Norwegian University of Life Sciences
Faculty of Chemistry, Biotechnology
and Food Science

Philosophiae Doctor (PhD)
Thesis 2024:33

Interplay between LPMOs and cellulases during enzymatic degradation of cellulose - effects of time, lignin, light and substrate concentration

Samspillet mellom LPMOer og cellulaser under enzymatisk nedbrytning av cellulose - effekter av tid, lignin, lys og substratkonsentrasjon

Camilla Fløien Angeltveit

Interplay between LPMOs and cellulases during enzymatic degradation of cellulose - effects of time, lignin, light and substrate concentration

Samspillet mellom LPMOer og cellulaser under enzymatisk nedbrytning av cellulose - effekter av tid, lignin, lys og substratkonsentrasjon

Philosophiae Doctor (PhD) Thesis

Camilla Fløien Angeltveit

Norwegian University of Life Sciences
Faculty of Chemistry, Biotechnology and Food Science

Ås, 2024

Thesis number 2024:33
ISSN 1894-6402
ISBN 978-82-575-2159-2

TABLE OF CONTENTS

ACKNOWLEDGMENT

The work presented in this thesis was carried out at the Faculty of Chemistry, Biotechnology, and Food Science (KBM), department of Bioprocess Technology and Biorefining (BioRef) at the Norwegian University of Life Sciences (NMBU) from 2020 to 2024. The Norwegian Research Council funded the work as a part of the FME research center Bio4Fuels (project number 257622).

I would like to express my sincere gratitude to my main supervisor, Svein Jarle Horn, for the opportunity to complete my PhD in the BioRef group. Thank you for always being available, for your dedication, enthusiasm, encouragement, and for sharing your vast knowledge. I couldn't have asked for a better supervisor!

To my co-supervisors, Vincent Eijsink and Anikó Várnai, thank you for your thorough feedback on manuscripts. Vincent, thank you for always providing insightful solutions and explanations, your extensive knowledge is inspiring!

I'm incredibly thankful to be a member of the BioRef group. I have genuinely been looking forward to coming to work every day. A special thanks to Pernille, Line, and Lars, who have been there with me from the beginning. I would also like to thank Eirik for all discussions and support throughout my MSc and PhD.

I have also had the opportunity to travel abroad, work in Tina Jeoh's lab at the University of California, Davis, and experience California with my friend and college, Lauren, for which I'm truly grateful. I'm very happy that our collaborative efforts resulted in a publication!

A huge thanks to my friends and family for their unwavering support throughout this journey. Finally, I don't know what I would have done without the endless support of my partner, Fredrik. Thank you for always being there, encouraging, cheering, and listening to my endless chatter about work.

Camilla Angeltveit
Ås, March 2024

SUMMARY

The recent discovery of lytic polysaccharide monooxygenases (LPMOs) marked a paradigm shift in our understanding of enzymatic saccharification of lignocellulosic biomass. Under aerobic conditions, interactions between oxygen and redox-active components such as ascorbic acid or lignin produce the LPMO co-substrate H_2O_2. The presence of H_2O_2 is pivotal for maintaining LPMO activity during saccharification processes, but *in situ* production is challenging to regulate. This is problematic since H_2O_2 accumulation in the system may lead to reactive oxygen species production and inactivation of the enzymes. LPMOs' flat active site surface facilitates direct oxidation in crystalline cellulose, which makes the substrate accessible to classical hydrolytic cellulases. However, the interplay between cellulases and LPMOs is still not fully understood, which restricts practical applications. The aim of this thesis was to improve our understanding of the LPMO-cellulase interplay by investigating the effects of time, light, lignin, and substrate concentration on LPMO activity and saccharification performance. This study is based on four research articles:

In **Paper I,** a positive effect of LPMO pretreatment on the productive binding capacity of a reducing end cellulase, *Tl*CBHI, was demonstrated. Despite the fact that LPMO inactivation occurred before the first time point (5 h), a pronounced enhancement of *Tl*CBHI's productive binding capacity on LPMO-pretreated cellulose was observed after 24 h. This indicates that the LPMO cleavage of the crystalline cellulose does not directly serve as new access points for cellulases but that this is followed by a non-enzymatic amorphization that makes the substrate accessible for cellulase activity.

In **Paper II,** the importance of maintaining LPMO activity throughout the reaction to ensure efficient cellulase activity, especially at high substrate loadings, was demonstrated. The positive effect of including LPMOs in a cellulase cocktail

increased with dry matter concentrations and reaction time. The impact of LPMO regioselectivity varied depending on the substrate, but a clear increase in cellulose conversion was observed when combining C1 and C4 LPMO activity. The study also indicates that chelating of free copper with EDTA might hinder transition metal-induced side reactions following LPMO inactivation.

In **Papers III** and **IV,** light-exposed lignin was shown to promote LPMO activity on cellulose by improving *in situ* generation of H_2O_2 compared to similar reactions in the dark. These studies further demonstrated that the H_2O_2 production and thus LPMO activity could be controlled by lignin concentration, light intensity, and light-specific wavelengths. The findings of **Paper III** indicate that when lignin is exposed to light, it enhances LPMO activity by converting O_2 to H_2O_2, most likely via $O_2^{\bullet-}$. In contrast, the results in **Paper IV** showed that light exposure of lignin-containing reactions negatively affected cellulose saccharification by cellulolytic enzyme cocktails. Interestingly, LPMO activity could help mitigate this negative effect on the glucose yield by their productive H_2O_2 consumption, delaying the accumulation of reactive oxygen species and subsequent enzyme inactivation.

SAMMENDRAG

Den nylige oppdagelsen av lytisk polysakkarid monooxygenaser (LPMOer) markerte et paradigmeskifte i vår forståelse av enzymatisk sakkarifisering av lignocellulose. Under aerobe forhold blir LPMOenes ko-substrat, H_2O_2, produsert gjennom interaksjoner mellom oksygen og redoksaktive komponenter som askorbinsyre eller lignin. Tilstedeværelsen av H_2O_2 er avgjørende for å opprettholde LPMO-aktiviteten under enzymatisk sakkarifisering, men *in situ* produksjon av H_2O_2 er utfordrende å regulere. Dette er problematisk siden akkumulering av H_2O_2 i systemet kan føre til produksjon av reaktive oksygenarter og inaktivering av enzymene. LPMOenes flate aktive sete tillater direkte oksidasjon i krystallinsk cellulose og gjør dermed substratet mer tilgjengelig for klassiske hydrolytiske cellulaser. Imidlertid er samspillet mellom cellulaser og LPMOer fortsatt ikke helt forstått, noe som begrenser praktiske anvendelser. Målet med denne avhandlingen var å forbedre forståelsen vår om samspillet mellom LPMOer og cellulaser ved å undersøke effekter av tid, lignin, lys-eksponering og substratkonsentrasjon på LPMO-aktivitet og glukose-utbytte. Denne studien er basert på fire forskningsartikler:

I **Artikkel I** ble det vist at LPMO-forbehandling økte den produktive bindingskapasiteten til *Tl*CBHI, en cellulase med affinitet for reduserende celluloseender. En markant økning i den produktive bindingskapasiteten til *Tl*CBHI var synlig etter 24 t med LPMO-forbehandling, og dette til tross for at LPMOene var inaktivert allerede etter 5 t. Dette tyder på at LPMO-kutt i den krystallinske celluloseoverflaten ikke direkte fungerer som nye tilgangspunkter for cellulasene, men at LPMO-oksideringen er etterfulgt av en ikke-enzymatisk dekrystallisering som gjør substratet mer tilgjengelig for cellulase-aktivitet.

I **Artikkel II** ble det vist at stabil LPMO-aktivitet gjennom hele reaksjonsforløpet fremmer cellulase-aktivitet, spesielt ved høye substratkonsentrasjoner. Den

positive effekten av å inkludere LPMO i cellulase-cocktailer økte i takt med substratkonsentrasjonen og gjennom reaksjonsforløpet. Effekten av C1- vs C4-aktive LPMOer varierte avhengig av substratet, men en tydelig økning i glukose-utbytte ble observert ved å kombinere C1- og C4-aktive LPMOer. Studien viste også at chelatering av fri kobber med EDTA kan forhindre sidereaksjoner med innskuddsmetaller som en følge av LPMO-inaktivering.

I **Artikkel III** og **IV** ble det vist at lys-eksponering av lignin fører til økt *in situ* H_2O_2-produksjon og dermed økt LPMO-aktivitet sammenlignet med reaksjoner i mørket. Disse studiene viste også at H_2O_2-produksjonen og LPMO-aktiviteten kunne kontrolleres ved hjelp av ligninkonsentrasjon, lysintensitet og lys-spesifikke bølgelengder. **Artikkel III** viste at lyseksponering av lignin økte omdannelsen av O_2 til H_2O_2, mest sannsynlig via $O_2^{\bullet-}$, og ga derfor økt LPMO-aktivitet. Samtidig viste resultatene i **Artikkel IV** at lys-eksponering av reaksjoner med lignin hadde en negativ påvirkning på cellulase-aktivitet. Tilstedeværelsen av LPMO kunne hjelpe til med å motvirke den negative effekten på glukoseutbyttet til cellulasene. Dette er mest sannsynlig et resultat av LPMOens konsumering av H_2O_2, som vil forsinke produksjonen av reaktive oksygenarter og enzym inaktivering.

ABBREVIATIONS

AA	Auxiliary activity
BG	β-glucosidase
CAZy	Carbohydrate-active enzyme
CBM	Cellulose binding module
CBH	Cellobiohydrolase
CBP	Chitin-binding protein
CCS	Carbon capture and storage
CD	Catalytic domain
CDH	Cellobiose dehydrogenase
Chl	Chlorophyllin
DM	Dry matter
EDTA	Ethylenediaminetetraacetic acid
EG	Endoglucanase
G	Guaiacyl
GH	Glycoside hydrolase
GHG	Greenhouse gas
H	p-hydroxyl phenol
HRP	Horseradish peroxidase
IPCC	Intergovernmental panel on climate change
LPMO	Lytic polysaccharide monooxygenase
NR	Non-reducing end
R	Reducing end
RE	Redox enzyme
ROS	Reactive oxygen species
S	Syringyl
SOD	Superoxide dismutase
UPO	Unspecific peroxygenase

LIST OF PAPERS

Paper I:

Angeltveit CF, Jeoh T & Horn SJ. (2023). Lytic polysaccharide monooxygenase activity increases productive binding capacity of cellobiohydrolases on cellulose. *Bioresource Technology*, 389, 129806.

Paper II:

Angeltveit CF, Várnai A, Eijsink VGH & Horn SJ. (2024). Enhancing enzymatic saccharification yields of cellulose at high solid loadings by combining different LPMO activities. *Biotechnology for Biofuels and Bioproducts,* 17, 39.

Paper III:

Kommedal EG, **Angeltveit CF,** Klau LJ, Ayuso-Fernández I, Arstad B, Antonsen SG, Stenstrøm Y, Ekeberg D, Gírio F, Carvalheiro F, Horn SJ, Achmann FL & Eijsink VGH. (2023). Visible light-exposed lignin facilitates cellulose solubilization by lytic polysaccharide monooxygenases. *Nature Communication*, *14*, 1063.

Paper IV:

Angeltveit CF, Kommedal EG, Stepnov AA, Eijsink VGH & Horn SJ. Light exposure of lignin affects the saccharification efficiency of LPMO-containing cellulolytic enzyme cocktails. *Manuscript submitted to ACS Sustainable Chemistry and Engineering.*

1 INTRODUCTION

1.1 Navigating the path towards a greener future

1.1.1 Global warming

The carbon cycle has ensured a stable global temperature for centuries, but in the last 200 years, human use of fossil fuels such as coal, oil, and natural gas has resulted in a system imbalance. Carbon is the fundamental building block for life on Earth, with Nature continuously repurposing and cycling carbon atoms through the carbon cycle. The carbon cycle is a complex system of interactions between the atmosphere, land, oceans, and living organisms, influencing Earth's climate and ecosystems [1]. For the last 800,000 years, the carbon cycle has maintained a CO_2 level in the range of 170 to 300 ppm [2], while as of March 2024, the level has exceeded 420 ppm [3]. The combustion of fossil fuels for generating heat and electricity, and for use in the transportation sector releases large quantities of CO_2 and other greenhouse gases (GHGs) that adsorb and radiate heat, which is a pivotal factor in today's climate change.

During the decade from 2011 to 2020, the global temperature rose 1.1°C compared to the pre-industrial level (1850 to 1900). The greenhouse effect is Earth's mechanism for keeping the average global temperature above freezing, making life on Earth possible. The increased GHG emissions exceed the carbon sinks' limits, resulting in carbon accumulation in the atmosphere and causing the global temperature to rise **(Fig. 1)** [4]. The increasing global temperature is causing more extreme weather, drought, melting glaciers, rising sea levels, and ocean acidification. These changes may have catastrophic consequences for the Earth, threatening the food supply, animal diversity, and human health [5].

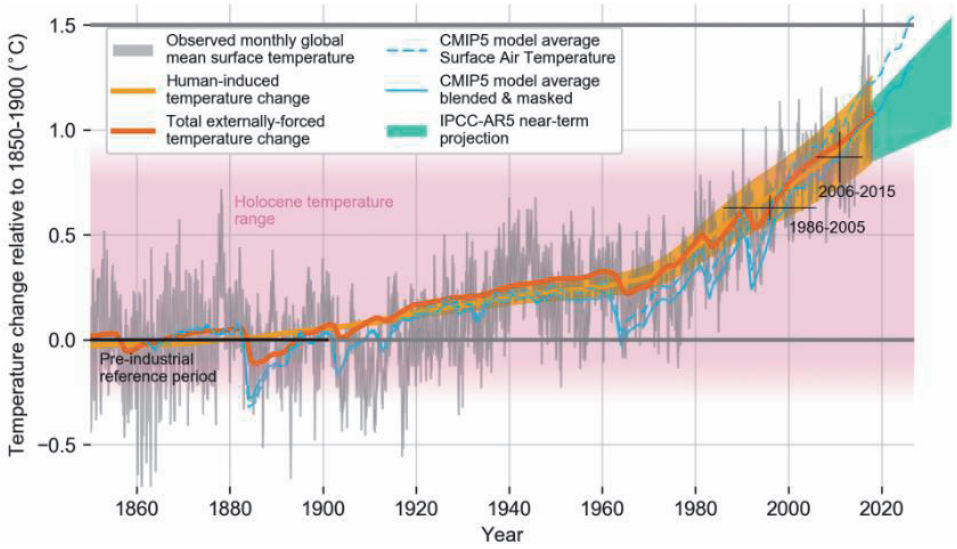

Figure 1. Development and projection of the average global temperature. The figure shows the monthly average global temperature **(grey)**, human-induced temperature change **(yellow)**, total temperature change (human and naturally forced; **orange)**, surface air temperature **(dashed blue line)**, air and sea surface temperature **(solid blue line)**, and the IPCC-AR5 near time temperature projection by Kirtman et al. [6] **(green)**. The temperature change is relative to the average global temperature between 1850 and 1900. The figure was taken from [4].

National low-emissions strategies are necessary to reverse the course of global warming before it becomes irreversible. In 2015, the Paris Agreement came into form, which aims to limit global warming to well below 2°C (preferably 1.5°C) above the pre-industrial level and achieve climate neutrality by 2050 [7]. Climate neutrality means a balance between the total GHG emissions and the removal of the gasses absorbed by carbon sinks [8] and, for example, carbon capture and storage (CCS) systems [9].

Only lowering the current GHG emissions is insufficient because of the current level of GHG in the atmosphere. Hence, helping the natural carbon cycle with the removal of CO_2, often referred to as negative emissions, is another crucial action to mitigate global warming [4]. This can be achieved by helping the natural CO_2 fixation capacities through afforestation and reforestation, which involves planting or replanting new trees. Another potentially necessary action is CCS, a process in which atmospheric CO_2 is captured and transported for long-term underground storage [9]. The cost-effective and long-term value of this process can be

debated, but the negative emissions can be a deciding factor in turning around this global crisis before it is too late.

The most recent Intergovernmental Panel on Climate Change (IPCC) report from 2023 suggests that according to their models, the chance of reaching or surpassing a global temperature rise of 1.5°C compared to before the industrial revolution is more than 50% between 2021 and 2040 [10]. Therefore, transitioning from a fossil fuel-based society to using renewable energy sources and sustainable alternatives for producing energy, fuel, and high-value chemicals is crucial to disprove IPCC's projection.

The transport sector, which relies heavily on gasoline and diesel, is a major contributor to GHG emissions. As of 2021, almost a third of the GHG emissions in Norway are from the transportation sector [11]. Renewable energy sources, such as hydropower, wind, solar, and geothermal, offer a way to generate electricity and power electric vehicles. However, electrification cannot replace fuels for heavy road transport, the marine sector, or jet fuels. Replacing fossil chemicals and fuels with renewable bioethanol, biodiesel, and sustainable aviation fuel is essential in combating global warming.

1.1.2 The production of carbon-neutral biofuels

Biofuels produced from biomass offer an environmentally friendly alternative to traditional fossil fuels. During photosynthesis, plants and algae use sunlight to convert CO_2 and water into glucose and oxygen. Fossil fuels have been sequestered underground for millions of years and are not part of the carbon cycle. Using carbon-containing biomass already within the global carbon cycle for biofuels production instead of fossil fuels will not increase the net atmospheric CO_2 levels.

In total volume, bioethanol is the most important biofuel consumed worldwide. Corn and sugar cane are the two primary sources for bioethanol production in the United States and Brazil, accounting for 84% of the global bioethanol production

[12]. Utilizing the sucrose and starch content of edible biomass, which is "easily" converted into bioethanol, is generally referred to as first-generation biofuels. The need to avoid conflicts with food production and land use and improve sustainability drives a transition from first-generation to subsequent generations of biofuels [13]. Second-, third-, and fourth-generation biofuels aim to overcome these challenges by using diverse feedstocks, improving production processes, and reducing environmental impacts. While these newer generations hold promise, they face technical, economic, and regulatory hurdles as they continue to develop.

Second-generation (or advanced biofuels) are produced from non-edible biomass such as food waste, agricultural residue, wood chips, and spent cooking oil [14]. Algal biomass can be used for the third-generation of biofuels due to the high lipid content [15], while fourth-generation biofuels can be produced from genetically modified crops and algae [16]. The carbohydrates found in these sources can be used for bioethanol or biogas production, while the lipid content can be used to produce biodiesel. In addition to processing biomass, there is some interest in developing power-X technologies to produce e-fuels from CO_2 [17].

In general, biofuels can be produced via thermochemical or biochemical processes. Thermochemical processes include pyrolysis, hydrothermal liquefaction, or gasification [18,19], while biochemical methods use enzymes and microorganisms to break down biomass and produce liquid or gaseous fuels [20]. Thermochemical methods typically demand high energy and acidic inputs but operate at considerably higher rates compared to biochemical methods. In comparison, the biochemical methods use milder operating conditions, have lower energy requirements, higher selectivity, and lower production of byproducts. The choice between these methods ultimately depends on factors such as specific feedstock availability, desired product portfolio, and economic feasibility [21,22].

1.1.3 Valorization of forest biomass and its limitations

Valorization of forest biomass holds significant promise for addressing the world's energy needs while mitigating environmental impacts. Leveraging lignocellulosic biomass for producing biofuels, value-added biochemicals, and bioenergy comes with several challenges and limitations related to feedstock availability and transportation, feedstock recalcitrance, technological barriers, and sustainable forest management.

One-third of the terrestrial surface area of the world is covered by forests [23]. Transportation of biomass from forest land to processing plants can be logistically challenging, especially in remote or densely forested areas. Transportation costs can significantly impact the overall economics of biofuels production, and it is therefore crucial to minimize transport distances to ensure minimal cost and energy requirements.

Non-edible biomass is significantly more challenging to process than edible biomass. Wood processing residues such as sawdust and bark or residues from forestry operations such as branches, tops, and thinnings are typical non-edible biomasses [24]. Given the diversity and heterogeneity of the biomass, the production of a range of products, from biofuels to pharmaceuticals, is crucial to utilize lignocellulosic biomass economically **(Fig. 2)**, where biofuels comprise the highest volume yet the lowest value and pharmaceuticals the lowest volume and the highest value. The recalcitrant structure possesses extensive challenges, and better and more efficient technology is still needed to achieve cost-effective conversion of lignocellulosic biomass.

Mono-feedstock biorefineries producing first-generation biofuels are already commercialized, while second-generation biofuels production is still economically challenging. For example, the enzymatic hydrolysis processes for second-generation biofuels account for around 25-30% of the total operating costs, while first-generation biofuels from corn are below 3% [25]. In any case, petroleum-derived fuels (0.29 USD/L) are still cheaper than biodiesel production, for

example, compared to biodiesel production from soybeans in the United States (0.42 USD/L) [26]. Today, the companies GranBio and Raizen in Brazil are rare examples of successful industrial production of second-generation bioethanol [27].

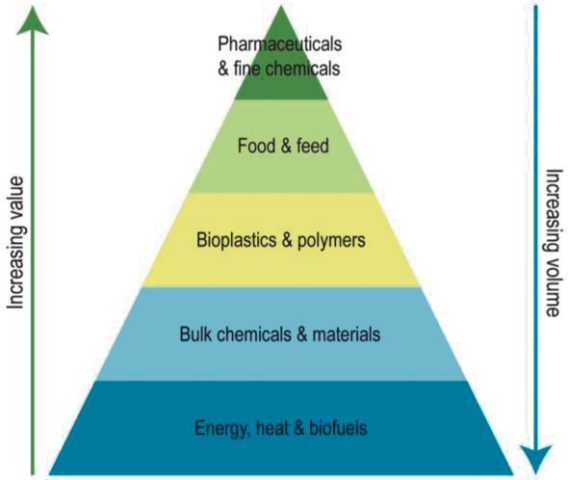

Figure 2. Valorization of forest biomass requires a large product profile. The figure shows the value vs volume of biobased end products. The figure is a modified version of the one appearing in [28].

Maintaining sustainable forest management while utilizing woody biomass for biofuels production requires a balanced approach that prioritizes conservation efforts and resource utilization. Implementing strict harvesting practices, such as selective cutting and rotation cycles, ensures minimal impact on forest ecosystems and allows for natural regeneration. Additionally, reforestation and afforestation activities are essential for facilitating the natural regeneration and growth of forests, thereby preserving the rich biodiversity of plant and animal species within these ecosystems. Overall, collaborative efforts between industries, governments, and communities are crucial for harnessing the potential of woody biomass for biofuels while maintaining the long-term sustainability of biofuels production from lignocellulosic biomass [29].

1.2 Lignocellulosic biomass

Over millions of years of evolution, plants have developed complex cell wall structures composed of cellulose (40-50%), hemicellulose (20-40%), and lignin

(10-30%), along with minor components like pectin, minerals, proteins, lipids, and soluble sugars [30]. These components are embedded in a structural matrix **(Fig. 3)** and are usually referred to as lignocellulosic biomass. Lignocellulosic biomass accounts for a significant portion of the five gigatons of carbon available on Earth [31], which includes materials such as crop residues (e.g., corn stover, wheat straw), forestry residues (e.g., wood chips, sawdust), and energy crops (e.g., switchgrass, miscanthus) [32]. The plant cell wall structure provides structural support and protection to plant cells and tissues, allowing them to withstand abiotic and biotic stress [33]. The complex structure and large compositional variation of lignocellulosic materials make the utilization of the ubiquitous material challenging [34].

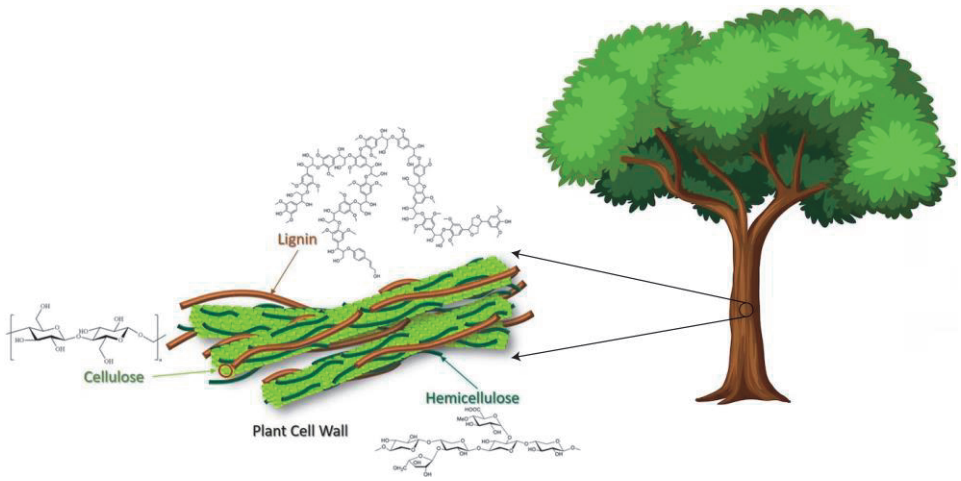

Figure 3. Illustration of lignocellulosic biomass structure. The figure shows lignocellulosic biomass and its main components: cellulose, hemicellulose, and lignin. The figure is a modified version of the one appearing in [35].

1.2.1 Cellulose

The widespread distribution of cellulose in plant biomass has made it a valuable resource for human societies, serving as an energy source and raw material for various industrial processes, including the production of paper, fibers, textiles, and biofuels [36,37]. Cellulose is the most resilient polysaccharide in plant cell walls, consisting of linear polymers composed of β-1,4-linked D-glucose units with significant resistance towards depolymerization [38]. The cellulose repeating

unit is cellobiose, wherein two glucose monomers are rotated 180° relative to each other **(Fig. 4)**. These polysaccharide chains form an insoluble material with crystalline and amorphous regions. The native crystalline cellulose structure arises from the aggregation of parallel microfibril chains, strengthened by van der Waals interactions and intra- and intermolecular hydrogen bonds. The most prevalent native form is Cellulose I, composed of microfibrils formed by parallel glucan chains, while Cellulose II comprises microfibrils of antiparallel glucan chains [39]. The breakdown of cellulose is particularly challenging due to the complex interactions between the polymer chains and the limited accessibility of surface-exposed cellulose chains for degradation by classical cellulolytic enzymes [40]. Despite its recalcitrance, the uniformity of cellulose presents a considerable advantage, as the depolymerization of cellulose results in one singular product, glucose.

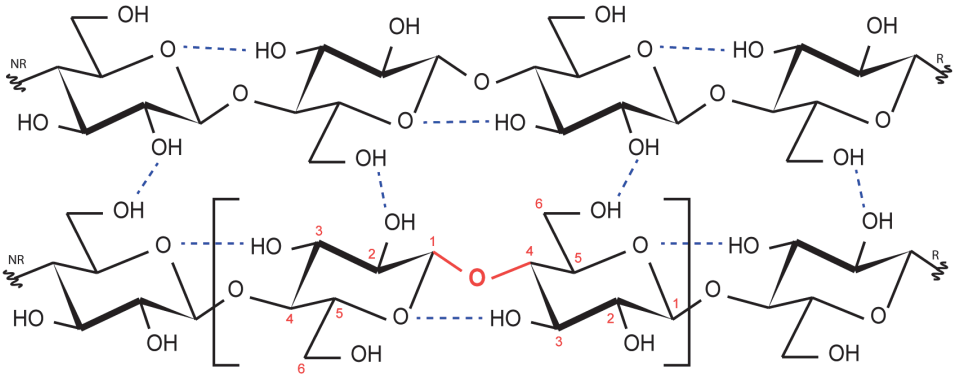

Figure 4. Chemical structure of cellulose. The figure shows the structure of Cellulose I, consisting of cellobiose repeating units shown in **square brackets** connected by β-1,4-glycosidic bonds marked in **red.** The Cellulose I structure consists of multiple linear parallel glucan chains interconnected by hydrogen bonds, shown in **blue**. The reducing **(R)** and non-reducing **(NR)** cellulose chain ends are marked.

1.2.2 Hemicellulose

Hemicellulose comprises various non-cellulosic polysaccharides playing a crucial biological role in strengthening the cell wall by interconnecting cellulose and lignin [41,42]. It is a branched polysaccharide with a linear backbone composed of a β-1,4-linked homopolymer and different pentamers and hexamers such as xylans, xyloglucans, glucomannans, mannans, and β-(1,3;1,4)-glucans. For

example, glucomannan is the most prominent constituent of softwood (e.g., spruce), while hardwood (e.g., birch) contains mostly xylan [43]. Hemicellulose degradation requires a wide diversity of enzymes due to the heterogeneous structure, including specific enzymes for removing side chains and acetylation [44]. Generally, the degradation of hemicelluloses is more accessible than the degradation of cellulose but results in a diverse mix of pentamer and hexamer sugars **(Fig. 5)**.

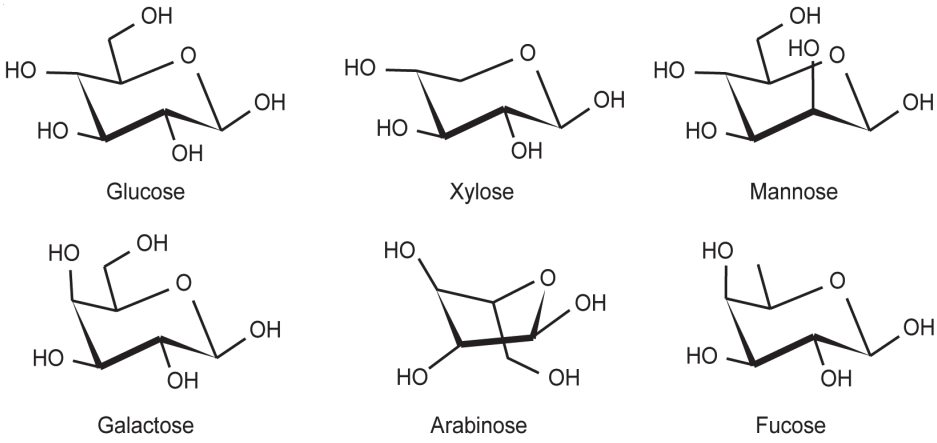

Figure 5. Overview of hemicellulose monomers. The figure shows a selection of the most common hemicellulose monomers.

1.2.3 Lignin

Lignin is the most abundant aromatic biopolymer found on Earth. As a component of the plan cell wall, it provides structural stability, transportation of nutrients and water, and protection against biological and chemical attacks. Lignin is regarded as the principal contributor to the recalcitrance of lignocellulose and poses a considerable challenge in the industrial processing of lignocellulosic biomass [45].

Lignin is a hydrophobic polymer with a highly complex and branched chemical structure. Generally, the lignin structure is comprised of three cross-linked monolignols: coniferyl alcohol, p-coumaryl alcohol, and sinapyl alcohol, each differing in their extent of methoxylation. These units are incorporated into the

lignin structure in the form of guaiacyl (G), p-hydroxyl phenol (H), and syringyl (S) groups, respectively, linked by different ether or carbon-carbon bonds **(Fig. 6)**. The relative composition varies depending on the biomass source, e.g., softwood lignin consists primarily of G units, hardwood lignin consists mainly of G and S units, while grass lignin encompasses all three units. However, the exact structure of native lignin is unknown due to side reactions occurring when separating lignin from the carbohydrate polymers, such as repolymerization [46].

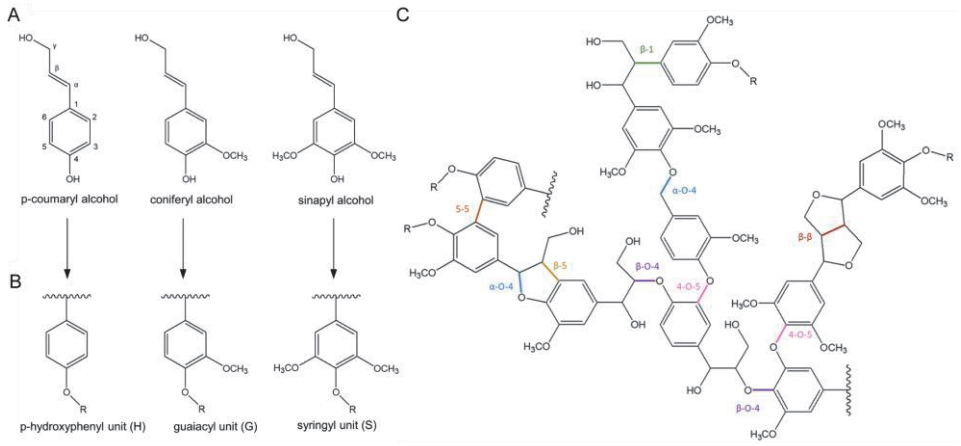

Figure 6. Illustration of a possible lignin structure. The figure shows the three monolignol components **(A)** and the corresponding lignin subunits **(B)**. **Panel C** shows an example lignin structure and a selection of different linkages: β-O-4, α-O-4, 4-O-5, β-β, β-1, 5-5, and β-5. The figure was taken from [47].

1.2.4 Lignocellulosic biorefineries

A biorefinery is an industrial plant, or network of plants, converting biomass into biofuels, biochemicals, biopolymers, and other bio-based materials. Biorefineries are divided into different phases based on their feedstock type(s), product type(s), and process(es). Phase I biorefineries utilize one process to produce one product, while phase II uses multiple processes and produces multiple products. The use of one single feedstock is typical for both phase I and phase II biorefineries. Phase III is the most advanced biorefineries, utilizing multiple feedstocks and processes to make a wide range of products [48].

A lignocellulosic biorefinery converts lignocellulosic biomass into a diverse array of high-value products [48]. The idea behind a lignocellulosic biorefinery parallels that of a petroleum refinery, but instead of refining crude oil into a range of products, it employs chemical, biological, and thermal processes to convert biomass into valuable bioproducts [49]. Biochemical processing is the most environmentally friendly and selective approach (as discussed above), encompassing the three main processes: pretreatment, enzymatic depolymerization forming platform sugars, and microbial fermentation and downstream processing producing the desired products **(Fig. 7)**. The robust structure of plant cell walls, developed to resist degradation, poses great challenges for effectively processing lignocellulosic biomass [32,50].

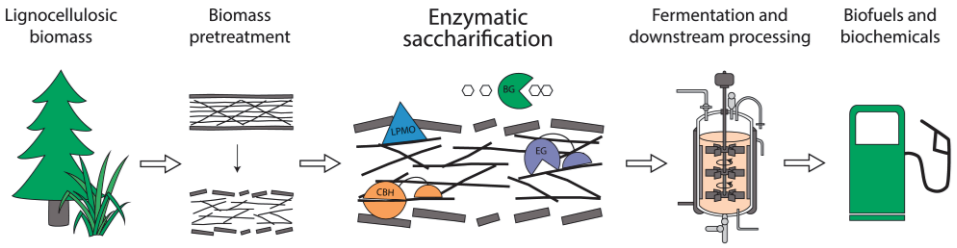

Figure 7. Overview of the biochemical processes involved in lignocellulose vaporization. Biochemical conversion of lignocellulose starts with harvesting and pretreatment of the biomass, followed by enzymatic degradation, fermentation, and downstream processing to produce the desired products.

Pretreatment is a critical step in lignocellulose conversion because it significantly influences the efficiency of the subsequent processes, enzymatic hydrolysis and fermentation. The aim is to alter the composition, increase the surface area, and/or remove lignin to make the substrate more accessible for enzymatic hydrolysis [51]. The pretreatment usually comprises a combination of mechanical and chemical treatment. Mechanical pretreatment often involves grinding, while chemical pretreatment includes, e.g., steam explosion and acid- or alkali-based treatment of the biomass. The goal is to maximize the release of fermentable sugars while minimizing the production of inhibitory compounds that can interfere with microbial growth and fermentation [43].

The process of removing lignin from lignocellulosic biomass requires a substantial amount of energy. Generally, the pretreatment processes can be divided into two main routes: removing or retaining (only partially removed) lignin in the biomass. The presence of lignin may hamper cellulase activity due to unproductive binding and shielding of the cellulose microfibrils [52], but lignin may also facilitate H_2O_2 production and promote the activity of critical redox-active enzymes [53]. Thus, effective and well-adapted pretreatment of the substrate is essential to increase the effectiveness of the next step, enzymatic hydrolysis, which currently comprises a substation contribution to the overall cost of second-generation biofuels production [54,55].

Following the enzymatic hydrolysis processes (which will be discussed in detail in **Section 1.3.**), the resulting sugar syrups are used for microbial fermentation. Microbial fermentation is a biological process in which microorganisms, such as bacteria, yeast, and fungi, are used to convert organic substrates into various products through metabolic pathways. The fermentation process starts with glycolysis, where glucose monomers from the enzymatic hydrolysis processes are converted into pyruvate. Pyruvate can be converted to a range of products, including ethanol and CO_2, using yeast (e.g., *Saccharomyces cerevisiae*) [56], and lastly, the products are concentrated and purified. Of note, *S. cerevisiae* cannot ferment pentamers, such as xylose, without genetic modification [57]. High ethanol production from lignocellulose is crucial for the feasibility of lignocellulosic biorefineries [58].

1.3 Enzymatic degradation of recalcitrant polysaccharides

In Nature, the degradation of recalcitrant polysaccharides is carried out by diverse communities of microorganisms such as bacteria, fungi, and archaea. These microorganisms have evolved complex enzymatic systems capable of breaking down polysaccharides into simpler sugars and other molecules that can be used as energy and carbon sources. Among the different carbohydrate-active enzymes, glycoside hydrolases (GHs) are the most abundant, breaking down

single polysaccharide and oligosaccharide chains by hydrolytically cleaving glycosidic bonds and releasing metabolizable sugars [59].

A complex synergistic relationship between a wide diversity of proteins is required for the degradation of lignocellulosic biomass, a simplified illustration is shown in **Fig. 8**. The most important enzymes for lignocellulose valorization are exoglucanases, also called cellobiohydrolases (CBHs), endoglucanases (EGs), and β-glucosidases (BGs), together targeting amorphous cellulose and producing easily fermentable glucose molecules [23]. To degrade the hemicellulose content of lignocellulose, hemicellulose active enzymes such as hemicellulases acting on the backbone and enzymes debranching the heterogeneous polymer are needed. Hemicellulose partly coats the cellulose fibrils, and therefore, hemicellulase activity may also increase cellulase activity.

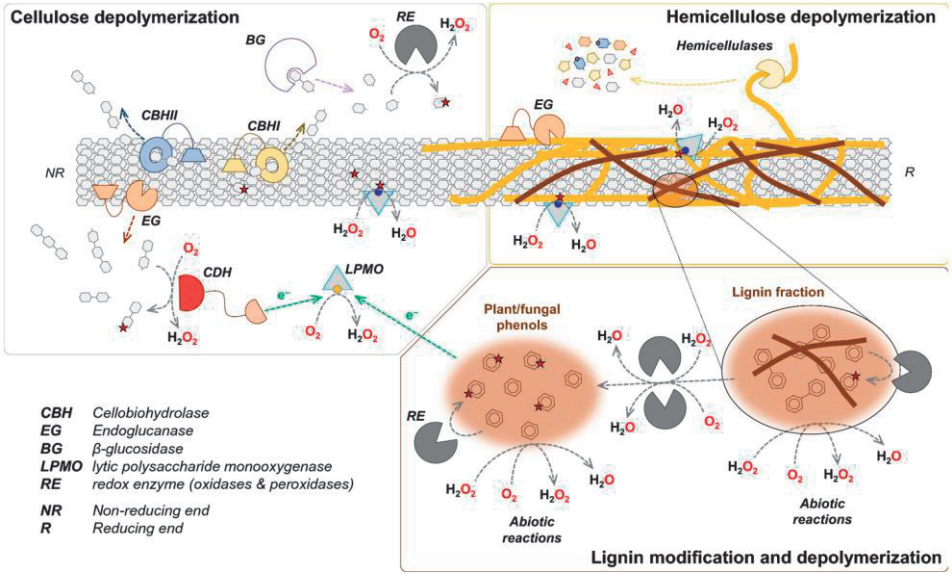

Figure 8. An illustration of enzymes involved in depolymerization of lignocellulosic biomass. The figure shows the key enzymes involved in the degradation of cellulose **(grey)**, hemicellulose **(orange)**, and lignin **(brown)**. The main cellulose-degrading enzymes are CBHI, acting from the reducing end, and CBHII, acting from the non-reducing end, EG, and BG. To simplify the illustration, the various enzymes that act on hemicellulose are referred to as hemicellulases, while lignin-modifying enzymes are denoted as redox enzymes (RE). Multiple sources can provide LPMOs with reducing equivalents and H_2O_2, e.g., cellobiose dehydrogenase (CDH) and phenols. An activated LPMO is illustrated with a blue sphere, while the resting state LPMO has an orange sphere. Oxidized sugars from LPMO activity or other RE are marked with stars. The figure was taken from [60].

To increase the accessibility of the polysaccharide polymers for the cellulolytic and hemicellulolytic enzymes, lignin active enzymes, such as peroxidases and laccases, to modify and (to a certain degree) depolymerize lignin are needed [61]. In recent years, including lytic polysaccharide monooxygenases (LPMOs) in the enzyme blends has shown greatly increased degradation efficiencies due to their oxidative action on material such as crystalline cellulose, hemicellulose, and chitin [62]. A positive synergistic relationship between these enzymes **(Fig. 8)**, increasing the saccharification yield while maintaining low enzyme usage, is vital for the cost-effective and sustainable manufacture of biofuels and high-value chemicals from lignocellulosic biomass [60].

1.3.1 Cellulases

Essential glycoside hydrolases for the efficient breakdown of cellulose are the three classical types of cellulolytic enzymes: CBHs, EGs, and BGs [59], where CBHs are considered the most important. CBHs have a tunnel-shaped active-site structure and are usually multi-domain enzymes with a catalytic domain (CD) and a carbohydrate-binding module (CBM), allowing for multiple different binding modes [63]. They are processive enzymes that, when successfully adsorbed and complexed to the substrate, release cellobiose from the reducing or non-reducing cellulose chain end, depending on their specific regioselectivity, before moving along the cellulose chain and release more cellobiose **(Fig. 9)** [64]. Conversely, endoglucanases attack the internal β-1,4-glycosidic bonds in cellulose chains, randomly cleaving the cellulose molecules and creating new attack points for CBHs [65]. β-glucosidases cleave cellobiose into two glucose molecules and are crucial in preventing cellobiose accumulation and inhibition of the CBHs [66].

Classical cellulolytic enzymes need accessible single cellulose chains (amorphous regions and cellulose chain ends) to initiate hydrolysis [61]. Cellulases usually exhibit a characteristic high initial degradation rate followed by a gradually slower degradation rate [67,68]. The initial rapid phase results from all the productive binding sites available on the substrate from the beginning of the reaction and the following slower degradation rate is limited by the rate at

which more binding sites become available [69,70]. The time-dependent exposure of access points for cellulases to complex cannot fully explain the decrease in the degradation efficiency. Thus, other important aspects to consider are physical obstacles at the substrate hindering the processive action and tightly or irreversibly adsorbed enzymes resulting in stalling of the enzyme activity, categorized as non-productive binding **(Fig. 9)**. Auxiliary enzymes such as LPMOs are beneficial to increase the accessibility of the crystalline substrate for the cellulases.

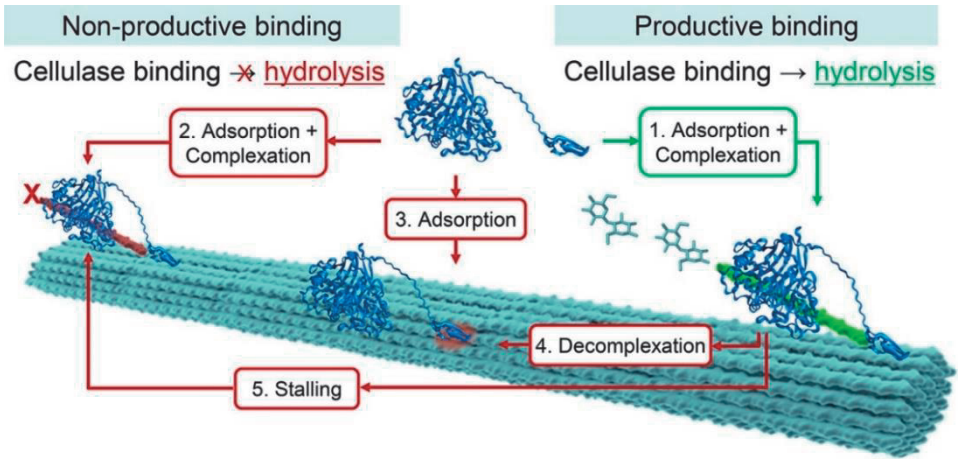

Figure 9. Productive and non-productive cellulase binding to cellulose. The figure illustrates a cellulose fibril and different binding modes for a processive reducing end cellulase with a CBM, Cel7A from *Trichoderma reesei.* Hydrolysis occurs when Cel7A is adsorbed and complexed to a productive binding site on the cellulose fibril **(1)**. In contrast, non-productive binding can occur if the Cel7A is adsorbed and complexed with a nonhydrolyzable chain end **(2)**, only the CBM is absorbed to the cellulose fibril **(3)**, the CD decomplex from the substrate while the CBM remains adsorbed **(4)**, or the Cel7A activity is blocked by the presence of surface obstacle resulting in stalled activity **(5)**. The figure was taken from [70].

1.3.2 Hemicellulases

Depolymerization of hemicellulose requires a wide diversity of enzymes due to the heterogenous and branched structure. Hemicellulases are often divided into two groups: enzymes responsible for depolymerization by cleaving the backbone and enzymes cleaving side chains that can cause steric hindrance for the depolymerization enzymes. The main backbone active enzymes are endo-β-1,4-xylanases and endo-β-1,4-mannanases, while enzymes such as arabinosidases, deacetylases, and galactosidases are essential for removing substitutions from

the main chain. In addition, β-xylosidases and β-mannosidases are crucial for the complete saccharification of hemicellulose to monomers [71,72].

1.3.3 Lytic polysaccharide monooxygenases

1.3.3.1 Discovery of the LPMO activity

Already in 1950, it was proposed that the classical cellulolytic enzymes required an enzymatic activation step carried out by a non-hydrolytic protein to help facilitate hydrolysis initiation of the crystalline cellulose structure [73]. Later, it was suggested that this non-hydrolytic protein was actually an oxidative enzyme. This hypothesis emerged from research demonstrating enhanced degradation efficiency by culture filtrates of white-rot fungi under aerobic conditions as opposed to anaerobic conditions [74]. Still, 60 years had to pass before the novel enzyme activity was discovered.

In 2005, Vaaje-Kolstad et al. showed that a chitin-binding protein (CBP21; today named *Sm*AA10A) from the gram-negative bacteria *Serratia marcescens*, which at the time belonged to family CBM33, had a boosting effect on the degradation of chitin by classical chitinases [75]. The groundbreaking discovery came in 2010 when the same authors showed that the boosting effect was a result of CBP21 catalyzing the oxidative cleavage of β-1,4-glycosidic bonds in chitin [76]. The study further showed that the enzyme required molecular oxygen and the delivery of electrons to perform its catalytic activity.

Shortly after, proteins performing similar catalytic activity on cellulose were discovered: CelS2 from the gram-positive bacteria *Streptomyces coelicolor* (today named *Sc*AA10C) [77], and in fungal proteins with structural similarities to CBM33, family GH61 [78,79]. In the following decade, enzyme activity on hemicelluloses [80], starch [81], pectin [82], and β-glucans [83] was discovered. Today, these enzymes are known as lytic polysaccharide monooxygenases (LPMO) [84] and are found in all kingdoms of life, demonstrating the importance of these proteins for breaking down recalcitrant polysaccharides in Nature.

1.3.3.2 LPMO classification and structure

The initially discovered LPMOs were categorized as GH61 and CBM33, which today belong to the auxiliary activity (AA) classification, AA9 and AA10, respectively. The Carbohydrate-Active Enzyme (CAZy) database created a new family in 2013 to include the redox-active AA enzymes acting on lignocellulosic polysaccharides [85]. As of March 2024, the CAZy database includes 17 AA families, eight of which are LPMOs: AA9-AA11 and AA13-AA17 [86].

LPMOs can be single- and two-domain (some cases of multi-modular LPMOs are also shown [87]). The main task of a CBM is to promote substrate binding [88], although new studies indicate that their role is more complex. The presence or absence of CBMs influences the LPMO cutting pattern, where a CBM results in more localized surface oxidation, while the LPMOs without CBMs oxidize more randomly in the crystalline structure [89]. The cutting pattern impacts sugar solubilization, which is important since most studies of LPMO activity depend on soluble-sugar analysis. It is worth mentioning that a recent study introduced a novel technique for analyzing non-soluble oxidized sugars through fluorescent labeling [90]. Moreover, substrate-bound LPMOs are less vulnerable to high H_2O_2 concentrations and autocatalytic inactivation (see below). Thus, the presence of a CBM can positively affect the stability of LPMOs, especially at low substrate concentrations [89].

Already in the seminal study by Vaaje-Kolstad et al. [76], LPMOs' dependency on a metal ion was suggested. Shortly after, it was shown that a copper ion in the active sites was crucial for the activity of the enzymes [78,91]. Two conserved histidines coordinate the copper ion in a T-shaped geometry, making up the LPMO's active site, often referred to as a "histidine brace" [78]. A recent study has shown that the amino acids surrounding the active site, the so-called second sphere residues, have important roles in fine-tuning the catalytic activity of the LPMOs [92]. Despite significant sequence variations, all LPMO families share a pyramidal core structure and a flat surface exposed activity site, illustrated in **Fig.**

10. These features are essential for executing their powerful oxidative catalytic mechanism.

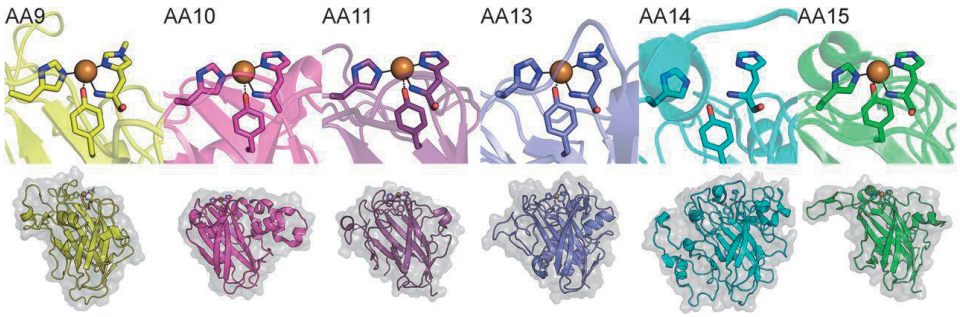

Figure 10. Structure and active site of different LPMO families. The figure shows the structure of six different LPMO families and their respective active site configurations. The LPMO-family and PDB codes from left to right are: AA9 (5ACH), AA10 (5OPF), AA11 (4MAI), AA13 (4OPB), AA14 (5NO7), and AA15 (5MSZ). The figure was taken from [93].

1.3.3.3 LPMO reaction mechanism

LPMOs perform oxidative cleavage of glycosidic bonds in polysaccharides, and in the seminal study by Vaaje-Kolstad et al., the monooxygenase paradigm was proposed [76]. In the monooxygenase paradigm, the LPMO requires the delivery of one molecular oxygen and two externally delivered electrons for every catalytic cycle ($R\text{-}H + O_2 + 2e^- + 2H^+ \rightarrow R\text{-}OH + H_2O$) **(Fig. 11, grey)**. A few years later, hydrogen peroxide instead of molecular oxygen was proposed by Bissaro et al. as the true co-substrate for the LPMO mechanism [94]. At the time, this theory was highly controversial, but it also offered a plausible explanation for the hitherto unexplained phenomena of how the second electron in the monooxygenase mechanism was delivered, since H_2O_2 as a co-substrate would provide the required electrons, protons, and hydrogen, all at once. Isotope labeling confirmed the theory, showing that despite the presence of 10-fold more O_2 than H_2O_2 in the reaction, the LPMO preferred H_2O_2 [94,95]. Thus, in 2017, the peroxygenase paradigm was proposed ($R\text{-}H + H_2O_2 \rightarrow R\text{-}OH + H_2O$), and with H_2O_2 as co-substrate, the LPMO requires only an initial priming reduction, after which the LPMO can perform multiple catalytic cycles **(Fig. 11, black)** [94].

The reaction mechanism of LPMOs has been heavily debated. However, consensus is emerging as several recent studies emphasize H_2O_2 as the preferred co-substrate. For example, a recent study employing online sensors monitoring both O_2 and H_2O_2 showed that only H_2O_2 was consumed by LPMOs [96]. Early studies suggesting monooxygenase activity overlooked the fact that H_2O_2 can be generated *in situ* under typical reaction conditions where oxygen and reactants are present. Importantly, the proposed LPMO peroxygenase mechanism is a clear advantage because of the so-called “oxygen dilemma”, avoiding wasting redox equivalence and hindering side reactions generating detrimental levels of reactive oxygen species (ROS) [97]. Studies have also shown that the H_2O_2-driven LPMO reaction is much faster than the O_2-driven [94,98], with a catalytic activity similar to true peroxygenases of approximately 10^6 $M^{-1}s^{-1}$ [99,100]. True peroxygenases such as unspecific peroxygenases (UPO) feature a heam iron active site and a catalytic mechanism resembling the LPMO peroxygenase mechanism [101].

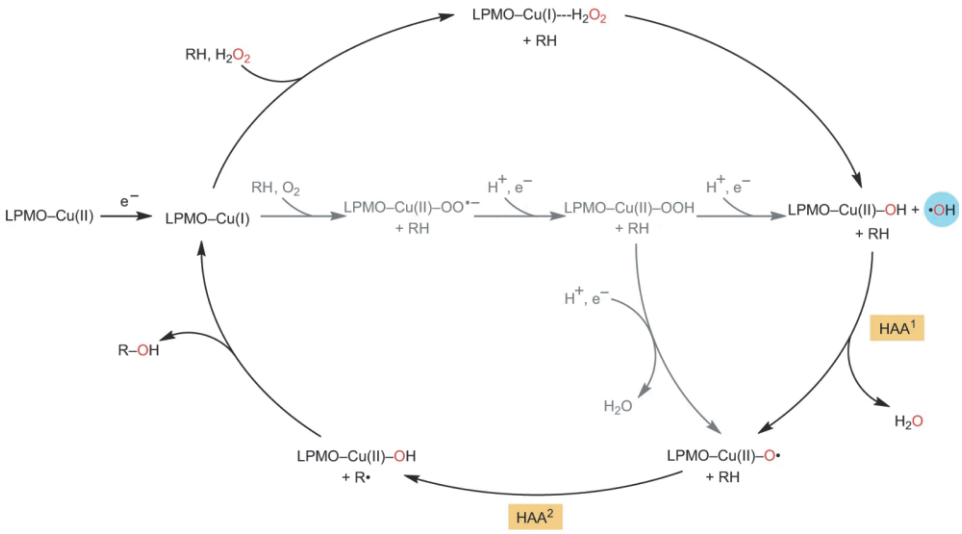

Figure 11. LPMO reaction mechanism. The figure shows the peroxygenase **(black)** and monooxygenase **(grey)** LPMO reaction mechanism. The figure was taken from [101].

A wide variety of electron donors facilitate the reductive activation of the LPMOs: enzymatic redox partners such as cellobiose dehydrogenase (CDH) [91], small-

molecule reductants such as ascorbic acid [76], gallic acid [102,103] or cysteine [104,105], or lignin and fragments thereof [106,107]. The choice of reductant may significantly affect LPMO activity. This is due to the role of reductants in both reducing the LPMOs and contributing to the *in situ* generation of H_2O_2. It should also be mentioned that the different reductants show big variations in the effect of pH and the presence of transition metals [108].

The powerful oxidative mechanism of LPMO relies on the formation of a complex capable of abstracting a hydrogen atom from the carbons in a glycosidic bond **(Fig. 11, black)**. The species responsible for the hydrogen abstraction has been extensively discussed, yet clear evidence remains elusive. However, most studies suggest Cu(II)-oxyl as the responsible species [109-114]. The Cu(II)-oxyl species will abstract a hydrogen atom either from the C1 or C4 position, whereases some LPMOs are mixed C1/C4 oxidizers, and hydroxylate the carbon in the scissile glycosidic bond in the polysaccharides. The hydroxylation destabilizes the glycosidic bond and results in chain breakage, producing aldonic acid or a gemdiol, for C1- or C4-active LPMOs, respectively, as illustrated in **Fig. 12** [76,115-118]. Of note, the complementary reducing or non-reducing chain end can have implications for the subsequent cellulase activity [119,120]. Since this lytic chain break is non-enzymatic, some researchers refer to the enzymes as polysaccharide monooxygenases (PMOs) [121].

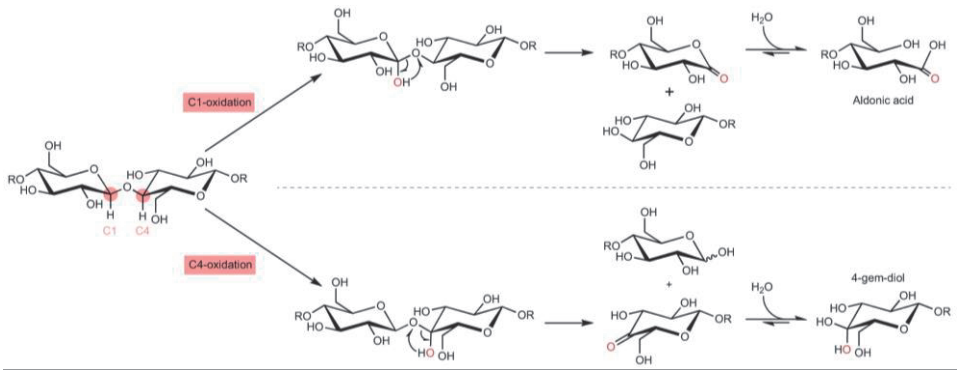

Figure 12. Hydroxylation and cleavage of glycosidic bonds by LPMOs. The figure shows the formation of C1- and C4-oxidized products following LPMO oxidation**.** The figure was taken from [101].

When adsorbed to its substrate, LPMOs carry out the **peroxygenase** reaction **(Fig. 13, PO pathway)**, as described in detail in **Fig. 11**. However, in the absence of a substrate, various side reactions can occur when the LPMO is in its reduced form **(Fig. 13)**. The LPMO can function as an **oxidase** and facilitate *in situ* H_2O_2 production from O_2 by oxidizing the reductant accompanied by Cu(I) being re-oxidized to Cu(II) **(Fig. 13, O pathway)** [118,122,123], which may be an evolutional trait for the LPMOs to being self-sufficient with their desired co-substrate. The **oxidase** activity depends on the type of reductant being oxidized [124-126], and may vary depending on the LPMO [124,127]. Of note, the truncation of LPMOs' CBM can increase their oxidase activity [128]. An LPMO can also perform **peroxidase** activity, catalyzing the oxidation of a non-carbohydrate substrate while consuming H_2O_2, similar to the **oxidase** activity, Cu(I) will be re-oxidized to Cu(II) **(Fig. 13, P pathway)**.

Hydrogen peroxide is a multi-edged sword, typically limiting the LPMO activity [129], but LPMOs are also vulnerable to high levels of H_2O_2 [94]. Production of H_2O_2 can be facilitated by abiotic oxidation of reducing compounds such as ascorbic acid or lignin **(Fig. 13, A pathway)**. A reduced LPMO not bound to a substrate can react with H_2O_2 and produce ROS, resulting in the inactivation of the enzymes [94,130] **(Fig. 13, I pathway)**. The binding of LPMOs to the carbohydrate substrate will have a protective effect and, to some degree, prevent LPMO inactivation [94,99,131]. As an additional consequence of LPMO inactivation, the coordinated copper atom of the active site of inactivated LPMOs may leak into the solution [128,132]. Fenton-like chemistry, facilitated by transition metals like copper, induces the generation of hydroxyl radicals from H_2O_2 **(Fig. 13, F pathway)** that may influence the lignocellulose matrix and enzyme activity [133]. When using reductants such as ascorbic acid, whose abiotic oxidation is promoted by transition metals, LPMO inactivation may be a self-reinforcing process [128]. Altogether, LPMO activity and the unavoidable side reactions, both enzymatic and non-enzymatic **(illustrated in Fig. 13)**, present a clear challenge in terms of process control and optimization.

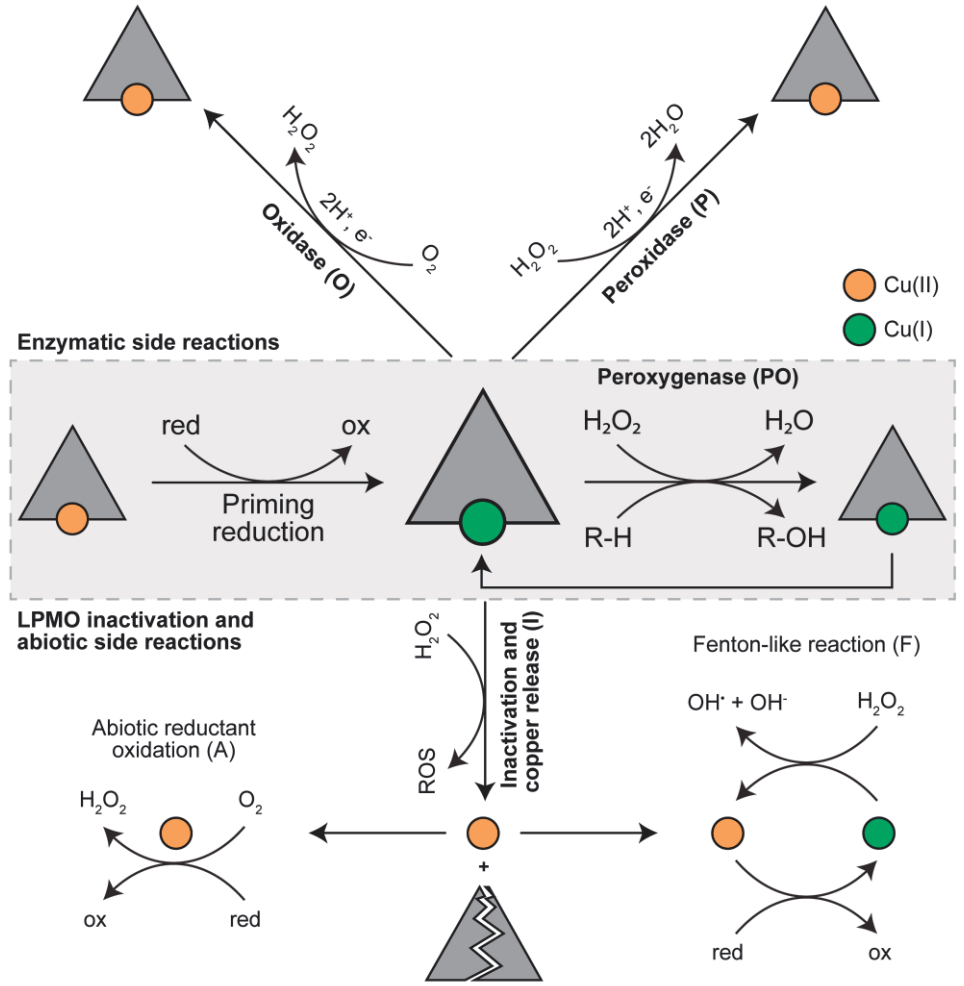

Figure 13. Overview of important LPMO reactions and abiotic reactions. The LPMO peroxygenase reaction **(PO)** is shown in the grey square and starts with a priming reduction, followed by multiple turnovers of carbohydrate cleavage using H_2O_2 before occasional re-oxidation of the active site copper. In the absence of a substrate, the LPMO contributes to various side reactions; it can function as an oxidase producing H_2O_2 **(O)** or a peroxidase consuming H_2O_2 **(P)**. The LPMO will, in the presence of too much H_2O_2, be non-reversibly inactivated and release its active site copper into solution **(I)**. H_2O_2 can also be produced by abiotic reductant oxidation, a process promoted by the presence of copper **(A)**. Lastly, Fenton-like chemistry from the presence of copper generates hydroxyl radicals from H_2O_2 **(F)**. red: reductant, ox: oxidized reductant.

1.3.4 Commercial enzyme preparations

Fungi have a central role among biomass-degrading organisms, accounting for the majority of biomass degradation in Nature. Wood decomposition by these fungi is important to the global carbon cycle. Wood-rotting fungi are divided into

two groups based on substrate preferences and wood-decaying strategies. White-rot and soft-rot fungi can degrade cellulose, hemicelluloses, and lignin by using a wide arsenal of hydrolytic and oxidative enzymes, whereas brown-rot fungi mostly rely on non-enzymatic oxidative reactions (Fenton chemistry) to depolymerize plant biomass and are not capable of lignin metabolization [134]. Efforts to mimic Nature's strategies for enzymatic degradation of recalcitrant polysaccharides have led to the development of fungal-derived commercial enzyme cocktails aimed at industrial biomass degradation and valorization.

Trichoderma reesei (synonym *Hypocrea jecorina*), a model system for degrading plant biomass to platform sugar, has gained significant attention due to its remarkable cellulase-producing abilities. *T. reesei* is a well-known soft-rot filamentous fungus discovered and isolated in the South Pacific during the 1940s [135]. It secretes high levels of endo- and exo-glucanases but low levels of accessory enzymes, e.g., hemicellulases, BGs, and LPMOs. An example of a commercial enzyme preparation based on *T. reesei* is Celluclast 1.5 L [136]. *T. reesei* has been subjected to extensive research to better understand its physiology, genetics, and enzymatic capabilities [137]. For example, customized enzyme mixtures can be efficiently generated by harnessing the innate adaptability of *T. reesei* [138].

In the wake of the LPMO discovery [76], LPMOs have been implemented into commercial enzyme cocktails (e.g., Cellic CTec2 and Cellic CTec3) and have shown greatly improved saccharification yields [62,139-142]. Higher levels of BG with better tolerance towards cellobiose feedback inhibition are also found in the more modern cocktails [143,144]. The commercial enzyme cocktails available today are tailored for agricultural waste biomass with high xylan content and thus are not optimal for the degradation of softwood due to the high glucomannan content. Spruce is an example of a softwood species, accounting for the majority of available woody-biomass in Norway. This is a good example of the importance of customizing the enzyme cocktails to the specific feedstock, guided by the composition of the biomass.

1.3.4.1 LPMO-cellulase synergy

Until recently, the synergistic relationship between LPMOs and cellulases was mainly attributed to enzymes' regioselectivity. Meaning that a positive synergistic relationship was limited to C1-active LPMOs and processive cellulases attacking the non-reducing end, and C4-active LPMOs and reducing end cellulases [119,120]. A mechanism similar to the known endo-exo synergism between cellulases, where the random action of endolytic enzymes created new access points for processive exolytic enzymes [145,146].

Recent studies suggest that the impact of LPMO oxidation on cellulase activity extends beyond the creation of new chain ends [147-151]. LPMO oxidation enables nearby water molecules of the breaking point to infiltrate the tightly organized fibril structure, thereby increasing solvent accessibility within the cellulose fibril. The production of aldonic acids through C1 oxidation is believed to have the most significant impact, as the open-ring structure enables greater penetration of water into the crystalline structure [147-149], and the negative surface charge promotes electrostatic repulsion and separation of the individual microfibrils [151]. Generally, the amorphization caused by LPMO oxidation of crystalline substrates will enhance the overall accessibility of the crystalline substrate for the classical cellulolytic enzymes.

The increased hydrophilicity of the substrate can also play a significant role in addressing challenges associated with high dry matter (DM) content [150]. Conducting enzymatic saccharification at high DM concentrations is known to impede yields and conversion rates, a phenomenon commonly termed "the high-solids effect" [152]. A high DM content indicates a scenario where minimal to no free water is available at the beginning of a reaction. This implies that the substrate retains all the water [153,154]. Water availability during enzymatic saccharification is crucial for multiple reasons: it serves as a reactant, a solvent facilitating the interaction between enzyme and substrate, and facilitates the diffusion of products [155]. The increased hydrophilicity of high DM reactions from LPMO activity may increase water availability and help alleviate the

negative effects of high DM conditions on cellulase activity. However, further research is still needed to unravel the mechanism of LPMO-cellulase synergism.

1.4 Photobiocatalysis to facilitate redox reactions

Photosynthesis is the conversion of light energy into chemical energy and is predominantly carried out by green plants, algae, and certain microorganisms such as cyanobacteria. Chlorophyll is the primary pigment used in photosynthesis and is responsible for capturing light photons. The light-dependent reaction (Photosystem I and Photosystem II) takes place in the thylakoid membrane of the chloroplast and produces NAPHD, ATP, and O_2, using energy produced by excited electrons and H_2O as a sacrificial electron donor. The energy produced in the light-dependent reaction facilitates the fixation of atmospheric CO_2 and the production of sugars by the light-independent reaction, which is happening in the stroma **(Fig. 14A)**.

Photobiocatalysis is a promising field of renewable and environmentally friendly technologies inspired by plant photosynthesis. This approach aims at the photochemical generation of redox equivalents to promote the activity of redox-active enzymes [156]. Redox enzymes play multiple important roles in Nature [157], such as LPMOs' crucial role in the enzymatic breakdown of lignocellulosic biomass [62,129]. A photobiocatalytic system usually consists of four main elements: an electron donor (or sacrificial molecule), a photoredox catalyst, an electron mediator/cofactor, and a biocatalyst (i.e., redox enzyme) **(Fig. 14B)** [158]. A photoredox catalyst is a single molecule or a complex that can adsorb light and excite an electron from its highest occupied molecular orbital (ground state) to the lowest unoccupied molecular orbital (a high energy state). The photoexcited electron can directly reduce the biocatalyst or indirectly through an electron mediator/cofactor. The presence of an electron donor is crucial for the photoredox catalyst to return to its ground state. Photoredox catalysts naturally adsorb light at specific wavelengths. Thus, selecting the appropriate light wavelength is crucial for successful photobiocatalytic reactions [159].

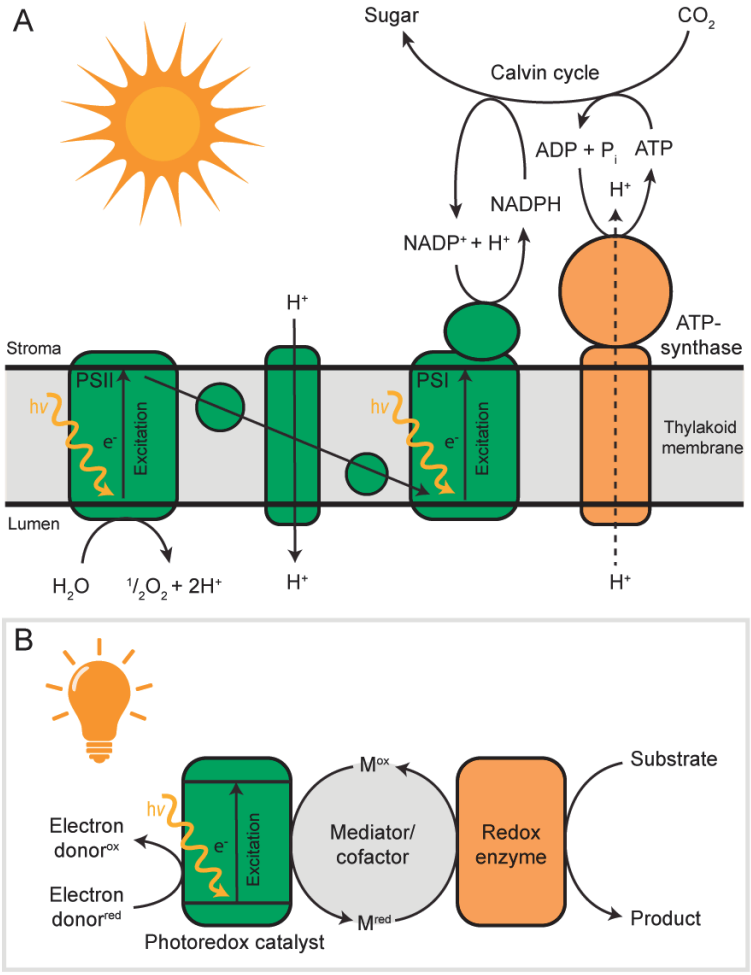

Figure 14. Photobiocatalysis inspired by plant photosynthesis. The figure shows a simplified illustration of photosynthesis in plants **(A)** and an illustration of a photobiocatalytic redox reaction combining photocatalysis and biocatalysis **(B)**.

Harnessing water as a sacrificial electron donor, as demonstrated in plant photosynthesis, poses a challenge because of the stability and low oxidation potential of water. Exposing gold- or vanadium-doped titanium dioxide (Au-TiO_2 or V-TiO_2, respectively) to visible or UV-light combined with a flavin redox mediator, could create the required thermodynamic driving force to oxidize water and sustain the activity of an oxidoreductase [160]. Later, it was demonstrated that visible light-exposed V-TiO_2 could also facilitate LPMO activity (family AA9 and AA10) without any additional reductant or redox mediator [161].

In 2016, Cannella et al. showed that visible light-exposed pigments [thylakoids or chlorophyllin (Chl)], in combination with ascorbic acid, dramatically improved the catalytic activity of an AA9 LPMO on both Avicel and phosphoric acid swollen cellulose [162]. The same study showed that the LPMO activity varied depending on the specific light wavelength. In a follow-up study, the presence of both $O_2^{\bullet-}$ and H_2O_2 in the reactions was observed. However, these two compounds did not seem to promote LPMO activity since reactions with superoxide dismutase (enzyme facilitating the conversion of $O_2^{\bullet-}$ to H_2O_2) or catalase (enzyme facilitating the conversion of H_2O_2 to O_2 and H_2O) did not affect LPMO activity [163].

After the LPMO peroxygenase activity was discovered [94], the study of Cannella et al. [162] was revisited. The new study showed that H_2O_2 was essential to facilitate LPMO activity in the light-exposed Chl-system [98], and that $O_2^{\bullet-}$ was produced and could function as a reductant for the LPMO [98,164], thus eliminating the necessity for an external reductant. It should be mentioned that Bissaro et al. used a higher light intensity and AA10s, while Cannella et al. and Möllers et al. used AA9s and a light source emitting a lower light intensity. Additionally, the required illumination to sustain AA9 activity in a light-exposed Chl-system is highly dependent on the DM content, where illumination of 1 s/min gave the best result at low DM (1 and 2.5%), while at high DM (10 and 15%), constant illumination gave the most LPMO products [165]. Using a photobiocatalytic system offers a new way of controlling enzyme activity through light intensity [98], light wavelength [162], and light exposure time [165]. This approach may help to utilize the full LPMO potential by providing enough H_2O_2 while hindering LPMO inactivation.

1.4.1 Lignin as a photoredox catalyst

Sunlight promotes the microbial decomposition of biomass in Nature. This phenomenon is usually associated with the degradation of lignin induced by light, which enhances the accessibility of polysaccharides [166-169]. Lignin is known to be light-sensitive, and discoloration over time is a direct indication of chemical

modification of lignin when exposed to light. This is typically referred to as a photo-yellowing process, which involves the oxidation of free phenolic groups and hydroquinones [170].

Hydrogen peroxide generation from light-induced oxidation of lignin has recently been demonstrated [171,172]. This may promote the activity of important peroxidases and peroxygenases, offering a new enzymatic rationale for the observed impact of visible light on biomass conversion. It was recently demonstrated that light-exposed kraft lignin and lignosulfonate could be used to facilitate H_2O_2 production and sustain the activity of a true peroxygenase, UPO [171]. Two different mechanisms for light-exposed lignin-induced H_2O_2 production have been proposed. Either a two-electron reduction directly from O_2 to H_2O_2, or a two-step mechanism, starting with a reduction of O_2 to $O_2^{\bullet-}$ followed by the reduction of $O_2^{\bullet-}$ to H_2O_2 [171,172]. The H_2O_2 production may be coupled with autooxidation of lignin or oxidation of sacrificial electron donors [172]. It was recently suggested that the reduction of O_2 to H_2O_2 is accompanied by the oxidation of the Cα-OH moieties of β-O-4 bonds in lignin, forming Cα = O [171]. Overall, this suggests that lignin may be used as a photoredox catalyst to promote H_2O_2 production and increase LPMO activity in aerobic conditions upon light irradiation, which is usually limited by the *in situ* production of H_2O_2 under normal dark conditions.

2 THE PURPOSE AND OUTLINE OF THIS STUDY

Harnessing lignocellulosic biomass as a source of fermentable sugars poses significant challenges due to the recalcitrant structure of the biomass, which makes it hard to degrade enzymatically. The characteristic flat active site of LPMOs allows them to cut directly into crystalline structures found in lignocellulosic biomass, improving the accessibility of polysaccharides for classical hydrolytic enzymes. The work described in this thesis aims to improve the enzymatic degradation efficiency of lignocellulosic biomass by getting a better understanding of the interaction between LPMOs and cellulases **(Papers I, II & IV)** and by obtaining new insights about lignin-catalyzed H_2O_2 production in light-exposed reactions and its effects on LPMO and cellulase activity **(Papers III & IV)**.

In **Paper I**, the effect of LPMO activity on the productive binding capacity of a reducing end cellobiohydrolase (*Tl*CBHI, *Trichoderma longibrachiatum*) on microcrystalline cellulose was investigated by employing online biosensor measurements and sugar analysis. The study employed a sequential experimental procedure, pretreating the substrate with LPMOs before adding *Tl*CBHI and monitoring the effect on initial cellulase activity. The LPMO pretreatment was performed for 5 and 24 h with three different LPMOs (*Sc*AA10C and *Sc*AA10C-N from *S. coelicolor* and *Nc*AA9C from *Neurospora crassa*) or combinations thereof, providing insights into the impact of LPMO regioselectivity and, importantly, the understanding that LPMO cleavage of cellulose does not necessarily affect cellulase activity directly but rather via a non-enzymatic decrystallization of the substrate following the LPMO oxidation.

In **Paper II**, the impact of LPMO regioselectivities on the saccharification efficiency of cellulose at high dry matter concentrations was investigated by using a commercial cellulase cocktail, Celluclast 1.5 L, spiked with a β-glucosidase (NZ-BG) and two different LPMOs; *Ta*AA9A from *Thermoascus aurantiacus* and *Tt*AA9E from *Thermothielavioides* (previously *Thielavia*) *terrestris.* A modern cellulase cocktail, Cellic CTec2, was also employed for comparison. The study provides valuable insights into the effect of combining LPMOs with different regioselectivities and the time and feedstock influence on LPMO-cellulase interactions. Additionally, the study shows the detrimental consequences of LPMO inactivation on cellulase activity.

In **Paper III**, the use of soluble and insoluble lignin as photoredox catalysts to induce *in situ* H_2O_2 production upon light exposure and its impact on cellulose solubilization by LPMOs were investigated. The activity of *Sc*AA10C on microcrystalline cellulose showed a clear dose-response to lignin, substrate, and LPMO concen trations, as well as light intensities. A chitin-active LPMO, *Sm*AA10A from *S. marcescens*, was used to study the reduction kinetics, and NMR was used to study the physical changes in the lignin structure arising from light exposure and LPMO activity. The results showed that light-exposed lignin boosts LPMO activity by reducing O_2 to H_2O_2, most likely via $O_2^{\bullet-}$, and that LPMOs can oxidize lignin to acquire reducing power, but at a much lower rate than light-induced H_2O_2 production.

In **Paper IV**, a combined LPMO-cellulase system similar to **Paper II** was used to study cellulose saccharification in the presence of light-induced H_2O_2 production by lignin. This included investigating the effect of different light wavelengths on H_2O_2 production and enzyme activity. In general, the study shows that light exposure negatively affects glucan conversion by cellulases. However, LPMO activity can counteract this negative effect by consuming H_2O_2 and protecting cellulases from enzyme inactivation.

3 MAIN RESULTS AND DISCUSSION

I Lytic polysaccharide monooxygenase activity increases productive binding capacity of cellobiohydrolases on cellulose

In **Paper I,** the ability of LPMOs to increase the productive binding capacity on microcrystalline cellulose was studied using fungal and bacterial LPMOs with different regioselectivities. Cellobiohydrolases are the workhorses of cellulose depolymerization but rely on auxiliary activities to increase saccharification efficiencies due to their limited activity on crystalline substrates. The novel LPMO activity discovered in 2010 directly targets the crystalline cellulose surface, introducing chain breakage and facilitating cellulase activity by increasing productive binding sites. A productive binding site is a substrate position where the processive cellulase can complex and successfully perform hydrolysis, releasing cellobiose, while productive binding capacity is the total number of accessible binding sites on the substrate.

The sequential reaction setup employed in this study allowed for better insight into the effects of LPMO activity on the cellulose surface and the subsequent impact on cellulase activity. Microcrystalline cellulose (Avicel; 0.5 g/L) was pretreated with *Sc*AA10C, *Sc*AA10C-N, or *Nc*AA9C, or combinations thereof, in the presence of ascorbic acid. After pretreatment, the initial cellobiose release of the reducing end cellulase, *Tl*CBHI, was measured using a biosensor with a CDH working electrode. The productive binding capacity was calculated by ensuring complete saturation of all initially available productive binding sites **(Fig. 1A; Paper I)**.

After 5 h, LPMO activity had no effect or even a slightly negative effect on the productive binding capacity of *Tl*CBHI on insoluble LPMO-pretreated cellulose, except when both *Sc*AA10C and *Nc*AA9C activities were combined (i.e., C1 and C4-active LPMO, respectively). However, after 24 h, all LPMO pretreatment conditions enhanced the productive binding capacity of *Tl*CBHI. No significant variation was observed among the various LPMOs or LPMO combinations after 24 h **(Fig. 1B; Paper I)**. Thus, the LPMO effect on *Tl*CBHI productive binding capacity on cellulose is time-dependent and unaffected by the regioselectivity of the LPMOs when given adequate time.

Analysis of the LPMO-pretreated soluble sugar fractions revealed substantial differences in soluble oxidized and native sugars between the different LPMOs and LPMO combinations. *Sc*AA10C released 20-fold more soluble oxidized sugar than *Sc*AA10C-N after 24 h, only differing in the presence or absence of a CBM, respectively **(Fig. 2A; Paper I)**. LPMOs without CBM will cut more randomly in the cellulose crystal [173], and thus result in lower product solubilization. CBM removal will also weaken the substrate binding, which is crucial for activity and stability toward inactivation, especially at low DM concentrations.

Interestingly, the reaction combining *Sc*AA10C and *Sc*AA10C-N activities was the only reaction with some product formation between 5 and 24 h. For all other reactions, LPMO activity stopped before 5 h **(Figs. 2A & B; Paper I)**. A positive synergistic relationship between *Sc*AA10C and *Sc*AA10C-N has been demonstrated previously and attributed to the increased oxidase activity of the truncated LPMO facilitating *in situ* production of H_2O_2 for the full-length LPMO to perform peroxygenase activity [128].

Reactivation experiments were performed to investigate the stopped LPMO activity. Under stable reaction conditions, levels of ascorbic acid remain constant throughout the reaction. However, in these reactions, all ascorbic acid was consumed within 7 h **(Fig. 4A; Paper I)**. The stopped enzyme activity could only be reactivated by adding more ascorbic acid and fresh LPMO **(Figs. 4B & S4;**

Paper I). The reactivated activity observed upon adding fresh LPMO supports the theory of H_2O_2 accumulation and subsequent generation of transition metal-induced ROS, leading to irreversible inactivation of the LPMOs (see **Section 1.3.3.3.** for more details).

Combining different LPMO regioselectivities released the highest level of soluble oxidized sugars **(Figs. 2A & B; Paper I)** and was the only LPMO pretreatment condition facilitating increased productive binding capacity after 5 h **(Fig. 1B; Paper I)**.The oxidative regioselectivity of the LPMO is usually regarded as a main contributor to the synergistic relationship with cellulases, where reducing end cellulases favors C4-active LPMOs, and C1-active LPMOs are more beneficial for non-reducing end cellulases. The C1-oxidized sugar (aldonic acid) interacts favorably with the CD of reducing end cellulases and may facilitate non-productive binding [148]. However, the results show that both C1- and C4-active LPMOs positively affect the productive binding capacity of a reducing end cellulase. In **Papers II** and **IV**, we will further explore the effects of combining LPMOs with different regioselectivities on cellulase activity.

There was no direct correlation between productive binding capacity and soluble oxidized sugars. Despite the early cessation of LPMO activity and no effect on cellulases after 5 h (except the reaction combining C1 and C4 activity), all LPMOs significantly affected the productive binding capacity after 24 h. This suggests a time-dependent, non-enzymatic decrystallization of the substrate following the LPMO oxidation. The chain breakage will allow more water to penetrate the crystalline structure, facilitating hydrogen bonding with water molecules in the cut site. The increasing solvent accessibility may be more pronounced for C1-active LPMOs because of the open ring structure and the negative surface charge of the carboxyl group of the aldonic acid sugar [149,151]. Thus, even though C1-oxidized sugars can result in non-productive binding with the CD of reducing end cellulases, the positive effect of the amorphization of the substrate facilitating cellulase activity will probably be more significant.

II Enhancing enzymatic saccharification yields of cellulose at high solid loadings by combining different LPMO activities

In **Paper II**, the effect of two fungal LPMOs with different regioselectivities, C1-active and C4-active, *Tt*AA9E and *Ta*AA9A, respectively, together with a commercial cellulase cocktail, Celluclast 1.5 L + NZ-BG, were employed to study LPMOs role in high-solids saccharification of Avicel or steam-exploded wheat straw. The high-solids effect refers to the typical decreasing cellulose degradation yields observed at increasing dry matter loadings, resulting from a complex repertoire of factors that are still not fully understood. Among those factors is water accessibility, which is crucial for enzyme activity and diffusion of products. A key factor for enhanced cellulose degradation efficiencies has been the incorporation of LPMOs into commercial cellulase cocktails [62].

As expected, the cellulose conversion after 24 h dropped significantly (from 45 to 20%) when increasing the DM (from 5 to 25%) and using the cellulase cocktail only **(Fig. 1B; Paper II)**. For similar reactions, including C1- or C4-active LPMOs, the impact of LPMO incorporation ranged from a 30% decrease to a 30% increase in glucose conversion, depending on the DM content. At the highest DM concentration, the inclusion of LPMOs had the biggest impact on glucan conversion. *Ta*AA9A had the biggest effect on the glucan conversion after 5 h, while after 24 h, *Tt*AA9E gave a higher or equal effect **(Fig. 1; Paper II)**. The relative native to oxidized sugar ratio differed after 5 h reaction depending on LPMO and DM, while it was more similar after 24 h for all DM concentrations **(Figs. 2C & D; Paper II).**

The highest DM (25%) was chosen for further experiments with blends of C1- and C4-active LPMOs. After 72 h, all reactions with combined C1 and C4 LPMO activity gave higher saccharification yields than those with only one LPMO. The combination with more *Ta*AA9A than *Tt*AA9E (7:3) gave significantly higher glucan conversion than the reaction with only *Tt*AA9E, while the reaction with

only *Ta*AA9A showed the lowest glucan conversion except from the reaction without LPMO inclusion **(Fig. 3A; Paper II)**. In the reaction with only *Ta*AA9A supplement, no glucan release was observed between 48 and 72 h, and the level of C4-oxidized sugars decreased between 24 and 72 h. C4-oxidized sugars are known to be unstable in systems with high H_2O_2 levels. When LPMOs are inactivated, they release copper into the solution, thereby accelerating the generation of ROS [132,174] (as illustrated in **Fig. 13**), which may also detrimentally affect cellulase activity **(Fig. 5; Paper II).** Interestingly, the reactions with combined C1 and C4 LPMO activity delayed the degradation of C4-oxidized sugars **(Fig. 3C; Paper II)**, suggesting that the C1-active LPMO positively affected the stability of the system.

In an attempt to reduce enzyme inactivation, the LPMO activity was initiated later by adding ascorbic acid after 24 or 48 h. The delayed LPMO activity affected the rate of the reactions, but after 72 h, all reactions reached similar glucan yields **(Fig. 4A; Paper II).** Thus, delayed initiation of LPMO activity was not beneficial. This could be related to the time-dependent decrystallization phase following the LPMO cleavage, as discussed in **Paper I.** The effect of adding ethylenediaminetetraacetic acid (EDTA) to chelate free copper in solution was also probed and showed a slight reduction in oxidized sugar formation although an increased glucan conversion after 48 h **(Fig. 4; Paper II),** which may be a result of a lower level of transition metal-induced side reactions.

The impact of *Ta*AA9A or *Tt*AA9E on the degradation of steam-exploded wheat straw revealed clear differences compared to their effect on Avicel degradation. *Ta*AA9A alone or with *Tt*AA9E gave much higher glucan yields than *Tt*AA9E alone after 72 h, showing that the *Ta*AA9A has a more important role in saccharification of this substrate than Avicel **(Figs. 3A & 7A; Paper II)**. Cellic CTec2 gave significantly higher glucan yields than all LPMO-cellulase combinations. Cellic CTec2 naturally contains LPMOs and has improved hemicellulose activity, especially towards xylan, compared to Celluclast 1.5 L. The wheat straw substrate contains 20% xylan that partly coats the cellulose fibrils **(Table 1; Paper II)**. Thus, the hemicellulase activity of Cellic CTec2 will not

only result in increased xylan conversion **(Fig. 7B; Paper II)** but also help increase the cellulose yields by removing hemicellulose shielding the cellulose.

The result of **Paper II** highlights the importance of customizing the enzyme composition for the specific substrate and maintaining LPMO activity for optimal saccharification efficiency. High DM reactions will hamper the mixing, delay the liquefaction stage, and decrease the available free water at the catalytic site, resulting in reduced enzyme activity. Limited water accessibility will also contribute to diffusion problems, making it physically more challenging for the enzymes to access the substrate and a higher chance of non-productive adsorption and glucose feedback inhibition (also demonstrated in **Fig. 6; Paper II**). Our findings indicate that the beneficial effect of LPMOs becomes more pronounced as the reaction progresses and as the DM concentrations increase. This is not only due to the positive effect of LPMO activity on cellulose depolymerization and water accessibility, but also due to LPMOs' productive turnover of H_2O_2, because free copper in the solution can lead to harmful side reactions with H_2O_2, possibly damaging all enzymes involved.

III Visible light-exposed lignin facilitates cellulose solubilization by lytic polysaccharide monooxygenases

Since LPMO reactions are usually limited by H_2O_2 availability, we investigated the use of lignin as a photoredox catalyst for H_2O_2 production in **Paper III**. In aerobic reactions, H_2O_2 is produced from abiotic reactions between oxygen and reducing compounds such as ascorbic acid or lignin. However, this process is typically slow unless transition metals are present. Lignin is a photosensitive compound recently shown to function as a photoredox catalyst and promote H_2O_2 production upon light exposure [171,172].

First, we probed the ability of light-exposed kraft lignin to facilitate LPMO activity at different lignin and LPMO concentrations using the C1-active *Sc*AA10C and Avicel. Overall, the LPMO activity increased with increasing lignin concentration, both in terms of initial reaction rates and the total amount of oxidized (soluble + insoluble) products obtained after 6 h **(Fig. 1A; Paper III)**. When combining high lignin concentration with high LPMO concentration, no H_2O_2 was detected in the reaction, while in the absence of LPMO or low LPMO concentrations, H_2O_2 accumulated **(Fig. 1B; Paper III).** This demonstrated that H_2O_2 production can be manipulated by lignin concentration and fuel LPMO activity in light-exposed reactions.

Moreover, the dose-response of LPMO, lignin, and Avicel concentration and the effect of light intensity was evaluated. The LPMO activity increased with increasing light intensity and lignin concentration, while increasing Avicel concentrations had a negative effect on the product formation due to attenuation of the light. Thus, high Avicel concentration resulted in lower light intensity and reduced lignin-catalyzed H_2O_2 formation **(Figs. 2B & S3; Paper III)**. Low LPMO concentrations (25 and 50 nM) resulted in fast inactivation **(Fig. 2A; Paper III)**, while the two highest LPMO concentrations (75 and 500 nM) gave similar results

(Fig. 2A; Paper III), demonstrating that H_2O_2 production was the limiting factor for LPMO activity**.**

To better understand the process by which lignin catalyzes LPMO activity upon light irradiation in aerobic reactions, the role of ROS was studied by probing the effect of horseradish peroxidase (HRP) and superoxide dismutase (SOD). HRP removes H_2O_2 from the reaction, while SOD increases the H_2O_2 level by speeding up the conversion of $O_2^{\bullet-}$ to H_2O_2. As expected, HRP reduced the activity while SOD increased the activity, confirming the presence of both H_2O_2 and $O_2^{\bullet-}$ in the reaction **(Figs. 3A & C; Paper III)**. It should be mentioned that $O_2^{\bullet-}$ also can reduce the LPMOs [98,164].

To exclude the presence of small phenolics or transition metals in the commercial kraft lignin preparation as being responsible for LPMO reduction, the difference between native and dialyzed lignin on LPMO activity was investigated using stopped-flow kinetic measurements. Because lignin quenches the fluorescence signal and *Sc*AA10C showed a weak signal, *Sm*AA10A with a stronger fluorescence signal was used. Of note, control experiments demonstrated an increase in *Sm*AA10A activity on chitin in the presence of lignin when exposed to light compared to in the dark **(Fig. S6; Paper III).** The effect of lignin dialysis was minimal for the reduction rate of *Sm*AA10A **(Fig. 4B; Paper III).** Although no reliable data on *Sc*AA10C reduction was obtained, comparing the fluorescence measurements of the two enzymes shows that *Sc*AA10C reduction by lignin is slower than *Sm*AA10A reduction **(Fig. S5; Paper III).** Both native and dialyzed lignin resulted in equal levels of oxidized sugars with *Sc*AA10C after 6 h when exposed to light, while in the dark, the dialyzed lignin showed lower activity than native lignin **(Fig. 4A; Paper III).** This showed that priming reduction is not a rate-limiting step, and the decreased LPMO activity with dialyzed lignin indicates that low molecular weights reductant from the lignin preparation might affect the already low H_2O_2 production in the dark reactions.

In addition to the soluble kraft lignin, insoluble organosolv lignin from spruce and birch was used to investigate light- and LPMO-induced changes in the lignin

structure. Of note, organosolv lignin from spruce and birch showed LPMO activity similar to kraft lignin in light-exposed reactions **(Fig. 5; Paper III).** Overall, the NMR spectra of light-exposed lignin showed a decreased signal for olefins and an increased signal for aldehydes compared to in the dark, which indicates oxidation in the light-exposed lignin structure **(Figs. 6, S7-11; Paper III).** However, it cannot be excluded that light-induced production of ROS is responsible for the changes in the lignin structure. Additionally, we investigated the impact of LPMO activity on the lignin (in the dark). The results showed that LPMO activity can modify the lignin structure, albeit at a much lower rate and in a manner distinct from that of light exposure **(Fig. S11; Paper III).**

It was recently proposed that the H_2O_2 production from light-exposed lignin could use H_2O as a sacrificial electron donor [171], performing the thermodynamically challenging reaction of splitting water. This suggests that lignin-catalyzed H_2O_2 production from light exposure should be able to sustain LPMO activity in anaerobic conditions. However, light-exposed anaerobic LPMO reactions performed with kraft lignin, spruce organosolv lignin, or ascorbic acid all showed equal trace levels of oxidized sugars after 22 h **(Fig. S13; Paper III)**. Control reaction with added H_2O_2 showed higher product formation, indicating that trace amounts of oxygen limited all reactions and that no water oxidation occurred under these conditions. The reactions were performed with $H_2{}^{18}O$ and the control reaction with $H_2{}^{18}O_2$, with the aim of using MS analysis to confirm the absence of water oxidation. Unfortunately, the MALDI-ToF MS analysis was inconclusive due to the very low levels of oxidized sugars and the presence of lignin.

IV Light exposure of lignin increases *in situ* H_2O_2 production and LPMO activity in cellulolytic enzyme cocktails

In **Paper VI**, we investigated glucan conversion by cellulase cocktails supplemented with LPMOs, where LPMO activity was modified through the *in situ* production of H_2O_2 from irradiated lignin. The same LPMOs (*Tt*AA9E and *Ta*AA9A) and cellulase systems (Celluclast 1.5 L + NZ-BG or Cellic CTec2) as **Paper II** were used to degrade a model system of Avicel (10 g/L) and soluble kraft lignin. We demonstrated in **Paper III** that lignin can promote AA9 and AA10 activity by light-induced H_2O_2 production, and we showed in **Papers I** and **II** that LPMO-cellulase interactions are time-, LPMO-, and substrate-dependent. However, the impact of light-exposed lignin on combined LPMO-cellulase activity has not been addressed.

The applied light system in **Paper IV** differed from that in **Paper III.** Multiple LED light sources of significantly lower light intensities than the mercury-xenon lamp (equipped with a filter for 400-700 nm wavelength) used in **Paper III** were applied in **Paper IV**. In **Paper III,** the vials were irradiated from above, while the setup applied in **Paper IV** allowed for complete irradiation of the whole reaction vials and possibly better utilization of the applied light.

First, the effect of light exposure and lignin concentration on the LPMO and cellulase activity was tested. Similar to **Paper III,** the LPMO activity increased under light exposure, but interestingly, light exposure led to decreased glucan conversion **(Fig. 1; Paper IV)**. The glucan conversion also decreased in the absence of lignin, although control experiments showed that light pretreatment of the cellulase cocktail did not negatively affect the glucan conversion **(Fig. S3; Paper IV).** Generally, the highest glucan yields were found in the reactions performed in the dark.

Exposure to light of varying wavelengths revealed a distinct relationship: shorter wavelengths resulted in reduced saccharification yields and enhanced LPMO effects **(Figs. 2A-D; Paper IV)**. For instance, in the reaction exposed to 365 nm, glucose release increased by 61% when LPMOs were included, compared to only 6% increase from LPMO inclusion for a similar reaction performed in the dark. Despite the positive LPMO effect, the glucose yield after 24 h in the dark was 100% higher than for the reaction exposed to 365 nm.

A direct effect of light intensity (white light; 400 to 700 nm) on LPMO activity was shown in **Paper III (Fig. 1B).** The adsorption spectra of kraft lignin show strong adsorption between 250 and 400 nm and significantly weaker adsorption between 400 and 700 nm **(Fig. S4; Paper IV).** With the adsorption spectra of lignin in mind, the effect of light wavelength on lignin-induced H_2O_2 production was investigated. **Fig. 2F (Paper IV)** shows a clear correlation between wavelength and H_2O_2 production, where the shorter wavelengths increased the *in situ* H_2O_2 production from lignin. The wavelength effect can also be seen reflected in the initial production of oxidized sugars **(Fig. 2D; Paper IV),** confirming the H_2O_2 dependency of the system and that H_2O_2 is the factor limiting the LPMO activity.

The effect of light-exposed lignin on Avicel degradation with Cellic CTec2 showed slightly higher glucan conversion (approximately 10 to 30% after 24 h) as compared to the reactions with Celluclast 1.5 L + NZ-BG + *Ta*AA9A **(Figs. 1C-D & 4A; Paper IV).** When exposed to light, both enzyme cocktails showed similar levels of oxidized sugars, where the amount of oxidized sugars increased up to 0.3 g/L lignin after 24 h, while the level decreased at the higher lignin concentrations. In contrast, Cellic CTec2 showed lower oxidized sugar levels in the dark than the *Ta*AA9A spiked Celluclast 1.5 L cocktail **(Figs. 1G-H & 4B; Paper IV).**

As discussed in **Paper II,** LPMO inactivation will promote ROS production and cellulase inactivation. Decreasing levels of C4-oxidized sugars serve as an indirect indication of accumulating H_2O_2 levels and LPMO inactivation **(Fig. 3;**

Paper IV). The increased glucose conversion of the light-exposed reactions in the presence of LPMO is likely due to LPMO's H_2O_2 consumption during cellulose cleavage, which limits ROS production and protects the cellulases. However, LPMO inactivation and copper release will increase ROS production, demonstrating the importance of avoiding LPMO inactivation.

The light exposure effect at higher DM (50 g/L) was also probed, showing a negative effect from the LPMOs at the earlier time points but a positive effect on the glucan conversion after 24 h **(Fig. 5; Paper IV).** Contrary to the lower DM concentration reaction, the LPMO effect did not seem light-dependent. High DM concentrations generally have a negative effect on the saccharification yields (as discussed in **Paper II**) and may also decrease the LPMO activity due to attenuation of the light photons, lowering the *in situ* H_2O_2 production from lignin, as shown in **Paper III (Figs. 2B & S3).** The impact of LPMOs on glucan conversion was thus less pronounced at the higher DM reaction because of the lower lignin-induced H_2O_2 production.

The study showed that combining light and lignin suppress cellulase activity. Moreover, the presence of LPMOs is important to counteract the negative effect of light-exposed lignin, not only because of increased oxidative cleavage of cellulose, but also because the LPMO consumes H_2O_2 that otherwise could harm the cellulolytic enzymes. The study further emphasizes the importance of considering abiotic factors such as light exposure when planning and conducting enzymatic hydrolysis of lignin-containing substrates.

4 CONCLUDING REMARKS AND FUTURE PERSPECTIVES

The thesis comprises four Papers that provide new insights into the LPMO-cellulase interactions and the importance of controlling H_2O_2 levels for better utilization of the LPMOs and preventing enzyme inactivation. Lignocellulosic biomass has a big potential as feedstock for the production of biofuels and value-added chemicals, but to date, enzymatic saccharification is still considered a major bottleneck. Although it is clear that both LPMOs and cellulases are needed to facilitate efficient conversion of this renewable and ubiquitous material, further optimization and insights into their interplay are needed.

LPMOs are particularly effective at breaking down crystalline materials and enhancing the efficient utilization of recalcitrant materials by classical hydrolytic enzymes. This synergistic action becomes increasingly valuable as the hydrolysis reaction progresses and the substrate becomes more challenging to degrade. The delayed LPMO effect shown in **Paper I** suggests that the enhanced productive binding capacity on LPMO-pretreated cellulose for cellulases is not directly linked to cellulose chain cleavage by LPMOs. This was likely a result of a non-enzymatic decrystallization phase following the LPMO oxidative cleavage, resulting in enhanced water accessibility and overall amorphization of the crystalline substrate, which is crucial for the subsequent cellulase activity. A time-dependent LPMO effect was also visible when spiking a cellulase cocktail with LPMOs, especially at high dry matter loading **(Paper II).**

Degradation of soluble C4-oxidized sugars late in enzyme reactions is a commonly observed phenomenon and can be used as an indicator of unstable reaction conditions, as shown in **Papers II and IV**. Recently, it was shown that the active-site copper of LPMOs may leak into the solution when the LPMOs are

inactivated. Free copper in solution will promote transition metal-induced reactions producing ROS, resulting in both degradation of C4-oxidized sugars and cellulase inactivation. An increased saccharification efficiency of microcrystalline cellulose and an apparent delay in the degradation of C4-oxidized sugars were seen when combining C1 and C4 LPMO activity **(Paper II).** The inclusion of C1-active LPMOs was clearly beneficial in this case. However, for a different substrate, pretreated wheat straw, the inclusion of only C4-active LPMOs worked very well, showing the importance of tailoring the enzyme composition to the specific feedstock to hinder enzyme inactivation and achieve high saccharification yields.

LPMO activity can be manipulated by utilizing light-exposed lignin to facilitate *in situ* H_2O_2 production, as demonstrated in **Papers III and IV**. However, careful control is essential to avoid triggering ROS production and enzyme inactivation. **Paper III** showed that light exposure and LPMO activity resulted in distinct changes in the lignin structure, and that H_2O_2 was produced by the reduction of O_2 in light-exposed reactions. Light exposure might negatively affect the overall efficiency of cellulolytic enzyme cocktails acting on lignin-containing cellulosic materials by inducing excessive H_2O_2 production **(Paper IV)**. Our findings indicate that LPMOs not only aid in cellulose cleavage but also mitigate the accumulation of H_2O_2, which could otherwise harm cellulases. These studies highlight the importance of considering light exposure when employing enzymatic saccharification of lignocellulosic biomass, especially in applied settings using cellulase enzyme cocktails.

Based on the result of this thesis, the following is suggested for future work in this field. For further insights into the time-dependent LPMO effect on the productive binding capacity of cellulases, a detailed kinetic study of LPMO-pretreated substrates should be performed. Although LPMO activity can be manipulated by light-exposed lignin, intermittent light exposure should be investigated as a strategy to boost LPMO activity without producing too much H_2O_2 to avoid ROS production and enzyme inactivation. Moreover, scavenging free copper during enzyme reactions, such as using EDTA or including apo-

LPMOs, should clearly be investigated as strategies to avoid enzyme inactivation. Working with undefined cellulase formulations complicates the interpretations of data, and to further understand the effect of different LPMO regioselectivities and LPMO combinations, studies using purified and known cellulases are needed. For downstream applications of lignocellulosic sugars, it should be mentioned that oxidized sugars are not easily fermented by microbes such as yeast. Thus, the main goal of applying LPMO activity is to alter the cellulose substrate physically to promote cellulase activity rather than producing high levels of oxidized sugars.

5 REFERENCES

1. Bolin B. (1970). The carbon cycle. *Sci Am*. **223**, 124-35.
2. Lüthi D, Le Floch M, Bereiter B, Blunier T, Barnola J-M, Siegenthaler U, Raynaud D, Jouzel J, Fischer H & Kawamura K. (2008). High-resolution carbon dioxide concentration record 650,000–800,000 years before present. *Nature*. **453**, 379-82.
3. NOAA. (2024). *Trends in Atmospheric Carbon Dioxide*. Available at: https://gml.noaa.gov/ccgg/trends/gl_trend.html (accessed: 07.03.24).
4. IPCC. (2018). Special Report on Global Warming of 1.5°C.
5. NOAA. (2021). *Climate change impacts*. Available at: https://www.noaa.gov/education/resource-collections/climate/climate-change-impacts (accessed: 07.03.24).
6. Kirtman B, Power SB, Adedoyin AJ, Boer GJ, Bojariu R, Camilloni I, Doblas-Reyes F, Fiore AM, Kimoto M & Meehl G. (2013). Near-term climate change: projections and predictability. Stocker T, Qin D, Plattner G, Tignor M, Allen S, Boschung J, et al. (eds) *Climate Change 2013: The Physical Science Basis*, pp. 953-1028: Cambridge Univ. Press.
7. UNFCCC. *The Paris Agreement. What is the Paris Agreement?* Available at: https://unfccc.int/process-and-meetings/the-paris-agreement (accessed: 07.03.24).
8. UNFCCC. (2021). *A Beginner's Guide to Climate Neutrality*. Available at: https://unfccc.int/news/a-beginner-s-guide-to-climate-neutrality (accessed: 06.03.24).
9. Bui M, Adjiman CS, Bardow A, Anthony EJ, Boston A, Brown S, Fennell PS, Fuss S, Galindo A & Hackett LA. (2018). Carbon capture and storage (CCS): the way forward. *Energy Environ Sci*. **11**, 1062-176.
10. IPCC. (2023). AR6 Synthesis Report on Climate Change 2023
11. Regjeringen. (2021). National Transport Plan 2022–2033.
12. IEA. (2019). *How competitive is biofuel production in Brazil and the United States?* Available at: https://www.iea.org/articles/how-competitive-is-biofuel-production-in-brazil-and-the-united-states (accessed: 19.02.24).
13. Naik SN, Goud VV, Rout PK & Dalai AK. (2010). Production of first and second generation biofuels: a comprehensive review. *Renew Sustain Energy Rev*. **14**, 578-97.
14. Balat M. (2011). Production of bioethanol from lignocellulosic materials via the biochemical pathway: a review. *Energy Convers Manag*. **52**, 858-75.
15. Banu JR, Kavitha S, Gunasekaran M & Kumar G. (2020). Microalgae based biorefinery promoting circular bioeconomy-techno economic and life-cycle analysis. *Bioresour Technol*. **302**, 122822.

16. Abdullah B, Muhammad SAFaS, Shokravi Z, Ismail S, Kassim KA, Mahmood AN & Aziz MMA. (2019). Fourth generation biofuel: A review on risks and mitigation strategies. *Renew Sustain Energy Rev*. **107**, 37-50.
17. d'Amore F, Nava A, Colbertaldo P, Visconti CG & Romano MC. (2023). Turning CO_2 from fuel combustion into e-Fuel? Consider alternative pathways. *Energy Convers Manag*. **289**, 117170.
18. Molino A, Chianese S & Musmarra D. (2016). Biomass gasification technology: The state of the art overview. *J Energy Chem*. **25**, 10-25.
19. Gollakota A, Kishore N & Gu S. (2018). A review on hydrothermal liquefaction of biomass. *Renew Sustain Energy Rev*. **81**, 1378-92.
20. Straathof AJ. (2014). Transformation of biomass into commodity chemicals using enzymes or cells. *Chem Rev*. **114**, 1871-908.
21. Li C, Aston JE, Lacey JA, Thompson VS & Thompson DN. (2016). Impact of feedstock quality and variation on biochemical and thermochemical conversion. *Renew Sustain Energy Rev*. **65**, 525-36.
22. Yu IK, Chen H, Abeln F, Auta H, Fan J, Budarin VL, Clark JH, Parsons S, Chuck CJ & Zhang S. (2021). Chemicals from lignocellulosic biomass: a critical comparison between biochemical, microwave and thermochemical conversion methods. *Crit Rev Environ Sci Technol*. **51**, 1479-532.
23. Wood TM. (1985). Properties of cellulolytic enzyme systems. *Biochem Soc Trans*. 407-10.
24. Kittler B, Stupak I & Smith CT. (2020). Assessing the wood sourcing practices of the US industrial wood pellet industry supplying European energy demand. *Energ Sustain Soc*. **10**, 23.
25. Valdivia M, Galan JL, Laffarga J & Ramos JL. (2016). Biofuels 2020: biorefineries based on lignocellulosic materials. *Microb Biotechnol*. **9**, 585-94.
26. Mizik T & Gyarmati G. (2021). Economic and sustainability of biodiesel production—a systematic literature review. *Clean Technologies*. **3**, 19-36.
27. Correa C, Alves YA, Souza CG & Boloy RAM. (2023). Brazil and the world market in the development of technologies for the production of second-generation ethanol. *Alex Eng J*. **67**, 153-70.
28. Stegmann P, Londo M & Junginger M. (2020). The circular bioeconomy: Its elements and role in European bioeconomy clusters. *Resour Conserv Recycl: X*. **6**, 100029.
29. Eggers J, Melin Y, Lundström J, Bergström D & Öhman K. (2020). Management strategies for wood fuel harvesting—Trade-offs with biodiversity and forest ecosystem services. *Sustainability*. **12**, 4089.
30. Pauly M & Keegstra K. (2008). Cell-wall carbohydrates and their modification as a resource for biofuels. *Plant J*. **54**, 559-68.
31. Bar-On YM, Phillips R & Milo R. (2018). The biomass distribution on Earth. *Proc Natl Acad Sci*. **115**, 6506-11.
32. Isikgor FH & Becer CR. (2015). Lignocellulosic biomass: a sustainable platform for the production of bio-based chemicals and polymers. *Polym Chem*. **6**, 4497-559.

33. Showalter AM. (1993). Structure and function of plant cell wall proteins. *Plant Cell*. **5**, 9-23.
34. Zoghlami A & Paës G. (2019). Lignocellulosic biomass: understanding recalcitrance and predicting hydrolysis. *Front Chem*. **7**, 874.
35. Jensen CU, Rodriguez Guerrero JK, Karatzos S, Olofsson G & Iversen SB. (2017). Fundamentals of Hydrofaction™: Renewable crude oil from woody biomass. *Biomass Conv Bioref*. **7**, 495-509.
36. Solomon BD, Barnes JR & Halvorsen KE. (2007). Grain and cellulosic ethanol: History, economics, and energy policy. *Biomass Bioenergy*. **31**, 416-25.
37. Klemm D, Heublein B, Fink HP & Bohn A. (2005). Cellulose: fascinating biopolymer and sustainable raw material. *Angew Chem Int Ed*. **44**, 3358-93.
38. Himmel ME, Ding S-Y, Johnson DK, Adney WS, Nimlos MR, Brady JW & Foust TD. (2007). Biomass recalcitrance: engineering plants and enzymes for biofuels production. *Science*. **315**, 804-7.
39. Gardner K & Blackwell J. (1974). The structure of native cellulose. *Biopolymers*. **13**, 1975-2001.
40. Béguin P & Aubert J-P. (1994). The biological degradation of cellulose. *FEMS Microbiol Rev*. **13**, 25-58.
41. Silveira RL, Stoyanov SR, Gusarov S, Skaf MS & Kovalenko A. (2013). Plant biomass recalcitrance: effect of hemicellulose composition on nanoscale forces that control cell wall strength. *J Am Chem Soc*. **135**, 19048-51.
42. Scheller HV & Ulvskov P. (2010). Hemicelluloses. *Annu Rev Plant Biol*. **61**, 263-89.
43. McMillan JD. (1994). Pretreatment of lignocellulosic biomass. *ACS Symposium Series*. 292-324.
44. Puls J. (1997). Chemistry and biochemistry of hemicelluloses: Relationship between hemicellulose structure and enzymes required for hydrolysis. *Macromol Symp*. **120**, 183-96.
45. Chen F & Dixon RA. (2007). Lignin modification improves fermentable sugar yields for biofuel production. *Nat Biotechnol*. **25**, 759-61.
46. Wang H, Pu Y, Ragauskas A & Yang B. (2019). From lignin to valuable products–strategies, challenges, and prospects. *Bioresour Technol*. **271**, 449-61.
47. Morena AG & Tzanov T. (2022). Antibacterial lignin-based nanoparticles and their use in composite materials. *Nanoscale Adv*. **4**, 4447-69.
48. Kamm B & Kamm M. (2004). Principles of biorefineries. *Appl Microbiol Biotechnol*. **64**, 137-45.
49. Stöcker M. (2008). Biofuels and biomass-to-liquid fuels in the biorefinery: Catalytic conversion of lignocellulosic biomass using porous materials. *Angew Chem Int Ed*. **47**, 9200-11.
50. Chundawat SP, Beckham GT, Himmel ME & Dale BE. (2011). Deconstruction of lignocellulosic biomass to fuels and chemicals. *Annu Rev Chem Biomol Eng*. **2**, 121-45.
51. Stone J, Scallan A, Donefer E & Ahlgren E. (1969). Digestibility as a simple function of a molecule of similar size to a cellulase enzyme. *Advances in Chemistry*. 219-41.

52. Haviland ZK, Nong D, Zexer N, Tien M, Anderson CT & Hancock WO. (2024). Lignin impairs Cel7A degradation of in vitro lignified cellulose by impeding enzyme movement and not by acting as a sink. *Biotechnol Biofuels*. **17**, 7.
53. Kont R, Pihlajaniemi V, Borisova AS, Aro N, Marjamaa K, Loogen J, Büchs J, Eijsink VG, Kruus K & Väljamäe P. (2019). The liquid fraction from hydrothermal pretreatment of wheat straw provides lytic polysaccharide monooxygenases with both electrons and H 2 O 2 co-substrate. *Biotechnol Biofuels*. **12**, 1-15.
54. Jørgensen H, Kristensen JB & Felby C. (2007). Enzymatic conversion of lignocellulose into fermentable sugars: challenges and opportunities. *Biofuels Bioprod Biorefin*. **1**, 119-34.
55. Jaiswal A, Bhattacharya R, Srivastava S, Singh A & Bose D. (2024). Bioethanol Production and Its Impact on a Future Bioeconomy. *Clean and Renewable Energy Production*. 375-411.
56. Olsson L & Hahn-Hägerdal B. (1993). Fermentative performance of bacteria and yeasts in lignocellulose hydrolysates. *Process Biochem*. **28**, 249-57.
57. Novy V, Krahulec S, Longus K, Klimacek M & Nidetzky B. (2013). Co-fermentation of hexose and pentose sugars in a spent sulfite liquor matrix with genetically modified *Saccharomyces cerevisiae*. *Bioresour Technol*. **130**, 439-48.
58. Viikari L, Vehmaanperä J & Koivula A. (2012). Lignocellulosic ethanol: from science to industry. *Biomass Bioenergy*. **46**, 13-24.
59. Cragg SM, Beckham GT, Bruce NC, Bugg TD, Distel DL, Dupree P, Etxabe AG, Goodell BS, Jellison J & McGeehan JE. (2015). Lignocellulose degradation mechanisms across the Tree of Life. *Curr Opin Chem Biol*. **29**, 108-19.
60. Østby H, Hansen LD, Horn SJ, Eijsink VG & Várnai A. (2020). Enzymatic processing of lignocellulosic biomass: principles, recent advances and perspectives. *J Ind Microbiol Biotechnol*. **47**, 623-57.
61. Arantes V & Saddler JN. (2010). Access to cellulose limits the efficiency of enzymatic hydrolysis: the role of amorphogenesis. *Biotechnol Biofuels*. **3**, 4.
62. Johansen KS. (2016). Discovery and industrial applications of lytic polysaccharide mono-oxygenases. *Biochem Soc Trans*. **44**, 143-9.
63. Mudinoor AR, Goodwin PM, Rao RU, Karuna N, Hitomi A, Nill J & Jeoh T. (2020). Interfacial molecular interactions of cellobiohydrolase Cel7A and its variants on cellulose. *Biotechnol Biofuels*. **13**, 10.
64. Igarashi K, Koivula A, Wada M, Kimura S, Penttilä M & Samejima M. (2009). High speed atomic force microscopy visualizes processive movement of *Trichoderma reesei* cellobiohydrolase I on crystalline cellulose. *J Biol Chem*. **284**, 36186-90.
65. Juturu V & Wu JC. (2014). Microbial cellulases: Engineering, production and applications. *Renew Sustain Energy Rev*. **33**, 188-203.
66. Teugjas H & Väljamäe P. (2013). Product inhibition of cellulases studied with ^{14}C-labeled cellulose substrates. *Biotechnol Biofuels*. **6**, 104.

67. Kipper K, Väljamäe P & Johansson G. (2005). Processive action of cellobiohydrolase Cel7A from *Trichoderma reesei* is revealed as 'burst' kinetics on fluorescent polymeric model substrates. *Biochem J*. **385**, 527-35.
68. Praestgaard E, Elmerdahl J, Murphy L, Nymand S, McFarland KC, Borch K & Westh P. (2011). A kinetic model for the burst phase of processive cellulases. *FEBS J*. **278**, 1547-60.
69. Väljamäe P, Sild V, Pettersson G & Johansson G. (1998). The initial kinetics of hydrolysis by cellobiohydrolases I and II is consistent with a cellulose surface - erosion model. *Eur J Biochem*. **253**, 469-75.
70. Nill JD & Jeoh T. (2020). The role of evolving interfacial substrate properties on heterogeneous cellulose hydrolysis kinetics. *ACS Sustain Chem Eng*. **8**, 6722-33.
71. Malgas S, Mafa MS, Mkabayi L & Pletschke BI. (2019). A mini review of xylanolytic enzymes with regards to their synergistic interactions during hetero-xylan degradation. *World J Microbiol Biotechnol*. **35**, 187.
72. Malgas S, van Dyk JS & Pletschke BI. (2015). A review of the enzymatic hydrolysis of mannans and synergistic interactions between β-mannanase, β-mannosidase and α-galactosidase. *World J Microbiol Biotechnol*. **31**, 1167-75.
73. Reese ET, Siu RG & Levinson HS. (1950). The biological degradation of soluble cellulose derivatives and its relationship to the mechanism of cellulose hydrolysis. *J Bacteriol*. **59**, 485-97.
74. Eriksson K-E, Pettersson B & Westermark U. (1974). Oxidation: an important enzyme reaction in fungal degradation of cellulose. *FEBS Lett*. **49**, 282-5.
75. Vaaje-Kolstad G, Horn SJ, van Aalten DM, Synstad B & Eijsink VG. (2005). The non-catalytic chitin-binding protein CBP21 from *Serratia marcescens* is essential for chitin degradation. *J Biol Chem*. **280**, 28492-7.
76. Vaaje-Kolstad G, Westereng B, Horn SJ, Liu Z, Zhai H, Sorlie M & Eijsink VG. (2010). An oxidative enzyme boosting the enzymatic conversion of recalcitrant polysaccharides. *Science*. **330**, 219-22.
77. Forsberg Z, Vaaje-Kolstad G, Westereng B, Bunaes AC, Stenstrom Y, MacKenzie A, Sorlie M, Horn SJ & Eijsink VG. (2011). Cleavage of cellulose by a CBM33 protein. *Protein Sci*. **20**, 1479-83.
78. Quinlan RJ, Sweeney MD, Lo Leggio L, Otten H, Poulsen JCN, Johansen KS, Krogh KBRM, Jorgensen CI, Tovborg M, Anthonsen A, Tryfona T, Walter CP, Dupree P, Xu F, Davies GJ & Walton PH. (2011). Insights into the oxidative degradation of cellulose by a copper metalloenzyme that exploits biomass components. *Proc Natl Acad Sci*. **108**, 15079-84.
79. Harris PV, Welner D, McFarland K, Re E, Navarro Poulsen J-C, Brown K, Salbo R, Ding H, Vlasenko E & Merino S. (2010). Stimulation of lignocellulosic biomass hydrolysis by proteins of glycoside hydrolase family 61: structure and function of a large, enigmatic family. *Biochemistry*. **49**, 3305-16.

80. Agger JW, Isaksen T, Varnai A, Vidal-Melgosa S, Willats WGT, Ludwig R, Horn SJ, Eijsink VGH & Westereng B. (2014). Discovery of LPMO activity on hemicelluloses shows the importance of oxidative processes in plant cell wall degradation. *Proc Natl Acad Sci*. **111**, 6287-92.
81. Vu VV, Beeson WT, Span EA, Farquhar ER & Marletta MA. (2014). A family of starch-active polysaccharide monooxygenases. *Proc Natl Acad Sci*. **111**, 13822-7.
82. Sabbadin F, Urresti S, Henrissat B, Avrova AO, Welsh LRJ, Lindley PJ, Csukai M, Squires JN, Walton PH, Davies GJ, Bruce NC, Whisson SC & McQueen-Mason SJ. (2021). Secreted pectin monooxygenases drive plant infection by pathogenic oomycetes. *Science*. **373**, 774-9.
83. Martinez-D'Alto A, Yan X, Detomasi TC, Sayler RI, Thomas WC, Talbot NJ & Marletta MA. (2023). Characterization of a unique polysaccharide monooxygenase from the plant pathogen *Magnaporthe oryzae*. *Proc Natl Acad Sci*. **120**, e2215426120.
84. Horn SJ, Vaaje-Kolstad G, Westereng B & Eijsink VG. (2012). Novel enzymes for the degradation of cellulose. *Biotechnol Biofuels*. **5**, 45.
85. Levasseur A, Drula E, Lombard V, Coutinho PM & Henrissat B. (2013). Expansion of the enzymatic repertoire of the CAZy database to integrate auxiliary redox enzymes. *Biotechnol Biofuels*. **6**, 41.
86. CAZy-database. *Auxiliary Activities family classification*. Available at: http://www.cazy.org/Auxiliary-Activities.html (accessed: 18.03.24).
87. Mutahir Z, Mekasha S, Loose JS, Abbas F, Vaaje-Kolstad G, Eijsink VG & Forsberg Z. (2018). Characterization and synergistic action of a tetra-modular lytic polysaccharide monooxygenase from *Bacillus cereus*. *FEBS Lett*. **592**, 2562-71.
88. Forsberg Z, Mackenzie AK, Sorlie M, Rohr AK, Helland R, Arvai AS, Vaaje-Kolstad G & Eijsink VG. (2014). Structural and functional characterization of a conserved pair of bacterial cellulose-oxidizing lytic polysaccharide monooxygenases. *Proc Natl Acad Sci*. **111**, 8446-51.
89. Courtade G, Forsberg Z, Heggset EB, Eijsink VGH & Aachmann FL. (2018). The carbohydrate-binding module and linker of a modular lytic polysaccharide monooxygenase promote localized cellulose oxidation. *J Biol Chem*. **293**, 13006-15.
90. Sulaeva I, Budischowsky D, Rahikainen J, Marjamaa K, Støpamo FG, Khaliliyan H, Melikhov I, Rosenau T, Kruus K & Várnai A. (2024). A novel approach to analyze the impact of lytic polysaccharide monooxygenases (LPMOs) on cellulosic fibres. *Carbohydr Polym*. **328**, 121696.
91. Phillips CM, Beeson IV WT, Cate JH & Marletta MA. (2011). Cellobiose dehydrogenase and a copper-dependent polysaccharide monooxygenase potentiate cellulose degradation by *Neurospora crassa*. *ACS Chem Biol*. **6**, 1399-406.
92. Hall KR, Joseph C, Ayuso-Fernández I, Tamhankar A, Rieder L, Skaali R, Golten O, Neese F, Røhr ÅK & Jannuzzi SA. (2023). A conserved second sphere residue tunes copper site reactivity in lytic polysaccharide monooxygenases. *J Am Chem Soc*. **145**, 18888-903.
93. Tandrup T, Frandsen KE, Johansen KS, Berrin J-G & Lo Leggio L. (2018). Recent insights into lytic polysaccharide monooxygenases (LPMOs). *Biochem Soc Trans*. **46**, 1431-47.

94. Bissaro B, Rohr AK, Muller G, Chylenski P, Skaugen M, Forsberg Z, Horn SJ, Vaaje-Kolstad G & Eijsink VGH. (2017). Oxidative cleavage of polysaccharides by monocopper enzymes depends on H_2O_2. *Nat Chem Biol*. **13**, 1123-8.
95. Bissaro B, Røhr ÅK, Skaugen M, Forsberg Z, Horn SJ, Vaaje-Kolstad G & Eijsink VG. (2016). Fenton-type chemistry by a copper enzyme: molecular mechanism of polysaccharide oxidative cleavage. *bioRxiv*. 097022.
96. Chang H, Gacias Amengual N, Botz A, Schwaiger L, Kracher D, Scheiblbrandner S, Csarman F & Ludwig R. (2022). Investigating lytic polysaccharide monooxygenase-assisted wood cell wall degradation with microsensors. *Nat Commun*. **13**, 6258.
97. Holtmann D & Hollmann F. (2016). The oxygen dilemma: a severe challenge for the application of monooxygenases? *ChemBioChem*. **17**, 1391-8.
98. Bissaro B, Kommedal E, Røhr ÅK & Eijsink VG. (2020). Controlled depolymerization of cellulose by light-driven lytic polysaccharide oxygenases. *Nat Commun*. **11**, 890.
99. Kuusk S, Bissaro B, Kuusk P, Forsberg Z, Eijsink VG, Sørlie M & Väljamäe P. (2018). Kinetics of H_2O_2-driven degradation of chitin by a bacterial lytic polysaccharide monooxygenase. *J Biol Chem*. **293**, 523-31.
100. Kont R, Bissaro B, Eijsink VG & Väljamäe P. (2020). Kinetic insights into the peroxygenase activity of cellulose-active lytic polysaccharide monooxygenases (LPMOs). *Nat Commun*. **11**, 5786.
101. Munzone A, Eijsink VG, Berrin J-G & Bissaro B. (2024). Expanding the catalytic landscape of metalloenzymes with lytic polysaccharide monooxygenases. *Nat Rev Chem*. **8**, 106-19.
102. Kracher D, Scheiblbrandner S, Felice AK, Breslmayr E, Preims M, Ludwicka K, Haltrich D, Eijsink VG & Ludwig R. (2016). Extracellular electron transfer systems fuel cellulose oxidative degradation. *Science*. **352**, 1098-101.
103. Frommhagen M, Westphal AH, van Berkel WJ & Kabel MA. (2018). Distinct substrate specificities and electron-donating systems of fungal lytic polysaccharide monooxygenases. *Front Microbiol*. **9**, 358610.
104. Frommhagen M, Koetsier MJ, Westphal AH, Visser J, Hinz SW, Vincken J-P, Van Berkel WJ, Kabel MA & Gruppen H. (2016). Lytic polysaccharide monooxygenases from *Myceliophthora thermophila* C1 differ in substrate preference and reducing agent specificity. *Biotechnol Biofuels*. **9**, 186.
105. Lo Leggio L, Simmons TJ, Poulsen J-CN, Frandsen KE, Hemsworth GR, Stringer MA, Von Freiesleben P, Tovborg M, Johansen KS & De Maria L. (2015). Structure and boosting activity of a starch-degrading lytic polysaccharide monooxygenase. *Nat Commun*. **6**, 5961.
106. Cannella D, Hsieh CWC, Felby C & Jorgensen H. (2012). Production and effect of aldonic acids during enzymatic hydrolysis of lignocellulose at high dry matter content. *Biotechnol Biofuels*. **5**, 26.

107. Westereng B, Cannella D, Wittrup Agger J, Jørgensen H, Larsen Andersen M, Eijsink VG & Felby C. (2015). Enzymatic cellulose oxidation is linked to lignin by long-range electron transfer. *Sci Rep*. **5**, 18561.
108. Golten O, Ayuso-Fernández I, Hall KR, Stepnov AA, Sørlie M, Røhr ÅK & Eijsink VG. (2023). Reductants fuel lytic polysaccharide monooxygenase activity in a pH-dependent manner. *FEBS Lett*. **597**, 1363-74.
109. Hedegård ED & Ryde U. (2017). Targeting the reactive intermediate in polysaccharide monooxygenases. *J Biol Inorg Chem*. **22**, 1029-37.
110. Bissaro B, Streit B, Isaksen I, Eijsink VG, Beckham GT, DuBois JL & Røhr ÅK. (2020). Molecular mechanism of the chitinolytic peroxygenase reaction. *Proc Natl Acad Sci*. **117**, 1504-13.
111. Wang B, Johnston EM, Li P, Shaik S, Davies GJ, Walton PH & Rovira C. (2018). QM/MM studies into the H_2O_2-dependent activity of lytic polysaccharide monooxygenases: evidence for the formation of a caged hydroxyl radical intermediate. *ACS Catal*. **8**, 1346-51.
112. Hedegård ED & Ryde U. (2018). Molecular mechanism of lytic polysaccharide monooxygenases. *Chem Sci*. **9**, 3866-80.
113. Kim S, Ståhlberg J, Sandgren M, Paton RS & Beckham GT. (2014). Quantum mechanical calculations suggest that lytic polysaccharide monooxygenases use a copper-oxyl, oxygen-rebound mechanism. *Proc Natl Acad Sci*. **111**, 149-54.
114. Wang B, Wang Z, Davies GJ, Walton PH & Rovira C. (2020). Activation of O_2 and H_2O_2 by lytic polysaccharide monooxygenases. *ACS Catal*. **10**, 12760-9.
115. Beeson WT, Phillips CM, Cate JH & Marletta MA. (2012). Oxidative cleavage of cellulose by fungal copper-dependent polysaccharide monooxygenases. *J Am Chem Soc*. **134**, 890-2.
116. Beeson WT, Vu VV, Span EA, Phillips CM & Marletta MA. (2015). Cellulose degradation by polysaccharide monooxygenases. *Annu Rev Biochem*. **84**, 923-46.
117. Walton PH & Davies GJ. (2016). On the catalytic mechanisms of lytic polysaccharide monooxygenases. *Curr Opin Chem Biol*. **31**, 195-207.
118. Kjaergaard CH, Qayyum MF, Wong SD, Xu F, Hemsworth GR, Walton DJ, Young NA, Davies GJ, Walton PH & Johansen KS. (2014). Spectroscopic and computational insight into the activation of O_2 by the mononuclear Cu center in polysaccharide monooxygenases. *Proc Natl Acad Sci*. **111**, 8797-802.
119. Keller MB, Badino SF, Blossom BMl, McBrayer B, Borch K & Westh P. (2020). Promoting and impeding effects of lytic polysaccharide monooxygenases on glycoside hydrolase activity. *ACS Sustain Chem Eng*. **8**, 14117-26.
120. Tokin R, Ipsen ØJ, Westh P & Johansen KS. (2020). The synergy between LPMOs and cellulases in enzymatic saccharification of cellulose is both enzyme- and substrate-dependent. *Biotechnol Lett*. **42**, 1975-84.
121. Vu VV & Marletta MA. (2016). Starch-degrading polysaccharide monooxygenases. *Cell Mol Life Sci*. **73**, 2809-19.

122. Isaksen T, Westereng B, Aachmann FL, Agger JW, Kracher D, Kittl R, Ludwig R, Haltrich D, Eijsink VGH & Horn SJ. (2014). A C4-oxidizing Lytic Polysaccharide Monooxygenase Cleaving Both Cellulose and Cello-oligosaccharides. *J Biol Chem*. **289**, 2632-42.
123. Kittl R, Kracher D, Burgstaller D, Haltrich D & Ludwig R. (2012). Production of four *Neurospora crassa* lytic polysaccharide monooxygenases in *Pichia pastoris* monitored by a fluorimetric assay. *Biotechnol Biofuels*. **5**, 79.
124. Rieder L, Stepnov AA, Sørlie M & Eijsink VG. (2021). Fast and specific peroxygenase reactions catalyzed by fungal mono-copper enzymes. *Biochemistry*. **60**, 3633-43.
125. Stepnov AA, Christensen IA, Forsberg Z, Aachmann FL, Courtade G & Eijsink VGH. (2022). The impact of reductants on the catalytic efficiency of a lytic polysaccharide monooxygenase and the special role of dehydroascorbic acid. *FEBS Lett*. **596**, 53-70.
126. Hegnar OA, Petrovic DM, Bissaro B, Alfredsen G, Várnai A & Eijsink VG. (2019). pH-dependent relationship between catalytic activity and hydrogen peroxide production shown via characterization of a lytic polysaccharide monooxygenase from *Gloeophyllum trabeum*. *Appl Environ Microbiol*. **85**, e02612-18.
127. Petrović DM, Varnai A, Dimarogona M, Mathiesen G, Sandgren M, Westereng B & Eijsink VG. (2019). Comparison of three seemingly similar lytic polysaccharide monooxygenases from *Neurospora crassa* suggests different roles in plant biomass degradation. *J Biol Chem*. **294**, 15068-81.
128. Stepnov AA, Eijsink VGH & Forsberg Z. (2022). Enhanced *in situ* H_2O_2 production explains synergy between an LPMO with a cellulose-binding domain and a single-domain LPMO. *Sci Rep*. **12**, 6129.
129. Chylenski P, Bissaro B, Sørlie M, Røhr ÅK, Várnai A, Horn SJ & Eijsink VG. (2019). Lytic polysaccharide monooxygenases in enzymatic processing of lignocellulosic biomass. *ACS Catal*. **9**, 4970-91.
130. Kuusk S, Eijsink VG & Väljamäe P. (2023). The “life-span” of lytic polysaccharide monooxygenases (LPMOs) correlates to the number of turnovers in the reductant peroxidase reaction. *J Biol Chem*. **299**, 105094.
131. Hangasky JA, Iavarone AT & Marletta MA. (2018). Reactivity of O_2 versus H_2O_2 with polysaccharide monooxygenases. *Proc Natl Acad Sci*. **115**, 4915-20.
132. Østby H, Tuveng TR, Stepnov AA, Vaaje-Kolstad G, Forsberg Z & Eijsink VG. (2023). Impact of copper saturation on lytic polysaccharide monooxygenase performance. *ACS Sustain Chem Eng*. **11**, 15566-76.
133. Arantes V & Goodell B. (2014). Current understanding of brown-rot fungal biodegradation mechanisms: a review. Nicholas D, Goodell B & Schultz T (eds) *Biodeterioration and Protection of Sustainable Biomaterials*, pp. 147-58. ACS Symposium Series: Oxford University Press

134. Goodell B, Jellison J, Liu J, Daniel G, Paszczynski A, Fekete F, Krishnamurthy S, Jun L & Xu G. (1997). Low molecular weight chelators and phenolic compounds isolated from wood decay fungi and their role in the fungal biodegradation of wood. *J Biotechnol*. **53**, 133-62.
135. Reese E. (1976). *History of the cellulase program at the US army Natick Development Center*. Biotechnol Bioeng Symp: Army Natick Development Center, MA.
136. Agrawal R, Semwal S, Kumar R, Mathur A, Gupta RP, Tuli DK & Satlewal A. (2018). Synergistic enzyme cocktail to enhance hydrolysis of steam exploded wheat straw at pilot scale. *Front Energy Res*. **6**, 122.
137. Bischof RH, Ramoni J & Seiboth B. (2016). Cellulases and beyond: the first 70 years of the enzyme producer *Trichoderma reesei*. *Microb Cell Fact*. **15**, 106.
138. Novy V, Nielsen F, Cullen D, Sabat G, Houtman CJ & Hunt CG. (2021). The characteristics of insoluble softwood substrates affect fungal morphology, secretome composition, and hydrolytic efficiency of enzymes produced by *Trichoderma reesei*. *Biotechnol Biofuels*. **14**, 105.
139. Costa TH, Kadic' A, Chylenski P, Várnai A, Bengtsson O, Lidén G, Eijsink VG & Horn SJ. (2020). Demonstration-scale enzymatic saccharification of sulfite-pulped spruce with addition of hydrogen peroxide for LPMO activation. *Biofuels Bioprod Biorefin*. **14**, 734-45.
140. Müller G, Chylenski P, Bissaro B, Eijsink VG & Horn SJ. (2018). The impact of hydrogen peroxide supply on LPMO activity and overall saccharification efficiency of a commercial cellulase cocktail. *Biotechnol Biofuels*. **11**, 209.
141. Qu X-S, Hu B-B & Zhu M-J. (2017). Enhanced saccharification of cellulose and sugarcane bagasse by *Clostridium thermocellum* cultures with Triton X-100 and β-glucosidase/Cellic® CTec2 supplementation. *RSC Adv*. **7**, 21360-5.
142. Rodrigues AC, Haven MØ, Lindedam J, Felby C & Gama M. (2015). Celluclast and Cellic® CTec2: saccharification/fermentation of wheat straw, solid–liquid partition and potential of enzyme recycling by alkaline washing. *Enzyme Microb Technol*. **79**, 70-7.
143. Sukumaran RK, Singhania RR & Pandey A. (2005). Microbial cellulases-production, applications and challenges. *J Sci Ind Res*. **64**, 832-44.
144. Hsieh C-wC, Cannella D, Jørgensen H, Felby C & Thygesen LG. (2014). Cellulase inhibition by high concentrations of monosaccharides. *J Agric Food Chem*. **62**, 3800-5.
145. Boisset C, Pétrequin C, Chanzy H, Henrissat B & Schülein M. (2001). Optimized mixtures of recombinant *Humicola insolens* cellulases for the biodegradation of crystalline cellulose. *Biotechnol Bioeng*. **72**, 339-45.
146. Väljamäe P, Sild V, Nutt A, Pettersson G & Johansson G. (1999). Acid hydrolysis of bacterial cellulose reveals different modes of synergistic action between cellobiohydrolase I and endoglucanase I. *Eur J Biochem*. **266**, 327-34.
147. Uchiyama T, Uchihashi T, Ishida T, Nakamura A, Vermaas JV, Crowley MF, Samejima M, Beckham GT & Igarashi K. (2022). Lytic polysaccharide monooxygenase increases cellobiohydrolases activity by promoting decrystallization of cellulose surface. *Sci Adv*. **8**, eade5155.

148. Vermaas JV, Crowley MF, Beckham GT & Payne CM. (2015). Effects of lytic polysaccharide monooxygenase oxidation on cellulose structure and binding of oxidized cellulose oligomers to cellulases. *J Phys Chem B*. **119**, 6129-43.
149. Mudedla SK, Vuorte M, Veijola E, Marjamaa K, Koivula A, Linder MB, Arola S & Sammalkorpi M. (2021). Effect of oxidation on cellulose and water structure: a molecular dynamics simulation study. *Cellulose*. **28**, 3917-33.
150. Cannella D, Weiss N, Hsieh C, Magri S, Zarattini M, Kuska J, Karuna N, Thygesen LG, Polikarpov I & Felby C. (2023). LPMO-mediated oxidation increases cellulose wettability, surface water retention and hydrolysis yield at high dry matter. *Cellulose*. **30**, 6259–72.
151. Koskela S, Wang S, Li L, Zha L, Berglund LA & Zhou Q. (2023). An oxidative enzyme boosting mechanical and optical performance of densified wood films. *Small*. **19**, 2205056.
152. Kristensen JB, Felby C & Jørgensen H. (2009). Yield-determining factors in high-solids enzymatic hydrolysis of lignocellulose. *Biotechnol Biofuels*. **2**, 11.
153. Jørgensen H, Vibe-Pedersen J, Larsen J & Felby C. (2007). Liquefaction of lignocellulose at high-solids concentrations. *Biotechnol Bioeng*. **96**, 862-70.
154. Hodge DB, Karim MN, Schell DJ & McMillan JD. (2009). Model-based fed-batch for high-solids enzymatic cellulose hydrolysis. *Appl Biochem Biotechnol*. **152**, 88-107.
155. Roberts KM, Lavenson DM, Tozzi EJ, McCarthy MJ & Jeoh T. (2011). The effects of water interactions in cellulose suspensions on mass transfer and saccharification efficiency at high solids loadings. *Cellulose*. **18**, 759-73.
156. Maciá-Agulló JA, Corma A & Garcia H. (2015). Photobiocatalysis: the power of combining photocatalysis and enzymes. *Chem - Eur J*. **21**, 10940-59.
157. Martínez AT, Ruiz-Dueñas FJ, Camarero S, Serrano A, Linde D, Lund H, Vind J, Tovborg M, Herold-Majumdar OM & Hofrichter M. (2017). Oxidoreductases on their way to industrial biotransformations. *Biotechnol Adv*. **35**, 815-31.
158. Lee SH, Choi DS, Kuk SK & Park CB. (2018). Photobiocatalysis: activating redox enzymes by direct or indirect transfer of photoinduced electrons. *Angew Chem Int Ed*. **57**, 7958-85.
159. Magri S & Cannella D. (2022). Producing Value-Added Products from Organic Bioresources via Photo-BioCatalytic Processes. *Production of Biofuels and Chemicals from Sustainable Recycling of Organic Solid Waste*, pp. 245-82: Springer.
160. Mifsud M, Gargiulo S, Iborra S, Arends IW, Hollmann F & Corma A. (2014). Photobiocatalytic chemistry of oxidoreductases using water as the electron donor. *Nat Commun*. **5**, 3145.
161. Bissaro B, Forsberg Z, Ni Y, Hollmann F, Vaaje-Kolstad G & Eijsink VG. (2016). Fueling biomass-degrading oxidative enzymes by light-driven water oxidation. *Green Chem*. **18**, 5357-66.

162. Cannella D, Möllers K, Frigaard N-U, Jensen P, Bjerrum M, Johansen K & Felby C. (2016). Light-driven oxidation of polysaccharides by photosynthetic pigments and a metalloenzyme. *Nat Commun*. **7**, 11134.
163. Möllers K, Mikkelsen H, Simonsen T, Cannella D, Johansen K, Bjerrum M & Felby C. (2017). On the formation and role of reactive oxygen species in light-driven LPMO oxidation of phosphoric acid swollen cellulose. *Carbohydr Res*. **448**, 182-6.
164. Koppenol WH, Stanbury DM & Bounds PL. (2010). Electrode potentials of partially reduced oxygen species, from dioxygen to water. *Free Radic Biol Med*. **49**, 317-22.
165. Blossom BM, Russo DA, Singh RK, Van Oort B, Keller MB, Simonsen TI, Perzon A, Gamon LF, Davies MJ & Cannella D. (2020). Photobiocatalysis by a lytic polysaccharide monooxygenase using intermittent illumination. *ACS Sustain Chem Eng*. **8**, 9301-10.
166. Austin AT & Ballaré CL. (2010). Dual role of lignin in plant litter decomposition in terrestrial ecosystems. *Proc Natl Acad Sci*. **107**, 4618-22.
167. Austin AT, Méndez MS & Ballaré CL. (2016). Photodegradation alleviates the lignin bottleneck for carbon turnover in terrestrial ecosystems. *Proc Natl Acad Sci*. **113**, 4392-7.
168. Austin AT & Vivanco L. (2006). Plant litter decomposition in a semi-arid ecosystem controlled by photodegradation. *Nature*. **442**, 555-8.
169. Berenstecher P, Vivanco L, Pérez LI, Ballaré CL & Austin AT. (2020). Sunlight doubles aboveground carbon loss in a seasonally dry woodland in Patagonia. *Curr Biol*. **30**, 3243-51.
170. Paulsson M & Parkås J. (2012). Light-induced yellowing of lignocellulosic pulps-mechanisms and preventive methods. *BioResources*. **7**, 5995-6040.
171. Kim J, Nguyen TVT, Kim YH, Hollmann F & Park CB. (2022). Lignin as a multifunctional photocatalyst for solar-powered biocatalytic oxyfunctionalization of C–H bonds. *Nat Synth*. **1**, 217-26.
172. Miglbauer E, Gryszel M & Głowacki ED. (2020). Photochemical evolution of hydrogen peroxide on lignins. *Green Chem*. **22**, 673-7.
173. Koskela S, Wang SN, Xu DF, Yang X, Li K, Berglund LA, McKee LS, Bulone V & Zhou Q. (2019). Lytic polysaccharide monooxygenase (LPMO) mediated production of ultra-fine cellulose nanofibres from delignified softwood fibres. *Green Chem*. **21**, 5924-33.
174. Stepnov AA, Forsberg Z, Sørlie M, Nguyen G-S, Wentzel A, Røhr ÅK & Eijsink VG. (2021). Unraveling the roles of the reductant and free copper ions in LPMO kinetics. *Biotechnol Biofuels*. **14**, 28.

6 PUBLICATIONS

Paper I

Lytic polysaccharide monooxygenase activity increases productive binding capacity of cellobiohydrolases on cellulose

Angeltveit CF, Jeoh T & Horn SJ

Bioresource Technology 389 (2023) 129806

Contents lists available at ScienceDirect

Bioresource Technology

journal homepage: www.elsevier.com/locate/biortech

Lytic polysaccharide monooxygenase activity increases productive binding capacity of cellobiohydrolases on cellulose

Camilla F. Angeltveit [a], Tina Jeoh [b], Svein J. Horn [a,*]

[a] Faculty of Chemistry, Biotechnology, and Food Science, Norwegian University of Life Sciences (NMBU), Ås, Norway
[b] Biological and Agricultural Engineering, University of California, Davis, United States

HIGHLIGHTS

- Application of CDH biosensor for productive binding capacity determination.
- LPMO pretreatment increased the productive binding capacity of *Tl*CBHI on cellulose.
- Both C1 and C4 LPMO activity was beneficial for the reducing end cellulase.
- Non-enzymatic decrystallization phase following the LPMO activity.

GRAPHICAL ABSTRACT

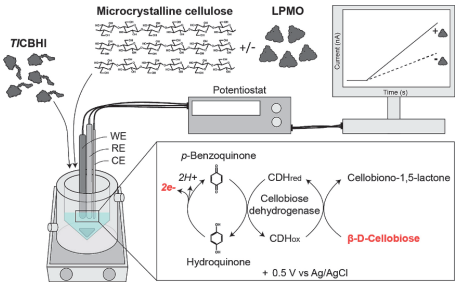

ARTICLE INFO

Keywords:
Enzymatic saccharification
LPMO pretreatment
Microcrystalline cellulose
*Tl*CBHI
Amperometric biosensor

ABSTRACT

Cellobiohydrolases are crucial for cellulose breakdown, but their efficiency on crystalline cellulose is hampered by limited access to single chain ends to initiate hydrolysis. As a result, they depend on enzymes like lytic polysaccharide monooxygenases (LPMOs), which directly target the crystalline cellulose surface. This study investigated how LPMO pretreatment affected the productive binding capacity of a *Trichoderma longibrachiatum* cellobiohydrolase, *Tl*CBHI, on crystalline cellulose by applying an amperometric cellobiose dehydrogenase biosensor. After the 24-hour of LPMO pretreatment, the productive binding capacity of *Tl*CBHI significantly increased in all reactions. However, with a shorter 5-hour LPMO pretreatment, minimal to no effect on productive binding capacity was observed. Of note, all LPMO reactions were inactivated around this time point. This delayed LPMO effect suggests that the improved binding capacity for cellulases does not directly result from cellulose chain cleavage by LPMOs but rather from the cellulose decrystallization following the oxidative cleavage.

Abbreviations: AA, Auxiliary activity; AscA, Ascorbic acid; BG, β-glucosidase; CBH, Cellobiohydrolase; CBM, Carbohydrate binding module; CDH, Cellobiose dehydrogenase; DP, Degree of polymerization; HPAEC-PAD, High-performance anion-exchange chromatography with pulsed amperometric detection; LPMO, Lytic polysaccharide monooxygenase; PASC, Phosphoric acid-swollen cellulose.

* Corresponding author.
E-mail address: svein.horn@nmbu.no (S.J. Horn).

https://doi.org/10.1016/j.biortech.2023.129806
Received 14 August 2023; Received in revised form 25 September 2023; Accepted 25 September 2023
Available online 27 September 2023

1. Introduction

Cellulases are well-known workhorses for the enzymatic saccharification of lignocellulosic biomass, an abundant renewable carbon source that can be applied as feedstock to produce biofuels and biochemicals (Payne et al., 2015). The term lignocellulose refers to plant biomass rich in lignin and the carbohydrate polymers cellulose and hemicellulose. The classical scheme for enzymatic cellulose degradation uses fungal enzyme cocktails with three main classes of glycoside hydrolases; cellobiohydrolases (CBHs), endoglucanases, and β-glucosidases (BGs). Exo-acting processive CBHs rely on the presence of a free chain end to initiate hydrolysis. These enzymes are the predominant components of the *Trichoderma reesei* secretome (Gritzali and Brown, 1979). Consequently, the inclusion of enzymes such as endoglucanases or lytic polysaccharide monooxygenases (LPMOs) that cleave cellulose can significantly enhance the effectiveness of enzyme cocktails (Horn et al., 2012).

Cellulose hydrolysis by cellulases is characterized by an initial rapid degradation phase (burst kinetics) followed by a gradual much slower degradation phase (Praestgaard et al., 2011). This rapid initial phase is based on the high number of productive binding sites that are accessible on the surface from the start of the reaction, while the second phase relies on the new binding sites that get exposed during the course of hydrolysis (Nill and Jeoh, 2020; Väljamäe et al., 1998). A productive binding site is a location on the substrate where the enzyme can complex and successfully perform hydrolysis (Karuna and Jeoh, 2017). Thus, in order to increase the cellulose degradation efficiency, the amount of productive binding sites must be increased.

The discovery of LPMOs has revolutionized the field of polysaccharide saccharification because of LPMOs' ability to cleave crystalline cellulose (Forsberg et al., 2011; Quinlan et al., 2011), chitin (Vaaje-Kolstad et al., 2010), hemicelluloses (Agger et al., 2014), starch (Vu et al., 2014), pectin (Sabbadin et al., 2021) and beta-glucans (Martinez-D'Alto et al., 2023). LPMOs can be found in all kingdoms of life (Voshol et al., 2017) and are classified as auxiliary activity (AA) in the Carbohydrate-Active Enzyme Database in families 9–11 and 13–17 (Levasseur et al., 2013). The powerful oxidative mechanism of LPMOs relies on a priming reduction of their coordinated copper (Quinlan et al., 2011) and the supply of an oxygen species (Vaaje-Kolstad et al., 2010), later shown to be H_2O_2 (Bissaro et al., 2017) to cleave the β-1,4-glycoside bonds in polysaccharides by oxidizing sugars in the C1 or C4 position. C1 activity results in the formation of a lactone in equilibrium with an aldonic acid, while C4 activity results in a ketoaldose in equilibrium with a gemdiol-aldose (Horn et al., 2012).

LPMOs' regioselectivity is often discussed in connection to LPMO-cellulase synergism. The most common hypothesis for LPMO-cellulase synergism is that LPMOs create new chain ends for the cellulases to complex and perform hydrolysis (Eibinger et al., 2014), indicating that the synergism is restricted to C1 active LPMOs and non-reducing end cellulases, and C4 active LPMOs and reducing end cellulases (Tokin et al., 2020). However, synergism has been observed between endoglucanases and LPMOs (Keller et al., 2020), and it should be noted that several cellobiohydrolases also show some endo-activity (Fox et al., 2012; Kurašin and Väljamäe, 2011). LPMO-cellulase synergism is typically studied by adding the enzymes simultaneously, making it challenging to evaluate LPMOs' physical effect on the substrate and how this influences the cellulase activity.

A recent molecular dynamic study showed that the glycoside bond breakage following LPMO oxidation allows surrounding water molecules to penetrate the highly ordered fibril structure, promoting decrystallization of the material (Uchiyama et al., 2022). Where the decrystallization effect is promoted by the increased negative surface charge from the introduction of carboxylate groups from C1 oxidizing LPMOs, resulting in the separation of the individual microfibrils due to electrostatic repulsion (Koskela et al., 2023). Suggesting that the oxidation and chain cleavage are followed by a non-enzymatic process where individual cellulose chains are decrystallized from the surface and exposed to the water phase.

In this study, a cellobiose dehydrogenase amperometric biosensor was used for online monitoring of cellobiose release to investigate how pretreatment with LPMOs influenced the productive binding capacity of cellulose for the reducing end cellobiohydrolase, *Tl*CBHI. Both C1 and C4 active LPMOs, derived from *Streptomyces coelicolor* and *Neurospora crassa*, respectively, were employed. The findings of this study provide new important insights into the collaborative interactions of LPMOs and cellulases.

2. Materials and methods

2.1. Enzymes

*Tl*CBHI from *Trichoderma longibrachiatum* was purchased from Neogen (E-CBHI; Neogen Corporation, Lansing, MI, USA). The enzyme was buffer exchanged to sodium acetate buffer (50 mM, pH 5.0; Sigma-Aldrich, St. Louis, MO, USA) and stored at −18 °C. The full-length *Sc*AA10C (UniProt Q9RJY2) and the N-terminal LPMO domain (*Sc*AA10C-N; residues 35–230, UniProt Q9RJY2) from *Streptomyces coelicolor* was recombinantly expressed in *Escherichia coli* and purified as previously described (Forsberg et al., 2014). *Nc*AA9C from *Neurospora crassa* (Uniprot NCU02916) was produced and purified as described elsewhere (Kittl et al., 2012). All LPMOs were copper saturated (Loose et al., 2014), followed by desalting using a PD MidiTrap column (G-25; GE Healthcare, Chicago, IL, USA) and stored at 4 °C.

2.2. Preparation of phosphoric acid-swollen cellulose

Phosphoric acid-swollen cellulose (PASC) was prepared by soaking 5 g of Whatman #1 filter paper (Sigma-Aldrich) in 250 mL of 85 % phosphoric acid (Sigma-Aldrich) at 4 °C overnight (Wood, 1988). It was then precipitated by adding a large amount of ice-cold water and washed until its pH approached neutrality. The cellulose was subsequently resuspended in water and autoclaved. Substrate concentration was determined using an Anthrone assay with a glucose standard curve (Morris, 1948).

2.3. LPMO pretreatment of Avicel

Microcrystalline cellulose (Avicel® PH-101, 50 μm particles; Sigma-Aldrich) was pretreated for 5 or 24 h with either *Sc*AA10C, *Sc*AA10C-N, or *Nc*AA9C alone or a combination of *Sc*AA10C with *Sc*AA10C-N or *Nc*AA9C in a 1:1 ratio. The Avicel and LPMO concentrations were 0.5 g/L and 100 nM for all reactions, respectively. L-ascorbic acid (Sigma-Aldrich) was present in all reactions at 1 mM. The LPMO pretreatment was performed in sodium acetate buffer (50 mM, pH 5.0) in 4 mL reaction volume at 50 °C with 25 rpm end-over-end rotation. The reactions were stopped by separating the reaction liquid from the insoluble substrate by centrifugation using 5 mL CENTREX 0.45 μm Nylon filter tubes (Sigma-Aldrich). The filtrate was stored at −18 °C for further analysis of soluble oxidized and native cello-oligosaccharides, while the insoluble substrate was washed using a similar procedure as described in previous publications (Jung et al., 2002; Nill and Jeoh, 2020). In brief, the insoluble substrate was washed with NaCl (0.5 M; Sigma-Aldrich) three consecutive times. After the last cycle of NaCl washing, the process was repeated with sodium acetate buffer (50 mM, pH 5.0). The pretreated and washed insoluble cellulose samples were resuspended in buffer and stored at 4 °C prior to further analysis. LPMO pretreatment led to very low cellulose solubilization (in all cases below 1 %).

2.4. Cellobiose biosensor

The three-electrode amperometric cellobiose biosensor was set up as previously described (Cruys-Bagger et al., 2012; Nill and Jeoh, 2020). Briefly, a cellobiose dehydrogenase (CDH) working electrode, Ag/AgCl

reference electrode (MF-2052; BASi® Research Products, West Lafayette, IN, USA), and platinum counter electrode (MW-4130; BASi® Research Products) were placed in a stirred jacked cell connected to a water bath and held at + 0.5 V by a potentiostat. The current detected by the potentiostat was monitored and recorded using an in-house program written in LabView.

2.5. Preparation of cellobiose dehydrogenase working electrode

The CDH electrode was prepared in a carbon paste holder (MF-2010; BASi® Research Products) with p-benzoquinone as described previously (Cruys-Bagger et al., 2012) with minor adjustments. Briefly, a paste of graphite (Thermo Scientific, Waltham, MA, United States), p-benzoquinone (Sigma-Aldrich), and paraffin (Sigma-Aldrich) were thoroughly mixed until homogenous before the carbon paste was packed into the carbon paste holder. The surface of the carbon paste holder was polished until it was flat and shiny. A drop of CDH enzyme solution (4 μL, approximately 6 g/L; Novozymes, Bagsværd, Denmark) was carefully added to the polished carbon paste surface and dried completely. Then it was stored overnight in an inverted position in a closed container containing sodium acetate buffer (50 mM, pH 5.0) at 4 °C, creating a humid environment, followed by one day immersed in the buffer before use.

2.6. Determination of saturating concentrations of productively bound *Tl*CBHI

Saturating concentrations of productively bound *Tl*CBHI on Avicel or PASC were determined based on maximum cellobiose release rates as previously described (Nill and Jeoh, 2020). Initial (maximum) cellobiose release at varying enzyme loadings was determined using time-resolved cellobiose measurements made with the CDH amperometric biosensor. Each reaction was performed with enzyme loadings in the 60–150 μmol/g cellulose range for the Avicel samples (0.1 g/L) and 40–350 μmol/g cellulose range for the PASC sample (0.05 g/L) in sodium acetate buffer (50 mM, pH 5.0) and 2 mL reaction volumes. Substrate and buffer were equilibrated in the jacketed stir cell with the biosensor probe at the predetermined reaction temperature (40 °C), and the reaction was initiated by adding *Tl*CBHI to the target enzyme loading. Sub-second resolved amperometric signal was recorded at a 10 per second sampling rate converted to cellobiose concentration using cellobiose standard curves (see supplementary materials). The steepest initial slope of the cellobiose vs time curve determined the initial rate of cellobiose release (r_{CB}). Saturating concentrations of productively bound *Tl*CBHI were determined empirically from fits to the following saturation relationship:

$$r_{CB} = \frac{a*(\frac{[E_T]}{[S]})}{b + (\frac{[E_T]}{[S]})} \quad (1)$$

where, r_{CB} = rate of cellobiose release (μM/s), $\frac{[E_T]}{[S]}$ = enzyme loading (μmol/g), and a and b are fitting parameters corresponding to the estimate of the productively bound enzyme concentration at saturation, and the half-saturation constant, respectively (Karuna and Jeoh, 2017).

2.7. Determination of the intrinsic catalytic rate constant of *Tl*CBHI

Using a previously estimated productive binding capacity of PASC of 5.75 μmol/g (Nill and Jeoh, 2020), the catalytic rate constant (k_{cat}) of *Tl*CBHI was determined from initial cellobiose release rates at saturation, as shown in Equation (2).

$$k_{cat} = \frac{r_{CB_{max}}}{[E_{BP}]*[S]} \quad (2)$$

where k_{cat} = catalytic rate constant (s^{-1}), $[E_{BP}]$ = concentration of productively bound enzymes at saturation = 5.75 μmol/g, $[S]$ = substrate concentration (g/L), and $r_{CB_{max}}$ = maximum rate of cellobiose release at saturation (μM/s).

2.8. Determination of the productive binding capacity of *Tl*CBHI on cellulose

The initial cellobiose release and the experimentally determined catalytic rate constant (2.6 s^{-1}) were used to calculate the concentration of productively bound *Tl*CBHI on Avicel (Karuna and Jeoh, 2017; Nill et al., 2018). When applying high *Tl*CBHI concentrations that ensure occupation of all cellulose binding sites, the initial cellobiose release will directly indicate the amount of productively bound enzymes (Nill and Jeoh, 2020). Thus, the *Tl*CBHI productive binding capacity ($[S_{PT}]$) will be equal to the initial concentration of productively bound *Tl*CBHI, as shown in Equations (3)–(5):

$$[E_{BP}] = \frac{r_{CB}}{k_{cat}*[S]} \quad (3)$$

$$[S_P] = [S_{PT}] - [E_{BP}] \quad (4)$$

$$[S_{PT}] = [E_{BP}]|_{r_{CB_{max}}} (where\ S_p = 0) \quad (5)$$

where, $[S_P]$ = productive binding sites (μmol/g) and $[S_{PT}]$ = productive binding capacity of the substrate (μmol/g).

2.9. Analysis of soluble oxidized and native cello-oligosaccharides by high-performance anion-exchange chromatography

The soluble oxidized and native cello-oligosaccharides after LPMO pretreatment were analyzed by high-performance anion-exchange chromatography with pulsed amperometric detection (HPAEC-PAD) using a Dionex ICS-5000 (Thermo Scientific) equipped with a CarboPac PA1 column, as previously described (Westereng et al., 2013). Freshly made eluents (A: 100 mM NaOH; B: 1 M NaOAc + 100 mM NaOH), an operational flow of 500 μL/min, and a sample loop volume of 5 μL were used. An eluent gradient from 0 to 100 % B was used to analyze oxidized and native cello-oligosaccharides as described previously (Ostby et al., 2022). For quantification purposes, the samples were treated with 2 μM *Tf*Cel6A from *Thermobifida fusca* (produced in-house, as described previously (Spezio et al., 1993)), or a cellulase cocktail (Celluclast® 1.5 + NZ-BG (Novozymes)) overnight to convert soluble oxidized and native cello-oligosaccharides to a degree of polymerization (DP) of 2–3 or 1, respectively.

C1-oxidized standards for DP2-6, $Glc_{2\text{-}5}GlcA$, were made by treating native cello-oligosaccharides (Neogen Corporation) with 0.2 μM *Mt*CDH from *Myriococcum thermophilum* (produced in-house, as described previously (Zamocky et al., 2008) in sodium acetate buffer (50 mM, pH 5.0) at 40 °C for 20 h in an Eppendorf Thermomixer (Eppendorf, Hamburg, Germany). C4-oxidized standards of DP2-3, $Glc_4gemGlc_{1\text{-}2}$, were made by treating cellopentaose with 2 μM *Nc*AA9C in Tris buffer (10 mM, pH 8.0; Sigma-Aldrich) with 2 mM L-ascorbic acid at 33 °C for 24 h in an Eppendorf Thermomixer, after which the reactions were stopped by boiling at 100 °C for 15 min (Ostby et al., 2022). The C4 oxidized standards were quantified assuming equal molar products of cellobiose and $Glc_4gemGlc_2$ and cellotriose and $Glc_4gemGlc$ (Muller et al., 2015).

2.10. Spectrophotometrically determination of ascorbic acid depletion

The depletion of ascorbic acid during the reaction course was measured spectrophotometrically by quenching the LPMO reactions at various time points by removing the insoluble substrate using a 96-well filter plate (Sigma-Aldrich) rapidly followed by measuring the absorbance at 255 nm (Stepnov et al., 2022b). L-ascorbic acid standard solutions were prepared in metal-free TraceSELECT water (VWR, Radnor, PA, United States).

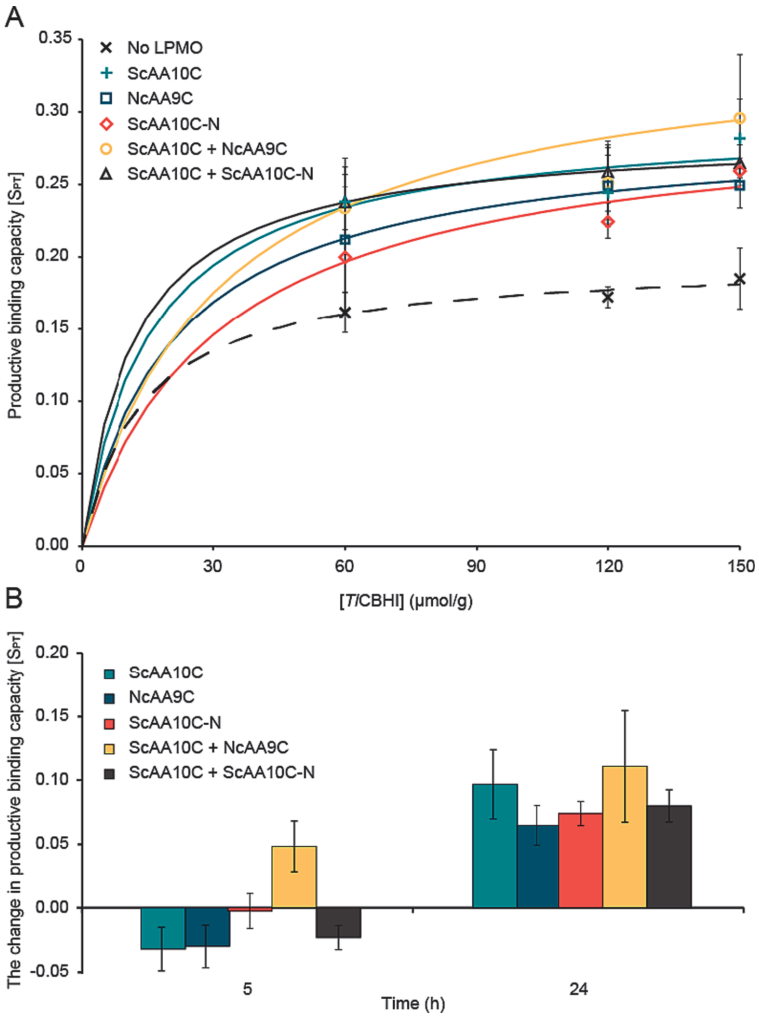

Fig. 1. The effect of LPMO pretreatment on the productive binding capacity of *Tl*CBHI on cellulose. (**A**) *Tl*CBHI productive binding capacity (S_{PT}) on Avicel, either untreated or pretreated with LPMO for 24 h. (**B**) The net change in *Tl*CBHI productive binding capacity on Avicel after 5 and 24 h of LPMO pretreatment. Markers represent biosensor measurements, and curves are determined empirically from fits to Equation (1). Standard deviation is shown as error bars from three biological replicates.

3. Results and discussion

3.1. LPMO activity increases the productive TlCBHI binding capacity of microcrystalline cellulose

Two different LPMO families were compared in this study. The wild-type *Sc*AA10C is a two-domain C1 active LPMO with a catalytic domain and a carbohydrate-binding module (CBM) and is a well-studied bacterial LPMO (Forsberg et al., 2011, 2014; Quinlan et al., 2011). *Nc*AA9C is a well-studied fungal two-domain LPMO with C4 activity towards crystalline cellulose, xyloglucan, and soluble oligosaccharides (Isaksen et al., 2014). Removal of the CBM from the wild-type *Sc*AA10C has previously been shown to considerably impact enzyme stability, the ability to produce oxidized products, and the resulting oligosaccharide product profile (Courtade et al., 2018; Forsberg and Courtade, 2023). Synergy between the wild-type and the truncated AA10 enhancing release of soluble oxidized products from cellulose has been shown before (Courtade et al., 2018; Forsberg and Courtade, 2023; Stepnov et al., 2022b), but the impact on available productive cellobiohydrolase binding sites on cellulose has not been investigated.

Microcrystalline cellulose was incubated with different LPMOs to investigate if this affected the productive binding capacity of *Tl*CBHI on this substrate. Binding was evaluated using a biosensor equipped with a CDH working electrode to measure initial cellobiose release from *Tl*CBHI on cellulose. Biosensors are a relatively new tool allowing continuous real-time measurements of soluble sugars. In recent years, this has been used both in single-component studies (Cruys-Bagger et al., 2012; Nill and Jeoh, 2020) and studies mimicking natural environments both in terms of enzyme and substrate composition (Chang et al., 2022), allowing faster and more accurate determination of initial substrate

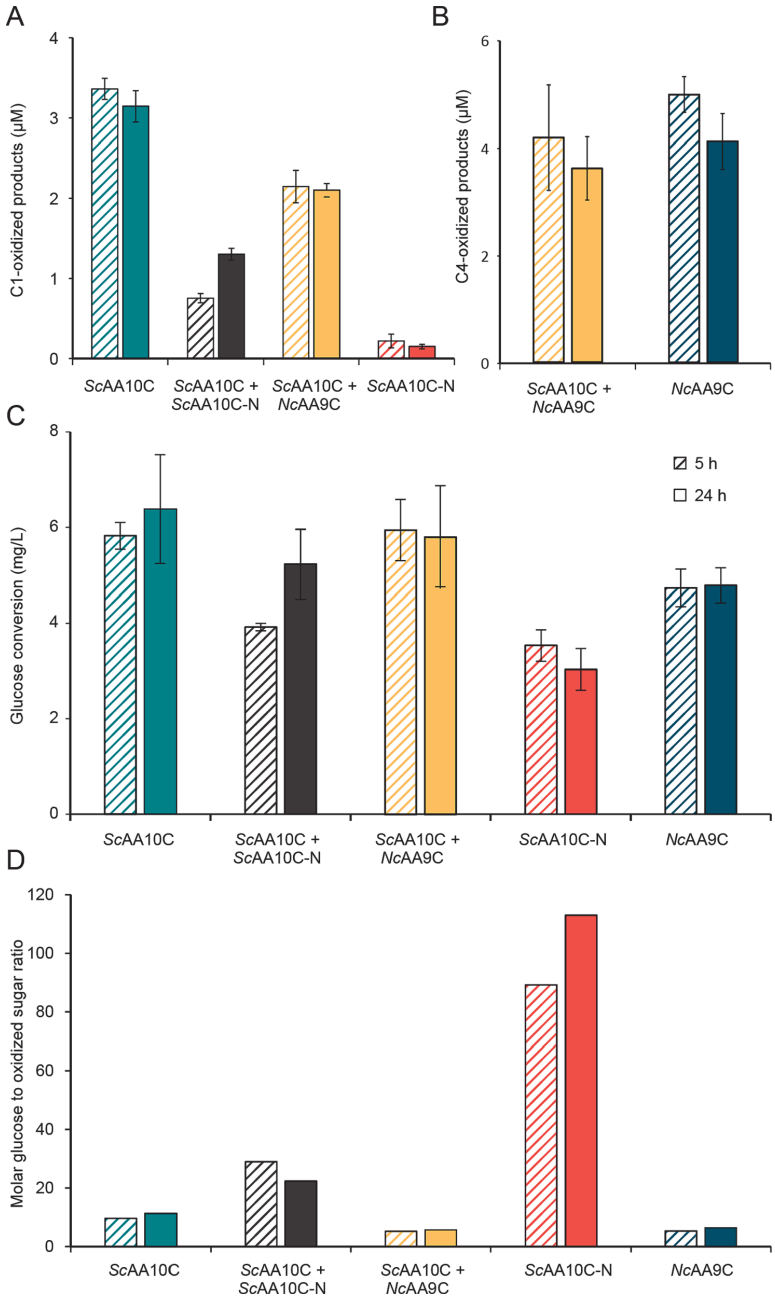

Fig. 2. Release of soluble native, C1- and C4-oxidized sugars from LPMO pretreated cellulose. (**A**) C1-oxidized soluble sugars, (**B**) C4-oxidized soluble sugar, (**C**) glucose conversion, and (**D**) the molar ratio of glucose to oxidized sugars from LPMO pretreated cellulose. Standard deviation is shown as error bars from three biological replicates.

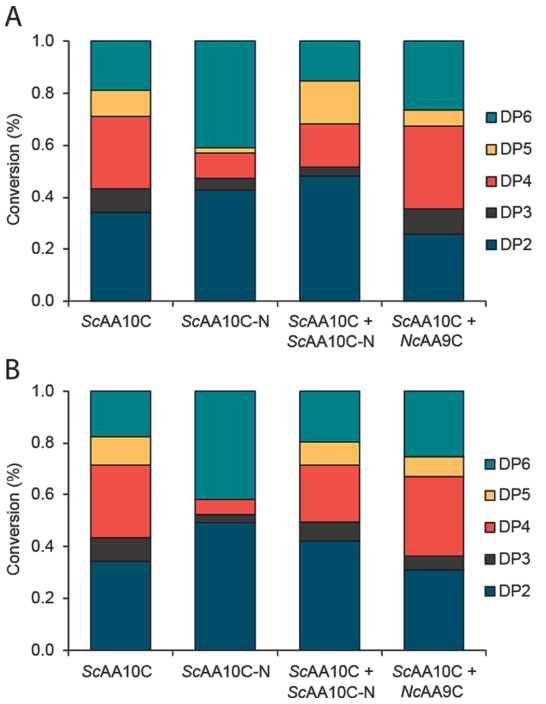

Fig. 3. Relative product profiles showing the distribution of DP2 to DP6 soluble oxidized sugars after LPMO pretreatment of Avicel (0.5 g/L) with 100 nM *Sc*AA10C, *Sc*AA10C-N, or *Sc*AA10C combined with *Nc*AA9C or *Sc*AA10C-N in the presence of 1 mM ascorbic acid for (**A**) 5 or (**B**) 24 h.

effects. So-called "inverse Michaelis-Menten kinetics" were carried out where the roles of enzyme and substrate are interchanged, i.e., performing measurements with low substrate concentration and high enzyme concentrations (Kari et al., 2017). Biosensor measurements were performed at different *Tl*CBHI concentrations to identify saturating concentrations where *Tl*CBHI enzymes occupy all productive binding sites of the substrate.

First, the catalytic rate constant of *Tl*CBHI was experimentally determined (Equation (2)) to be 2.6 s^{-1} at 40 °C by measuring the initial cellobiose release rates on PASC because of its predetermined productive binding capacity (Karuna and Jeoh, 2017; Nill and Jeoh, 2020). Then, the productive binding capacity of the Avicel samples was calculated (Equations (3)–(5)) using the catalytic rate constant and the initial cellobiose release, assuming that the initial rate of cellobiose release under saturated enzyme conditions is directly a function of the amount of productively bound enzymes (Nill and Jeoh, 2020). All curves leveled off (Fig. 1**A**), indicating saturation of all productive binding sites on the substrate at the higher *Tl*CBHI concentrations (120–150 μmol/g) after 24 h of LPMO incubation. Thus, it was decided to use the initial cellobiose release from experiments with 150 μmol/g *Tl*CBHI to investigate the effect on the substrate from LPMO pretreatment. The productive binding capacity of *Tl*CBHI on microcrystalline cellulose was 0.19 μmol/g (Fig. 1**A**), which was used as the baseline for all further comparisons. This is an order of magnitude lower than the previously reported *Tr*Cel7A binding capacity of microcrystalline cellulose (Nill and Jeoh, 2020). However, variability in the binding capacities of different cellulases has been shown, indicating differences in the ability of the enzymes to form active complexes on cellulose (Kari et al., 2017).

Fig. 1**B** shows the net change in *Tl*CBHI productive binding capacity of microcrystalline cellulose after 5 and 24 h of LPMO pretreatment. Five hours of LPMO incubation resulted in no or even a slight decrease in *Tl*CBHI binding capacity. The only exception was the combination of *Sc*AA10C and *Nc*AA9C, which improved the binding by 0.05 ± 0.02 μmol/g. After 24 h, all LPMO incubations yielded an increased productive binding capacity (in the range 0.06 ± 0.02 to 0.11 ± 0.04 μmol/g) of *Tl*CBHI on cellulose (Fig. 1**B**). Thus, LPMO pretreatment of microcrystalline cellulose increased the number of productive binding sites for *Tl*CBHI, but the effect depended on the LPMO incubation time. There was no significant difference between the different LPMO pretreatments, except that the combination of *Sc*AA10C (C1 active) and *Nc*AA9C (C4 active) seemed to act faster, yielding more productive binding sites for *Tl*CBHI after 5 h.

3.2. LPMO production of soluble oxidized and native sugars

To confirm LPMO activity, the soluble sugars released during LPMO pretreatment were analyzed (see supplementary materials). Fig. 2**A** and Fig. 2**B** show that oxidized sugars were produced in all reactions but also reveal significant differences in the amount of oxidized soluble sugars produced. In general, the amount of oxidized sugars was quite similar at 5 and 24 h, meaning that LPMOs were mainly active in the initial phase of the reactions. After 24 h of LPMO pretreatment, *Sc*AA10C had produced 20-fold more soluble C1 oxidized sugars than *Sc*AA10C-N, and twice as much C1 oxidized products as the reaction containing *Sc*AA10C and *Sc*AA10C-N. C1 oxidized sugars from DP2 to DP6 were detected in these reactions, and all C1 oxidized sugar profiles are highly dominated by even-numbered oxidized products (Fig. 3), as has been shown before and which indicates that LPMOs act directly on the crystalline surface (Forsberg et al., 2011). The combination of *Sc*AA10C and *Sc*AA10C-N was the only reaction where a significant difference in the soluble oxidized sugar profile was observed for the 5 and 24 h time points (Fig. 3). As for the soluble C4 oxidized products, there were similar levels of oxidized products in the two reactions including *Nc*AA9C, alone or together with *Sc*AA10C. When summing the soluble C1 and C4 oxidized products, the reaction with the highest total oxidized sugar production was the reaction including both *Nc*AA9C and *Sc*AA10C (Fig. 2**A** and Fig. 2**B**).

Generally, two-domain LPMOs with a CBM will have stronger affinities to the substrate, which is particularly beneficial at low substrate concentrations (Courtade et al., 2018). This is evident for *Sc*AA10C-N, which produces much less soluble oxidized products than *Sc*AA10C (Fig. 2**A**). However, the role of the CBM is complex and does not only affect binding to the substrate in general. It has been suggested that CBMs lead to binding to internal positions on the substrate, which promotes multiple cleavages in the same region before they desorb from the substrate and are absorbed somewhere else (Courtade et al., 2018). Accordingly, LPMOs lacking a CBM will oxidize in a more dispersed manner over the entire cellulose (Koskela et al., 2019) and may result in more LPMO cleavage close to chain ends, releasing native cello-oligosaccharides (Forsberg and Courtade, 2023). Fig. 2**C** shows the amount of glucose in the liquid phase produced by further hydrolysis of the released oligosaccharides by an enzyme cocktail. Interestingly, the molar ratio of glucose and oxidized sugars showed a large range for the different reactions (Fig. 2**D**). The reactions with *Nc*AA9C, either alone or together with *Sc*AA10C, had the lowest molar ratio of glucose to oxidized sugar, followed by the reaction with *Sc*AA10C. In contrast, the reaction with only *Sc*AA10C-N had a 10-fold higher ratio compared to *Sc*AA10C alone, clearly indicating that more native oligos are produced with LPMOs lacking a CBM.

3.3. Reductant depleted early in the reaction

The availability of hydrogen peroxide is typically the limiting factor for LPMO activity (Bissaro et al., 2017; Stepnov et al., 2022a). Under aerobic conditions, H_2O_2 will be produced *in situ* from oxidizing

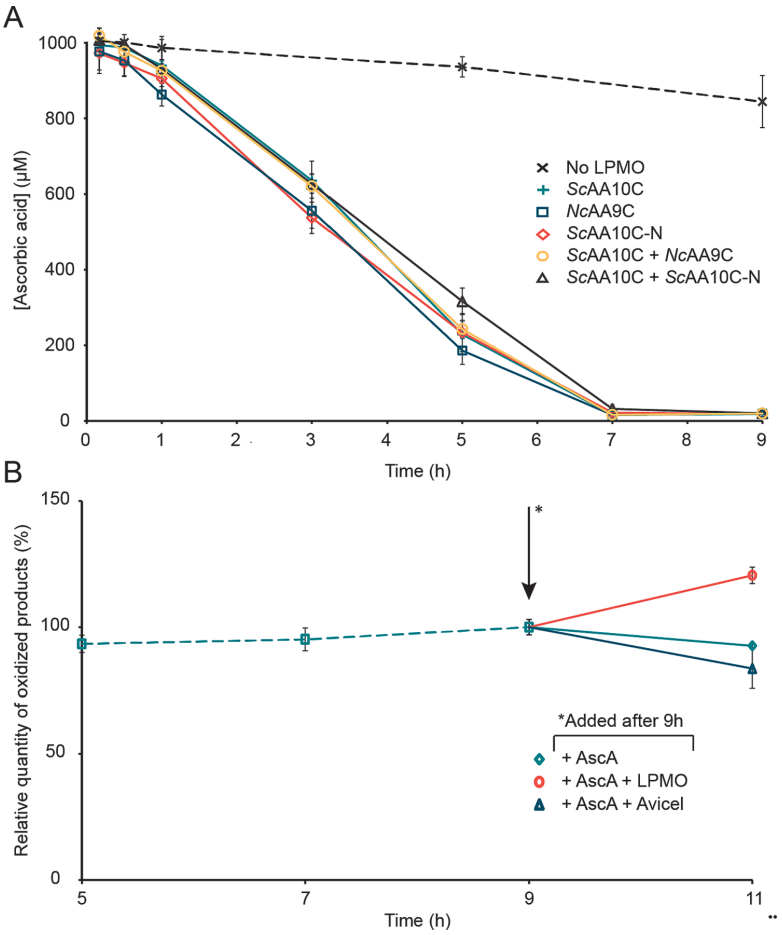

Fig. 4. Probing the cause of the early cessation of LPMO activity. (**A**) Spectrophotometrically determination of ascorbic acid depletions during LPMO pretreatment of Avicel. (**B**) Reactivation of the *Sc*AA10C reaction (from panel A) by supplementing the reactions with 1 mM ascorbic acid, either alone or with fresh LPMO or Avicel after 9 h reaction time. The change in oxidized sugars is shown as the relative product formation, where 100 % is the level after 9 h. Standard deviation is shown as error bars from three biological replicates.

compounds such as gallic acid, ascorbic acid, or lignin. The LPMOs themselves will also contribute to H_2O_2 production when not absorbed to the cellulose substrate. However, reduced LPMOs in solution are at higher risk for inactivation due to non-reversible oxidation of the active site in reactions with high H_2O_2 levels (Bissaro et al., 2017).

To probe the reason for the halted LPMO activity after 5 h (Fig. 2**A & B**), the consumption of ascorbic acids in the LPMO reactions were measured, indicating *in situ* H_2O_2 production. Interestingly, all LPMO reactions exhausted ascorbic acids between 5 and 7 h (Fig. 4**A**), meaning no more H_2O_2 could be produced from ascorbic acid later in the reactions. Rapid and accelerated consumption of ascorbic acid could be due to release of free copper from the active site of inactivated LPMOs, as observed previously (Stepnov et al., 2022b). A reactivation experiment was performed to further investigate the reason for the halted LPMO activity. Reactivation of the stagnated LPMO reactions (here using the *Sc*AA10C reaction as an example, see supplementary materials for additional experiments) was only successful when adding more ascorbic acid and LPMOs, indicating that the LPMO activity stopped due to LPMO inactivation (Fig. 4**B**).

3.4. Delayed effect of LPMO activity on cellulase binding

Despite different regioselectivities and the presence or absence of a CBM, all LPMOs tested in this study ultimately increased the productive *Tl*CBHI binding capacity of microcrystalline cellulose to similar extents (Fig. 1). Interestingly, for most of the LPMO combinations, this enhancement of available *Tl*CBHI productive binding sites on the cellulose was not evident during the early stages of the reaction while LPMO activity released solubilized oxidized and native sugars (Fig. 2**A, B & C**), and only evident after apparent cessation of LPMO activity (Fig. 4**B**). Consequently, LPMO activity alone cannot explain the increased productive binding capacity between 5 and 24 h.

Indeed, in a recent molecular dynamics study by Uchiyama et al. (2022), they show that the effect of LPMOs on cellulose is not limited by the creation of new chain ends, but by increasing hydrogen bonding with water molecules in the cut sites to increase solvent accessibility into the cellulose fibril, which overall makes the substrate more accessible for the cellulases. The effect is most pronounced for the C1-oxidized aldonic acid because of the increased solvent exposed area from the

open ring structure allowing more water to penetrate the crystalline structure (Mudedla et al., 2021) combined with the electrostatic repulsion promoting separation of the individual microfibrils because of the negative surface charge from the introduced carboxylate groups (Koskela et al., 2023). These findings imply that the enzymatic cleavage of glycosidic bonds within the crystalline cellulose structure by LPMOs may not directly provide productive binding sites for cellobiohydrolases. Instead, a subsequent non-enzymatic phase of decrystallization following the oxidative cleavage appears necessary to enhance the productive binding capacity of the substrate to the cellulases.

Decrystallization of cellulose has been shown to take place gradually over time (Eibinger et al., 2017) and is dependent on the type of oxidized products (C1 vs C4) and on the configuration of the oxidized sugar (lactone vs aldonic acid and keto-aldose vs geminal-diol) (Mudedla et al., 2021; Uchiyama et al., 2022; Vermaas et al., 2015). The C1-oxidized products are in an equilibrium between lactone and aldonic acid, and the typical reaction conditions used for enzymatic hydrolysis favor the aldonic acid configuration (Cannella et al., 2012). The open chain formation of aldonic acid has a greater solvent-accessible surface area with more favorable interactions with the interior of the commonly used cellulase *Tr*Cel7A than the exterior. As a result, the aldonic acid can lead to non-productive binding and stalling of the cellulase activity (Vermaas et al., 2015). With this in mind, an inhibitory relationship between C1-oxidizing LPMOs and reducing end cellulases has been suggested. On the other hand, the negative charge of aldonic acid will have a positive decrystallization effect on the substrate resulting in separation of the individual microfibrils. Thus, the decrystallization effect on the substrate could explain the increased productive binding capacity of reducing end cellulase *Tl*CBHI on cellulose pretreated with C1 active LPMOs even though they produce non-reducing chain ends.

This study showed similar effects on cellulase binding for all LPMO pretreatment conditions after 24 h. However, the decrystallization effect seemed to occur earlier when combining C1 and C4 activity, where a significant increase in the productive binding capacity was detected already after 5 h (Fig. 1). This was also the reaction that clearly produced the most oxidized sugars. Thus, the combination of different LPMOs may be beneficial for improving saccharification rate.

Previous studies have proposed that LPMOs play a more significant role in the later stages of hydrolysis, which is often attributed to the increased recalcitrance of the remaining cellulose substrate. However, the delayed LPMO effect presented here suggests that glycosidic bond cleavage in the crystalline cellulose structure by LPMOs may not immediately provide accessible binding sites for *Tl*CBHI but is followed by a non-enzymatic phase where increasing hydrogen bonding between the cellulose cut sites and water result in a gradual decrystallization, overall making the material more accessible for the cellulases. This effect may have been overlooked in previous studies due to the lack of time courses or limited time spans in the experimental setups, or the simultaneous addition of both enzymes rather than their sequential addition, as applied in this study.

4. Conclusion

This study provides new insight into cellulase-LPMO synergism, showing that both C1 oxidizing LPMOs and C4 oxidizing LPMOs have a positive effect on the cellulose binding capacity of the reducing end cellulase *Tl*CBHI after an extended pretreatment time. Taken together, these findings highlight the complex interplay between LPMOs, cellulose decrystallization, and cellulase activity. An improved understanding of the LPMO and cellulase synergy can aid in the design of more efficient saccharification processes and facilitate the conversion of cellulose into valuable bio-based products.

CRediT authorship contribution statement

Camilla F. Angeltveit: Writing – original draft, Writing – review & editing, Conceptualization, Investigation, Formal analysis, Methodology, Visualization, Funding acquisition. **Tina Jeoh:** Conceptualization, Investigation, Formal analysis, Methodology, Supervision, Writing – review & editing. **Svein J. Horn:** Writing – original draft, Writing – review & editing, Conceptualization, Project administration, Supervision, Funding acquisition.

Declaration of competing interest

The authors declare that they have no known competing financial interests or personal relationships that could have appeared to influence the work reported in this paper.

Data availability

Data will be made available on request.

Acknowledgments

This work was supported by the Research Council of Norway through grant number 257622 (Bio4Fuels). Celluclast® 1.5 L, NZ-BG and CDH were kindly gifted from Novozymes, Denmark. We thank Dr. Thales Costa at NMBU for providing *Nc*AA9C, and NMBU for granting Angeltveit a scholarship for a research visit to UC Davis.

Appendix A. Supplementary data

Supplementary data to this article can be found online at https://doi.org/10.1016/j.biortech.2023.129806.

References

Agger, J.W., Isaksen, T., Varnai, A., Vidal-Melgosa, S., Willats, W.G.T., Ludwig, R., Horn, S.J., Eijsink, V.G.H., Westereng, B., 2014. Discovery of LPMO activity on hemicelluloses shows the importance of oxidative processes in plant cell wall degradation. PNAS 111 (17), 6287–6292. https://doi.org/10.1073/pnas.1323629111.

Bissaro, B., Rohr, A.K., Muller, G., Chylenski, P., Skaugen, M., Forsberg, Z., Horn, S.J., Vaaje-Kolstad, G., Eijsink, V.G.H., 2017. Oxidative cleavage of polysaccharides by monocopper enzymes depends on H(2)O(2). Nat. Chem. Biol. 13 (10), 1123–1128. https://doi.org/10.1038/nchembio.2470.

Cannella, D., Hsieh, C.W.C., Felby, C., Jorgensen, H., 2012. Production and effect of aldonic acids during enzymatic hydrolysis of lignocellulose at high dry matter content. Biotechnol. Biofuels 5 (1), 1–10. https://doi.org/10.1186/1754-6834-5-26.

Chang, H., Gacias Amengual, N., Botz, A., Schwaiger, L., Kracher, D., Scheiblbrandner, S., Csarman, F., Ludwig, R., 2022. Investigating lytic polysaccharide monooxygenase-assisted wood cell wall degradation with microsensors. Nat. Commun. 13 (1), 6258. https://doi.org/10.1038/s41467-022-33963-w.

Courtade, G., Forsberg, Z., Heggset, E.B., Eijsink, V.G.H., Aachmann, F.L., 2018. The carbohydrate-binding module and linker of a modular lytic polysaccharide monooxygenase promote localized cellulose oxidation. JBC 293 (34), 13006–13015. https://doi.org/10.1074/jbc.RA118.004269.

Cruys-Bagger, N., Ren, G., Tatsumi, H., Baumann, M.J., Spodsberg, N., Andersen, H.D., Gorton, L., Borch, K., Westh, P., 2012. An amperometric enzyme biosensor for real-time measurements of cellobiohydrolase activity on insoluble cellulose. Biotechnol. Bioeng. 109 (12), 3199–3204. https://doi.org/10.1002/bit.24593.

Eibinger, M., Ganner, T., Bubner, P., Rosker, S., Kracher, D., Haltrich, D., Ludwig, R., Plank, H., Nidetzky, B., 2014. Cellulose surface degradation by a lytic polysaccharide monooxygenase and its effect on cellulase hydrolytic efficiency. JBC 289 (52), 35929–35938. https://doi.org/10.1074/jbc.M114.602227.

Eibinger, M., Sattelkow, J., Ganner, T., Plank, H., Nidetzky, B., 2017. Single-molecule study of oxidative enzymatic deconstruction of cellulose. Nat. Commun. 8 (1), 894. https://doi.org/10.1038/s41467-017-01028-y.

Forsberg, Z., Courtade, G., 2023. On the impact of carbohydrate-binding modules (CBMs) in lytic polysaccharide monooxygenases (LPMOs). Essays Biochem. 67 (3), 561–574. https://doi.org/10.1042/EBC20220162.

Forsberg, Z., Vaaje-Kolstad, G., Westereng, B., Bunaes, A.C., Stenstrom, Y., MacKenzie, A., Sorlie, M., Horn, S.J., Eijsink, V.G., 2011. Cleavage of cellulose by a CBM33 protein. Protein Sci. 20 (9), 1479–1483. https://doi.org/10.1002/pro.689.

Forsberg, Z., Mackenzie, A.K., Sorlie, M., Rohr, A.K., Helland, R., Arvai, A.S., Vaaje-Kolstad, G., Eijsink, V.G., 2014. Structural and functional characterization of a conserved pair of bacterial cellulose-oxidizing lytic polysaccharide monooxygenases. PNAS 111 (23), 8446–8451. https://doi.org/10.1073/pnas.1402771111.

Fox, J.M., Levine, S.E., Clark, D.S., Blanch, H.W., 2012. Initial-and processive-cut products reveal cellobiohydrolase rate limitations and the role of companion enzymes. Biochemistry 51 (1), 442–452. https://doi.org/10.1021/bi2011543.
Gritzali, M., Brown, R.D., 1979. The cellulase system of Trichoderma: Relationships between purified extracellular enzymes from induced or cellulose-grown cells. ACS Adv. Chem. 181, 238–260. https://doi.org/10.1021/ba-1979-0181.ch012.
Horn, S.J., Vaaje-Kolstad, G., Westereng, B., Eijsink, V.G., 2012. Novel enzymes for the degradation of cellulose. Biotechnol. Biofuels 5 (1), 45. https://doi.org/10.1186/1754-6834-5-45.
Isaksen, T., Westereng, B., Aachmann, F.L., Agger, J.W., Kracher, D., Kittl, R., Ludwig, R., Haltrich, D., Eijsink, V.G.H., Horn, S.J., 2014. A C4-oxidizing Lytic Polysaccharide Monooxygenase Cleaving Both Cellulose and Cello-oligosaccharides. JBC 289 (5), 2632–2642. https://doi.org/10.1074/jbc.M113.530196.
Jung, H., Wilson, D.B., Walker, L.P., 2002. Binding of Thermobifida fusca CDCel5A, CDCel6B and CDCel48A to easily hydrolysable and recalcitrant cellulose fractions on BMCC. Enzymeand Microbial Technol. 31 (7), 941–948. https://doi.org/10.1016/S0141-0229(02)00181-3.
Kari, J., Andersen, M., Borch, K., Westh, P., 2017. An inverse Michaelis-Menten approach for interfacial enzyme kinetics. ACS Catal. 7 (7), 4904–4914. https://doi.org/10.1021/acscatal.7b00838.
Karuna, N., Jeoh, T., 2017. The productive cellulase binding capacity of cellulosic substrates. Biotechnol. Bioeng. 114 (3), 533–542. https://doi.org/10.1002/bit.26193.
Keller, M.B., Badino, S.F., Blossom, B.M.l., McBrayer, B., Borch, K., Westh, P., 2020. Promoting and impeding effects of lytic polysaccharide monooxygenases on glycoside hydrolase activity. ACS Sustain Chem Eng. 8 (37), 14117–14126. https://doi.org/10.1021/acssuschemeng.0c04779v.
Kittl, R., Kracher, D., Burgstaller, D., Haltrich, D., Ludwig, R., 2012. Production of four Neurospora crassa lytic polysaccharide monooxygenases in Pichia pastoris monitored by a fluorimetric assay. Biotechnol. Biofuels 5 (1), 79. https://doi.org/10.1186/1754-6834-5-79.
Koskela, S., Wang, S.N., Xu, D.F., Yang, X., Li, K., Berglund, L.A., McKee, L.S., Bulone, V., Zhou, Q., 2019. Lytic polysaccharide monooxygenase (LPMO) mediated production of ultra-fine cellulose nanofibres from delignified softwood fibres. Green Chem. 21 (21), 5924–5933. https://doi.org/10.1039/c9gc02808k.
Koskela, S., Wang, S., Li, L., Zha, L., Berglund, L.A., Zhou, Q., 2023. An Oxidative Enzyme Boosting Mechanical and Optical Performance of Densified Wood Films. Small 19 (17), e2205056. https://doi.org/10.1002/smll.202205056.
Kurašin, M., Väljamäe, P., 2011. Processivity of cellobiohydrolases is limited by the substrate. JBC 286 (1), 169–177. https://doi.org/10.1074/jbc.M110.161059.
Levasseur, A., Drula, E., Lombard, V., Coutinho, P.M., Henrissat, B., 2013. Expansion of the enzymatic repertoire of the CAZy database to integrate auxiliary redox enzymes. Biotechnol. Biofuels 6 (1), 41. https://doi.org/10.1186/1754-6834-6-41.
Loose, J.S.M., Forsberg, Z., Fraaije, M.W., Eijsink, V.G.H., Vaaje-Kolstad, G., 2014. A rapid quantitative activity assay shows that the Vibrio cholerae colonization factor GbpA is an active lytic polysaccharide monooxygenase. FEBS Lett. 588 (18), 3435–3440. https://doi.org/10.1016/j.febslet.2014.07.036.
Martínez-D'Alto, A., Yan, X., Detomasi, T.C., Sayler, R.I., Thomas, W.C., Talbot, N.J., Marletta, M.A., 2023. Characterization of a unique polysaccharide monooxygenase from the plant pathogen Magnaporthe oryzae. PNAS 120 (8), e2215426120. https://doi.org/10.1073/pnas.2215426120.
Morris, D.L., 1948. Quantitative determination of carbohydrates with Dreywood's anthrone reagent. Science 107 (2775), 254–255. https://doi.org/10.1126/science.107.2775.254.
Mudedla, S.K., Vuorte, M., Veijola, E., Marjamaa, K., Koivula, A., Linder, M.B., Arola, S., Sammalkorpi, M., 2021. Effect of oxidation on cellulose and water structure: a molecular dynamics simulation study. Cellul. 28 (7), 3917–3933. https://doi.org/10.1007/s10570-021-03751-8.
Muller, G., Varnai, A., Johansen, K.S., Eijsink, V.G., Horn, S.J., 2015. Harnessing the potential of LPMO-containing cellulase cocktails poses new demands on processing conditions. Biotechnol. Biofuels 8 (1), 187. https://doi.org/10.1186/s13068-015-0376-y.
Nill, J.D., Jeoh, T., 2020. The role of evolving interfacial substrate properties on heterogeneous cellulose hydrolysis kinetics. ACS Sustain. Chem. Eng. 8 (17), 6722–6733. https://doi.org/10.1021/acssuschemeng.0c00779.
Nill, J., Karuna, N., Jeoh, T., 2018. The impact of kinetic parameters on cellulose hydrolysis rates. Process Biochem. 74, 108–117. https://doi.org/10.1016/j.procbio.2018.07.006.
Ostby, H., Jameson, J.K., Costa, T., Eijsink, V.G.H., Arntzen, M.O., 2022. Chromatographic analysis of oxidized cello-oligomers generated by lytic polysaccharide monooxygenases using dual electrolytic eluent generation. J. Chromatogr. A 1662, 462691. https://doi.org/10.1016/j.chroma.2021.462691.
Payne, C.M., Knott, B.C., Mayes, H.B., Hansson, H., Himmel, M.E., Sandgren, M., Stahlberg, J., Beckham, G.T., 2015. Fungal cellulases. ACS Chem. Rev. 115 (3), 1308–1448. https://doi.org/10.1021/cr500351c.
Praestgaard, E., Elmerdahl, J., Murphy, L., Nymand, S., McFarland, K.C., Borch, K., Westh, P., 2011. A kinetic model for the burst phase of processive cellulases. FEBS J. 278 (9), 1547–1560. https://doi.org/10.1111/j.1742-4658.2011.08078.x.
Quinlan, R.J., Sweeney, M.D., Lo Leggio, L., Otten, H., Poulsen, J.C.N., Johansen, K.S., Krogh, K.B.R.M., Jorgensen, C.I., Tovborg, M., Anthonsen, A., et al., 2011. Insights into the oxidative degradation of cellulose by a copper metalloenzyme that exploits biomass components. PNAS 108 (37), 15079–15084. https://doi.org/10.1073/pnas.1105776108.
Sabbadin, F., Urresti, S., Henrissat, B., Avrova, A.O., Welsh, L.R.J., Lindley, P.J., Csukai, M., Squires, J.N., Walton, P.H., Davies, G.J., et al., 2021. Secreted pectin monooxygenases drive plant infection by pathogenic oomycetes. Science 373 (6556), 774–779. https://doi.org/10.1126/science.abj1342.
Spezio, M., Wilson, D.B., Karplus, P.A., 1993. Crystal structure of the catalytic domain of a thermophilic endocellulase. Biochemistry 32 (38), 9906–9916. https://doi.org/10.1021/bi00089a006.
Stepnov, A.A., Christensen, I.A., Forsberg, Z., Aachmann, F.L., Courtade, G., Eijsink, V.G.H., 2022a. The impact of reductants on the catalytic efficiency of a lytic polysaccharide monooxygenase and the special role of dehydroascorbic acid. FEBS Lett. 596 (1), 53–70. https://doi.org/10.1002/1873-3468.14246.
Stepnov, A.A., Eijsink, V.G.H., Forsberg, Z., 2022b. Enhanced in situ H2O2 production explains synergy between an LPMO with a cellulose-binding domain and a single-domain LPMO. Sci. Rep. 12 (1), 1–11. https://doi.org/10.1038/s41598-022-10096-0.
Tokin, R., Ipsen, Ø.J., Westh, P., Johansen, K.S., 2020. The synergy between LPMOs and cellulases in enzymatic saccharification of cellulose is both enzyme-and substrate-dependent. Biotechnol. Lett. 42, 1975–1984. https://doi.org/10.1007/s10529-020-02922-0.
Uchiyama, T., Uchihashi, T., Ishida, T., Nakamura, A., Vermaas, J.V., Crowley, M.F., Samejima, M., Beckham, G.T., Igarashi, K., 2022. Lytic polysaccharide monooxygenase increases cellobiohydrolases activity by promoting decrystallization of cellulose surface. Sci. Adv. 8 (51), eade5155. https://doi.org/10.1126/sciadv.ade5155.
Vaaje-Kolstad, G., Westereng, B., Horn, S.J., Liu, Z., Zhai, H., Sorlie, M., Eijsink, V.G., 2010. An oxidative enzyme boosting the enzymatic conversion of recalcitrant polysaccharides. Science 330 (6001), 219–222. https://doi.org/10.1126/science.1192231.
Väljamäe, P., Sild, V., Pettersson, G., Johansson, G., 1998. The initial kinetics of hydrolysis by cellobiohydrolases I and II is consistent with a cellulose surface–erosion model. Eur. J. Biochem. 253 (2), 469–475. https://doi.org/10.1046/j.1432-1327.1998.2530469.x.
Vermaas, J.V., Crowley, M.F., Beckham, G.T., Payne, C.M., 2015. Effects of lytic polysaccharide monooxygenase oxidation on cellulose structure and binding of oxidized cellulose oligomers to cellulases. J. Phys. Chem. B 119 (20), 6129–6143. https://doi.org/10.1021/acs.jpcb.5b00778.
Voshol, G.P., Vijgenboom, E., Punt, P.J., 2017. The discovery of novel LPMO families with a new Hidden Markov model. BMC. Res. Notes 10 (1), 105. https://doi.org/10.1186/s13104-017-2429-8.
Vu, V.V., Beeson, W.T., Span, E.A., Farquhar, E.R., Marletta, M.A., 2014. A family of starch-active polysaccharide monooxygenases. PNAS 111 (38), 13822–13827. https://doi.org/10.1073/pnas.1408090111.
Westereng, B., Agger, J.W., Horn, S.J., Vaaje-Kolstad, G., Aachmann, F.L., Stenstrom, Y. H., Eijsink, V.G., 2013. Efficient separation of oxidized cello-oligosaccharides generated by cellulose degrading lytic polysaccharide monooxygenases. J. Chromatogr. A 1271 (1), 144–152. https://doi.org/10.1016/j.chroma.2012.11.048.
Wood, T. M. (1988). Preparation of crystalline, amorphous, and dyed cellulase substrates. In vol. 160 *Methods Enzymol*, pp. 19-25: Elsevier.
Zamocky, M., Schumann, C., Sygmund, C., O'Callaghan, J., Dobson, A.D., Ludwig, R., Haltrich, D., Peterbauer, C.K., 2008. Cloning, sequence analysis and heterologous expression in Pichia pastoris of a gene encoding a thermostable cellobiose dehydrogenase from Myriococcum thermophilum. Protein Expr. Purif. 59 (2), 258–265. https://doi.org/10.1016/j.pep.2008.02.007.

Supplementary material

Lytic polysaccharide monooxygenase activity increases productive binding capacity of cellobiohydrolases on cellulose

Camilla F. Angeltveit[1], Tina Jeoh[2], Svein J. Horn[1*]

[1]Faculty of Chemistry, Biotechnology, and Food Science, Norwegian University of Life Sciences (NMBU), Ås, Norway

[2]Biological and Agricultural Engineering, University of California, Davis, United States

[*] Corresponding author, e-mail address: svein.horn@nmbu.no

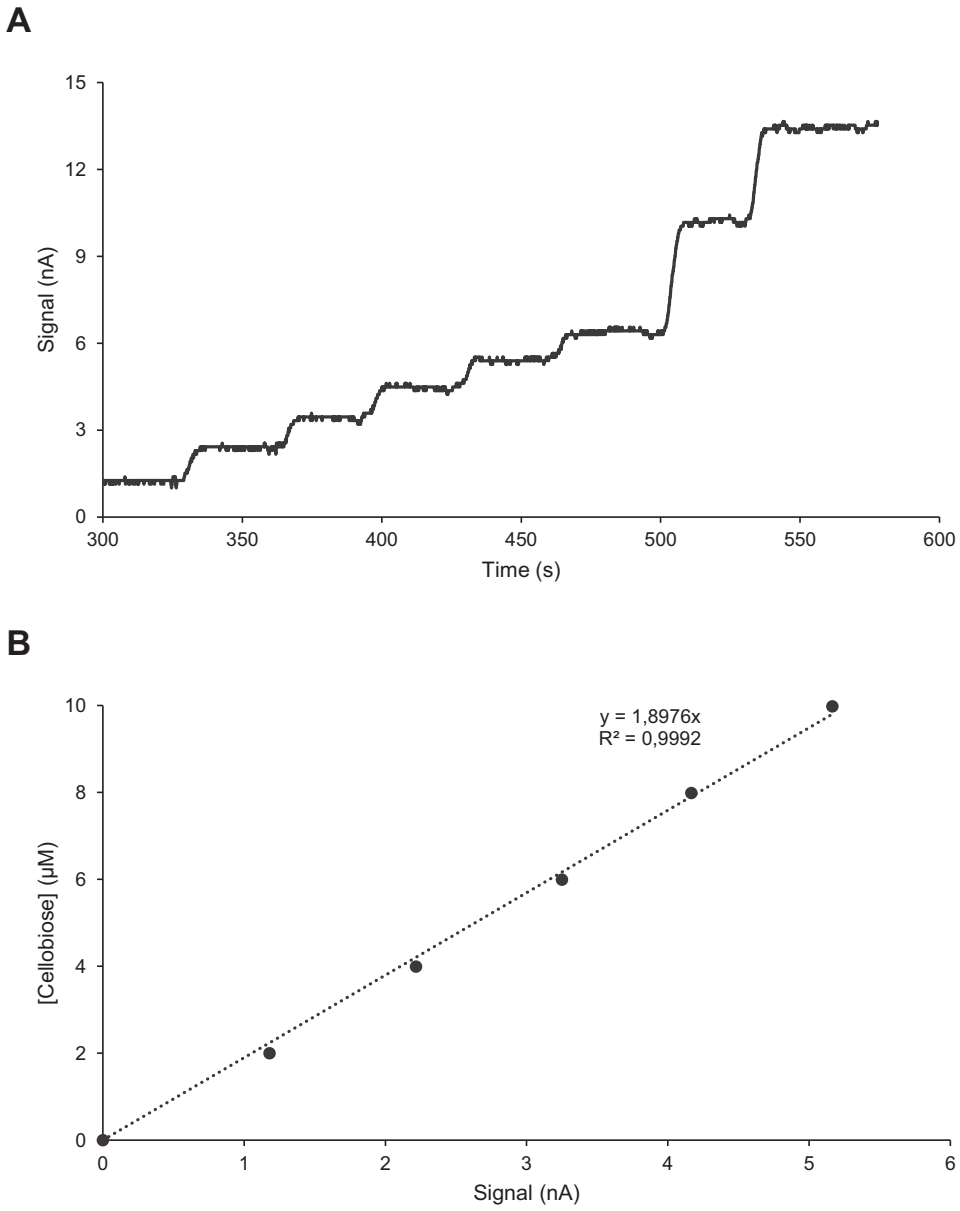

Figure S1. Calibration of CDH working electrode with cellobiose. (**A**) Raw data from the injection of 2 µM β-cellobiose five times, followed two injections of by 10 µM β-cellobiose, each injection corresponding to a stair in the staircase. (**B**) The calibration curve from 0 to 10 µM β-cellobiose vs signal (nA).

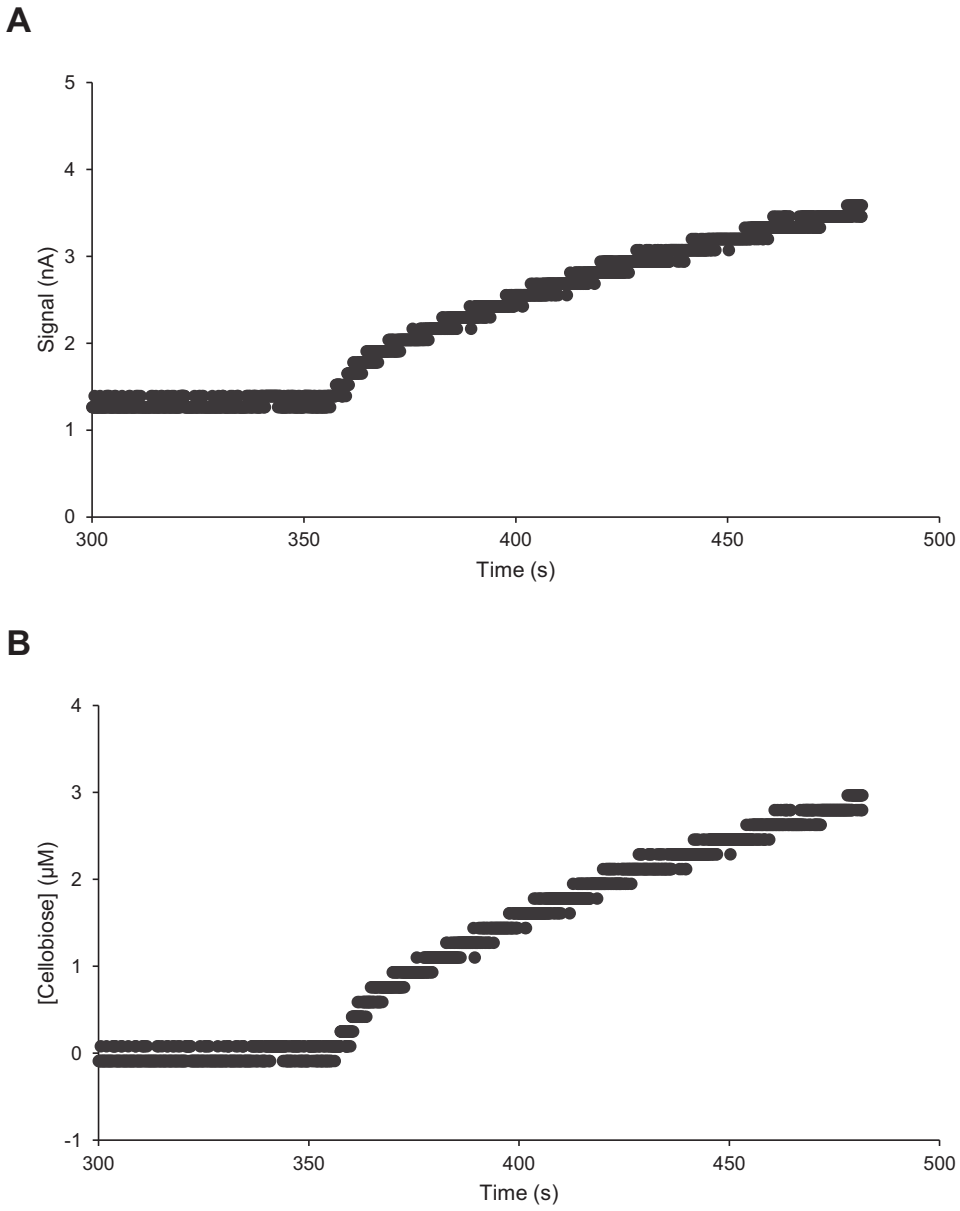

Figure S2. Biosensor measurement of LPMO pretreated Avicel**.** (**A**) Biosensor measurements of *Tl*CBHI added to Avicel (0.5 g/L) pretreated with *Sc*AA10C (100 nM) for 24 hours in 50 mM NaOAc pH 5.0 at 50°C. (**B**) The signal from Panel A converted into the corresponding cellobiose concentration vs time by using the standard curve in **Figure S1**.

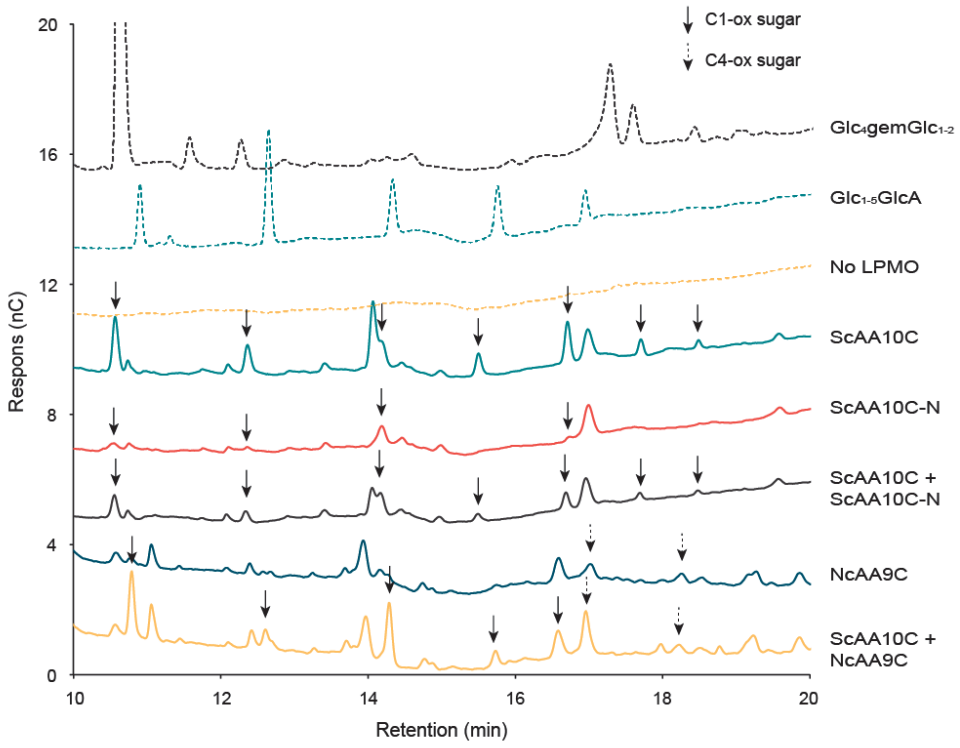

Figure S3. Soluble oxidized sugar profiles from 24 hours of LPMO pretreatment. C1 oxidized products are marked with solid arrows, while C4 oxidized products are marked with dotted arrows. A control reaction without LPMO, C1-oxidized standard showing 0.001 g/L $Glc_{1-5}GlcA$, and C4-oxidized standard showing 0.005 g/L $Glc_4gemGlc_{1-2}$ are included.

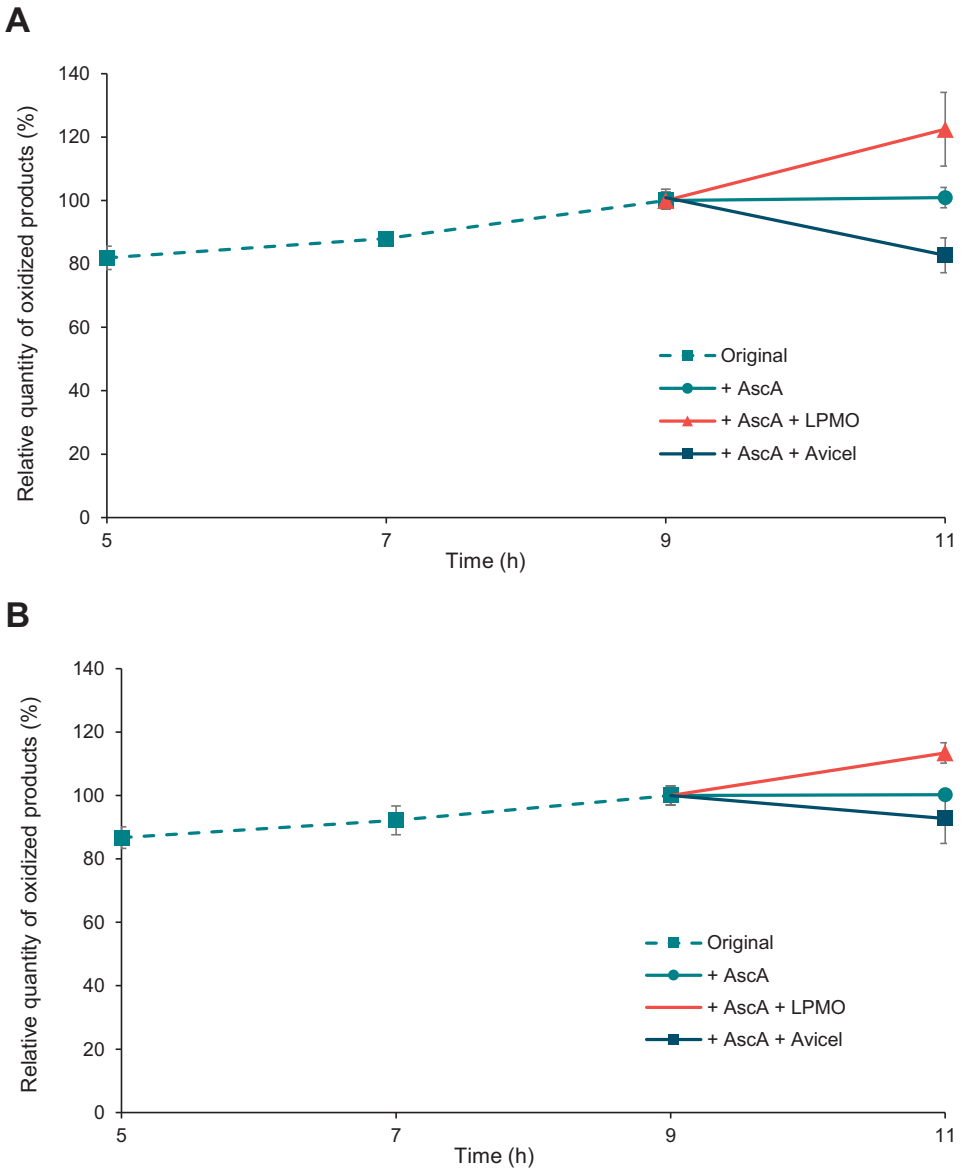

Figure S4. Reactivation of reactions with *Sc*AA10C together with *Sc*AA10C-N or *Nc*AA9C after ceased LPMO activity. (**A**) Reactivation of the *Sc*AA10C + *Sc*AA10C-N or (**B**) *Sc*AA10C + *Nc*AA9C reaction (from **Figure 4A**) by supplementing the reactions with 1 mM ascorbic acid, either alone or with fresh LPMO or Avicel after 9 hours reaction time. The change in oxidized sugars is shown as the relative product formation, where 100% is the level after 9 hours. Standard deviation is shown as error bars from three biological replicates.

Paper II

Enhancing enzymatic saccharification yields of cellulose at high solid loadings by combining different LPMO activities

Angeltveit CF, Várnai A, Eijsink VGH & Horn SJ

Angeltveit *et al.*
Biotechnology for Biofuels and Bioproducts (2024) 17:39
https://doi.org/10.1186/s13068-024-02485-6

Biotechnology for Biofuels and Bioproducts

RESEARCH

Open Access

Enhancing enzymatic saccharification yields of cellulose at high solid loadings by combining different LPMO activities

Camilla F. Angeltveit[1], Anikó Várnai[1], Vincent G. H. Eijsink[1] and Svein J. Horn[1*]

Abstract

Background The polysaccharides in lignocellulosic biomass hold potential for production of biofuels and biochemicals. However, achieving efficient conversion of this resource into fermentable sugars faces challenges, especially when operating at industrially relevant high solid loadings. While it is clear that combining classical hydrolytic enzymes and lytic polysaccharide monooxygenases (LPMOs) is necessary to achieve high saccharification yields, exactly how these enzymes synergize at high solid loadings remains unclear.

Results An LPMO-poor cellulase cocktail, Celluclast 1.5 L, was spiked with one or both of two fungal LPMOs from *Thermothielavioides terrestris* and *Thermoascus aurantiacus, Tt*AA9E and *Ta*AA9A, respectively, to assess their impact on cellulose saccharification efficiency at high dry matter loading, using Avicel and steam-exploded wheat straw as substrates. The results demonstrate that LPMOs can mitigate the reduction in saccharification efficiency associated with high dry matter contents. The positive effect of LPMO inclusion depends on the type of feedstock and the type of LPMO and increases with the increasing dry matter content and reaction time. Furthermore, our results show that chelating free copper, which may leak out of the active site of inactivated LPMOs during saccharification, with EDTA prevents side reactions with in situ generated H_2O_2 and the reductant (ascorbic acid).

Conclusions This study shows that sustaining LPMO activity is vital for efficient cellulose solubilization at high substrate loadings. LPMO cleavage of cellulose at high dry matter loadings results in new chain ends and thus increased water accessibility leading to decrystallization of the substrate, all factors making the substrate more accessible to cellulase action. Additionally, this work highlights the importance of preventing LPMO inactivation and its potential detrimental impact on all enzymes in the reaction.

Keywords Lytic polysaccharide monooxygenase, LPMO, AA9, Cellulolytic enzyme cocktails, Enzymatic saccharification, Inactivation, Hydrogen peroxide, High-solids effect

Background

There is a critical need for technology that allows efficient utilization of renewable resources like lignocellulosic biomass to combat the environmental effects of human fossil fuel consumption. Lignocellulosic plant biomass is a ubiquitous source of the carbohydrate polymers cellulose and hemicellulose, which may be depolymerized to yield fermentable sugars that can be converted to biofuels and value-added chemicals [1]. Efficient depolymerization of these polysaccharides is hampered by the recalcitrant structure of plant cell walls. At the same time, efficient production of concentrated sugar syrups is essential for cost-effective conversion of lignocellulosic biomass into valuable products [2–5]. Performing enzymatic

*Correspondence:
Svein J. Horn
svein.horn@nmbu.no
[1] Faculty of Chemistry, Biotechnology, and Food Science, Norwegian University of Life Sciences (NMBU), Ås, Norway

saccharification processes efficiently at elevated solid loadings is pivotal in reducing the overall expenses associated with lignocellulosic biorefineries, thereby enhancing the feasibility of lignocellulose valorization.

Performing enzymatic saccharification at high dry matter (DM) levels is known to hamper yields and conversion rates, an effect that is referred to as "the high-solids effect" [6]. A high DM content refers to a situation in which little-to-no free water is present at the beginning of a reaction, meaning that the substrate holds all the water [4, 7]. The amount of free water will depend on the substrate composition and pretreatment methods. However, a DM content of 15–20% (w/w) is typically considered "high" [2]. Several studies employing commercial enzyme cocktails predominantly composed of endo- and exo-acting cellulases have demonstrated a linear reduction in the enzymatic conversion yield with increasing substrate concentration [6, 8–14].

A direct consequence of elevated solid loadings is increased slurry viscosity, which hampers adequate mixing. Additional challenges arise from non-productive cellulase adsorption to phenolic compounds [15, 16], enzyme inhibition by compounds like furan derivatives formed during commonly used pretreatment methods such as steam explosion [16], and feedback inhibition of cellobiohydrolases or β-glucosidases (BGs) due to the accumulation of cellobiose or glucose, respectively [17, 18]. Nevertheless, recent literature suggests that water constraints are the most prominent contributor to the high-solids effect [2, 5, 19]. Water has multiple roles during enzymatic saccharification: it functions as a solvent facilitating the contact between enzymes and their substrate, it acts as a reactant during hydrolysis, and it is responsible for the diffusion of products from the site of enzymatic reaction [20]. Despite efforts in the last decades, the challenges posed by high-solids conditions remain a subject of ongoing studies.

Lytic polysaccharide monooxygenases (LPMOs) were discovered in 2010 [21] and are included in current commercial cellulase cocktails [22]. LPMOs are copper-dependent redox enzymes that require a priming reduction and an oxygen species as co-substrate [21], most probably H_2O_2 [23], to perform catalysis. The reduced LPMO-Cu(I) complex will oxidatively break the scissile glycosidic bond in cellulose, leading to the formation of an aldonic acid or gemdiol-aldose for C1- or C4-oxidizing LPMOs, respectively [24, 25]. LPMOs are prone to non-reversible inactivation in the presence of excess H_2O_2 [23], which can lead to release of the active-site copper that may fuel transition metal-dependent futile side reactions, such as abiotic oxidation of reducing compounds [26, 27]. Numerous studies have shown that LPMOs improve the efficiency of classical hydrolytic cellulases, likely due to LPMOs' ability to attack the more crystalline parts of the polysaccharide substrate [28–34].

Several studies have tried to shed light on the mechanism behind the synergistic relationship between LPMOs and cellulases [34–39], one important outcome being that the oxidative regioselectivity of the LPMOs plays a role. For example, C1-oxidizing LPMOs tend to synergize well with processive cellulases attacking the non-reducing-end, while C4-oxidizing LPMOs seem to have a better effect when combined with cellulases attacking the reducing ends of the cellulose chains [35, 38]. A recent study has shown that the LPMO effect may not be as "direct" as initially suggested. Studies of the effects of LPMO pretreatments showed that the chain ends introduced by LPMO action do not necessarily serve as immediate access points for cellulases. Instead, it was suggested that LPMO promotes time-dependent decrystallization of the substrate that improves accessibility for the classical hydrolytic enzymes [40]. Indeed, several studies support the notion that LPMO action promotes decrystallization of cellulose [41–44]. Recently, Cannella et al. [45] showed that oxidation of filter paper with an LPMO, or chemically, using TEMPO [(2,2,6,6-tetramethylpiperidin-1-yl)oxyl] increases the amount of water retained by the fibers, due to the increased negative surface charge. Thus, LPMO activity will increase the hydrophilicity and water content of the substrate, which could help mitigate the negative effects of high DM conditions on cellulase performance.

While the impact of LPMOs on the efficiency of cellulolytic enzyme cocktails has been studied extensively, little is known about the effect of the DM level and the role LPMOs may play in counteracting the high-solids effect. It is important to note that water availability depends on the DM content and, therefore, that saccharification performances cannot be directly compared across low and high DM experiments [19]. The effect of DM loading (1–15%) on AA9 LPMO activity was recently shown to vary a lot depending on the type of LPMO. Some LPMOs gave more product release as DM content was increased, while other LPMOs seemed to be substrate saturated and even inhibited at high DM [44]. To gain more insight into these matters, in this study, a commercial LPMO-poor enzyme cocktail, Celluclast 1.5L, was spiked with two different fungal AA9 LPMOs, C1-oxidizing *Tt*AA9E from *Thermothielavioides* (previously *Thielavia*) *terrestris* and predominantly C4-oxidizing *Ta*AA9A from *Thermoascus aurantiacus* to investigate the impact of LPMOs on cellulose saccharification at elevated DM concentrations. Using various experimental setups, we show that LPMOs are increasingly important for saccharification efficiency at higher substrate concentrations, notably in a manner that varies between LPMOs and substrates. We also show

the importance of preventing LPMO inactivation, not only because LPMO activity is needed, but also because copper leaking out of inactivated LPMOs [27, 46] facilitates unfavorable side reactions.

Methods

Steam-exploded wheat straw

Steam-exploded wheat straw was provided by Novozymes. The compositional analysis was performed based on the standard operating procedure developed by NREL [47] and is shown in Table 1. The DM content was measured using Karl Fischer titration as described elsewhere [48] and found to be 52% (w/w). The substrate was stored at − 20 °C.

Enzymes

*Ta*AA9A from *Thermoascus aurantiacus* and *Tt*AA9E from *Thermothielavioides (*previously *Thielavia) terrestris*, as well as Celluclast 1.5 L, NZ-BG (a β-glucosidase preparation), and Cellic CTec2 were kindly supplied by Novozymes (Novozymes, Bagsværd, Denmark). The protein concentrations were determined using the Bradford method with BSA (Sigma-Aldrich, St. Louis, MO, USA) as standard. Both LPMOs were copper saturated as described previously [49], followed by desalting using a PD MidiTrap column (G-25; GE Healthcare, Chicago, IL, USA). All enzymes were stored at 4 °C.

Standard reaction setup

The enzyme dosage was held constant at 4 mg protein per g substrate for all reactions. Reactions without LPMO were performed with Celluclast 1.5 L and NZ-BG in a 9:1 ratio (protein:protein). For the reactions supplemented with LPMO, the LPMO constituted 10% of the total protein dose (i.e., 0.4 mg/g substrate). The BG dose was held at 10% of total protein (0.4 mg/g substrate) in all reactions to ensure the complete conversion of cellobiose to glucose. Thus, Celluclast 1.5 L represented 80% of the protein (3.2 mg/g substrate) in reactions with added LPMO and 90% (3.6 mg/g substrate) in reactions without added LPMO. Reactions with Cellic CTec2 were performed without addition of BG at 4 mg protein per g substrate.

The substrates were microcrystalline cellulose (Avicel PH-101, 50 µm particles; Sigma-Aldrich) or steam-exploded wheat straw and reactions were run at 5–25% (w/w) DM concentrations in 50 mM sodium acetate buffer (Sigma-Aldrich), pH 5.0. If not specified otherwise, 10 mM ascorbic acid (Sigma-Aldrich) was added at the beginning of all reactions with Avicel. Glucose feedback inhibition of enzyme cocktails was probed by adding 2.5, 5.0, or 10% (w/w) glucose (Sigma-Aldrich) at the start of the reaction in addition to the cellulose substrate.

Reaction termination and dilution

All time points (5, 24, 48, and 72 h) were run as individual reactions in 2 mL Eppendorf tubes with 0.6 mL reaction volume in an Eppendorf Thermomixer (Eppendorf, Hamburg, Germany) at 50 °C and 1000 rpm. The reactions were terminated by boiling the samples at 100 °C for 20 min before samples were diluted to 1% DM (w/w) by transferring the whole reaction slurry to 15 mL Falcon tubes and diluting with sodium acetate buffer [6] to minimize errors associated with the higher DM contents [3]. Afterward, the samples were thoroughly mixed, 250 µL of each were filtered with a 96-well filter plate (0.2 µm; Sigma-Aldrich), and filtrates were stored at 4 °C before further analysis.

Cellulase inactivation by abiotic reactions

A mixture of Celluclast 1.5 L and NZ-BG (9:1 ratio, 0.6 mg protein in total) was preincubated in 50 mM sodium acetate buffer pH 5.0 at 50 °C and 1000 rpm for 24 h in an Eppendorf Thermomixer together with externally added 10 mM H_2O_2 (Sigma-Aldrich), 10 mM ascorbic acid, or 0.63 mM Cu(II)SO_4. The effects of different combinations of H_2O_2 or ascorbic acid with Cu(II) and EDTA (6.3 mM; Sigma-Aldrich) were also tested. After the preincubation, the saccharification reaction was initiated by transferring the preincubated cellulase cocktail (450 µL) to Eppendorf tubes containing 150 mg Avicel, yielding a reaction mixture with 25% DM (w/w) and 4 mg protein per gram of substrate. The saccharification reactions were run at the same conditions as for the preincubation reactions for 24 and 48 h after which they were terminated as described above.

Analysis of soluble native and oxidized sugars

Glucose levels were analyzed by high-performance liquid chromatography (HPLC) using a Dionex Ultimate 3000 (Dionex, Sunnyvale, CA, USA) connected to a refractive index detector 101 (Shodex, Japan) as described previously [29]. The analytical column was a Rezex

Table 1 Composition of steam-exploded wheat straw

Ash	Arabinan	Galactan	Glucan	Xylan	Mannan	Total lignin
7.70	1.62	0.71	47.48	19.19	0.33	22.51

ROA-organic acid H+(8%) 300×7.8 mm (Phenomenex, Torrance, CA, USA), the eluent was 5 mM H_2SO_4, the operating temperature was 65 °C, and the flow rate was 0.6 mL/min. Soluble oxidized sugars (Glc1A, Glc4gemGlc and Glc4gemGlc$_2$) were quantified by high-performance anion exchange chromatography with pulsed amperometric detection (HPAEC-PAD) using a Dionex ICS-5000 (Dionex) equipped with a CarboPac PA200 column, as previously described [50, 51]. An eluent gradient from 0 to 100% B (A: 100 mM NaOH; B: 1 M NaOAc+100 mM NaOH), an operational flow of 500 µL/min, and a sample loop volume of 5 µL were used, as described previously [51]. The results were analyzed using the Chromeleon 7 software program (Dionex).

Standards of glucose, cellobiose, and gluconic acid (C1-oxidized, DP1) were purchased from Sigma-Aldrich and diluted as appropriate. Cellobionic and cellotrionic acid (C1-oxidized, DP2-3) [52] and C4-oxidized standards of DP2-3 [29, 51] were produced as described previously using *Mt*CDH from *Myriococcum thermophilum* [52] or *Nc*AA9C from *Neurospora crassa* [53] respectively.

Statistical analysis

The statistical analysis was performed with a two-tailed Student's t-test using Microsoft Excel (Office 365).

Results and discussion

The role of LPMOs at different cellulose concentrations

Enzymatic saccharification experiments using Celluclast 1.5 L (supplemented with a β-glucosidase, NZ-BG) with or without LPMOs were run at five different cellulose (Avicel) concentrations ranging from 5 to 25% (w/w). The overall glucose conversion in the reactions with only the cellulolytic enzyme cocktail (90% Celluclast 1.5 L+10% NZ-BG) decreased with the increasing DM content, and this effect was visible both after 5 and 24 h of saccharification (Fig. 1). Interestingly, for reactions with added LPMOs (80% Celluclast 1.5 L+10% NZ-BG+10% LPMO), the high-solids effect was less pronounced after 24 h, as can be seen by comparing the blue and gray line with the orange line in Fig. 1B. This result shows that the importance of the LPMO increases with increasing DM concentrations and saccharification time (Fig. 1), as observed previously [45, 54]. Remarkably, at the lowest substrate concentration (5%), supplementing the cellulolytic enzyme cocktail with LPMOs decreased glucan conversion after 24 h substantially (by about one-third) (Fig. 1B). This result is noteworthy, since it provides an "extreme" illustration of how strongly LPMO effects depend on reaction conditions.

After 5 h of reaction, the concentration of soluble oxidized LPMO products was highest in the 10 and 15% (w/w) DM reactions. Reactions with higher cellulose concentrations yielded lower concentrations of soluble oxidized sugars (Fig. 2A, B), which could reflect lower LPMO activity or, more likely, that a larger fraction of the oxidized sites remains bound to the substrate (as expected based on the work of Courtade et al. [55]). Similar results have been shown recently for different DM concentrations of cellulose nano-crystals (1–15%), although Magri et al. observed a maximum release of soluble oxidized sugar at 5% DM for the same LPMOs used in our study [44]. However, these experiments were done with LPMOs alone (i.e., no presence of cellulases). Additionally, a recent study has shown that the LPMO oxidation profiles also vary depending on the substrate type [56]. Thus, the results cannot be compared directly.

The ratio of solubilized glucose to solubilized oxidized sugars after 5 h increases with increased DM (Fig. 2C). For the reaction containing *Tt*AA9E, the glucose-to-oxidized sugar ratio increased from 60 to 150 (i.e., approximately 0.7–1.7% of the soluble sugar were oxidized), while for the *Ta*AA9A-containing reaction, the ratio increased from 120 to 260 (i.e., approximately 0.4–0.8% of the soluble sugar were oxidized) when increasing the substrate concentration from 5 to 25% (w/w) (Fig. 2C). After longer incubation, i.e., at 24 h, the concentration of soluble LPMO products (Fig. 2A, B) followed the trends of the glucose concentration (Fig. 1B), meaning that the levels of solubilized oxidized products increased with DM and that the glucose-to-oxidized sugar ratios did not vary much with DM (around 100 for all reactions, i.e., approximately 1% of the soluble sugars were oxidized; Fig. 2D). The fraction of oxidized sugars are similar to that reported in a recent study by Cannella et al. [45], which also observed that the ratio of oxidized to native sugars increased at longer incubation times than 24 h at higher DM levels (10–25%), while the ratio remained stable at the lower DM levels (5%). Although these effects depend on multiple interrelated factors, such as solubilization effects and substrate concentration-dependent effects on LPMO stability, the trends in the levels of soluble oxidized products after 24 h that are visible in Fig. 2 align well with the notion, derived from Fig. 1, that the importance of LPMOs increases at higher DM levels.

In the early stages of saccharification, cellulases work on easily accessible regions of the polysaccharide substrate. As the reaction progresses, the remaining substrate becomes more recalcitrant, exposing regions that are more resistant to enzymatic attack. It is generally believed that LPMOs help break down these recalcitrant structures by introducing oxidative modifications, creating new sites of accessibility that enable cellulases and other enzymes to continue degrading the substrate. Importantly, recent studies indicate that

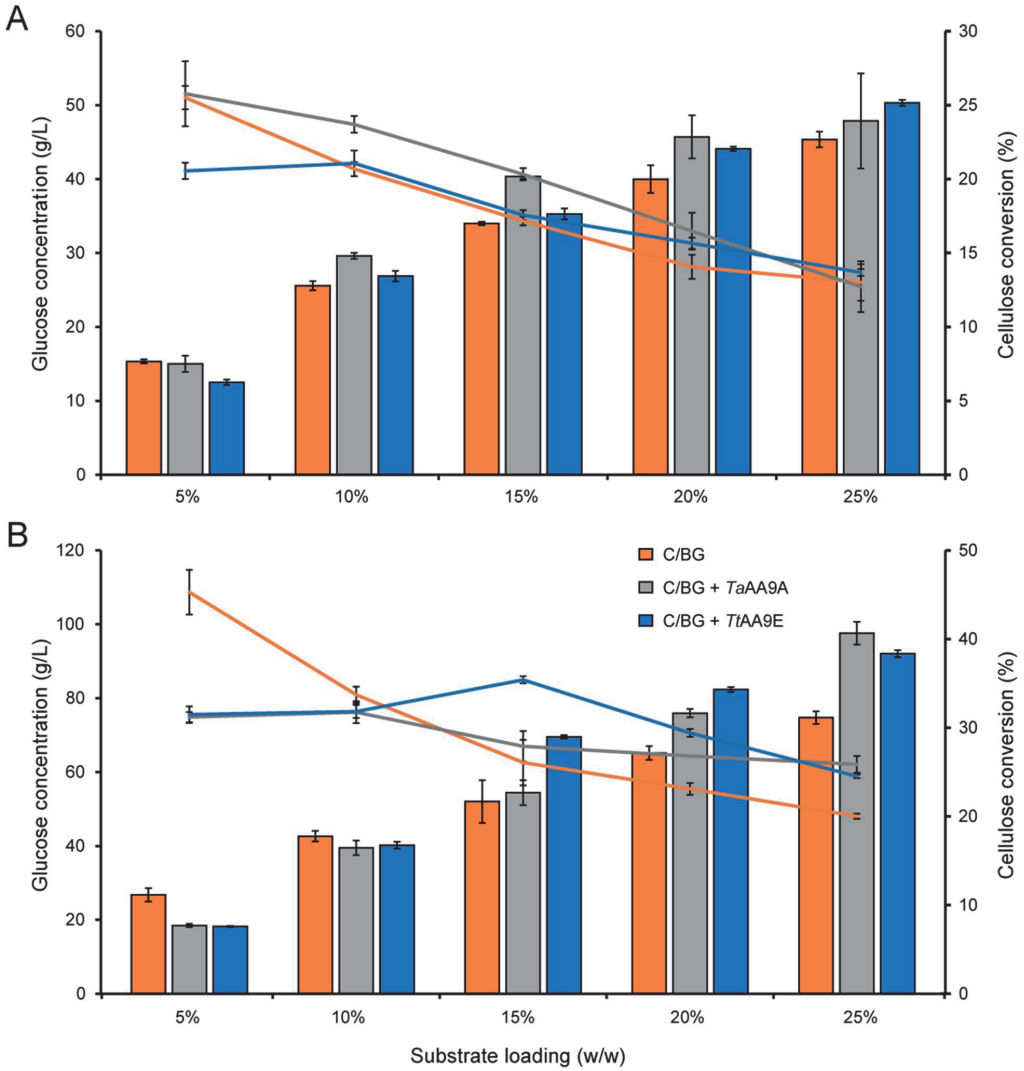

Fig. 1 The impact of LPMO supplementation on cellulose saccharification at increasing solids loading. Saccharification reactions containing 5–25% (w/w) Avicel were set up with 3.6 mg/g of Celluclast 1.5 L + 0.4 mg/g NZ-BG or with 3.2 mg/g Celluclast 1.5 L + 0.4 mg/g NZ-BG + 0.4 mg/g *Ta*AA9A or *Tt*AA9E. All reactions contained 10 mM AscA as reductant. Bars represent the glucose release in g/L (left y-axis), and lines show the percentage of cellulose conversion (right y-axis) after 5 (**A**) and 24 h (**B**). Standard deviations for three biological replicates are shown as error bars

the LPMO–cellulase synergism may be more complex than creating access points [40–43, 45]. The cleavage of a glycosidic bond and concomitant oxidation of the cleavage point allows surrounding water molecules to access the highly ordered fibril structure, leading to decrystallization and amorphization over time [45]. The extent of these larger, and potentially slower, effects will likely vary between C1- and C4-oxidizing LPMOs. Generation of aldonic acids (C1 oxidation) is thought to have the largest effect due to the open ring structure allowing more water to penetrate the crystalline structure [41–43]. On the other hand, recent work

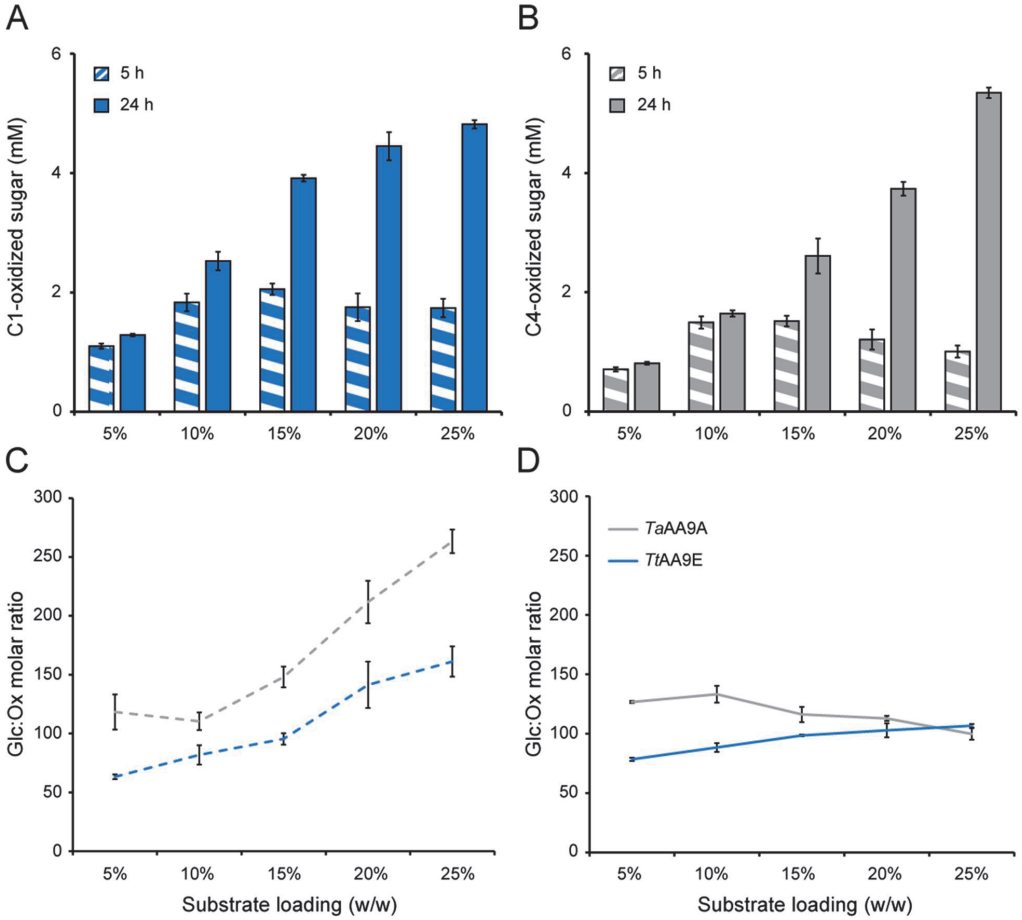

Fig. 2 Release of oxidized sugars during saccharification of Avicel at increasing dry matter concentrations. The figure shows the formation of soluble oxidized products in the reactions shown in Fig. 1. Panel **A** shows the soluble C1-oxidized products formed by *Tt*AA9E; panel **B** shows the soluble C4-oxidized products formed by *Ta*AA9A. Panels **C** and **D** show the molar ratio of glucose (from Fig. 1) to total soluble oxidized sugar after 5 and 24 h, respectively. Standard deviations are shown as error bars, for three biological replicates

by Angeltveit has shown that, with time, the increase in overall accessibility of the substrate for the traditional hydrolytic enzymes will be governed by a time-dependent non-enzymatic decrystallization phase that follows the oxidative action of LPMOs and that does not clearly depend on the oxidative regiospecificity of the enzymes [40]. This aligns with our data showing a significant LPMO effect after 24 h for both the C1- and C4-active LPMOs.

Increased saccharification efficiency by combining *Tt*AA9E and *Ta*AA9A activity

The highest DM content, 25% (w/w), was selected for experiments to investigate the impact of supplementing the reactions with varying ratios of the C1-active (*Tt*AA9E) and the predominantly C4-active (*Ta*AA9A) LPMOs in 72 h reactions with sampling after 5 h and every 24 h. Figure 3A shows a clear positive effect of LPMO inclusion on saccharification yield, with a

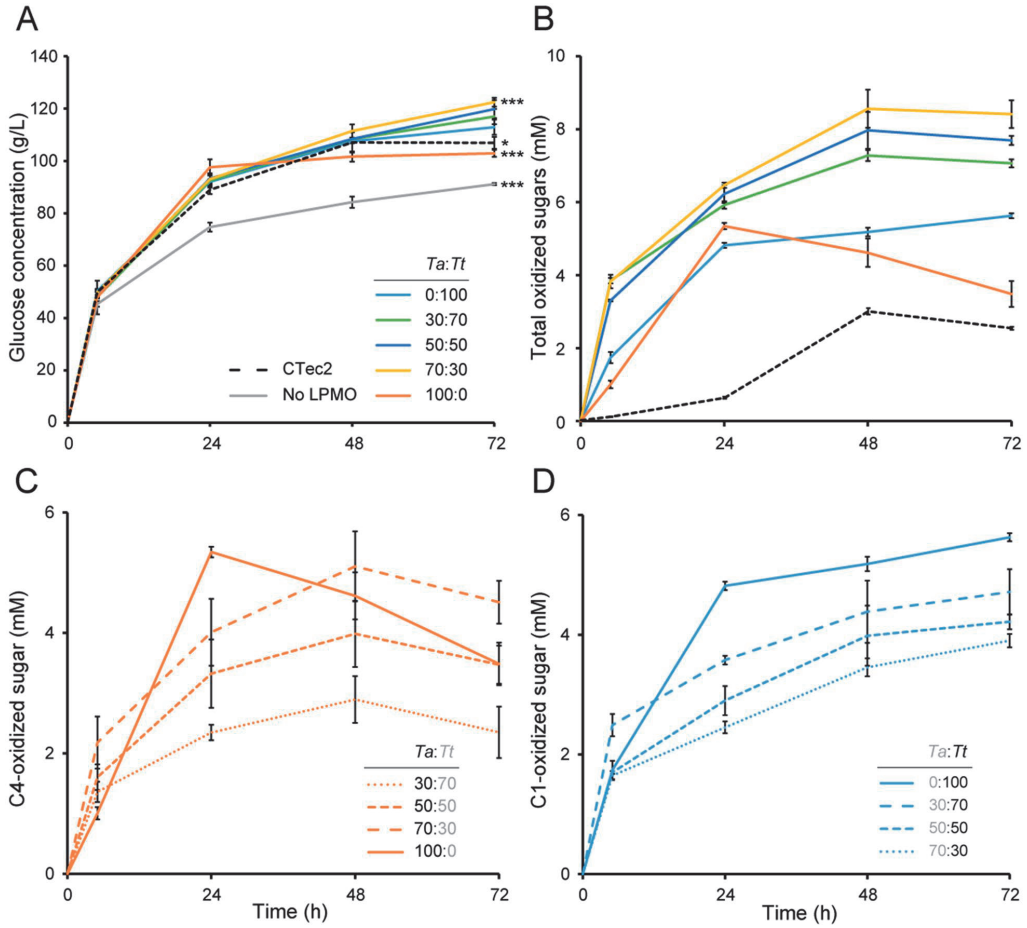

Fig. 3 Saccharification of Avicel with LPMO-containing cellulase cocktails at high dry matter. In the reactions, 25% (w/w) Avicel was incubated with either 3.2 mg/g Celluclast 1.5 L + 0.4 mg/g NZ-BG + 0.4 mg/g LPMO (*Ta*AA9A and *Tt*AA9E in varying ratios), or 3.6 mg/g Celluclast 1.5 L + 0.4 mg/g NZ-BG, or 4 mg/g Cellic CTec2. All reactions contained 10 mM AscA as reductant. Panel **A** shows the glucose release; panel **B** shows the total release of oxidized sugars, which is the sum of C4-oxidized products generated by *Ta*AA9A (**C**) and C1-oxidized products generated by *Tt*AA9E (**D**). The symbols * and *** in panel **A** indicate significant differences ($p \le 0.05$ and $p \le 0.01$, respectively) between the cellulase cocktail spiked with *Tt*AA9E only (0:100) and the other enzyme combinations after 72 h (by Student's t-test). Soluble oxidized products were not detected in the reactions without LPMO. Standard deviations are shown as error bars, for three biological replicates

maximum 38% increase when combining Celluclast 1.5 L with both LPMOs in a 7:3 ratio (*Ta*AA9A:*Tt*AA9E). Early work done prior to the discovery that LPMOs are redox enzymes has shown that each of these LPMOs improves the saccharification of pretreated corn stover, with *Ta*AA9A being the better enzyme [22]. Our results show that, for Avicel, *Tt*AA9E outperforms *Ta*AA9A. It is also worth noting that Celluclast 1.5 L supplemented with any *Tt*AA9E-containing LPMO mixture depolymerized Avicel more efficiently than the more modern LPMO-containing cellulase cocktail Cellic CTec2 (Fig. 3A, B).

The reaction with Celluclast 1.5 L and C4-active *Ta*AA9A showed peculiar kinetics: maximum glucose levels were reached after 24 h (Fig. 3A), and the concentration of C4-oxidized products started declining after 24 h (Fig. 3C). The latter indicates LPMO inactivation and concomitant release of free copper from the active site of oxidatively damaged LPMOs into solution [27].

Under such conditions, i.e., increased availability of H_2O_2 due to copper-catalyzed abiotic oxidation of the reductant and accumulation of this H_2O_2 because the LPMO no longer consumes it, the C4-oxidized products are unstable and degrade [28]. In reactions with *Tt*AA9E, the levels of C1-oxidized products kept increasing after 24 h (Fig. 3D), indicating that this enzyme stays active longer. In general, LPMO inactivation happens faster at low substrate concentrations [55]. The apparent difference in kinetics and levels of inactivation could be a direct consequence of differences in enzyme stabilities of the two LPMOs or a result of different substrate-binding preferences and thus the experience of different effective substrate concentrations during the reactions. Combining *Tt*AA9E with *Ta*AA9A (and the cellulases) led to an apparent delay in the degradation of C4-oxidized oligosaccharides (Fig. 3C), indicating a moderate stabilizing effect of *Tt*AA9E on *Ta*AA9A for example because *Tt*AA9E still can productively consume available H_2O_2. Overall, our data indicate that co-supplementation of *Tt*AA9E and *Ta*AA9A is beneficial, because it leads to less LPMO inactivation and a higher saccharification efficiency.

The role of LPMOs in enzyme inactivation

In the absence of lignin, like in our reactions with Avicel, LPMOs rely on H_2O_2 produced in situ either from abiotic oxidation of the reductant or from the reaction of reduced LPMOs in solution with oxygen [53, 57]. Free (i.e., not substrate-bound) reduced LPMOs lose their activity over time due to oxidative damage to the catalytic site that results from a peroxidase reaction, i.e., futile turnover of H_2O_2 [23, 58]. Thus, LPMO stability during a reaction depends on a combination of the level of available H_2O_2 and the effective substrate concentration. Of note, when using reductants whose abiotic oxidation is promoted by transition metals such as copper, such as ascorbic acid, LPMO inactivation may be a self-reinforcing process [27]: damage to the catalytic center leads to copper release, which again promotes production of H_2O_2, which again promotes LPMO inactivation.

Considering the above, we tested whether it could be beneficial to delay reduction of LPMOs and generation of H_2O_2 by adding ascorbic acid at specific time points later than 0 h, thus increasing the chance of keeping the LPMOs functional during the later phase of the reaction. The results show that, for the setup used here, delaying the reduction of the LPMOs was not beneficial (Fig. 4). Addition of ascorbic acid at the beginning of the reaction gave, as expected, the fastest initial glucose solubilization. Solubilization yields after 72 h were similar for reactions in which ascorbic acid was added at 0 or 24 h and reduced for the reaction in which ascorbic acid was added after 48 h. These results support the theory of a time-dependent amorphization of the material following the LPMO oxidation rather than the direct creation of access points, and hence, overall making the substrate more accessible for the cellulases.

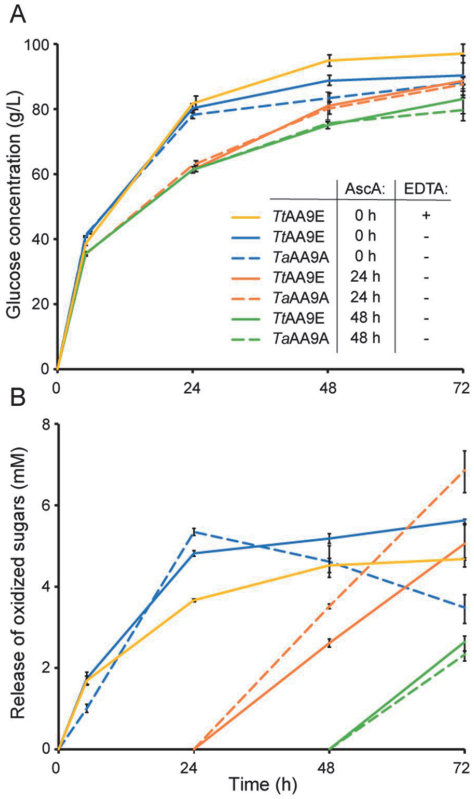

Fig. 4 Initiating LPMO activity by adding ascorbic acid at different time points. In the reactions, 25% (w/w) Avicel was incubated with 3.2 mg/g Celluclast 1.5 L + 0.4 mg/g NZ-BG + 0.4 mg/g of either *Ta*AA9A or *Tt*AA9E. The LPMO activity was initiated by adding AscA (10 mM) at different time points. If added, EDTA was present at 6.3 mM. Panel **A** shows glucose release; panel **B** shows the release of soluble oxidized sugars. Standard deviations are shown as error bars, for three biological replicates

Non-sufficient removal of unbound copper from the LPMO preparation after copper saturation, "copper-polluted" substrates, and copper leakage from the active site of inactivated LPMOs will influence the activity and inactivation of LPMOs [27, 46, 59]. Copper will speed up production of H_2O_2 through abiotic oxidation of ascorbic acid [60] and production of hydroxyl radicals through Fenton-like reactions [61]. To assess possible copper

effects, we used ethylenediaminetetraacetic acid (EDTA), which is a good chelator and, hence a scavenger of divalent metal cations such as Cu(II). The dissociation constant for Cu(II) binding by EDTA is between 10^{-6} M and $3.1 \cdot 10^{-16}$ M [62], i.e., quite similar to published K_d values for LPMOs, which are in the order of 1 nM for Cu(I) and 50 nM for Cu(II) [63–65]. Addition of 6.3 mM EDTA to a reaction with Celluclast 1.5 L and *Tt*AA9E led to a slight decrease in apparent LPMO activity (Fig. 4B), which may be due to reduced levels of available H_2O_2 as a result of reduced levels of transition metals in the reaction solution. Interestingly, despite the lower LPMO activity, the presence of EDTA was beneficial for the overall saccharification yield after 48 h; however, no significant effect was observed after 72 h (Fig. 4A). This suggests that chelation of free copper by EDTA may play a role in preventing additional side reactions that otherwise would damage the enzymes during the course of the reaction.

To gain a deeper insight into the potential impact of abiotic reactions involving ascorbic acid, H_2O_2, and free copper on the inactivation of cellulases, Celluclast 1.5 L was preincubated with various combinations of ascorbic acid, H_2O_2, Cu(II)SO_4, and EDTA for 24 h before initiating a saccharification reaction by the addition of Avicel. In general, no significant effects from preincubation with 10 mM H_2O_2, 10 mM ascorbic acid, or 0.63 mM Cu(II) alone were observed, except for the 24 h reaction with H_2O_2 pretreatment and the 48 h reaction with Cu(II) pretreatment (Fig. 5). However, when H_2O_2 or ascorbic acid was combined with Cu(II) during the preincubation, the 24 h conversion yield dropped to only 18% and 30%, respectively, compared to the yields obtained with the cellulase mixture that had not been exposed to any of these compounds. Incubating the cellulase mixture with H_2O_2 and free copper had the strongest impact on the cellulase mixture: next to giving the strongest reduction in the 24 h conversion yield, all cellulase activity was lost at this point. Although the applied concentrations of H_2O_2 and Cu(II) are higher than what would be seen in the enzyme reactions, a similar molar ratio of these compounds could be expected with H_2O_2 concentrations probably being lower than 100 µM [66]. The detrimental effect of H_2O_2 and free copper was counteracted by the addition of EDTA, which completely restored the activity of the cellulase cocktail (Fig. 5).

Excess levels of H_2O_2 have been shown to inactivate both LPMOs and cellulases [23, 28, 67]. The present results show that the enzymes are relatively stable in the presence of high H_2O_2 concentrations (10 mM) as long as transition metals are absent (Fig. 5). Adding copper ions to the system leads to the production of reactive oxygen species such as superoxide and hydroxyl radicals. Thus, observations that seem to indicate that autocatalytic

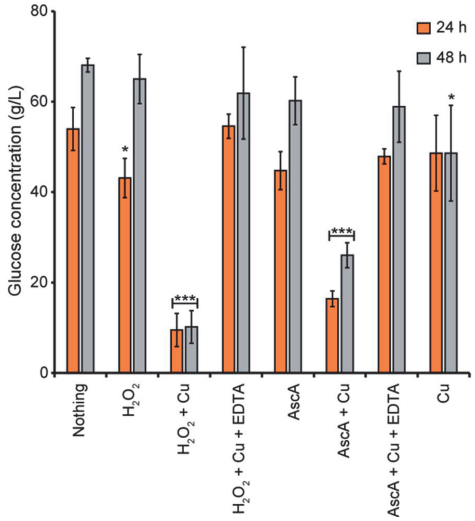

Fig. 5 Preincubation of Celluclast 1.5 L prior to Avicel degradation. A 90% Celluclast 1.5 L + 10% NZ-BG mixture was preincubated at 50 °C for 24 h in the presence of H_2O_2 (10 mM), AscA (10 mM), Cu(II)SO_4 (0.63 mM), and/or EDTA (6.3 mM). Following the preincubation, the saccharification reactions were initiated by adding 25% (w/w) Avicel to the preincubated cellulase cocktails, followed by incubation for 24 or 48 h under the same conditions as for the preincubation. The symbols * and *** indicate significant differences ($p \leq 0.05$ and $p \leq 0.01$, respectively) between no preincubation and the different preincubation conditions (by Student's t test). Standard deviations are shown as error bars, for three biological replicates

inactivation of LPMOs is accompanied by decreased cellulase activity [28], do not relate only to high H_2O_2 levels. Instead, this phenomenon likely arises from side reactions triggered by copper leakage from inactivated LPMOs combined with elevated H_2O_2 levels. As a result, the inactivation of LPMOs has significant implications on reaction kinetics and yields.

Cellulase feedback inhibition

It is well established that the initial substrate loading and the accumulation of products during the reaction, i.e., feedback inhibition, influence the saccharification rate, where high concentrations of cellobiose and glucose are known to be inhibitory for cellobiohydrolases and β-glucosidases, respectively [18, 68, 69]. In the present study, Celluclast 1.5 L was supplemented with BG to ensure complete conversion of cellobiose to glucose, and as expected, cellobiose levels in cellulose hydrolysates were negligible. To probe a possible effect of accumulating glucose levels on the saccharification efficiencies described above, cellulose saccharification reactions were

carried out with the Celluclast 1.5 L + NZ-BG cocktail spiked with *Ta*AA9A:*Tt*AA9E in a 1:1 ratio in the presence of externally added glucose (Fig. 6). The result shows approximately 10, 20, and 40% decrease in glucose release after 72 h when 2.5, 5.0, and 10% (w/w) glucose was included in the reactions from the start, respectively. The results presented illustrate the high-solids effect and show that glucose feedback inhibition plays a role.

However, several studies suggest that the high-solids effect primarily stems from rate-limiting reorganization of constrained water at the substrate surface upon enzymatic removal of soluble sugars and oligosaccharides [2, 5, 68, 70]. Water coordinating the released soluble mono- and oligosaccharides will take away water from the surface of the insoluble substrate, leading to limited availability of water at the site of catalysis and, consequently, lower enzymatic reactivity. As outlined above, it is conceivable that the substrate polarity and decrystallization that follow LPMO action contribute positively to water accessibility near the site of cellulase catalysis and show that LPMO action is important for overcoming the negative impact of high substrate concentrations. Of note, it has recently been shown that LPMOs are not inhibited by high glucose concentrations [45].

Saccharification efficiency of steam-exploded wheat straw

The high-solids effect, i.e., a decrease in saccharification efficiency at increasing substrate concentrations, is not only enzyme-dependent (as shown in Fig. 1) but also substrate-dependent. Yields at low- and high-solids concentrations do not correlate for a given biomass, and, thus, industrial evaluation of biomass saccharification should be carried out at high-solids conditions and with the target feedstock [19]. Therefore, we assessed the efficiency of the studied cellulase–LPMO cocktails on a commercial lignocellulosic feedstock, steam-exploded wheat straw provided by Novozymes, at 15% (w/w) substrate loading. Compositional analysis of the steam-exploded wheat straw showed that the feedstock contains around 22% (w/w) hemicelluloses, 22% (w/w) lignin, and 8% (w/w) ash in addition to 48% (w/w) glucan (Table 1).

The results of the saccharification reactions showed that the cellulase cocktail with 10% LPMO inclusion led to drastically increased cellulose solubilization. In this case, *Ta*AA9A, rather than *Tt*AA9E in the case of Avicel (Fig. 3A), had the largest effect: replacing 10% of the Celluclast 1.5 L + NZ-BG cocktail by *Ta*AA9A alone or by a 1:1 mixture of *Ta*AA9A and *Tt*AA9E improved the saccharification by about 75% both after 48 and 72 h (Fig. 7A). On the contrary to the Avicel reaction spiked with *Ta*AA9A, where the glucose release stopped after 24 h, a prolonged period of sugar release was observed in the wheat straw reactions. This shows that the LPMOs are even more important for cellulose solubilization when working with wheat straw at high solid loadings and that the choice of an optimal LPMO is substrate-dependent. The latter conclusion was also reached by Kim et al., in a 2017 study with 1–5% substrate loadings [71].

Xylan solubilization was not affected by replacing 10% of the cellulase cocktail, which includes xylanases, by LPMO (Fig. 7B). Although *Tt*AA9E has been shown to be active on cellulose-bound xylan [72], this activity did not have an apparent effect on the xylan conversion. While the efficiency of the Celluclast 1.5L + NZ-BG + LPMO cocktails surpassed that of Cellic CTec2 in reactions with pure cellulose (Avicel, containing about 1% (w/w) xylan [73]) (Fig. 3A), Cellic CTec2, a modern enzyme cocktail with improved hemicellulolytic activity and with LPMOs included, was more efficient on the xylan-rich wheat straw, releasing higher amounts of glucose and xylose throughout the saccharification reaction (Fig. 7). This aligns well with a study by Hu et al., who showed that supplementation of Celluclast 1.5 L with both xylanases and *Ta*AA9A is required to reach similar levels of cellulose saccharification of steam pretreated pine as when using Cellic CTec2 [32]. Of note, literature speculates that *Ta*AA9A is the dominant LPMO in Cellic CTec2 [29, 32].

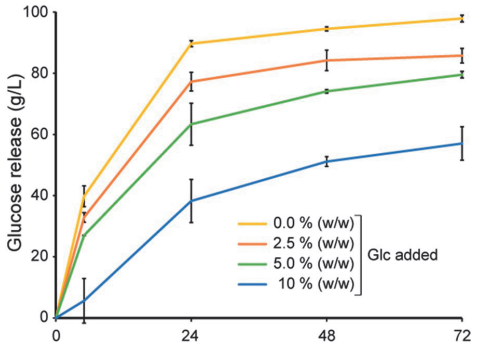

Fig. 6 Probing feedback inhibition by glucose. External glucose, up to 10% (w/w), was added to reactions containing 25% (w/w) Avicel and 3.2 mg/g Celluclast 1.5 L + 0.4 mg/g NZ-BG + 0.4 mg/g *Ta*AA9A and *Tt*AA9E in a 1:1 ratio. The figure shows the net glucose release where the externally added glucose concentrations have been subtracted. Standard deviations are shown as error bars, for three biological replicates

Conclusion

In recent years, multiple studies have addressed the interplay between LPMOs and cellulases. Many of these studies were done with low substrate concentrations, limiting their direct applicability to real-world high-solids

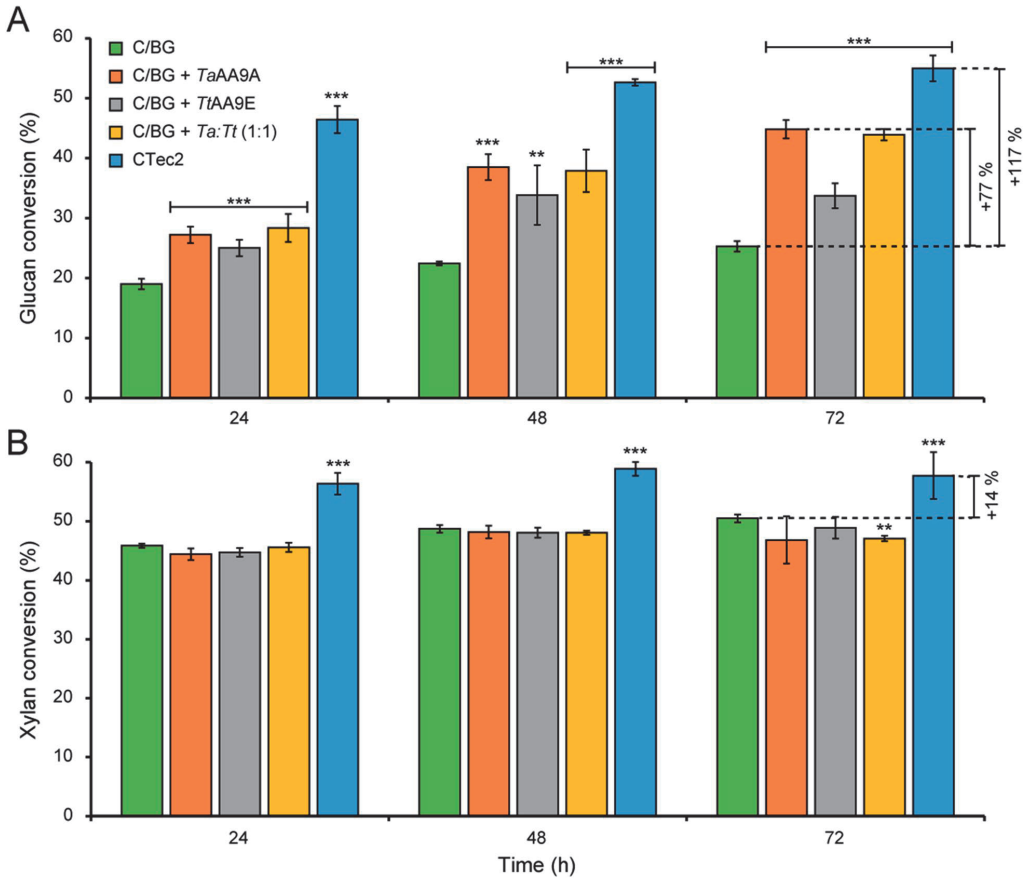

Fig. 7 Degradation of steam-exploded wheat straw with various cellulolytic enzyme cocktails. The degradation of 15% (w/w) steam-exploded wheat straw was performed by incubation with either 3.6 mg/g Celluclast 1.5 L + 0.4 mg/g NZ-BG or with 3.2 mg/g Celluclast 1.5 L + 0.4 mg/g NZ-BG + 0.4 mg/g *Ta*AA9A, *Tt*AA9E or a 1:1 *Ta*AA9A:*Tt*AA9E mixture, or with 4 mg/g Cellic CTec2. Panel **A** shows glucan solubilization; panel **B** shows xylan solubilization. The symbols ** and *** indicate significant differences ($p \leq 0.025$ and $p \leq 0.01$, respectively) between Celluclast 1.5 L/NZ-BG and Celluclast 1.5 L/ NZ-BG spiked with LPMO(s) or Cellic CTec2 (by Student's t-test). Standard deviations are shown as error bars, for three biological replicates

processing scenarios. Our study addresses the challenges associated with high-solids systems and shows the pivotal role of LPMOs in cellulolytic enzyme cocktails operating at high DM reactions that run over 24–72 h. Our results show that the positive impact of LPMOs increases throughout the reaction and with increasing DM concentrations.

Accumulating data in studies cited above suggest that the positive LPMO effect is multi-faceted. The increased importance of LPMOs late in saccharification reactions may be attributed to the increasing recalcitrance of the remaining substrate during the reaction, as well as to the relatively slow impact of oxidized cleavage sites on the substrate hydrophilicity and decrystallization. As to negative effects of the presence of LPMOs, recent discoveries highlight the potentially detrimental effects of copper leakage from damaged LPMOs, which may facilitate several side reactions. Our findings demonstrate that maintaining LPMO activity is crucial for the overall saccharification efficiency, not only because LPMO activity is useful, but also because free copper in solution results in

detrimental side reactions with H_2O_2 that may damage all enzymes in the reaction. Using a different experimental approach and unaware of the fact that LPMOs catalyze productive peroxygenase and potentially damaging peroxidase reactions Scott et al. [67] reached a similar conclusion.

Importantly, our study shows that LPMO effects differ between C1- and C4-oxidizing LPMOs in a DM- and substrate-dependent manner. Thus, despite substantial research efforts in the past decades, there remains a necessity for further optimization and customization of enzyme cocktails tailored to individual feedstocks with specific compositions to attain economically sustainable lignocellulose valorization.

Abbreviations

AscA	Ascorbic acid
BG	β-Glucosidase
BSA	Bovine serum albumin
C	Celluclast 1.5 L
DM	Dry matter
DP	Degree of polymerization
EDTA	Ethylenediaminetetraacetic acid
Glc	Glucose
HPAEC-PAD	High-performance anion exchange chromatography with pulsed amperometric detection
HPLC	High-performance liquid chromatography
LPMO	Lytic polysaccharide monooxygenase
NZ-BG	Novozymes β-glucosidase

Acknowledgements
*Ta*AA9A, *Tt*AA9E, Celluclast 1.5 L, NZ-BG, Cellic CTec2, and steam-exploded wheat straw were kindly supplied by Novozymes. The authors would like to thank Thales Costa for performing the compositional analysis of the steam-exploded wheat straw.

Author contributions
CFA and SJH designed the study. CFA performed the laboratory experiments and analyses. CFA and SJH wrote the first draft of the manuscript. SJH, AV, and VGHE supervised the work. All authors contributed to data interpretation and to writing the final version of the paper.

Funding
This work was supported by the Research Council of Norway under Grant No. 257622 (Bio4Fuels).

Availability of data and materials
All data generated or analyzed during this study are included in the published paper.

Declarations

Ethics approval and consent to participate
Not applicable.

Consent for publication
Not applicable.

Competing interests
The authors declare that there are no competing interests associated with the paper.

Received: 11 January 2024 Accepted: 24 February 2024
Published online: 09 March 2024

References

1. Menon V, Rao M. Trends in bioconversion of lignocellulose: biofuels, platform chemicals & biorefinery concept. Prog Energy Combust Sci. 2012;38(4):522–50. https://doi.org/10.1016/j.pecs.2012.02.002.
2. da Silva ASA, Espinheira RP, Teixeira RSS, de Souza MF, Ferreira-Leitão V, Bon EP. Constraints and advances in high-solids enzymatic hydrolysis of lignocellulosic biomass: a critical review. Biotechnol Biofuels. 2020;13(1):58. https://doi.org/10.1186/s13068-020-01697-w.
3. Kristensen JB, Felby C, Jørgensen H. Determining yields in high solids enzymatic hydrolysis of biomass. Appl Biochem Biotech. 2009;156:127–32. https://doi.org/10.1007/s12010-008-8375-0.
4. Jørgensen H, Vibe-Pedersen J, Larsen J, Felby C. Liquefaction of lignocellulose at high-solids concentrations. Biotechnol Bioeng. 2007;96(5):862–70. https://doi.org/10.1002/bit.21115.
5. Liu Z-H, Chen H-Z. Biomass–water interaction and its correlations with enzymatic hydrolysis of steam-exploded corn stover. ACS Sustain Chem Eng. 2016;4(3):1274–85. https://doi.org/10.1021/acssuschemeng.5b01303.
6. Kristensen JB, Felby C, Jørgensen H. Yield-determining factors in high-solids enzymatic hydrolysis of lignocellulose. Biotechnol Biofuels. 2009;2:11. https://doi.org/10.1186/1754-6834-2-11.
7. Hodge DB, Karim MN, Schell DJ, McMillan JD. Model-based fed-batch for high-solids enzymatic cellulose hydrolysis. Appl Biochem Biotech. 2009;152:88–107. https://doi.org/10.1007/s12010-008-8217-0.
8. Cara C, Moya M, Ballesteros I, Negro MJ, González A, Ruiz E. Influence of solid loading on enzymatic hydrolysis of steam exploded or liquid hot water pretreated olive tree biomass. Process Biochem. 2007;42(6):1003–9. https://doi.org/10.1016/j.procbio.2007.03.012.
9. Schwald W, Breuil C, Brownell H, Chan M, Saddler J. Assessment of pretreatment conditions to obtain fast complete hydrolysis on high substrate concentrations. Appl Biochem Biotech. 1989;20:29–44. https://doi.org/10.1007/BF02936471.
10. Tengborg C, Galbe M, Zacchi G. Influence of enzyme loading and physical parameters on the enzymatic hydrolysis of steam-pretreated softwood. Biotechnol Prog. 2001;17(1):110–7.
11. Jørgensen H, Kristensen JB, Felby C. Enzymatic conversion of lignocellulose into fermentable sugars: challenges and opportunities. Biofuel Bioprod Biorefin. 2007;1(2):119–34. https://doi.org/10.1002/bbb.4.
12. Xing Y, Ji L, Liu Z-p, Zhang W-m, Jiang J-x. Effects of *Gleditsia saponin* on high-solids enzymatic hydrolysis of furfural residues. Ind Crops Prod. 2015;64:209–14. https://doi.org/10.1016/j.indcrop.2014.09.055.
13. Jiang X, Zhai R, Jin M. Increased mixing intensity is not necessary for more efficient cellulose hydrolysis at high solid loading. Bioresour Technol. 2021;329:124911. https://doi.org/10.1016/j.biortech.2021.124911.
14. Du J, Cao Y, Liu G, Zhao J, Li X, Qu Y. Identifying and overcoming the effect of mass transfer limitation on decreased yield in enzymatic hydrolysis of lignocellulose at high solid concentrations. Bioresour Technol. 2017;229:88–95. https://doi.org/10.1016/j.biortech.2017.01.011.
15. Hodge DB, Karim MN, Schell DJ, McMillan JD. Soluble and insoluble solids contributions to high-solids enzymatic hydrolysis of lignocellulose. Bioresour Technol. 2008;99(18):8940–8. https://doi.org/10.1016/j.biortech.2008.05.015.
16. Kim Y, Ximenes E, Mosier NS, Ladisch MR. Soluble inhibitors/deactivators of cellulase enzymes from lignocellulosic biomass. Enzyme Microb Technol. 2011;48(4–5):408–15. https://doi.org/10.1016/j.enzmictec.2011.01.007.
17. Sukumaran RK, Singhania RR, Pandey A. Microbial cellulases-production, applications and challenges. J Sci Ind Res. 2005;64:832–44.
18. Hsieh C-wC, Cannella D, Jørgensen H, Felby C, Thygesen LG. Cellulase inhibition by high concentrations of monosaccharides. J Agric Food Chem. 2014;62(17):3800–5. https://doi.org/10.1021/jf5012962.
19. Weiss ND, Felby C, Thygesen LG. Enzymatic hydrolysis is limited by biomass–water interactions at high-solids: improved performance through substrate modifications. Biotechnol Biofuels. 2019;12:3. https://doi.org/10.1186/s13068-018-1339-x.

20. Roberts KM, Lavenson DM, Tozzi EJ, McCarthy MJ, Jeoh T. The effects of water interactions in cellulose suspensions on mass transfer and saccharification efficiency at high solids loadings. Cellulose. 2011;18:759–73. https://doi.org/10.1007/s10570-011-9509-z.
21. Vaaje-Kolstad G, Westereng B, Horn SJ, Liu Z, Zhai H, Sorlie M, Eijsink VG. An oxidative enzyme boosting the enzymatic conversion of recalcitrant polysaccharides. Science. 2010;330(6001):219–22. https://doi.org/10.1126/science.1192231.
22. Harris PV, Welner D, McFarland K, Re E, Navarro Poulsen J-C, Brown K, et al. Stimulation of lignocellulosic biomass hydrolysis by proteins of glycoside hydrolase family 61: structure and function of a large, enigmatic family. Biochem. 2010;49(15):3305–16. https://doi.org/10.1021/bi100009p.
23. Bissaro B, Rohr AK, Muller G, Chylenski P, Skaugen M, Forsberg Z, et al. Oxidative cleavage of polysaccharides by monocopper enzymes depends on H_2O_2. Nat Chem Biol. 2017;13(10):1123–8. https://doi.org/10.1038/nchembio.2470.
24. Horn SJ, Vaaje-Kolstad G, Westereng B, Eijsink VG. Novel enzymes for the degradation of cellulose. Biotechnol Biofuels. 2012;5(1):45. https://doi.org/10.1186/1754-6834-5-45.
25. Chylenski P, Bissaro B, Sørlie M, Røhr ÅK, Várnai A, Horn SJ, Eijsink VG. Lytic polysaccharide monooxygenases in enzymatic processing of lignocellulosic biomass. ACS Catal. 2019;9(6):4970–91. https://doi.org/10.1021/acscatal.9b00246.
26. Stepnov AA, Forsberg Z, Sørlie M, Nguyen G-S, Wentzel A, Røhr ÅK, Eijsink VG. Unraveling the roles of the reductant and free copper ions in LPMO kinetics. Biotechnol Biofuels. 2021;14:28. https://doi.org/10.1186/s13068-021-01879-0.
27. Stepnov AA, Eijsink VGH, Forsberg Z. Enhanced in situ H_2O_2 production explains synergy between an LPMO with a cellulose-binding domain and a single-domain LPMO. Sci Rep. 2022;12(1):6129. https://doi.org/10.1038/s41598-022-10096-0.
28. Müller G, Chylenski P, Bissaro B, Eijsink VG, Horn SJ. The impact of hydrogen peroxide supply on LPMO activity and overall saccharification efficiency of a commercial cellulase cocktail. Biotechnol Biofuels. 2018;11(1):209. https://doi.org/10.1186/s13068-018-1199-4.
29. Müller G, Varnai A, Johansen KS, Eijsink VG, Horn SJ. Harnessing the potential of LPMO-containing cellulase cocktails poses new demands on processing conditions. Biotechnol Biofuels. 2015;8(1):187. https://doi.org/10.1186/s13068-015-0376-y.
30. Cannella D, Jørgensen H. Do new cellulolytic enzyme preparations affect the industrial strategies for high solids lignocellulosic ethanol production? Biotechnol Bioeng. 2014;111(1):59–68. https://doi.org/10.1002/bit.25098.
31. Kadić A, Chylenski P, Hansen MAT, Bengtsson O, Eijsink VG, Lidén G. Oxidation-reduction potential (ORP) as a tool for process monitoring of H_2O_2/LPMO assisted enzymatic hydrolysis of cellulose. Process Biochem. 2019;86:89–97. https://doi.org/10.1016/j.procbio.2019.08.015.
32. Hu J, Chandra R, Arantes V, Gourlay K, Van Dyk JS, Saddler JN. The addition of accessory enzymes enhances the hydrolytic performance of cellulase enzymes at high solid loadings. Bioresour Technol. 2015;186:149–53. https://doi.org/10.1016/j.biortech.2015.03.055.
33. Costa TH, Kadic' A, Chylenski P, Várnai A, Bengtsson O, Lidén G, et al. Demonstration-scale enzymatic saccharification of sulfite-pulped spruce with addition of hydrogen peroxide for LPMO activation. Biofuel Bioprod Biorefin. 2020;14(4):734–45. https://doi.org/10.1002/bbb.2103.
34. Eibinger M, Ganner T, Bubner P, Rosker S, Kracher D, Haltrich D, et al. Cellulose surface degradation by a lytic polysaccharide monooxygenase and its effect on cellulase hydrolytic efficiency. J Biol Chem. 2014;289(52):35929–38. https://doi.org/10.1074/jbc.M114.602227.
35. Keller MB, Badino SF, Blossom BMI, Mcbrayer B, Borch K, Westh P. Promoting and impeding effects of lytic polysaccharide monooxygenases on glycoside hydrolase activity. ACS Sustain Chem Eng. 2020;8(37):14117–26. https://doi.org/10.1021/acssuschemeng.0c04779.
36. Keller MB, Badino SF, Rojel N, Sorensen TH, Kari J, McBrayer B, et al. A comparative biochemical investigation of the impeding effect of C1-oxidizing LPMOs on cellobiohydrolases. J Biol Chem. 2021;296:100504. https://doi.org/10.1016/j.jbc.2021.100504.
37. Zhou H, Li T, Yu Z, Ju J, Zhang H, Tan H, et al. A lytic polysaccharide monooxygenase from *Myceliophthora thermophila* and its synergism with cellobiohydrolases in cellulose hydrolysis. Int J Biol Macromol. 2019;139:570–6. https://doi.org/10.1016/j.ijbiomac.2019.08.004.
38. Tokin R, Ipsen ØJ, Westh P, Johansen KS. The synergy between LPMOs and cellulases in enzymatic saccharification of cellulose is both enzyme-and substrate-dependent. Biotechnol Lett. 2020;42:1975–84. https://doi.org/10.1007/s10529-020-02922-0.
39. Østby H, Várnai A, Gabriel R, Chylenski P, Horn SJ, Singer SW, Eijsink VG. Substrate-dependent cellulose saccharification efficiency and LPMO activity of cellic CTec2 and a cellulolytic secretome from thermoascus aurantiacus and the impact of H_2O_2-producing glucose oxidase. ACS Sustain Chem Eng. 2022;10(44):14433–44. https://doi.org/10.1021/acssuschemeng.2c03341.
40. Angeltveit CF, Jeoh T, Horn SJ. Lytic polysaccharide monooxygenase activity increases productive binding capacity of cellobiohydrolases on cellulose. Bioresour Technol. 2023;389:129806. https://doi.org/10.1016/j.biortech.2023.129806.
41. Vermaas JV, Crowley MF, Beckham GT, Payne CM. Effects of lytic polysaccharide monooxygenase oxidation on cellulose structure and binding of oxidized cellulose oligomers to cellulases. J Phys Chem B. 2015;119(20):6129–43. https://doi.org/10.1021/acs.jpcb.5b00778.
42. Mudedla SK, Vuorte M, Veijola E, Marjamaa K, Koivula A, Linder MB, et al. Effect of oxidation on cellulose and water structure: a molecular dynamics simulation study. Cellulose. 2021;28(7):3917–33. https://doi.org/10.1007/s10570-021-03751-8.
43. Uchiyama T, Uchihashi T, Ishida T, Nakamura A, Vermaas JV, Crowley MF, et al. Lytic polysaccharide monooxygenase increases cellobiohydrolases activity by promoting decrystallization of cellulose surface. Sci Adv. 2022;8(51):5155. https://doi.org/10.1126/sciadv.ade5155.
44. Magri S, Nazerian G, Segato T, Monclaro AV, Zarattini M, Segato F, et al. Polymer ultrastructure governs AA9 lytic polysaccharide monooxygenases functionalization and deconstruction efficacy on cellulose nanocrystals. Bioresour Technol. 2022;347:126375. https://doi.org/10.1016/j.biortech.2021.126375.
45. Cannella D, Weiss N, Hsieh C, Magri S, Zarattini M, Kuska J, et al. LPMO-mediated oxidation increases cellulose wettability, surface water retention and hydrolysis yield at high dry matter. Cellulose. 2023;30:6259–72. https://doi.org/10.1007/s10570-023-05271-z.
46. Østby H, Tuveng TR, Stepnov AA, Vaaje-Kolstad G, Forsberg Z, Eijsink VG. Impact of copper saturation on lytic polysaccharide monooxygenase performance. ACS Sustain Chem Eng. 2023;11(43):15566–76. https://doi.org/10.1021/acssuschemeng.3c03714.
47. Sluiter A, Hames B, Ruiz R, Scarlata C, Sluiter J, Templeton D, Crocker D. Determination of structural carbohydrates and lignin in biomass. Laboratory Analytical Procedure, NREL Technical Report. 2008:1–16.
48. Agger JW, Nilsen PJ, Eijsink VG, Horn SJ. On the determination of water content in biomass processing. Bioenergy Res. 2014;7:442–9. https://doi.org/10.1007/s12155-013-9388-2.
49. Loose JSM, Forsberg Z, Fraaije MW, Eijsink VGH, Vaaje-Kolstad G. A rapid quantitative activity assay shows that the *Vibrio cholerae* colonization factor GbpA is an active lytic polysaccharide monooxygenase. FEBS Lett. 2014;588(18):3435–40. https://doi.org/10.1016/j.febslet.2014.07.036.
50. Westereng B, Agger JW, Horn SJ, Vaaje-Kolstad G, Aachmann FL, Stenstrom YH, Eijsink VG. Efficient separation of oxidized cello-oligosaccharides generated by cellulose degrading lytic polysaccharide monooxygenases. J Chromatogr A. 2013;1271(1):144–52. https://doi.org/10.1016/j.chroma.2012.11.048.
51. Østby H, Jameson JK, Costa T, Eijsink VGH, Arntzen MO. Chromatographic analysis of oxidized cello-oligomers generated by lytic polysaccharide monooxygenases using dual electrolytic eluent generation. J Chromatogr A. 2022;1662:462691. https://doi.org/10.1016/j.chroma.2021.462691.
52. Zamocky M, Schumann C, Sygmund C, O'Callaghan J, Dobson AD, Ludwig R, et al. Cloning, sequence analysis and heterologous expression in *Pichia pastoris* of a gene encoding a thermostable cellobiose dehydrogenase from *Myriococcum thermophilum*. Protein Expr Purif. 2008;59(2):258–65. https://doi.org/10.1016/j.pep.2008.02.007.
53. Kittl R, Kracher D, Burgstaller D, Haltrich D, Ludwig R. Production of four *Neurospora crassa* lytic polysaccharide monooxygenases in *Pichia pastoris* monitored by a fluorimetric assay. Biotechnol Biofuels. 2012;5(1):79. https://doi.org/10.1186/1754-6834-5-79.
54. Tuveng TR, Jensen MS, Fredriksen L, Vaaje-Kolstad G, Eijsink VG, Forsberg Z. A thermostable bacterial lytic polysaccharide monooxygenase with high operational stability in a wide temperature range. Biotechnol Biofuels. 2020;13:194. https://doi.org/10.1186/s13068-020-01834-5.

55. Courtade G, Forsberg Z, Heggset EB, Eijsink VGH, Aachmann FL. The carbohydrate-binding module and linker of a modular lytic polysaccharide monooxygenase promote localized cellulose oxidation. J Biol Chem. 2018;293(34):13006–15. https://doi.org/10.1074/jbc.RA118.004269.
56. Sun P, Valenzuela SV, Chunkrua P, Javier Pastor FI, Laurent CV, Ludwig R, et al. Oxidized product profiles of AA9 lytic polysaccharide monooxygenases depend on the type of cellulose. ACS Sustain Chem Eng. 2021;9(42):14124–33. https://doi.org/10.1021/acssuschemeng.1c04100.
57. Golten O, Ayuso-Fernández I, Hall KR, Stepnov AA, Sørlie M, Røhr ÅK, Eijsink VG. Reductants fuel lytic polysaccharide monooxygenase activity in a pH-dependent manner. FEBS Lett. 2023;597(10):1363–74.
58. Kuusk S, Eijsink VG, Väljamäe P. The, "life-span" of lytic polysaccharide monooxygenases (LPMOs) correlates to the number of turnovers in the reductant peroxidase reaction. J Biol Chem. 2023;299(9):105094. https://doi.org/10.1016/j.jbc.2023.105094.
59. Eijsink VG, Petrovic D, Forsberg Z, Mekasha S, Røhr ÅK, Várnai A, et al. On the functional characterization of lytic polysaccharide monooxygenases (LPMOs). Biotechnol Biofuels. 2019;12(1):58.
60. Wilson R, Beezer AE, Mitchell JC. A kinetic study of the oxidation of L-ascorbic acid (vitamin C) in solution using an isothermal microcalorimeter. Thermochim Acta. 1995;264:27–40.
61. Goldstein S, Meyerstein D, Czapski G. The fenton reagents. Free Radic Biol Med. 1993;15(4):435–45.
62. Xiao Z, Wedd AG. The challenges of determining metal–protein affinities. Nat Prod Rep. 2010;27(5):768–89.
63. Quinlan RJ, Sweeney MD, Lo Leggio L, Otten H, Poulsen JCN, Johansen KS, et al. Insights into the oxidative degradation of cellulose by a copper metalloenzyme that exploits biomass components. Proc Natl Acad Sci. 2011;108(37):15079–84. https://doi.org/10.1073/pnas.1105776108.
64. Aachmann FL, Sørlie M, Skjåk-Bræk G, Eijsink VG, Vaaje-Kolstad G. NMR structure of a lytic polysaccharide monooxygenase provides insight into copper binding, protein dynamics, and substrate interactions. Proc Natl Acad Sci. 2012;109(46):18779–84.
65. Chaplin AK, Wilson MT, Hough MA, Svistunenko DA, Hemsworth GR, Walton PH, et al. Heterogeneity in the histidine-brace copper coordination sphere in auxiliary activity family 10 (AA10) lytic polysaccharide monooxygenases. J Biol Chem. 2016;291(24):12838–50.
66. Chang H, Gacias Amengual N, Botz A, Schwaiger L, Kracher D, Scheiblbrandner S, et al. Investigating lytic polysaccharide monooxygenase-assisted wood cell wall degradation with microsensors. Nat Chem Biol. 2022;13(1):6258. https://doi.org/10.1038/s41467-022-33963-w.
67. Scott BR, Huang HZ, Frickman J, Halvorsen R, Johansen KS. Catalase improves saccharification of lignocellulose by reducing lytic polysaccharide monooxygenase-associated enzyme inactivation. Biotechnol Lett. 2016;38:425–34. https://doi.org/10.1007/s10529-015-1989-8.
68. Selig MJ, Hsieh CWC, Thygesen LG, Himmel ME, Felby C, Decker SR. Considering water availability and the effect of solute concentration on high solids saccharification of lignocellulosic biomass. Biotechnol Prog. 2012;28(6):1478–90. https://doi.org/10.1002/btpr.1617.
69. Cannella D, Hsieh CWC, Felby C, Jorgensen H. Production and effect of aldonic acids during enzymatic hydrolysis of lignocellulose at high dry matter content. Biotechnol Biofuels. 2012;5(1):26. https://doi.org/10.1186/1754-6834-5-26.
70. Selig MJ, Thygesen LG, Johnson DK, Himmel ME, Felby C, Mittal A. Hydration and saccharification of cellulose Iβ, II and III I at increasing dry solids loadings. Biotechnol Lett. 2013;35:1599–607. https://doi.org/10.1007/s10529-013-1258-7.
71. Kim IJ, Seo N, An HJ, Kim J-H, Harris PV, Kim KH. Type-dependent action modes of *Tt*AA9E and *Ta*AA9A acting on cellulose and differently pretreated lignocellulosic substrates. Biotechnol Biofuels. 2017;10:46.
72. Tõlgo M, Hegnar OA, Østby H, Várnai A, Vilaplana F, Eijsink VG, Olsson L. Comparison of six lytic polysaccharide monooxygenases from *Thermothielavioides terrestris* Shows that functional variation underlies the multiplicity of LPMO genes in filamentous fungi. Appl Environ Microbiol. 2022;88(6):e0009622.
73. Várnai A, Siika-aho M, Viikari L. Restriction of the enzymatic hydrolysis of steam-pretreated spruce by lignin and hemicellulose. Enzyme Microb Technol. 2010;46(3–4):185–93.

Publisher's Note

Paper III

Visible light-exposed lignin facilitates cellulose solubilization by lytic polysaccharide monooxygenases

Kommedal EG, Angeltveit CF, Klau LJ, Ayuso-Fernández I, Arstad B, Antonsen SG, Stenstrøm Y, Ekeberg D, Gírio F, Carvalheiro F, Horn SJ, Aachmann FL & Eijsink VGH

nature communications

Article

https://doi.org/10.1038/s41467-023-36660-4

Visible light-exposed lignin facilitates cellulose solubilization by lytic polysaccharide monooxygenases

Received: 17 June 2022

Accepted: 10 February 2023

Published online: 24 February 2023

Check for updates

Eirik G. Kommedal[1], Camilla F. Angeltveit[1], Leesa J. Klau[2], Iván Ayuso-Fernández[1], Bjørnar Arstad[3], Simen G. Antonsen[1], Yngve Stenstrøm[1], Dag Ekeberg[1], Francisco Gírio[4], Florbela Carvalheiro[4], Svein J. Horn[1], Finn Lillelund Aachmann[2] & Vincent G. H. Eijsink[1]

Lytic polysaccharide monooxygenases (LPMOs) catalyze oxidative cleavage of crystalline polysaccharides such as cellulose and are crucial for the conversion of plant biomass in Nature and in industrial applications. Sunlight promotes microbial conversion of plant litter; this effect has been attributed to photochemical degradation of lignin, a major redox-active component of secondary plant cell walls that limits enzyme access to the cell wall carbohydrates. Here, we show that exposing lignin to visible light facilitates cellulose solubilization by promoting formation of H_2O_2 that fuels LPMO catalysis. Light-driven H_2O_2 formation is accompanied by oxidation of ring-conjugated olefins in the lignin, while LPMO-catalyzed oxidation of phenolic hydroxyls leads to the required priming reduction of the enzyme. The discovery that light-driven abiotic reactions in Nature can fuel H_2O_2-dependent redox enzymes involved in deconstructing lignocellulose may offer opportunities for bioprocessing and provides an enzymatic explanation for the known effect of visible light on biomass conversion.

Every year, 100 billion tons of CO_2 are converted to cellulose by photosynthetic organisms[1], making lignocellulosic plant biomass the most abundant natural material on Earth and a large reservoir of renewable carbon that can be transformed to chemicals and fuels. However, plant cell walls have evolved to become recalcitrant co-polymeric structures to provide mechanical strength and rigidity and to provide resistance against pathogen attack, and are, thus, hard to break down[2]. Plant cell wall-degrading microorganisms have solved this challenge by developing multi-component enzymatic tools that act synergistically to process this highly complex and recalcitrant biomass.

Selective oxidation of non-activated C-H bonds in crystalline cellulose by lytic polysaccharide monooxygenases (LPMOs) is crucial for efficient aerobic decomposition of plant biomass[3–6]. LPMOs are abundant in Nature and classified, based on their sequences, in the auxiliary activity (AA) families 9–11 and 13–17 of the Carbohydrate Active enZymes (CAZy) database[7]. LPMOs are mono-copper enzymes[4,5] that catalyze oxidative cleavage of glycosidic bonds in insoluble polysaccharides such as cellulose[5,6] and chitin[3], as well as in certain hemicelluloses[8,9]. LPMOs were first considered monooxygenases as the activity was shown to depend on the presence of molecular oxygen, but recent studies have demonstrated that H_2O_2 is the kinetically relevant co-substrate making these enzymes peroxygenases rather than monooxygenases[10–14]. The oxidative action of LPMOs disrupts the crystalline polysaccharide surface[15,16] thus promoting depolymerization by hydrolytic enzymes[3,17]. It is generally accepted that LPMOs are the C1 factor hypothesized by Elwyn Reese and co-workers in 1950[18] and that LPMOs explain why Eriksson et al. found, in 1974, that oxygen promotes biomass conversion by a fungal secretome[19].

[1]Faculty of Chemistry, Biotechnology and Food Science, Norwegian University of Life Sciences (NMBU), 1432 Ås, Norway. [2]Department of Biotechnology and Food Science, Norwegian University of Science and Technology (NTNU), 7491 Trondheim, Norway. [3]SINTEF Industry, Process Chemistry and Functional Materials, 0373 Oslo, Norway. [4]National Laboratory of Energy and Geology (LNEG), 1649-038 Lisboa, Portugal. e-mail: vincent.eijsink@nmbu.no

LPMO catalysis was first thought to require delivery of two electrons, two protons and molecular oxygen per catalytic cycle in what would be a monooxygenase reaction ($R\text{-}H + 2e^- + 2H^+ + O_2 \rightarrow R\text{-}OH + H_2O$), whereas in the peroxygenase reaction, a reduced LPMO can catalyze multiple turnovers with H_2O_2 ($R\text{-}H + H_2O_2 \rightarrow R\text{-}OH + H_2O$)[20]. A standard monooxygenase reaction set-up involves incubating the LPMO with substrate and a reductant under aerobic conditions and it has been shown that a wide variety of reducing compounds and reducing equivalent-delivering enzymes can drive LPMO reactions[4,21–27]. It is currently being debated whether observed monooxygenase reactions are in fact peroxygenase reactions that are limited by the in situ generation of H_2O_2 by LPMO-catalyzed or abiotic oxidation of the reductant (e.g., Bissaro et al.[28]). Importantly, like for other redox enzymes, high levels of H_2O_2 combined with low levels of substrate will lead to autocatalytic oxidative damage in the catalytic center of the enzyme[10,17,29]. H_2O_2-driven LPMO catalysis is a double-edged sword, enabling high enzymatic activity at the possible cost of enzyme inactivation.

Light represents an abundant and cheap source of energy that can be harvested by a photoredox catalyst to tailor H_2O_2 levels to enzymatic reactions[30,31]. Light-driven LPMO reactions were first described in 2016. Cannella et al.[32] showed that the activity of a fungal LPMO acting on amorphous cellulose (PASC) could be boosted dramatically by adding chlorophyllin, a photosynthetic pigment, and light, next to the reductant, ascorbic acid (AscA). Light-driven activity of a bacterial LPMO from *Streptomyces coelicolor* (*Sc*AA10C) on crystalline cellulose (Avicel) using irradiated vanadium-doped titanium dioxide (V-TiO_2) was demonstrated later the same year[33]. Both studies discussed molecular mechanisms for the observed LPMO activity, but neither considered light-induced formation of H_2O_2 from O_2 as the primary driver for LPMO activity, which, later, was shown to be the key driver of LPMO activity in these light-fueled reaction systems[23].

The impact of light on biomass conversion is of great interest, with repercussions spanning from the global carbon cycle to industrial biorefining. Light has been demonstrated to facilitate microbial decomposition of plant litter by increasing the accessibility of cell wall polysaccharides to enzymatic conversion[34–38]. Since secondary plant cell walls, the natural substrates of LPMOs, are rich in lignin, and since lignin is photoactive and can promote formation of H_2O_2[39,40], we hypothesized that light-driven redox processes involving lignin and LPMO activity can help explain the observed photofacilitation of biomass decomposition. Of note, possible effects of light may also be relevant for reactor design in industrial biorefining of lignocellulosic biomass, since pretreated feedstocks that are subjected to enzymatic saccharification with LPMO-containing cellulolytic enzyme cocktails usually contain large amounts of lignin.

Here we report a detailed biochemical study of cellulose degradation by *Sc*AA10C, a well-studied model LPMO from the soil actinomycete *Streptomyces coelicolor*, using light-exposed lignin to fuel the LPMO reaction. We show that light-exposure of lignin has a large effect on LPMO activity and that this effect is driven by the ability of lignin to promote generation of H_2O_2. We also show that the necessary priming reduction of the LPMO may be achieved through direct interactions with polymeric lignin and that LPMOs, thus, can oxidize lignin. Using NMR spectroscopy, we demonstrate the impact of visible light on the lignin structure, revealing effects on olefinic structures. Next to providing insight into how lignin and light-exposed lignin affect LPMO activity, this study offers an alternative, enzyme-based explanation for the effect of light on biomass turnover in the biosphere.

Results

Photocatalytic hydrogen peroxide generation by lignin fuels LPMO activity on cellulose

Previous studies have demonstrated lignin's ability to fuel LPMO reactions and this was thought to reflect the ability of lignin to deliver the electrons needed by the LPMO to carry out a monooxygenase reaction[24,25,32,41]. To gain more insight into lignin's ability to fuel LPMO reactions and to assess the impact of light, we used a well-studied cellulose-active C1-oxidizing LPMO from *Streptomyces coelicolor* (*Sc*AA10C, also known as CelS2) and Avicel (i.e., crystalline cellulose) as substrate.

In the first set of experiments, we used commercially available kraft lignin to fuel solubilization of crystalline cellulose by *Sc*AA10C and we measured both LPMO product formation and the accumulation of H_2O_2 in reactions exposed to light (Fig. 1). As expected, oxidized cello-oligosaccharides were not generated in reactions lacking the LPMO (Fig. 1a). At the lower lignin concentration (0.9 g L^{-1}), the reaction without LPMO showed accumulation of H_2O_2, whereas the reaction with 75 nM or 500 nM LPMO showed almost identical linear progress curves for LPMO product formation and no accumulation of H_2O_2. This suggests that, under these conditions, the LPMO reaction was limited by generation of H_2O_2. At the higher lignin concentration (9 g L^{-1}), accumulation of H_2O_2 in the reaction without LPMO was much higher (Fig. 1b). In the reaction with only 75 nM LPMO, product formation stopped within the first hour (Fig. 1a) and H_2O_2 accumulated at a rate similar to the reaction without LPMO (Fig. 1b), indicating that the

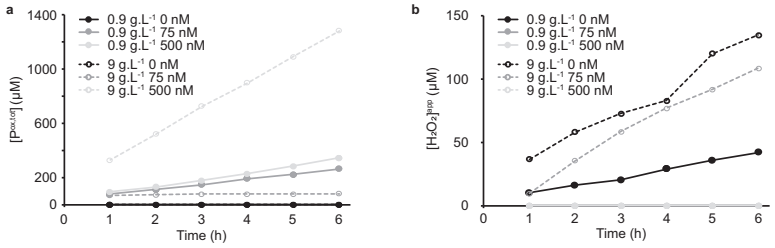

Fig. 1 | LPMO-catalyzed depolymerization of cellulose using kraft lignin as photoredox catalyst. The graphs show time-courses for the production of oxidized LPMO products (**a**) and apparent H_2O_2 levels (**b**) in photobiocatalytic reactions containing LPMO (*Sc*AA10C; 0, 75, or 500 nM; black, gray and light gray, respectively), substrate (Avicel, 10 g L^{-1}) and photoredox catalyst (kraft lignin; 0.9 or 9 g L^{-1}, closed symbols with solid lines and open symbols with dashed lines, respectively). All reactions were carried out in sodium phosphate buffer (50 mM, pH 7.0) at 40 °C under magnetic stirring and exposed to visible light ($I = 10\%\ I_{max}$, ~16.8 W cm^{-2}). 50 μL aliquots were taken every hour and diluted with 50 μL water prior to boiling for subsequent analysis of oxidized products (both soluble and insoluble) and quantification of H_2O_2. The data is reported as mean values from two individual experiments ($n = 2$). The values showed 10% or less variation between replicates except for the reaction with 0.9 g L^{-1} and 500 nM *Sc*AA10C where the deviations were less than 22% between replicates. No oxidized products were detected in reactions lacking LPMO (**a**) and H_2O_2 only accumulated in reactions without LPMO regardless of the lignin concentration except for the reaction with 9 g L^{-1} lignin and 75 nM LPMO (**b**) (see text for an explanation). Reactions in the dark showed much lower product levels, as shown in Fig. 2.

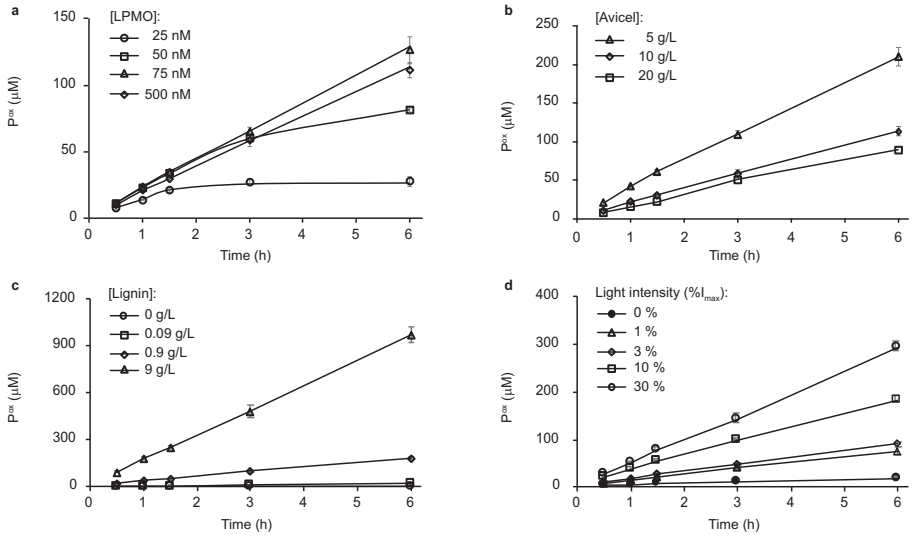

Fig. 2 | Influence of the LPMO, Avicel, and lignin concentrations and light intensity on LPMO-catalyzed solubilization of cellulose. The graphs show time-courses for the release of aldonic acid products in reactions with varying **a** LPMO concentration, **b** Avicel concentration, **c** kraft lignin concentration, and **d** light intensity. The values of the varied reaction parameter and the symbols used to discriminate different conditions are explained in the graphs. All reactions were carried out in sodium phosphate buffer (50 mM, pH 7.0) at 40 °C under magnetic stirring with exposure to visible light (10% I_{max}, ~16.8 W cm^{-2} unless otherwise specified), and contained LPMO (*Sc*AA10C, 0.5 μM), Avicel (10 g L^{-1}), and lignin (0.9 g L^{-1}), unless otherwise specified. Before quantification of soluble oxidized products, solubilized cello-oligosaccharides were hydrolyzed by *Tf*Cel6A to convert LPMO products with varying degree of polymerization (DP) to a mixture of DP 2 and 3 [GlcGlc1A, (Glc)2Glc1A], the amounts of which were summed up to yield the concentration of oxidized sites. The concentration of oxidized sites is reported as the mean value from the three independent experiments and error bars show ±s.d. ($n = 3$).

LPMO had been inactivated due to an overload of H_2O_2[23,42,43]. To demonstrate enzyme inactivation, three separate reactions identical to the 9 g L^{-1} lignin, 75 nM LPMO reaction of Fig. 1 were set up and after one hour, substrate, enzyme and substrate, or a reductant and substrate were added. Only the reaction to which fresh enzyme was added showed resumed LPMO activity (Supplementary Fig. 1), confirming that, indeed, enzyme inactivation had occurred. On the other hand, 500 nM LPMO was sufficient to productively convert all H_2O_2 generated during the course of the 6 h reaction with 9 g L^{-1} lignin into oxidized cello-oligosaccharides and no H_2O_2 accumulation was observed in this reaction (Fig. 1). Consequently, product formation in the reaction with 9 g L^{-1} lignin and 500 nM LPMO was much faster than in any of the other reactions.

While Fig. 1 shows that there is a clear correlation between the amount of H_2O_2 generated in the reaction system and LPMO activity, there is a marked difference between the H_2O_2 levels generated in absence of LPMO (Fig. 1b) and the amount of oxidized product formed in LPMO-containing reactions (Fig. 1a). If the apparent H_2O_2 levels in Fig. 1b equal the true levels and if one accepts the premise that access to H_2O_2 limits the LPMO reaction, H_2O_2 levels in the reaction without LPMO and LPMO product levels should be similar. One potential explanation resides in the HRP/Amplex Red assay used to determine H_2O_2 levels. Kraft lignin serves as substrate for HRP, which will suppress the Amplex Red signal. This effect was, however, compensated for since all H_2O_2 standard curves used to determine H_2O_2 accumulation with the HRP/Amplex Red assay contained the same lignin concentration as the reaction being analyzed. Another explanation lies in the abiotic consumption of H_2O_2 due to abiotic reactions with lignin[44]. The levels of H_2O_2 measured in the absence of the LPMO are the net result of formation (i.e., oxidation of lignin by O_2) and degradation (i.e., oxidation of lignin by H_2O_2), both of which may be dependent on light, as has been shown for a different photoredox catalyst[45]. Since LPMOs in presence of substrate have high affinity for H_2O_2 (K_m values in the low micromolar range)[11,29,43] it is conceivable that the LPMO peroxygenase reaction outcompetes consumption of H_2O_2 through reactions with lignin, which would explain the discrepancy between apparent H_2O_2 measured and LPMO product levels. A control experiment indicated that, indeed, H_2O_2 consumption by the LPMO is faster than abiotic H_2O_2 consumption (Supplementary Fig. 2).

To further understand the lignin/light/LPMO system, each reaction component in a standard reaction with *Sc*AA10C (0.5 μM), Avicel (10 g L^{-1}), lignin (0.9 g L^{-1}), and light ($I = 10\%$ I_{max}, corresponding to ~16.8 W cm^{-2}) was varied. In these, and subsequent, experiments only soluble LPMO products were quantified. Further reduction of the LPMO concentration to below 75 nM showed that the LPMO became limiting at lower concentrations (Fig. 2a). At 50 nM LPMO, product formation appeared to level off between 3 and 6 h, and further reducing the LPMO concentration to 25 nM resulted in cessation of product formation after 90 min due to enzyme inactivation (Fig. 2a).

Increasing the Avicel concentration led to a decrease in LPMO activity (Fig. 2b). While this may seem counterintuitive, it has been shown that higher Avicel concentrations attenuate more photons[42] which would reduce lignin-catalyzed H_2O_2 formation. Control reactions without enzyme showed that, indeed, the production of H_2O_2 in light-exposed reactions with a fixed amount of lignin is inversely correlated with the Avicel concentration (Supplementary Fig. 3). As for the lignin concentration, a clear dose-response effect was already visible in the data of Figs. 1 and 2c shows that further lowering of the lignin concentration leads to less LPMO activity, confirming the dose-response relationship. Figure 2d shows a clear dose-response effect for the light and shows that the reaction with the standard amount of light used here ($I = 10\%$ I_{max}) is one order of magnitude faster than a reaction in the dark. No LPMO activity was detected in absence of lignin (Fig. 2c). Taken together, the results displayed in Figs. 1 and 2

https://doi.org/10.1038/s41467-023-36660-4

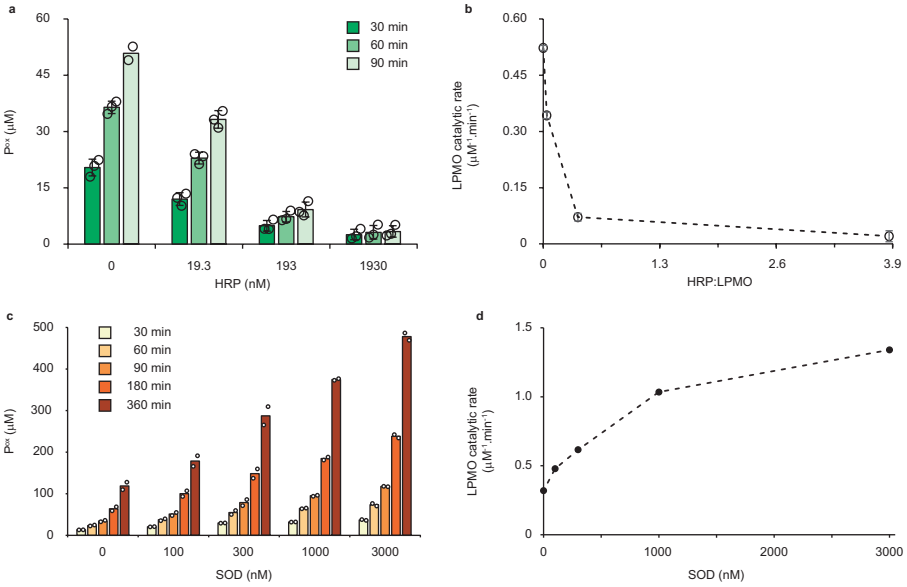

Fig. 3 | Probing the role of reactive oxygen species in the light/lignin/LPMO system. The graphs show time-courses for the formation of soluble oxidized products (**a**, **c**) and the corresponding apparent catalytic rates (**b**, **d**) for reactions with Avicel (10 g L^{-1}), *Sc*AA10C (0.5 μM), kraft lignin (0.9 g L^{-1}), and light-exposure in the presence of varying amounts of horseradish peroxidase (HRP) (**a**, **b**) and superoxide dismutase (SOD) (**c**, **d**). The varying colors in panels **a** and **c** indicate different time points of the reaction, as explained in the graphs. The rates shown in **b** were derived from linear regression analysis using all three time points in **a** with $R^2 > 0.99$ for all reactions with 0, 19.3, 193 nM HRP except for one replicate with 193 nM with $R^2 > 0.93$. For the reactions with 1930 nM HRP the product levels were very low and showed larger variability as these levels were close to the detection limit of the analytical method. The rates in **d** were derived using linear regression analysis for all time points displayed in **c** and all reactions gave progress curves with $R^2 > 0.99$. All reactions were carried out in sodium phosphate buffer (50 mM, pH 7.0) at 40 °C, under magnetic stirring and exposed to visible light ($I = 10\%\ I_{max}$, ~16.8 W cm^{-2}). Before quantification of soluble oxidized products, solubilized cello-oligosaccharides were hydrolyzed by *Tf*Cel6A to convert LPMO products with varying degree of polymerization (DP) to a mixture of DP 2 and 3 [GlcGlc1A, (Glc)2Glc1A], the amounts of which were summed up to yield the concentration of oxidized sites. The data presented are mean values derived from three (**a**, **b**) or two (**c**, **d**) independent experiments; error bars show ±s.d. (**a**, **b**; $n = 3$).

demonstrate that combining lignin and light enables fine-tuning of LPMO reactions and that increased LPMO activity correlates with conditions that favor H_2O_2 production. Preliminary experiments with fungal cellulose-active AA9 LPMOs showed that also in this case lignin-driven LPMO activity was boosted by visible light (Supplementary Fig. 4).

To demonstrate that light-driven H_2O_2 generation fuels the LPMO reaction, competition experiments were performed with increasing amounts of horseradish peroxidase (HRP). No additional substrate for HRP was needed as the soluble lignin used in these reactions is a suitable substrate for this enzyme. The reaction catalyzed by 0.5 μM LPMO was increasingly inhibited by increasing amounts of HRP (Fig. 3a). Plotting the rate of LPMO catalytic activity against the HRP concentration showed more than 85% inhibition of LPMO activity with 193 nM HRP and almost complete inhibition, >97% inhibition, with 1930 nM HRP (Fig. 3b). These experiments clearly show that the LPMO reaction is fueled by the H_2O_2 generated from light-irradiated lignin.

Two recent studies have demonstrated H_2O_2 generation by light-exposed lignin, which may be the result of two single-electron reductions of O_2 leading to $O_2^{\bullet-}$ and then H_2O_2, or of a one-step, two-electron reduction of O_2 to H_2O_2[39,40]. Of note, the superoxide radical can likely act as reductant for the LPMO[23,46]. To assess possible formation of superoxide we carried out reactions with superoxide dismutase (SOD), which converts superoxide to H_2O_2 and O_2. Adding increasing amounts of SOD (0–3000 nM) to an irradiated reaction with lignin (0.9 g L^{-1}), Avicel (10 g L^{-1}), and *Sc*AA10C (0.5 μM) led to a near four-fold increase in the LPMO rate (Fig. 3c, d), showing that superoxide was indeed generated from light-exposed lignin and that access to H_2O_2 limits LPMO activity in these conditions.

LPMO reduction by lignin

Superoxide and lignin have both been suggested as competent reducing agents for LPMOs[23–25]. To create insight into the role of lignin in LPMO reduction, we assessed the ability of lignin to reduce the LPMO using stopped-flow kinetic measurements. We first attempted to do so with *Sc*AA10C, but for this LPMO the combination of a weak signal and signal quenching by lignin prevented the determination of rates from the kinetic traces (see Supplementary Fig. 5 for data and further discussion). Changing from the cellulose-active *Sc*AA10C to the chitin-active *Sm*AA10A, with a stronger fluorescence signal, allowed proper determination of lignin oxidation rates (Supplementary Fig. 5). Of note, a control experiment showed that, just as cellulose degradation by *Sc*AA10C, chitin degradation by *Sm*AA10A was boosted by light-exposed lignin (Supplementary Fig. 6).

To rule out that LPMO reduction was caused by small phenolic or other low molecular weight compounds present in the commercial kraft lignin preparation, we measured LPMO reduction both with native kraft lignin and dialyzed kraft lignin. Such a dialysis step is often performed when studying lignin peroxidases to remove traces of Mn^{2+}[47]. The effect of lignin dialysis was minimal, both for light-driven (aerobic) cellulose oxidation by *Sc*AA10C and, importantly, for (anaerobic) reduction of *Sm*AA10A (Fig. 4 and Supplementary Fig. 5). Figure 4a shows that reactions with native and dialyzed kraft-lignin generated similar levels of oxidized products during a 6 h reaction with

https://doi.org/10.1038/s41467-023-36660-4

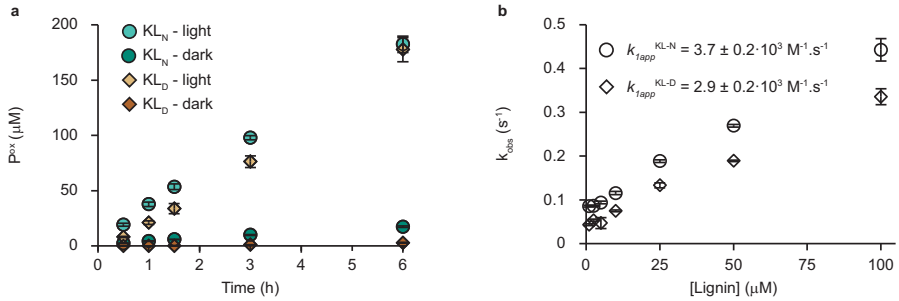

Fig. 4 | Lignin-driven *Sc*AA10C-catalyzed solubilization of cellulose and reduction kinetics for *Sm*AA10A. a The figure shows time courses for the formation of solubilized oxidized products by *Sc*AA10C (0.5 μM) in reactions with native (KL_N; circles) or dialyzed (KL_D; diamonds) kraft lignin (0.9 g L^{-1}) and Avicel (10 g L^{-1}) in sodium phosphate buffer (50 mM, pH 7.0) at 40 °C with magnetic stirring, in the dark (darker color) or when irradiated by white light (lighter color; $I = 10\%\ I_{max}$, ~16.8 W cm^{-2}). Before quantification of soluble oxidized products, solubilized cello-oligosaccharides were hydrolyzed by *Tf*Cel6A to convert LPMO products with varying degree of polymerization (DP) to a mixture of DP 2 and 3 [GlcGlc1A, (Glc)2Glc1A], the amounts of which were summed up to yield the concentration of oxidized sites. **b** The figure shows the observed pseudo-first-order constants, k_{obs}, for reduction of *Sm*AA10A-Cu(II) as a function the kraft lignin concentration, derived from the fluorescence traces shown in Supplementary Fig. 3a, b. Kraft lignin concentrations were calculated based on an average molecular mass (provided by the supplier) of 10,000 g/mol for both lignin preparations; since the average mass of the dialyzed lignin is expected to be somewhat higher, compared to the native lignin, the second order rate constant for the dialyzed lignin is underestimated. *Sm*AA10A-Cu(II) (10 μM) was anaerobically mixed with varying concentrations of native (KL_N; circles) and dialyzed (KL_D; diamonds) kraft lignin, and the change in fluorescence was monitored as a function of time. The reactions were carried out in sodium phosphate buffer (50 mM, pH 7.0) at 25 °C. Data were fit to single exponential functions to give observed rate constants (k_{obs}) at each lignin concentration. The apparent second order rate constant k_{1app}^{lignin} was determined from linear regression using the reported data points and displayed an $R^2 > 0.99$. The data in **a** and **b** are reported as mean values from three independent experiments and the error bars show ± s.d. ($n = 3$).

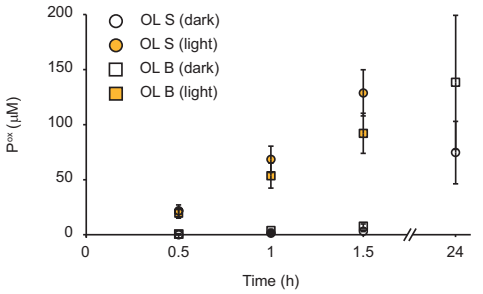

Fig. 5 | LPMO-catalyzed depolymerization of cellulose using organosolv lignin as photoredox catalyst. The graph shows time courses for the production of oxidized products in photobiocatalytic reactions containing *Sc*AA10C (500 nM), Avicel (10 g L^{-1}), and organosolv lignin (OL) from spruce (S; circles) or birch (B; squares) (2.5 g L^{-1}). All reactions were carried out in sodium phosphate buffer (50 mM, pH 6.0) at 40 °C under magnetic stirring and exposed (orange symbols) or not (white symbols) to visible light ($I = 10\%\ I_{max}$, ~16.8 W cm^{-2}). The light-exposed reactions were incubated for 1.5 h while the dark reactions were incubated for 24 h. Before quantification of soluble oxidized products, solubilized cello-oligosaccharides were hydrolyzed by *Tf*Cel6A to convert LPMO products with varying degree of polymerization (DP) to a mixture of DP 2 and 3 [GlcGlc1A, (Glc)2Glc1A], the amounts of which were summed up to yield the concentration of oxidized sites. The data is presented as mean values obtained from three independent experiments and error bars show ±s.d. ($n = 3$). OL was prepared as a stock suspension (25 g L^{-1}) in water, and thoroughly mixed prior to adding lignin to the reaction vials.

light-exposure. For reactions in the dark, the dialyzed lignin resulted in lower LPMO activity compared to the already slow reaction with native kraft lignin (Fig. 4a). It is conceivable that under these conditions, the presence of rapidly diffusing low molecular weight reductants has a notable impact on the (low) rate of in situ H_2O_2 generation that drives the reaction. Figure 4b shows that anaerobic reduction of *Sm*AA10A, and, thus oxidation of lignin, happens with similar second order rate constants, k_{1app}^{lignin}, of 3.7×10^3 M s^{-1} and 2.9×10^3 M s^{-1}, for non-dialyzed and dialyzed kraft lignin, respectively. These results demonstrate that the copper site of LPMOs can directly interact with and oxidize a high molecular weight lignin polymer. Although no reliable rates could be obtained for the cellulose-active *Sc*AA10C, the data suggested that reduction of this enzyme was slower than reduction of *Sm*AA10A (Supplementary Fig. 5).

Studies with other lignin types

Kraft lignin is produced from kraft pulping of wood to separate cellulose from hemicellulose and lignin using sodium hydroxide and sodium sulfide. This process generates a modified and condensed lignin structure with an increase in phenolic groups and recalcitrant C-C and C-O bonds, and a reduced number of less recalcitrant β-O-4 bonds, compared to native lignin[48,49]. To assess the impact of lignin type on light-enhanced LPMO activity, we performed experiments similar to those reported above in which the soluble kraft lignin was replaced by insoluble organosolv lignin obtained from either spruce or birch. Figure 5 shows that light-exposure drastically enhanced the ability of insoluble organosolv lignin to fuel the LPMO reaction, similar to what was observed with kraft lignin.

Light-induced structural changes of lignin

The boosting effect of light on lignin-driven LPMO-catalyzed oxidation of cellulose originates from the ability of lignin to photocatalytically reduce O_2 to $O_2^{\bullet-}$ and H_2O_2. Ring-conjugated double bonds, like those found in the cinnamyl alcohol building blocks, in β–1 stilbenes, and carbonyl moieties are known lignin structures that absorb light[50]. Irradiating Cα-carbonyls in lignin with UV-light leads to excited state carbonyls which may abstract phenolic hydrogens to yield phenoxyl radicals, but visible light does not provide the energy needed to excite Cα-carbonyls[51]. Recently, it has been proposed that the Cα-OH moieties of β-O-4 bonds in lignin are involved in O_2 reduction to H_2O_2, resulting in the conversion of Cα-OH to Cα = O[40]. Supporting this notion, Kim et al. showed photocatalytic reduction of O_2 to H_2O_2 using a model lignin dimer, guaiacylglycerol-β-guaiacyl ether, which contains two guaiacyl units linked together via a β-O-4 bond and harbors a

https://doi.org/10.1038/s41467-023-36660-4

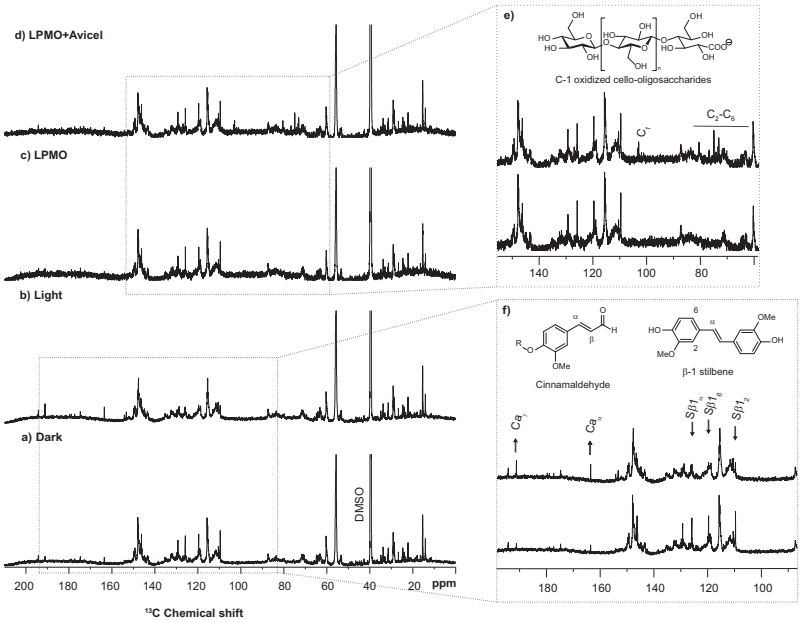

Fig. 6 | Light-induced and LPMO-induced changes in organosolv spruce lignin assessed by 1D carbon NMR spectroscopy. The panels show the spectra obtained for organosolv lignin from spruce (10 g L^{-1}) incubated for 24 h in the dark (**a**), with light-exposure (I = 10% I_{max}, corresponding to ~16.8 W cm^{-2}) (**b**), in the dark with *Sc*AA10C (500 nM) (**c**), or in the dark with *Sc*AA10C (500 nM) and Avicel (10 g L^{-1}) (**d**). Regions of the spectra displaying differences related to treatment with light (**f**) or an LPMO (**e**) are shown in the panels to the right. There were no detectable differences in the parts of the spectra that are not shown in panels **e** and **f**. All reactions were performed in sodium phosphate buffer (50 mM, pH 6.0) at 40 °C with magnetic stirring. The NMR samples were prepared by dissolving either ~40 mg for light-treated lignin (**a**, **b**, **f**) or ~20 mg for LPMO-treated lignin (**c**, **d**, **e**) in 480 µL DMSO-d_6 (99.96 atom % D) and the carbon spectrum was recorded at 25 °C on an 800 MHz instrument. To account for the differences in lignin concentration the intensity of all spectra was adjusted to be equal for the signal at ~28 ppm. Identified chemical moieties are based on partial assignment using ^{1}H–^{13}C-HSQC and previous values reported in the literature. Signals from β-1 stilbene ($S\beta1_\alpha$, $S\beta1_2$, and $S\beta1_6$)[49], cinnamaldehyde (Ca_α and Ca_γ)[49,53], and C-1 oxidized cello-oligosaccharides [C_1, C_2-C_6, where the number refers to the ring carbon for the monosaccharide[54]] are indicated. Changes in the abundance of selected chemical moieties are indicated with an up arrow for increase and a down arrow for decrease upon light treatment, and R indicates further coupling to the lignin polymer (**f**).

Cα-OH. The Cα-OH was shown to be photocatalytically oxidized to Cα = O with concomitant H_2O_2 formation, whereas the lignin monomers coniferyl alcohol and sinapyl alcohol were shown unable to photocatalytically reduce O_2 to H_2O_2[40]. When we employed the same lignin dimer in light-exposed LPMO reactions we did not observe H_2O_2 formation nor LPMO activity. Thus, we searched for other modifications (oxidations) in the lignin that are promoted by light exposure.

NMR spectroscopy was used to qualitatively investigate light-induced and LPMO-induced changes in the lignin structures directly. All lignins were incubated for 24 h with or without exposure to visible light (I = 10% I_{max}, corresponding to ~16.8 W cm^{-2}). For kraft lignin, light-exposure resulted in a decrease in the signal corresponding to hydroxyl groups (Supplementary Fig. 7), which could be due to generation of phenoxyl radicals (i.e., oxidation of phenolic hydroxyl groups) that radically couple with other parts of the lignin structure. More extensive analyses were done with the organosolv lignins. For organosolv lignin from both birch and spruce, the light treated sample showed an increase in cinnamaldehyde end groups (see Fig. 6a, b, f for spruce and Supplementary Fig. 8a, b, f for birch; more details in Supplementary Figs. 9 and 10), a decrease in carbon-carbon double bonds (Supplementary Figs. 9a and 10a), and, in the case of spruce, a notable decrease in β–1 stilbene signals ($SB1_\alpha$, $SB1_2$, $SB1_6$ in Fig. 6f). Overall, the spectra of light-exposed organosolv lignin showed a decrease in signals associated with olefins, accompanied by an increase in aldehyde signals (Supplementary Figs. 9 and 10). The decrease in olefinic signals and the concomitant increase in aldehydes are consistent with light-induced oxidation of ring-conjugated olefins[50].

Given that *Sc*AA10C oxidizes lignin and that organosolv lignin sustains slow cellulose solubilization by *Sc*AA10C in the dark, we attempted to measure changes in the organosolv lignin structure following reactions in the dark with LPMO, in the absence or presence of Avicel. Based on 1D carbon NMR, the lignin structure seemed unaffected by the LPMO regardless of the presence of Avicel (Fig. 6c–e, Supplementary Fig. 8c–e). When Avicel was included, the presence of soluble C-1 oxidized cello-oligosaccharides (Fig. 6e, Supplementary Figs. 8e, 9c, and 10c) was clearly detectable, showing that the LPMO was active. It should be noted that the spectra for LPMO-treated lignin have a higher signal-to-noise ratio compared to the spectra for light-treated lignin due to a 2-fold lower lignin concentration leading to ~4-fold lower sensitivity.

1D proton NMR of the treated organosolv lignins showed that protons of the hydroxyl groups in light-treated lignin occur at a higher chemical shift meaning that they are on average more deshielded compared to dark-incubated lignin. In contrast, addition of the LPMO resulted in hydroxyl protons becoming more shielded, as shown by a lower chemical shift (Supplementary Fig. 11). The degree of shielding may be interpretated as the degree of hydrogen bonding, as hydroxyl groups are strongly deshielded by hydrogen bonds[52]. These changes were observed for both the spruce and the birch lignin and suggest that light-driven oxidation and LPMO-catalyzed oxidation of lignin

have different chemical consequences. Oxidation of ring-conjugated olefins, promoted by light, could lead to some depolymerization of the lignin (as also suggested by the increase in cinnamaldehyde end groups; Fig. 6), resulting in increased hydrogen bonding and deshielded hydroxyl groups. On the other hand, LPMOs will oxidize hydroxyl groups[22], which could lead to radical formation and increased polymerization. It is not surprising that, apart from the observed changes in hydrogen bonding of the hydroxyl protons, no effects of LPMO treatment on the lignin structure could be detected, given that a reduced LPMO can catalyze multiple peroxygenase reactions and that, thus, oxidation of lignin by the LPMO may be much less frequent than the light-promoted oxidations that generate H_2O_2.

Probing for a possible role of water oxidation

It has been claimed, recently, that lignin may photocatalytically oxidize H_2O to H_2O_2 and O_2[40], which would mean that the formation of H_2O_2 by irradiated lignin does not depend on O_2, and that irradiated lignin should be able to fuel the LPMO reaction under anaerobic conditions. To assess this possibility, anaerobic experiments with ScAA10C and Avicel were performed, in the presence of lignins (soluble kraft lignin and insoluble organosolv lignin from spruce) or ascorbic acid. The reaction containing only AscA should not lead to any product formation in true anaerobic conditions whilst a control reaction containing AscA and H_2O_2 should generate oxidized products.

Chromatographic analysis of reaction mixtures after 22 h of incubation under anaerobic conditions, showed that all three reactions without added H_2O_2 had generated identical, low amounts of oxidized products, whereas, as expected, product levels were higher in the reaction with added H_2O_2 (Supplementary Fig. 13). The similar and low product levels in the reactions without added H_2O_2, regardless of the reductant (AscA or lignin), indicate that all reactions were limited by the same factor, which must be traces of O_2. The chromatographic analysis shows that, if water oxidation was happening at all in the reaction set-ups used here, this process must have been very slow, since neither kraft lignin nor organosolv spruce lignin were able to promote anaerobic LPMO activity above the level reached in the anaerobic reaction with AscA. We did these experiments in $H_2{}^{18}O$ and used $H_2{}^{18}O_2$ in the control reaction with hydrogen peroxide, because such an approach in principle could provide additional evidence for (the absence of) water oxidation, as explained in the legend of Supplementary Fig. 13. Unfortunately, due to the presence of lignin, the quality of MALDI-TOF MS spectra was too low to provide additional support for the conclusions drawn from chromatographic product analysis.

Discussion

Biotic degradation of recalcitrant carbohydrates in plant litter is promoted by sunlight. This effect is believed to stem from photodegradation of lignin in secondary plant cell walls, which would increase the availability of cell wall carbohydrates for enzymatic degradation[34–36,38]. LPMOs are key to aerobic solubilization of cellulose and other polysaccharides[55,56] from plant cell walls and, in the present study, we show that the impact of light on biomass degradation may relate to the activity of these enzymes. We show that irradiation of lignin promotes lignin oxidation and formation of H_2O_2, which fuels the LPMO reaction. Notably, abiotic generation of H_2O_2 in the biomass may also promote the activity of other biomass-converting and H_2O_2-consuming enzymes, for example lignin peroxidases.

This study provides further evidence for H_2O_2-driven LPMO activity and adds to the notion that LPMOs are peroxygenases, and that the monooxygenase activity of these enzymes, if existing at all, is of minor importance, kinetically. We demonstrate that LPMO activity is improved in conditions generating higher H_2O_2 levels and is inhibited by HRP, supporting the notion that the LPMO reaction is H_2O_2-dependent. Since LPMOs are susceptible to autocatalytic inactivation[10,57], as also demonstrated here, in Fig. 1 and Supplementary Fig. 1, regulating the amount of H_2O_2 available to the LPMO is important. The use of lignin and light not only offers a cheap and abundant source of reducing power for LPMO reactions, but could also be used to obtain better control and regulation, as previously shown for light-driven LPMO reactions with chlorophyllin[32,42,58]. It should be noted that the use of light to control LPMO activity in commercial bioreactors operating at high dry matter concentrations with for instance lignocellulose will be challenging as light is attenuated in reaction slurries. Still, light will penetrate to some extent and it is thus worth noting that the present results suggest that the outcome of lignocellulose saccharification experiments with LPMO-containing cellulase cocktails may depend on the vessel type (glass or steel) and the light conditions in the laboratory or the industrial plant. These light attenuation issues will not apply in light/lignin fueled reaction with other H_2O_2-dependent enzymes, for example the oxyfunctionalization of hydrocarbons recently reported by Kim et al.[40].

LPMO catalysis depends on reducing equivalents that are needed to bring the enzyme in its reduced, catalytically competent state. Since a once reduced LPMO can catalyze multiple peroxygenase reactions[14,17,59] and since most LPMO reactions likely are limited by available H_2O_2, the amount of LPMO reduction needed to maintain optimal reaction speed is somewhat unclear but is certainly much lower than the need for in situ generation of H_2O_2. We show here that LPMOs can oxidize polymeric lignin directly to recruit electrons and do so at an appreciable rate. The rates determined in our stopped-flow experiments are one order of magnitude lower than those observed for lignin oxidation by manganese peroxidase[60], between two and three orders of magnitude lower than the most efficient lignin peroxidases[61], and two orders of magnitude lower than LPMO reduction by one of the most efficient small molecule reductants, AscA[12].

While photoyellowing and photobleaching of lignin are well-known phenomena[50], and studies on the impact of visible light on lignin model compounds and lignin combined with (non-lignin) photoredox catalysts have been reported[62,63], to our knowledge not much is known about the structural modifications that may occur when polymeric lignin is exposed to visible light ($\lambda = 400–700$ nm). Our NMR analysis reveals that visible light-exposure of lignin results in oxidation of ring-conjugated carbon-carbon double bonds with a concomitant increase in cinnamaldehyde end groups (Fig. 6, Supplementary Figs. 8–11). Following light-exposure, the lignin hydroxyl groups experience an increase in hydrogen bonding, an effect that is opposite of what was found when the lignin was incubated in the presence of an LPMO, in the dark. This indicates that light-induced oxidation of lignin and LPMO-catalyzed lignin oxidation are distinct reactions

Importantly, while the structural studies of lignin show effects of both irradiation and LPMO action and clearly point at the chemical processes involved, further studies are needed to fully unravel structural changes in lignin. We used the highest practical sample concentrations in the NMR analyses, to maximize sensitivity. The complexity and heterogeneity of the lignin structures requires high sensitivity, while achieving complete dissolution of samples is challenging. It is likely that the structural changes in lignin observed in this study only provide part of the picture, due to low signal-to-noise ratios, particularly for the 1D carbon spectra. Of note, the apparent lack of an effect of LPMO treatment on the 1D carbon spectra of lignin (Fig. 6 and Supplementary Fig. 8) could to some extent be due to the lower signal-to-noise ratio in these spectra (compared to the spectra obtained in the experiments with light). Thus, we cannot fully exclude that LPMO action also leads to lignin oxidations similar to those occurring upon treatment with light. Further in-depth studies of treated and untreated lignin are needed to unravel the full impact of light and LPMO action of lignin. Such studies may eventually allow the determination of quantitative correlations between the degree of lignin oxidation, the amount of hydrogen peroxide produced and LPMO activity. Of note,

revealing such correlations would require accurate quantitative detection of all LPMO products and hydrogen peroxide levels under relevant conditions, which is challenging for reactions with lignin.

The present findings show that LPMO reactions can be fueled by light-exposed lignin and may have wide implications for how we understand biological processes related to biomass conversion in Nature. Lignin is abundant in plant biomass, which could make many processes involving biomass light sensitive. Interestingly, LPMO action was recently shown to be a major contributor to the infectivity of the potato pathogen *Phytophtora infestans*[64] and one may wonder if infectivity is affected by light. On another note, our findings suggest that changes in access to light may contribute to the well-known impact of tillage regimes on the turnover and sequestration of organic matter in soil[65]. It would be of interest to investigate whether the interplay between light, redox-active structural components, and enzymes such as LPMOs has had an impact on the (co-)evolution of lignin-rich materials and the enzyme systems that degrade these. While these are interesting possible implications and while the impact of light on biomass conversion in Nature is indisputable, the magnitude and relative importance of light/lignin-fueled catalysis by LPMOs and other H_2O_2-dependent biomass degrading enzymes remains to be established. No matter the width and magnitude of these implications, the present study provides important insight into the complex roles of lignin and light in Nature and the catalytic potential of LPMOs.

Methods

Materials

The crystalline cellulose used in this study was Avicel PH-101 (50 μm particles; Sigma-Aldrich). A 10 mM stock solution of AmplexRed (Thermo Fisher Scientific) was prepared in DMSO, aliquoted, and stored at −20 °C in the dark. Aliquots were thawed in the dark for 10 min before use and were used only once. Lignin stock solutions were prepared fresh in water each day in aluminum foil wrapped tubes and kept on ice. Kraft lignin, with an average molecular mass of 10 000 g/mol, was purchased from Sigma-Aldrich (Product number: 471003) and stored at room temperature in the dark. Dialyzed kraft lignin was prepared by dialyzing ~25 mL of a saturated kraft lignin solution against 5 L of ultrapure Milli-Q treated water overnight three times, in the dark, using a Spectra/Por® membrane with a MWCO of 3500 Da, after which the material was freeze-dried (Supplementary Fig. 12).

Organosolv lignins were obtained from spruce and birch. Debarked knife-milled wood (<2 mm) was used as feedstocks for organosolv treatments conducted in a 600 mL stirred high-pressure reactor (Parr) using 50 wt % aqueous ethanol as solvent and a biomass content in the reactor of 10 wt %. The wood suspensions were kept at 190 °C for 90 min or 120 min, for birch or spruce, respectively. After the treatment, the slurries were separated using a hydraulic press (Sotel) and the liquid phase was vacuum filtered (Whatman filter paper no.1). Lignin precipitation was performed by diluting the organosolv hydrolysates with water (1:4, w/w). Precipitation experiments were conducted at room temperature, with magnetic stirring for 2 h. After that, the suspension was centrifuged for 30 min at 12,000 *g*. Supernatants were discarded and lignin was dried at 45 °C for at least 48 h. Stock suspensions of organosolv lignins for photobiocatalytic LPMO reactions were suspended in water, not in DMSO or alcohols as these solvents may act as radical scavengers and/or sacrificial electron donors.

Enzymes

The model enzyme, *Sc*AA10C (UniProt ID Q9RJY2 [https://www.uniprot.org/uniprotkb/Q9RJY2/entry]) from *Streptomyces coelicolor*, was recombinantly produced and purified as previously described using anion exchange chromatography (HiTrap DEAE FF, GE Healthcare) followed by size exclusion chromatography (HiLoad 16/60 Superdex 75, GE Healthcare)[66], copper-saturated with three-fold molar excess Cu(II)SO_4[67], and desalted using a PD MidiTrap column [G-25, GE Healthcare][68] with buffer exchange to sodium phosphate (25 mM, pH 6.0). *Sm*AA10A (UniProt ID O83009) was produced and purified as previously described using chitin affinity chromatography (Chitin resin, New England Biolabs)[69], copper-saturated similarly to *Sc*AA10C, and stored in the same buffer. *Ta*AA9A (UniProt ID G3XAP7) was recombinantly produced and purified as described elsewhere using hydrophobic interaction chromatography (HiTrap Phenyl FF, GE Healthcare)[70] and copper-saturated prior to size-exclusion chromatography (HiLoad 16/60 Superdex 75, GE Healthcare)[71]. *Nc*AA9F (NCU03328; UniProt ID Q1K4Q1) was recombinantly produced and purified as described elsewhere[72] using hydrophobic interaction chromatography (HiTrap Phenyl FF, GE Healthcare) and anion exchange chromatography (HiTrap DEAE FF, GE Healthcare), and copper-saturated prior to size-exclusion chromatography (HiLoad 16/60 Superdex 75, GE Healthcare). *Ta*AA9A and *Nc*AA9F were stored in 50 mM Bis-Tris pH 6.5. Mn-dependent superoxide dismutase (Mn-SOD) from *E. coli* (Sigma-Aldrich, product number: S5639) was solubilized in Tris-HCl (10 mM, pH 8.0) and desalted (PD MidiTrap G-25, GE Healthcare) in the same buffer before use. Horseradish peroxidase (HRP, type II) (Sigma-Aldrich, product number: P8250) was solubilized in ultrapure Milli-Q treated water and filtered (Filtropur S, 0.2 μm PES, Sarstedt). All enzymes were stored at 4 °C.

Standard photobiocatalytic LPMO reactions

Standard photobiocatalytic reactions were carried out in a cylindrical glass vial (1.1 mL) with a conical bottom (Thermo Scientific) with 500 μL reaction volume, unless otherwise specified. The light source (Lightningcure L9588, Hamamatsu) was equipped with a filter with a spectral distribution of 400–700 nm (L9588-03, Hamamatsu) and placed 1 cm above the liquid surface. Standard reactions contained *Sc*AA10C (0.5 μM), Avicel (10 g L^{-1}), and kraft lignin (0.9 g L^{-1}) in sodium phosphate buffer (50 mM; pH 7.0), unless otherwise specified. The reactions were incubated for 15 min in the dark at 40 °C under magnetic stirring prior to adding lignin and starting the reactions by turning on the light (I = 10% I_{max}, equivalent to 16.8 W cm^{-2}). At regular intervals, 60 μL samples were removed from the reaction mixture and filtered using a 96-well filter plate (Millipore) and a vacuum manifold to stop the LPMO reaction. The filtered samples (35 μL) were stored at −20 °C prior to product quantification. A stock solution of recombinant, purified Cel6A from *Themobifida fusca* (*Tf*Cel6A)[73] was prepared in sodium phosphate buffer (50 mM; pH 6.0) and added to the filtrate to a final concentration of 2 μM, followed by incubation overnight at room temperature, to convert solubilized oxidized products to a mixture of C1-oxidized products with a degree of polymerization of 2 and 3 (GlcGlc1A and Glc_2Glc1A).

For measuring total oxidized products (i.e., both soluble and insoluble, as in Fig. 1), 50 μL samples were removed from the reaction, diluted with 50 μL H_2O and boiled for 15 min at 100 °C, cooled on ice, and stored at −20 °C prior to HPAEC-PAD analysis of oxidized products as described below. To prepare the samples for HPAEC-PAD analysis, 150 μL *Tf*Cel6A (5 μM final concentration) was added to 100 μL reaction suspension and the reaction was incubated in a thermomixer at 37 °C and 1200 rpm for 42 h to degrade all cellulosic material.

Detection and quantification of LPMO products

Oxidized cello-oligosaccharides were analyzed by HPAEC-PAD performed with a Dionex ICS5000 system equipped with a CarboPac PA200 analytical column (3 × 250 mm) as previously described[54]. Chromatograms were recorded and analyzed using Chromeleon 7.0 software. Quantitative analysis of C1-oxidizing LPMO activity was based on quantification of cellobionic acid (GlcGlc1A) and cellotrionic acid (Glc_2Glc1A), which were obtained after treating reaction mixtures or reaction filtrates with *Tf*Cel6A, as described above. Standards of

GlcGlc1A and Glc_2Glc1A were prepared by treating cellobiose and cellotriose, both purchased from Megazyme, with cellobiose dehydrogenase[74].

Oxidized chito-oligosaccharides were qualitatively analyzed using an Agilent 1290 HPLC system with a HILIC column using UV-detection, as described elsewhere[75,76]. Chito-oligosaccharides with a degree of polymerization from 2 to 6 (Megazyme) were treated with a chito-oligosaccharide oxidase[77] to generate the corresponding oxidized chito-oligosaccharides[67], which were used as standards.

H_2O_2 accumulation and consumption

The method for H_2O_2 detection was adapted from previously published methods[23,72] and modified as explained below. H_2O_2 accumulation in the light-exposed reactions containing lignin (0.9 or 9 g L^{-1}), LPMO (0, 75, or 500 nM), and Avicel (10 g L^{-1}) that are depicted in Fig. 1 was measured as follows: At given time points, 50 μL sample was withdrawn from the reaction and mixed with 50 μL H_2O before filtering as described above for LPMO reactions. 50 μL filtrate was recovered and diluted with water, after which 100 μL of diluted sample was mixed with 20 μL H_2O and 80 μL of a premix composed of HRP (0.4 μM) and AmplexRed (0.4 mM) in sodium phosphate buffer (0.4 M; pH 6.0). The H_2O_2 standard curve (0, 1, 2, 5, 10 μM) was prepared by mixing 80 μL of the same HRP/AmplexRed premix with 20 μL of an aqueous lignin solution to achieve approximately the same lignin concentration as for the reaction being measured, and lastly with 100 μL H_2O_2 solution (0, 2, 4, 10, 20 μM). All reaction mixtures were prepared in a non-transparent 96-well microtiter plate. The reaction mixtures were shaken for 30 s and incubated for 5 min at 30 °C prior to measuring fluorescence every 10 s for 2 min using 530/590 nm excitation/emission wavelengths in a Varioskan Lux plate reader (Thermo Fisher Scientific).

H_2O_2 consumption reactions were performed using the same conditions as the reactions for H_2O_2 production and were initiated by adding H_2O_2. Samples (50 μL) were withdrawn from the reaction at given time points (5, 10, 15, 40, 80, 120 min) and diluted with water prior to filtering the reaction mixture and measuring remaining H_2O_2, as described above.

Transient state kinetics of LPMO reduction by lignin

We used the differences in intrinsic fluorescence between the Cu(II) and Cu(I) states of *Sm*AA10A or *Sc*AA10C to measure the kinetics of LPMO reduction by kraft lignin. Single-mixing experiments were carried out with a stopped-flow rapid spectrophotometer (SFM4000, BioLogic Science Instruments) coupled to a photomultiplier with an applied voltage of 600 V for detection. The excitation wavelength was set to 280 nm, and fluorescence was collected with a 340 nm bandpass filter. Single-mixing experiments were carried out by mixing LPMO-Cu(II) (5 μM final concentration after mixing, 50 mM sodium phosphate buffer, pH 7.0) with different concentrations of lignin (ranging from 1 to 100 μM final concentrations after mixing), in triplicates. All reagents were deoxygenated using a Schlenk line with N_2 flux and subsequently prepared in sealed syringes in an anaerobic chamber. The stopped-flow rapid spectrophotometer was flushed with a large excess of anaerobic buffer before coupling the sealed syringes and performing the experiments.

Kinetics data analysis

The fluorescence data monitored with the stopped-flow was fitted to a single exponential function ($y = a + b \cdot e^{-kobs \cdot t}$) using the BioKine32 V4.74.2 software (BioLogic Science Instruments) to obtain the first order rate constant (k_{1obs}) for each lignin concentration. Plots of k_{1obs} vs lignin concentration were fitted using linear least squares regression to obtain the apparent second order rate constant of the reduction step (k_{1app}^{lignin}) with SigmaPlot v14.0.

NMR analyses

Kraft lignin (15 g L^{-1}) and organosolv lignin from birch or spruce (10 g L^{-1}) were incubated for 24 h in sodium phosphate buffer (50 mM, pH 7.0 for kraft lignin and pH 6.0 for organosolv lignin) at 40 °C under magnetic stirring, with or without exposure to visible light ($I = 10\%$ I_{max}, equivalent to 16.8 W cm^{-2}). For the incubations with organosolv lignin from birch or spruce, reactions were also performed in the presence of *Sc*AA10C (500 nM) alone or *Sc*AA10C (500 nM) in combination with Avicel (10 g L^{-1}), in the dark, to probe for putative LPMO-induced structural changes in the lignin. The reactions containing LPMO were performed as duplicates as opposed to the reactions treated with light or not in absence of LPMO, which were performed as four replicates. After 24 h, identical reactions were pooled and freeze-dried prior to NMR analyses.

Lyophilized organosolv lignin (20–40 mg) that had been incubated as described above was dissolved in 480 μL of deuterated dimethyl sulfoxide (DMSO-d_6 99.96 atom % D Sigma-Aldrich) and transferred to a 5 mm LabScape Stream NMR tube (Bruker LabScape). For NMR analyses, all homo- and heteronuclear experiments were recorded on a Bruker AV-IIIHD 800 MHz spectrometer (Bruker BioSpin AG) equipped with a 5 mm cryogenic CP-TCI z-gradient probe. The spectra were recorded, processed, and analyzed using TopSpin 3.6pl7 and TopSpin 4.0.7 software (Bruker BioSpin AG).

For chemical shift assignments, the following one- and two-dimensional NMR experiments were recorded at 25 °C for both the birch and spruce lignin sample series: 1D carbon with power-gated decoupling and 30° flip angle (spectral width 220 ppm, spectral resolution 64k points, number of scans 4096, interscan delay 4 s), 1D proton with 30° flip angle (spectral width 14 ppm, spectral resolution 64k points, number of scans 16, interscan delay 1 s), 2D $\{^1H\text{-}^{13}C\}$ heteronuclear single quantum coherence (HSQC) with multiplicity editing (spectral width C 200 ppm/ H 14 ppm, spectral resolution H 2k/ C 256k points, number of scans 32, interscan delay 2 s).

1D proton and carbon experiments were Fourier transformed using exponential windows function and line broadening of 0.3 Hz for proton and 5 Hz for carbon. Spectra were manually phase corrected with automatic baseline correction. HSQC experiments were Fourier transformed with the QSINE windows function (SSB = 2) in both dimensions, zero filling, linear prediction, and automatic baseline correction. All spectra were internally referenced to the residual DMSO signal (δ_C 39.5 and δ_H 2.50). Comparative analyses were only done for sets of reactions with similar lignin concentrations (i.e., those treated with LPMO containing ~20 mg lignin, and those treated with light, containing ~40 mg; the difference is due to sample availability). For presenting 1D spectra together, spectral intensities were scaled to the peak intensity at δ_C ~28ppm and/or δ_H 0.85 and 1.24, to compensate for differences in sample mass. Chemical moieties that changed, either in light-treated or LPMO-treated samples, were annotated based on comparison of chemical shift values with published literature values (see Figure captions for references).

^1H 1D NMR investigations of the kraft lignin were performed with a Bruker Avance III 400 MHz spectrometer equipped with a BBFO Plus double resonance probe head at 25 °C (Bruker BioSpin AG). 10–15 mg of lignin, treated as described above, was dissolved in 1500 μL of deuterated dimethyl sulfoxide (DMSO-d_6 99.9 atom % D Sigma-Aldrich) and transferred to a 5 mm NMR tube. The spectra were acquired with 30° flip angle, spectral width 16 ppm, spectral resolution 64k points, number of scans 80, interscan delay 10 s. The spectra were recorded with TopSpin 3.64 (Bruker BioSpin AG). MestreNova software v14.1.1 was used for processing and analysis (Mestrelab research S.L.).

Verification of superoxide dismutase activity

SOD activity was assessed using a published assay protocol[23,78]. In alkaline conditions, autooxidation of pyrogallol leads to formation

of $O_2^{\bullet-}$ which converts pyrogallol to purpurogallin, which absorbs strongly at 325 nm[78]. A stock solution of pyrogallol (15 mM in 10 mM HCl) was prepared in an aluminum foil wrapped tube and stored on ice and stock solutions of SOD were prepared in Tris-HCl (10 mM, pH 8.0) and kept on ice. All reactions were performed in 50 mM Tris-HCl pH 8.0 and were initiated by addition of pyrogallol (to 0.2 mM) immediately followed by addition of SOD (to 0, 10, 100, 1000 nM) and the absorbance at 325 nm was measured every 10 s for 3 min in a Hitachi U-1900 spectrophotometer. The inhibitory effect of SOD on pyrogallol autooxidation is shown in Supplementary Fig. 14.

Reporting summary

Further information on research design is available in the Nature Portfolio Reporting Summary linked to this article.

Data availability

The authors declare that all study data are included in the article and/or the supplementary information. Data is also available from the corresponding author upon request. The UniProt IDs of the enzymes used in this study are Q9RJY2 (*Sc*AA10C), O83009 (*Sm*AA10A), G3XAP7 (*Ta*AA9A), and Q1K4Q1 (*Nc*AA9F).

References

1. Field, C. B., Behrenfeld, M. J., Randerson, J. T. & Falkowski, P. Primary production of the biosphere: integrating terrestrial and oceanic components. *Science* **281**, 237–240 (1998).
2. Kirui, A. et al. Carbohydrate-aromatic interface and molecular architecture of lignocellulose. *Nat. Commun.* **13**, 538 (2022).
3. Vaaje-Kolstad, G. et al. An oxidative enzyme boosting the enzymatic conversion of recalcitrant polysaccharides. *Science* **330**, 219–222 (2010).
4. Phillips, C. M., Beeson, W. T., Cate, J. H. & Marletta, M. A. Cellobiose dehydrogenase and a copper-dependent polysaccharide monooxygenase potentiate cellulose degradation by *Neurospora crassa*. *ACS Chem. Biol.* **6**, 1399–1406 (2011).
5. Quinlan, R. J. et al. Insights into the oxidative degradation of cellulose by a copper metalloenzyme that exploits biomass components. *Proc. Natl Acad. Sci. USA* **108**, 15079–15084 (2011).
6. Forsberg, Z. et al. Cleavage of cellulose by a CBM33 protein. *Protein Sci.* **20**, 1479–1483 (2011).
7. Levasseur, A., Drula, E., Lombard, V., Coutinho, P. M. & Henrissat, B. Expansion of the enzymatic repertoire of the CAZy database to integrate auxiliary redox enzymes. *Biotechnol. Biofuels* **6**, 41 (2013).
8. Frommhagen, M. et al. Discovery of the combined oxidative cleavage of plant xylan and cellulose by a new fungal polysaccharide monooxygenase. *Biotechnol. Biofuels* **8**, 101 (2015).
9. Agger, J. W. et al. Discovery of LPMO activity on hemicelluloses shows the importance of oxidative processes in plant cell wall degradation. *Proc. Natl Acad. Sci. USA* **111**, 6287–6292 (2014).
10. Bissaro, B. et al. Oxidative cleavage of polysaccharides by monocopper enzymes depends on H_2O_2. *Nat. Chem. Biol.* **13**, 1123–1128 (2017).
11. Kuusk, S. et al. Kinetics of H_2O_2-driven degradation of chitin by a bacterial lytic polysaccharide monooxygenase. *J. Biol. Chem.* **293**, 523–531 (2018).
12. Bissaro, B. et al. Molecular mechanism of the chitinolytic peroxygenase reaction. *Proc. Natl Acad. Sci. USA* **117**, 1504–1513 (2020).
13. Jones, S. M., Transue, W. J., Meier, K. K., Kelemen, B. & Solomon, E. I. Kinetic analysis of amino acid radicals formed in H2O2-driven Cu^{I} LPMO reoxidation implicates dominant homolytic reactivity. *Proc. Natl Acad. Sci. USA* **117**, 11916–11922 (2020).
14. Hedison, T. M. et al. Insights into the H_2O_2-driven catalytic mechanism of fungal lytic polysaccharide monooxygenases. *FEBS J.* **288**, 4115–4128 (2021).
15. Eibinger, M. et al. Cellulose surface degradation by a lytic polysaccharide monooxygenase and its effect on cellulase hydrolytic efficiency. *J. Biol. Chem.* **289**, 35929–35938 (2014).
16. Song, B. et al. Real-time imaging reveals that lytic polysaccharide monooxygenase promotes cellulase activity by increasing cellulose accessibility. *Biotechnol. Biofuels* **11**, 41 (2018).
17. Müller, G., Chylenski, P., Bissaro, B., Eijsink, V. G. H. & Horn, S. J. The impact of hydrogen peroxide supply on LPMO activity and overall saccharification efficiency of a commercial cellulase cocktail. *Biotechnol. Biofuels* **11**, 209 (2018).
18. Reese, E. T., Siu, R. G. & Levinson, H. S. The biological degradation of soluble cellulose derivatives and its relationship to the mechanism of cellulose hydrolysis. *J. Bacteriol.* **59**, 485–497 (1950).
19. Eriksson, K.-E., Pettersson, B. & Westermark, U. Oxidation: an important enzyme reaction in fungal degradation of cellulose. *FEBS Lett.* **49**, 282–285 (1974).
20. Chylenski, P. et al. Lytic polysaccharide monooxygenases in enzymatic processing of lignocellulosic biomass. *ACS Catal.* **9**, 4970–4991 (2019).
21. Frommhagen, M., Westphal, A. H., van Berkel, W. J. H. & Kabel, M. A. Distinct substrate specificities and electron-donating systems of fungal lytic polysaccharide monooxygenases. *Front. Microbiol.* **9**, 1–22 (2018).
22. Kracher, D. et al. Extracellular electron transfer systems fuel cellulose oxidative degradation. *Science* **352**, 1098–1101 (2016).
23. Bissaro, B., Kommedal, E., Røhr, Å. K. & Eijsink, V. G. H. Controlled depolymerization of cellulose by light-driven lytic polysaccharide oxygenases. *Nat. Commun.* **11**, 890 (2020).
24. Westereng, B. et al. Enzymatic cellulose oxidation is linked to lignin by long-range electron transfer. *Sci. Rep.* **5**, 18561 (2015).
25. Muraleedharan, M. N. et al. Effect of lignin fractions isolated from different biomass sources on cellulose oxidation by fungal lytic polysaccharide monooxygenases. *Biotechnol. Biofuels* **11**, 296 (2018).
26. Chalak, A. et al. Influence of the carbohydrate-binding module on the activity of a fungal AA9 lytic polysaccharide monooxygenase on cellulosic substrates. *Biotechnol. Biofuels* **12**, 206 (2019).
27. Frommhagen, M. et al. Lytic polysaccharide monooxygenases from *Myceliophthora thermophila* C1 differ in substrate preference and reducing agent specificity. *Biotechnol. Biofuels* **9**, 1–17 (2016).
28. Bissaro, B., Várnai, A., Røhr, Å. K. & Eijsink, V. G. H. Oxidoreductases and reactive oxygen species in conversion of lignocellulosic biomass. *Microbiol. Mol. Biol. Rev.* **82**, e00029–18 (2018).
29. Kuusk, S. & Väljamäe, P. Kinetics of H_2O_2-driven catalysis by a lytic polysaccharide monooxygenase from the fungus *Trichoderma reesei*. *J. Biol. Chem.* **297**, 101256 (2021).
30. van Schie, M. M. C. H. et al. Cascading g-C_3N_4 and peroxygenases for selective oxyfunctionalization reactions. *ACS Catal.* **9**, 7409–7417 (2019).
31. Schmermund, L. et al. Photo-Biocatalysis: biotransformations in the presence of light. *ACS Catal.* **9**, 4115–4144 (2019).
32. Cannella, D. et al. Light-driven oxidation of polysaccharides by photosynthetic pigments and a metalloenzyme. *Nat. Commun.* **7**, 11134 (2016).
33. Bissaro, B. et al. Fueling biomass-degrading oxidative enzymes by light-driven water oxidation. *Green. Chem.* **18**, 5357–5366 (2016).
34. Austin, A. T. & Vivanco, L. Plant litter decomposition in a semi-arid ecosystem controlled by photodegradation. *Nature* **442**, 555–558 (2006).
35. Austin, A. T. & Ballaré, C. L. Dual role of lignin in plant litter decomposition in terrestrial ecosystems. *Proc. Natl Acad. Sci. USA* **107**, 4618–4622 (2010).
36. Austin, A. T., Méndez, M. S. & Ballaré, C. L. Photodegradation alleviates the lignin bottleneck for carbon turnover in terrestrial ecosystems. *Proc. Natl Acad. Sci. USA* **113**, 4392–4397 (2016).

37. Lin, Y., Karlen, S. D., Ralph, J. & King, J. Y. Short-term facilitation of microbial litter decomposition by ultraviolet radiation. *Sci. Total Environ.* **615**, 838–848 (2018).
38. Berenstecher, P., Vivanco, L., Pérez, L. I., Ballaré, C. L. & Austin, A. T. Sunlight doubles aboveground carbon loss in a seasonally dry woodland in Patagonia. *Curr. Biol.* **30**, 3243–3251.e3 (2020).
39. Miglbauer, E., Gryszel, M. & Głowacki, E. D. Photochemical evolution of hydrogen peroxide on lignins. *Green Chem.* **22**, 673–677 (2020).
40. Kim, J., Nguyen, T. V. T., Kim, Y. H., Hollmann, F. & Park, C. B. Lignin as a multifunctional photocatalyst for solar-powered biocatalytic oxyfunctionalization of C–H bonds. *Nat. Synth.* **1**, 217–226 (2022).
41. Hu, J., Arantes, V., Pribowo, A., Gourlay, K. & Saddler, J. N. Substrate factors that influence the synergistic interaction of AA9 and cellulases during the enzymatic hydrolysis of biomass. *Energy Environ. Sci.* **7**, 2308 (2014).
42. Blossom, B. M. et al. Photobiocatalysis by a lytic polysaccharide monooxygenase using intermittent illumination. *ACS Sustain. Chem. Eng.* **8**, 9301–9310 (2020).
43. Rieder, L., Petrović, D., Väljamäe, P., Eijsink, V. G. H. & Sørlie, M. Kinetic characterization of a putatively chitin-active LPMO reveals a preference for soluble substrates and absence of monooxygenase activity. *ACS Catal.* **11**, 11685–11695 (2021).
44. Kont, R. et al. The liquid fraction from hydrothermal pretreatment of wheat straw provides lytic polysaccharide monooxygenases with both electrons and H_2O_2 co-substrate. *Biotechnol. Biofuels* **12**, 235 (2019).
45. Burek, B. O., Bahnemann, D. W. & Bloh, J. Z. Modeling and optimization of the photocatalytic reduction of molecular oxygen to hydrogen peroxide over titanium dioxide. *ACS Catal.* **9**, 25–37 (2019).
46. Koppenol, W. H., Stanbury, D. M. & Bounds, P. L. Electrode potentials of partially reduced oxygen species, from dioxygen to water. *Free Radic. Biol. Med.* **49**, 317–322 (2010).
47. Sáez-Jiménez, V. et al. Role of surface tryptophan for peroxidase oxidation of nonphenolic lignin. *Biotechnol. Biofuels* **9**, 198 (2016).
48. Crestini, C., Lange, H., Sette, M. & Argyropoulos, D. S. On the structure of softwood kraft lignin. *Green Chem.* **19**, 4104–4121 (2017).
49. Lancefield, C. S., Wienk, H. L. J., Boelens, R., Weckhuysen, B. M. & Bruijnincx, P. C. A. Identification of a diagnostic structural motif reveals a new reaction intermediate and condensation pathway in kraft lignin formation. *Chem. Sci.* **9**, 6348–6360 (2018).
50. Paulsson, M. & Parkås, J. Light-induced yellowing of lignocellulosic pulps–mechanisms and preventive methods. *BioResources* **7**, 5995–6040 (2012).
51. Neumann, M. G. & Machado, A. E. H. The role of oxygen in the photodegradation of lignin in solution. *J. Photochem. Photobiol. B Biol.* **3**, 473–481 (1989).
52. Pretsch, E. et al. *Structure Determination Of Organic Compounds* (Springer, 2009).
53. Ralph, S. A., Ralph, J. & Landucci, L. L. *NMR Database of Lignin and Cell Wall Model Compounds*. http://www.glbrc.org/databases_and_software/nmrdatabase (2009).
54. Westereng, B. et al. Efficient separation of oxidized cello-oligosaccharides generated by cellulose degrading lytic polysaccharide monooxygenases. *J. Chromatogr. A* **1271**, 144–152 (2013).
55. Couturier, M. et al. Lytic xylan oxidases from wood-decay fungi unlock biomass degradation. *Nat. Chem. Biol.* **14**, 306–310 (2018).
56. Hegnar, O. A. et al. Quantifying oxidation of cellulose-associated glucuronoxylan by two lytic polysaccharide monooxygenases from *Neurospora crassa*. *Appl. Environ. Microbiol.* **87**, e01652–21 (2021).
57. Kadić, A., Várnai, A., Eijsink, V. G. H., Horn, S. J. & Lidén, G. In situ measurements of oxidation–reduction potential and hydrogen peroxide concentration as tools for revealing LPMO inactivation during enzymatic saccharification of cellulose. *Biotechnol. Biofuels* **14**, 46 (2021).
58. Dodge, N. et al. Water-soluble chlorophyll-binding proteins from *Brassica oleracea* allow for stable photobiocatalytic oxidation of cellulose by a lytic polysaccharide monooxygenase. *Biotechnol. Biofuels* **13**, 192 (2020).
59. Kuusk, S. et al. Kinetic insights into the role of the reductant in H_2O_2-driven degradation of chitin by a bacterial lytic polysaccharide monooxygenase. *J. Biol. Chem.* **294**, 1516–1528 (2019).
60. Ayuso-Fernández, I., Rencoret, J., Gutiérrez, A., Ruiz-Dueñas, F. J. & Martínez, A. T. Peroxidase evolution in white-rot fungi follows wood lignin evolution in plants. *Proc. Natl Acad. Sci. USA* **116**, 17900–17905 (2019).
61. Sánchez-Ruiz, M. I. et al. Agaricales mushroom lignin peroxidase: from structure–function to degradative capabilities. *Antioxidants* **10**, 1446 (2021).
62. Kärkäs, M. D., Matsuura, B. S., Monos, T. M., Magallanes, G. & Stephenson, C. R. J. Transition-metal catalyzed valorization of lignin: the key to a sustainable carbon-neutral future. *Org. Biomol. Chem.* **14**, 1853–1914 (2016).
63. Magallanes, G. et al. Selective C–O bond cleavage of lignin systems and polymers enabled by sequential palladium-catalyzed aerobic oxidation and visible-light photoredox catalysis. *ACS Catal.* **9**, 2252–2260 (2019).
64. Sabbadin, F. et al. Secreted pectin monooxygenases drive plant infection by pathogenic oomycetes. *Science* **373**, 774–779 (2021).
65. Jastrow, J. D., Amonette, J. E. & Bailey, V. L. Mechanisms controlling soil carbon turnover and their potential application for enhancing carbon sequestration. *Clim. Change* **80**, 5–23 (2007).
66. Forsberg, Z. et al. Structural and functional characterization of a conserved pair of bacterial cellulose-oxidizing lytic polysaccharide monooxygenases. *Proc. Natl Acad. Sci. USA* **111**, 8446–8451 (2014).
67. Loose, J. S. M., Forsberg, Z., Fraaije, M. W., Eijsink, V. G. H. & Vaaje-Kolstad, G. A rapid quantitative activity assay shows that the *Vibrio cholerae* colonization factor GbpA is an active lytic polysaccharide monooxygenase. *FEBS Lett.* **588**, 3435–3440 (2014).
68. Stepnov, A. A. et al. Unraveling the roles of the reductant and free copper ions in LPMO kinetics. *Biotechnol. Biofuels* **14**, 28 (2021).
69. Vaaje-Kolstad, G., Houston, D. R., Riemen, A. H. K., Eijsink, V. G. H. & van Aalten, D. M. F. Crystal structure and binding properties of the *Serratia marcescens* chitin-binding protein CBP21. *J. Biol. Chem.* **280**, 11313–11319 (2005).
70. Chylenski, P. et al. Enzymatic degradation of sulfite-pulped softwoods and the role of LPMOs. *Biotechnol. Biofuels* **10**, 177 (2017).
71. Petrović, D. M. et al. Methylation of the N-terminal histidine protects a lytic polysaccharide monooxygenase from auto-oxidative inactivation. *Protein Sci.* **27**, 1636–1650 (2018).
72. Kittl, R., Kracher, D., Burgstaller, D., Haltrich, D. & Ludwig, R. Production of four *Neurospora crassa* lytic polysaccharide monooxygenases in *Pichia pastoris* monitored by a fluorimetric assay. *Biotechnol. Biofuels* **5**, 79 (2012).
73. Calza, R. E., Irwin, D. C. & Wilson, D. B. Purification and characterization of two β-1,4-endoglucanases from *Thermomonospora fusca*. *Biochemistry* **24**, 7797–7804 (1985).
74. Zámocký, M. et al. Cloning, sequence analysis and heterologous expression in *Pichia pastoris* of a gene encoding a thermostable cellobiose dehydrogenase from *Myriococcum thermophilum*. *Protein Expr. Purif.* **59**, 258–265 (2008).
75. Nakagawa, Y. S. et al. A small lytic polysaccharide monooxygenase from *Streptomyces griseus* targeting α- and β-chitin. *FEBS J.* **282**, 1065–1079 (2015).
76. Mekasha, S. et al. A trimodular bacterial enzyme combining hydrolytic activity with oxidative glycosidic bond cleavage efficiently degrades chitin. *J. Biol. Chem.* **295**, 9134–9146 (2020).

77. Heuts, D. P. H. M., Winter, R. T., Damsma, G. E., Janssen, D. B. & Fraaije, M. W. The role of double covalent flavin binding in chito-oligosaccharide oxidase from *Fusarium graminearum*. *Biochem. J.* **413**, 175–183 (2008).
78. Li, X. Improved pyrogallol autoxidation method: a reliable and cheap superoxide-scavenging assay suitable for all antioxidants. *J. Agric. Food Chem.* **60**, 6418–6424 (2012).

Acknowledgements

This work was supported by the Norwegian Research Council through grants 262853 (V.G.H.E), 257622 (S.J.H), 315385 (F.L.A), 268002 (V.G.H.E.), and 269408 (V.G.H.E), and by the European Commission through the ERC-SyG-2019 project CUBE with grant number 856446 (V.G.H.E.).

Author contributions

E.G.K, S.J.H., and V.G.H.E designed the study. E.G.K., C.F.A., L.J.K., I.A.F., B.A., S.G.A., F.G., F.C., and F.L.A. performed the experiments. E.G.K., C.F.A., L.J.K., I.A.F., B.A., S.G.A., Y.S., D.E., F.G., F.C., S.J.H., F.L.A., and V.G.H.E. interpreted the data. E.G.K. and V.G.H.E. wrote the initial manuscript. All authors contributed to revising and writing the final version of the manuscript.

Competing interests

The authors declare no competing interests.

Additional information

Supplementary information The online version contains supplementary material available at https://doi.org/10.1038/s41467-023-36660-4.

Correspondence and requests for materials should be addressed to Vincent G. H. Eijsink.

Peer review information *Nature Communications* thanks the anonymous reviewer(s) for their contribution to the peer review of this work. Peer reviewer reports are available.

Supplementary information

Visible light-exposed lignin facilitates cellulose solubilization by lytic polysaccharide monooxygenases

Eirik G. Kommedal[1], Camilla F. Angeltveit[1], Leesa J. Klau[2], Iván Ayuso-Fernández[1], Bjørnar Arstad[3], Simen G. Antonsen[1], Yngve Stenstrøm[1], Dag Ekeberg[1], Francisco Gírio[4], Florbela Carvalheiro[4], Svein J. Horn[1], Finn Lillelund Aachmann[2], Vincent G. H. Eijsink[1*]

[1] Faculty of Chemistry, Biotechnology and Food Science, Norwegian University of Life Sciences (NMBU), 1432 Ås, Norway

[2] Department of Biotechnology and Food Science, Norwegian University of Science and Technology (NTNU), 7491 Trondheim, Norway

[3] SINTEF Industry, Process Chemistry and Functional Materials, 0373 Oslo, Norway

[4] National Laboratory of Energy and Geology (LNEG), 1649-038 Lisboa, Portugal

[*] Corresponding author: vincent.eijsink@nmbu.no

The supplementary information includes

Supplementary Figures

Supplementary Figure 10. Light-induced and LPMO-induced changes in organosolv birch lignin assessed by 2D HSQC NMR spectroscopy.

Supplementary Figure 11. Light-induced and LPMO-induced changes in organosolv birch and spruce lignin assessed by 1D proton NMR spectroscopy.

Supplementary Figure 12. UV-Vis absorption spectra of kraft lignin before and after dialysis.

Supplementary figure 13. Chromatographic analysis of oxidized products generated in anaerobic LPMO reactions with visible light-exposed lignin.

Supplementary Figure 14. Verification of Superoxide Dismutase (SOD) activity.

Supplementary references

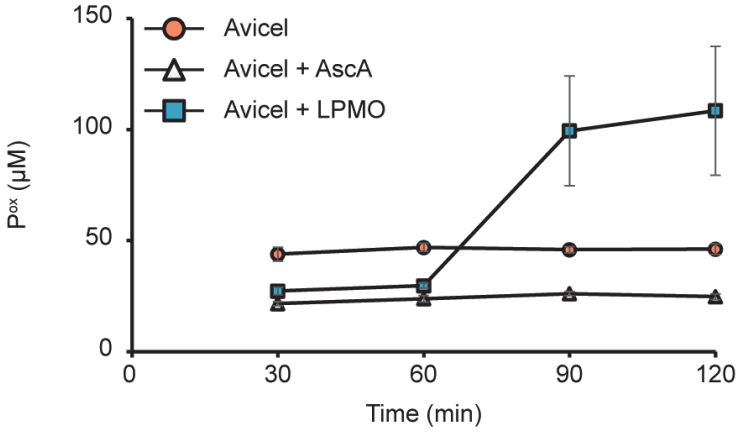

Supplementary Figure 1. Probing for LPMO inactivation. The graphs show time-courses for the release of aldonic acid products. All reactions were carried out with similar initial conditions: Avicel (10 $g.L^{-1}$), Kraft lignin (9 $g.L^{-1}$) and *Sc*AA10C (75 nM) in sodium phosphate buffer (50 mM, pH 7.0) at 40°C under magnetic stirring and exposed to visible light (I=10% I_{max}, approx. 16.8 $W.cm^{-2}$). After 60 min, Avicel (2.3 $g.L^{-1}$), Avicel (2.3 $g.L^{-1}$) and LPMO (100 nM), or Avicel (2.3 $g.L^{-1}$) and reductant (2.3 mM) were added to separate reactions, as indicated in the Figure. Upon sampling, reactions were stopped by filtration, separating the LPMO from its substrate. Before product quantification, solubilized cello-oligosaccharides were hydrolyzed with *Tf*Cel6A to convert LPMO products, with varying degree of polymerization (DP), to a mixture of DP 2 and 3 [GlcGlc1A, (Glc)2Glc1A], the amounts of which were summed up to yield the concentration of solubilized oxidized sites. The data is presented as mean values and error bars show ± s.d. (n = 3, independent experiments).

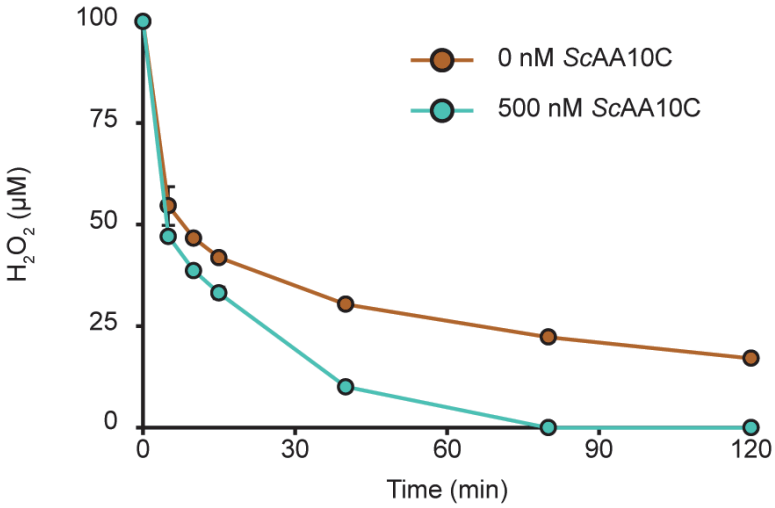

Supplementary Figure 2. Comparison of H_2O_2 consumption in standard dark reaction conditions in the presence or absence of LPMO. The graph shows time courses for consumption of H_2O_2 (added to 100 µM at t = 0) in the presence or absence of *Sc*AA10C (0.5 µM) in reactions with Avicel (10 g.L^{-1}) and kraft lignin (0.9 g.L^{-1}) in sodium phosphate buffer (50 mM, pH 7.0) at 40°C under magnetic stirring in the dark. The curves show that after an initial phase of equally fast H_2O_2 consumption lasting some 30 min, the reaction with the LPMO leads to faster H_2O_2 consumption in the later phase of the reaction (note that the LPMO reactions reported in the manuscript typically lasted 6 hours). The data points represent the mean of three independent experiments and error bars show ± s.d (n = 3).

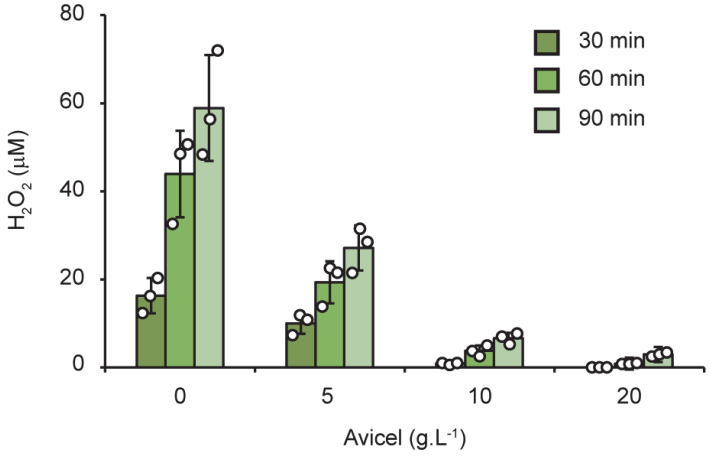

Supplementary Figure 3. The effect of Avicel on light-driven H_2O_2 production in the absence of LPMO. The graphs show time-courses for production of H_2O_2 in photobiocatalytic reactions containing lignin (0.9 g/L) and varying concentrations of Avicel. All reactions were carried out in sodium phosphate buffer (50 mM, pH 7.0) at 40 ºC under magnetic stirring with exposure to visible light (I=10 % I_{max}, approx., 16.8 W.cm^{-2}). H_2O_2 accumulation was measured as indicated in the main manuscript methods. The data is presented as mean values and error bars show ± s.d. (n = 3, independent experiments).

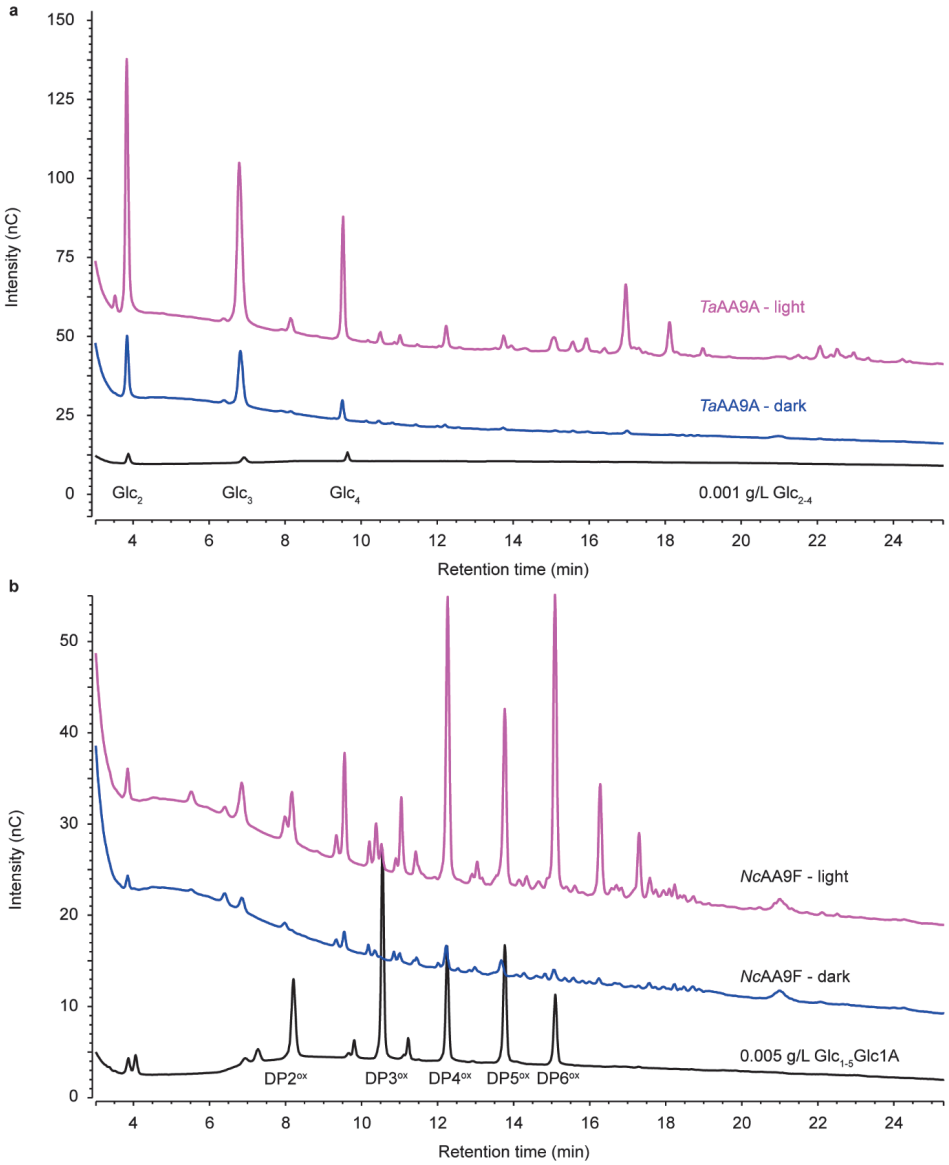

Supplementary Figure 4. Lignin-driven AA9 activity on cellulose. The figure shows chromatographic product profiles obtained for reactions containing kraft lignin (0.9 $g.L^{-1}$), Avicel (10 $g.L^{-1}$), and (**a**) *Ta*AA9A (0.5 µM) or (**b**) *Nc*AA9F (0.5 µM) after 6 h of reaction time. All reactions were performed in Bis-Tris buffer (50 mM, pH 7.0) at 40°C under magnetic stirring with or without light-exposure (I=10% I_{max}, approx. 16.8 $W.cm^{-2}$). All reactions were performed as two independent replicates (n = 2) and a representative product profile is shown. *Ta*AA9A is a primarily C4-oxidizing LPMO and, due to the nature of the analytics[1], its products are converted to native cello-oligomers; hence, the standard in the upper panel (black chromatogram) shows a mixture of native cello-oligomers (Glc_{2-4}). *Nc*AA9F is a C1-oxidizing LPMO; hence the standard in the lower panel (black chromatogram) shows a mixture of

C1-oxidized cello-oligomers ($Glc_{1-5}Glc1A$, referred to as $DP2^{ox}$ - $DP6^{ox}$). Both panels show that irradiation with visible light (upper chromatogram, magenta) increases product formation relative to the corresponding reaction in the dark (middle chromatogram, blue).

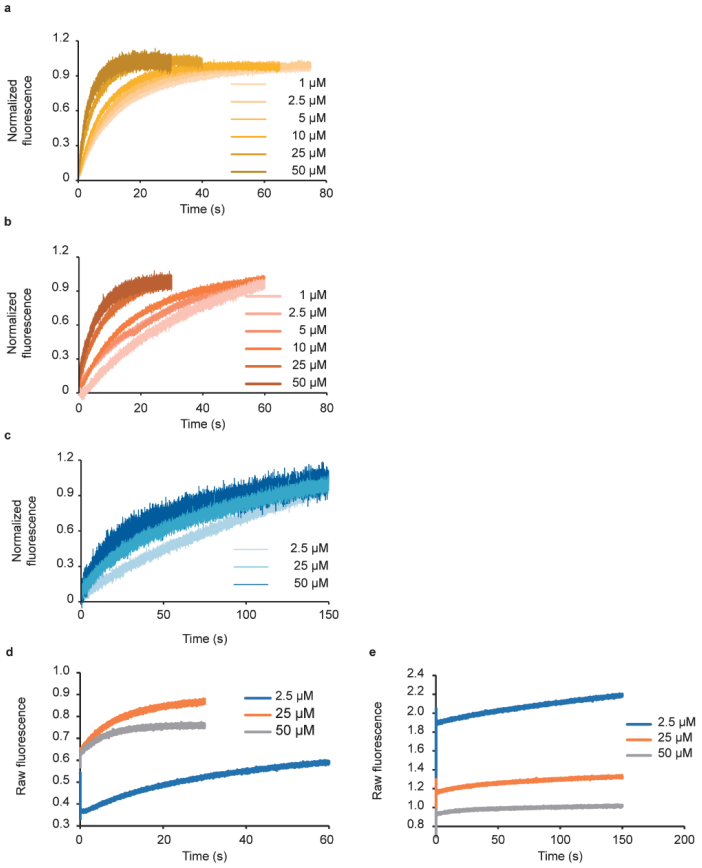

Supplementary Figure 5. Kinetic traces of lignin oxidation by bacterial LPMOs. The figure shows representative fluorescence traces for *Sm*AA10A (CBP21; chitin-active) catalyzed oxidation of native (a) and dialyzed (b) kraft lignin, and *Sc*AA10C (CelS2; cellulose-active) catalyzed oxidation of dialyzed kraft lignin (c). LPMO-Cu(II) (5 µM, final concentration after mixing) was anaerobically mixed with varying concentrations of kraft lignin and the change in fluorescence following reduction of LPMO-Cu(II) to LPMO-Cu(I) was monitored over time. The fluorescence signal was normalized as $F_N = (F_{max}-F(t))/(F_{max}-F_0)$, where F_{max} and F_0 are the fluorescence of the reduced and the oxidized LPMOs, respectively. All reactions were carried out in sodium phosphate buffer (50 mM; pH 7.0) at 25°C. Each experiment was performed in triplicates (n = 3) and a representative replicate is shown. Panels d and e show examples of the underlying raw data for reactions with dialyzed kraft lignin with *Sm*AA10A (corresponding to panel b) and *Sc*AA10C (corresponding to panel c), respectively.

Reliable data could only be obtained for the chitin-active LPMO, *Sm*AA10A, for which the difference in fluorescence signal between ground state and reduced copper state is higher, compared to *Sc*AA10C. Since the reactions contained spectroscopically active lignin, such a strong signal was needed to obtain reliable data. The stronger signal of *Sm*AA10A is likely due to the following: (1) *Sm*AA10A has more tryptophans near the copper ion; this improves signal strength; (2) *Sc*AA10C has an additional domain that contains tryptophans which give a high "background" fluorescence signal that is less affected by the redox state of the copper. Although no reliable rates could be obtained for cellulose-active *Sc*AA10C, comparison of panel c with panels a an b suggests that reduction of this enzyme is slower than reduction of *Sm*AA10A.

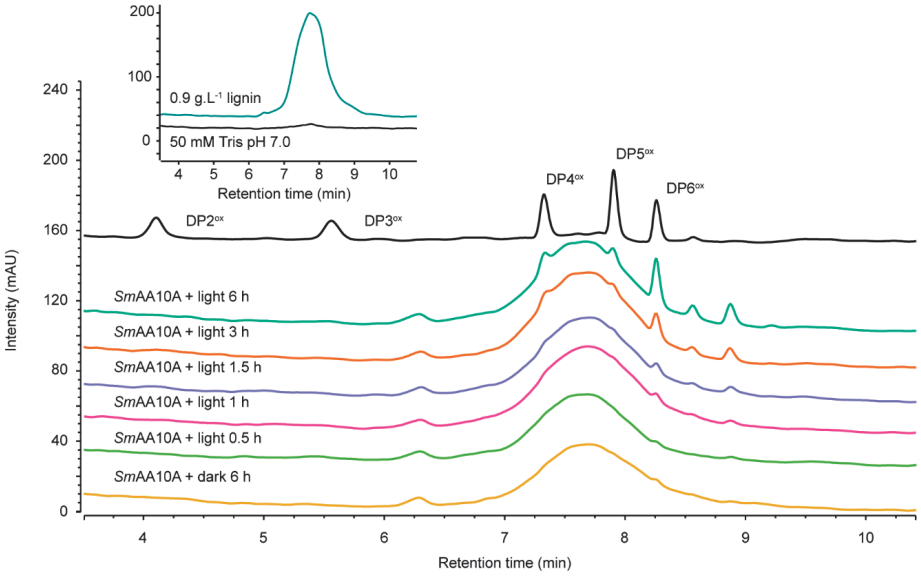

Supplementary Figure 6. Lignin-driven *Sm*AA10A activity on β-chitin. The figure shows chromatographic product profiles obtained for reactions with or without light-exposure containing kraft lignin (0.9 g.L^{-1}), β-chitin (10 g.L^{-1}), and *Sm*AA10A (0.5 µM). All reactions were performed in Tris buffer (50 mM, pH 7.0) at 40°C under magnetic stirring with or without light-exposure (I=10% I_{max}, approx. 16.8 W.cm^{-2}). All reactions were performed as three independent experiments (n = 3) and a representative product profile is shown. Only the final time point for the reaction with *Sm*AA10A in the dark is shown, as LPMO activity in this reaction was negligible. *Sm*AA10A activity on β-chitin was qualitatively assessed by comparing product profiles to product profile of oxidized chito-oligosaccharides with degree of polymerization ranging from 2 to 6 (DP2^{ox} - DP6^{ox}). Product formation over time is clearly visible, despite several product peaks being partially hidden by the broad peak from kraft lignin eluting between 7 and 9 minutes as shown in the inset.

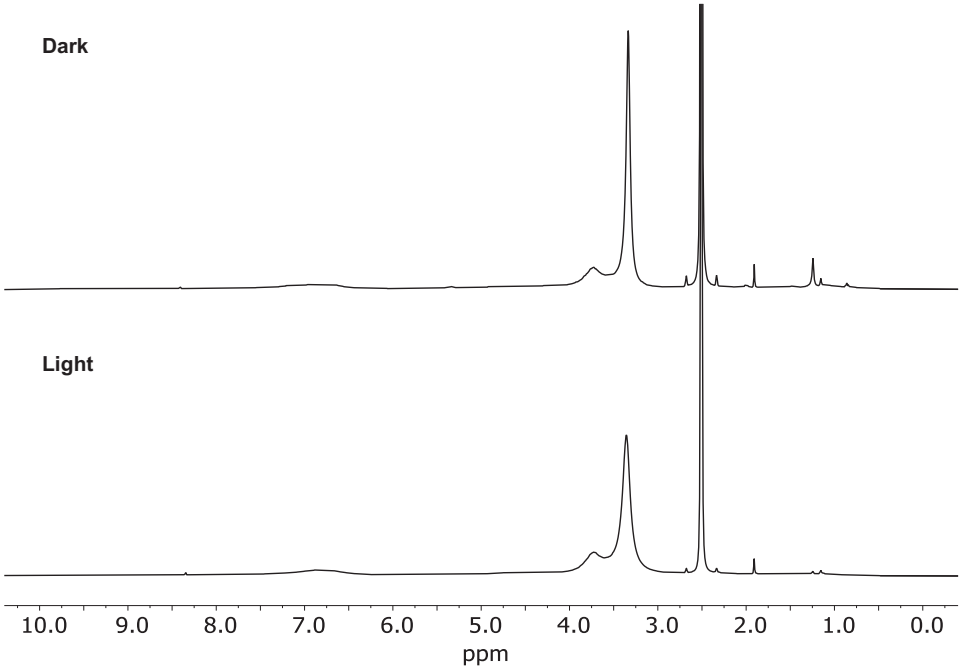

Supplementary Figure 7. Light-induced changes in kraft lignin assessed by 1D proton NMR spectroscopy. The figure shows 1D proton spectra of kraft lignin treated with light (lower spectrum) and non-treated kraft lignin (dark, top spectrum). The spectra were recorded in DMSO-d_6 (99.96 atom % D) and normalized using the peak at 3.75 ppm. Following light-exposure, the peaks at 1.23 and 3.35 ppm are reduced compared to the reference reaction in the dark. This figure is prepared from NMR data acquired with a Bruker Avance III 400 MHz spectrometer equipped with a BBFO Plus double resonance probe head at 25 °C. The 1H 1D spectra were acquired using 30-degree pulses, 8 single transients and a recycle delay of 10 s.

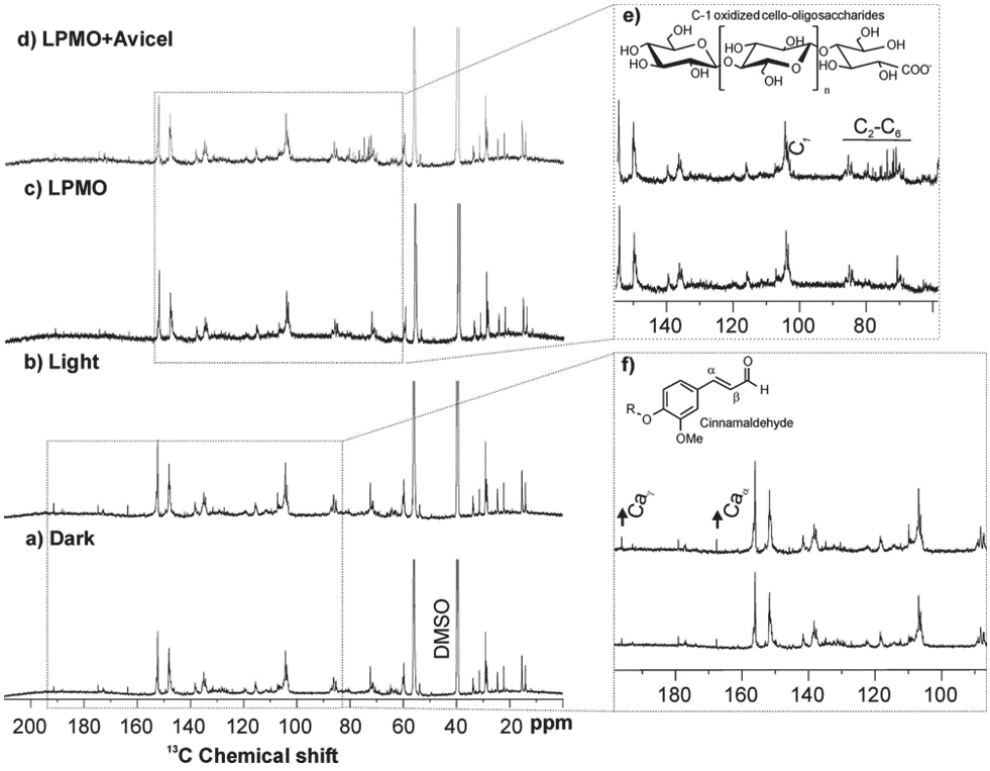

Supplementary Figure 8. Light-induced and LPMO-induced changes in organosolv birch lignin assessed by 1D carbon NMR spectroscopy. The panels show spectra obtained for organosolv lignin from birch (10 $g.L^{-1}$) incubated for 24 h in the dark (**a**), with light-exposure (I=10% I_{max}, corresponding to approx. 16.8 $W.cm^{-2}$) (**b**), in the dark with *Sc*AA10C (500 nM) (**c**), and in the dark with *Sc*AA10C (500 nM) and Avicel (10 $g.L^{-1}$) (**d**). Regions of the spectra displaying differences related to treatment with light (**f**) or an LMPO (**e**) are shown in the panels to the right. There were no detectable differences in the parts of the spectra that are not shown in panels **e** and **f**. All reactions were performed in sodium phosphate buffer (50 mM, pH 6.0) at 40°C with magnetic stirring. The NMR samples were prepared by dissolving either ~40 mg for light-treated lignin (**a**, **b**, **f**) or ~20 mg for LMPO-treated lignin (**c, d, e**) in 480 µL DMSO-d_6 (99.96 atom % D) and the carbon spectra were recorded at 25 °C on an 800 MHz instrument. To account for the differences in lignin concentration the intensity of all spectra was adjusted to be equal for the signal at ~28 ppm. Identification of chemical moieties, indicated in the spectra, is based on partial assignment using ^{1}H-^{13}C-HSQC and previous values reported in the literature (see Materials and Methods for more details). Signals representing the solubilised C-1 oxidized cello-oligosaccharides (C_1 [shoulder], C_2-C_6 where the number refers to the ring carbon of the monosaccharide)[2] are indicated. R indicates further coupling to the lignin polymer (**f**).

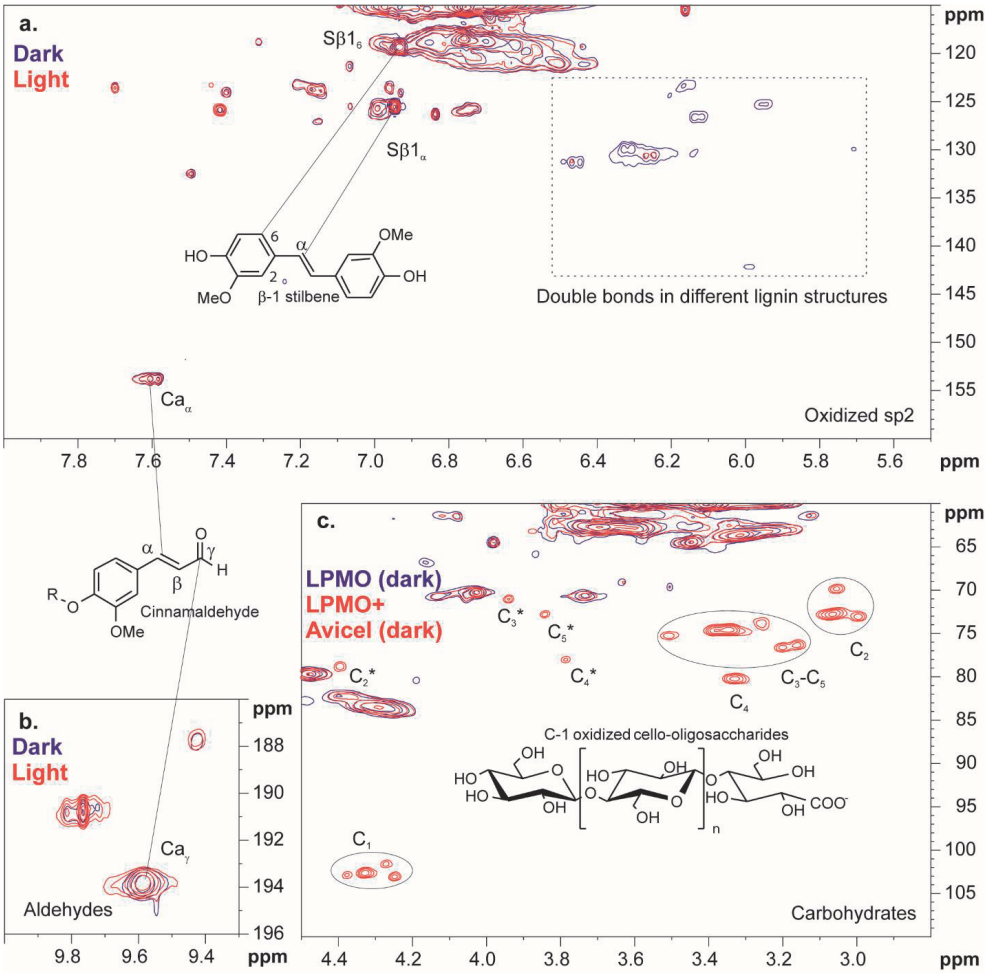

Supplementary Figure 9. **Light-induced and LPMO-induced changes in organosolv spruce lignin assessed by 2D HSQC NMR spectroscopy.** The figure shows comparisons between dark-incubated lignin (purple) and light-exposed lignin (red) for the olefinic region (**a**) and the aldehyde region (**b**). Panel (**c**) shows the region with signals from C-1 oxidized cello-oligosaccharides after incubation of lignin with LPMO (*Sc*AA10C, 500 nM) alone (cyan) or LPMO (*Sc*AA10C, 500 nM) and Avicel (10 g.L^{-1}) (red), in the dark. The NMR samples were prepared by dissolving either ~40 mg for light-treated lignin (**a**, **b**) or ~20 mg for LMPO-treated lignin (**c**) in 480 µL DMSO-d_6 (99.96 atom % D) and the HSQC spectra were recorded at 25 °C on an 800 MHz instrument. Identification of chemical moieties, indicated in the spectra, is based on partial assignment using ^{1}H-^{13}C-HSQC and previous values reported in the literature. Signals from β-1 stilbene (Sβ1$_\alpha$, Sβ1$_2$ and Sβ1$_6$)[3], cinnamaldehyde (Ca$_\alpha$ and Ca$_\gamma$)[3,4], and solubilised C-1 oxidized cello-oligosaccharides [C_1, C_2-C_6, where the number refers to the ring carbon for the monosaccharide and * indicates carbons belonging to an oxidized glucose residue[2]] are indicated. R indicates further coupling to the lignin polymer.

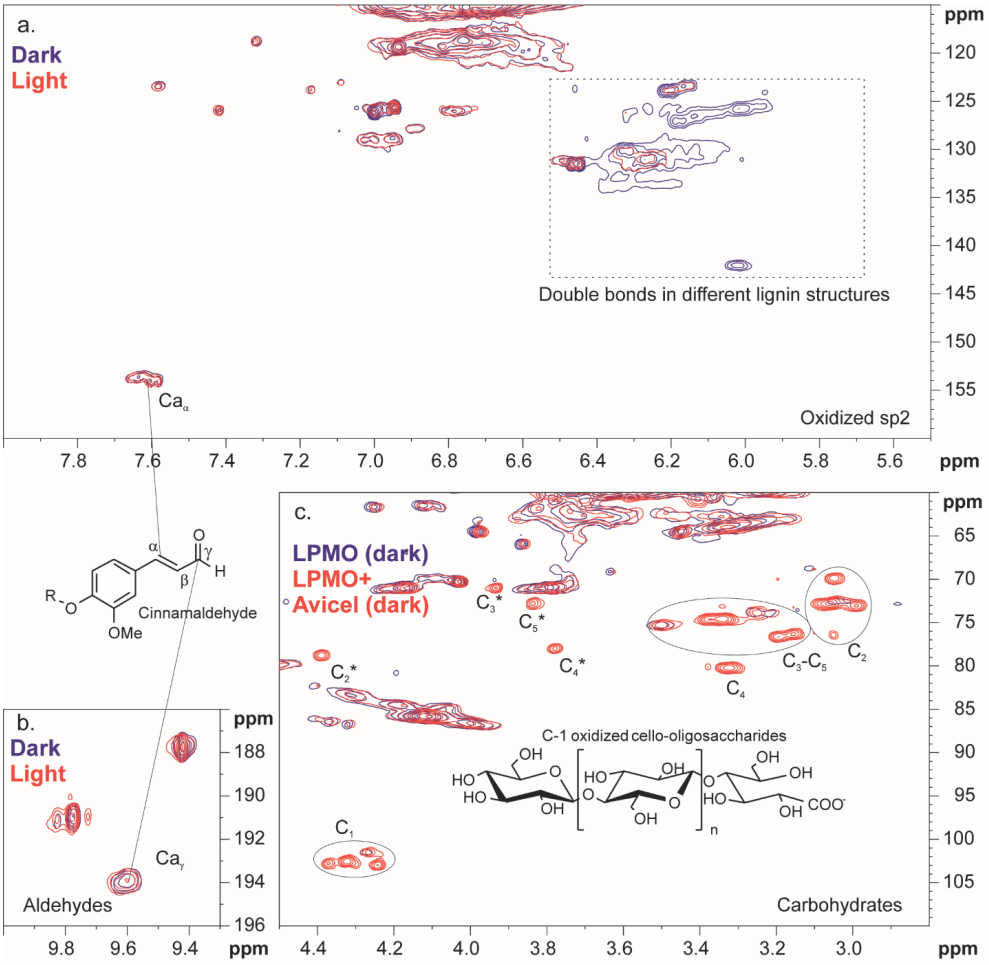

Supplementary Figure 10. **Light-induced and LPMO-induced changes in organosolv birch lignin assessed by 2D HSQC NMR spectroscopy.** The figure shows comparisons between dark-incubated lignin (purple) and light-exposed lignin (red) for the olefinic region (**a**) and the aldehyde region (**b**). Panel (**c**) shows the region with signals from C-1 oxidized cello-oligosaccharides after incubation of the lignin with LPMO (*Sc*AA10C, 500 nM) alone (purple) or LPMO (*Sc*AA10C, 500 nM) and Avicel (10 g.L^{-1}) (red), in the dark. The NMR samples were prepared by dissolving either ~40 mg for light-treated lignin (**a**, **b**) or ~20 mg for LMPO-treated lignin (**c**) in 480 µL DMSO-d_6 (99.96 atom % D) and the HSQC spectra were recorded at 25 °C on an 800 MHz instrument. Identification of chemical moieties, indicated in the spectra, is based on partial assignment using ^{1}H-^{13}C-HSQC and previous values reported in the literature. Signals from cinnamaldehyde (Ca$_\alpha$ and Ca$_\gamma$)[3,4] and solubilized C-1 oxidized cello-oligosaccharides [C_1, C_2-C_6, where the number refers to the ring carbon for the monosaccharide and * indicates the carbons belonging to an oxidized sugar residue[2]] are indicated. R indicates further coupling to the lignin polymer.

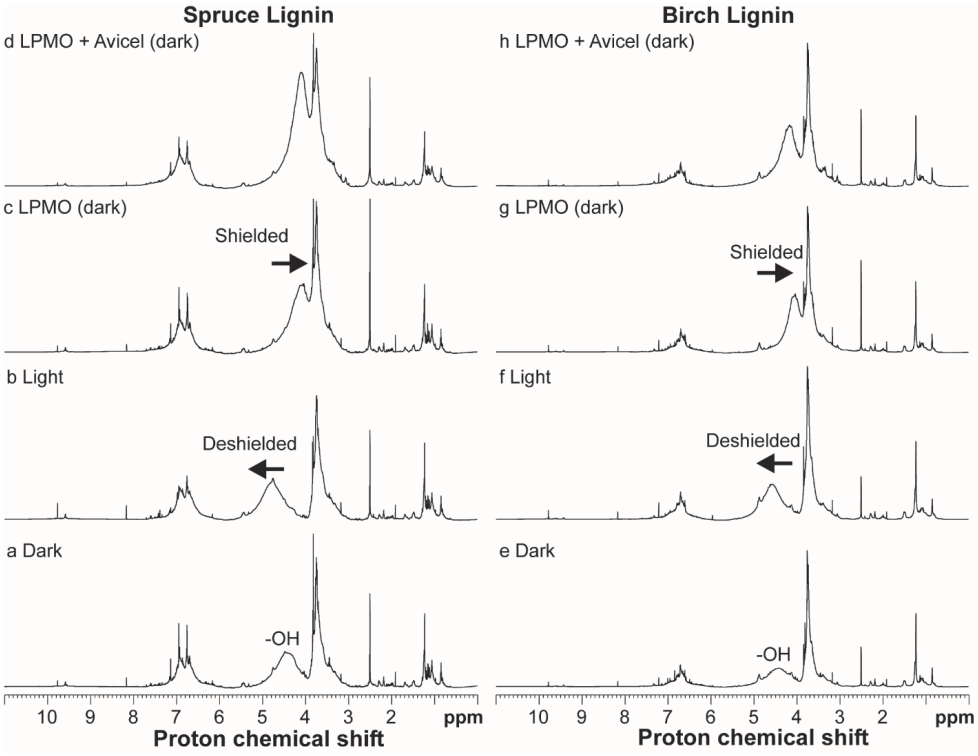

Supplementary Figure 11. Light-induced and LPMO-induced changes in organosolv birch and spruce lignin assessed by 1D proton NMR spectroscopy. The panels show spectra obtained for organosolv lignin from spruce (**a-d**) and birch (**e-h**). Lignin (10 $g.L^{-1}$) was incubated for 24 h in the dark (**a, e**), with light-exposure (I=10% I_{max}, corresponding to approximately 16.8 $W.cm^{-2}$) (**b, f**), in the dark with *Sc*AA10C (500 nM) (**c, g**), or in the dark with *Sc*AA10C (500 nM) and Avicel (10 $g.L^{-1}$) (**d, h**). The broad signal associated with protons of hydroxyl groups is shifted to higher frequency (deshielded) in light incubated reactions, and to a lower frequency (shielded) in reactions containing the LPMO. All reactions were performed in sodium phosphate buffer (50 mM, pH 6.0) at 40°C with magnetic stirring. The NMR samples were prepared by dissolving either ~40 mg for light-treated lignin (**a**, **b**, **e**, **f**) or ~20 mg for LMPO-treated lignin (**c**, **d**, **g**, **h**) in 480 µL DMSO-d_6 (99.96 atom % D) and the proton spectra were recorded at 25°C on an 800 MHz instrument. To account for the differences in lignin concentration the intensity of all spectra was adjusted using the lower frequency signals (δ_H 0.85, 1.24) belonging to aliphatic lignin groups that are expected to be unaffected by both light and LPMO.

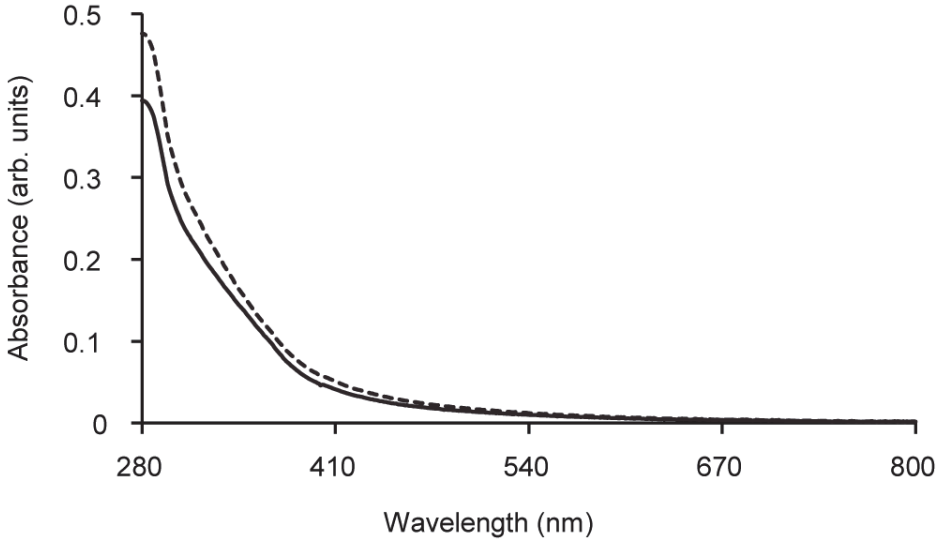

Supplementary Figure 12. UV-Vis absorption spectra of kraft lignin before and after dialysis. The figures show the absorption spectra of 0.1 $g.L^{-1}$ native (solid line) and dialyzed (dashed line) kraft lignin. The spectra were measured in triplicates and the figure shows a representative spectrum for each lignin.

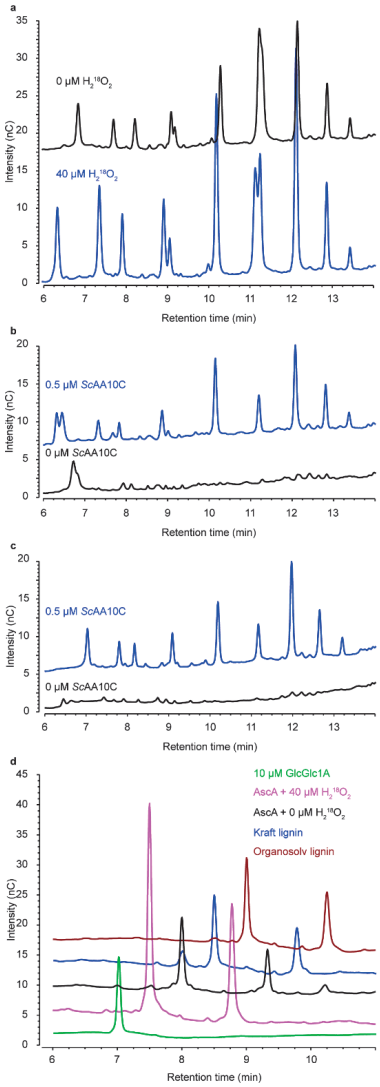

Supplementary figure 13. Chromatographic analysis of oxidized products generated in anaerobic LPMO reactions with visible light-exposed lignin. The panels show chromatographic analysis of soluble products generated in anaerobic reactions with *Sc*AA10C (500 nM) and Avicel (1 $g.L^{-1}$) containing 1 mM AscA with or without added ^{18}O-labelled $H_2{}^{18}O_2$ (**a**), kraft lignin (2 $g.L^{-1}$) (**b**), or organosolv lignin (2 $g.L^{-1}$) (**c**). Panel (**d**) shows the same product mixture after treatment with *Tf*Cel6A (converting oxidized products to oxidized cellobiose and cellotriose, which appear as two peaks). All reactions were conducted in ammonium bicarbonate buffer (20 mM, pH 6.9) and ^{18}O-labelled water ($H_2{}^{18}O$), and were performed in flat bottom vials with magnetic stirring, placed in an EvoluChem PhotoRedoxBox (HepatoChem) on a BioSan Mini-Shaker PSU-2T microtiter plate shaker set to 500 rpm and exposed to visible-light (EvoluChem™ LED 6200K white, with a light intensity of 29 $mW.cm^{-2}$) for 22 h. After 22 h, reaction mixtures were transferred to a 1.5 mL Eppendorf tube and spun down to recover the supernatants. The Eppendorf

tubes containing the supernatant were taken out of the anaerobic chamber and filtered using a 96-well filter plate (Millipore) and a vacuum manifold prior to HPAEC-PAD analysis. The samples were assessed for the presence of solubilized oxidized products before (**a**, **b**, and **c**) and, to obtain the best quantitative impression, after (**d**) treatment with *Tf*Cel6A. Product formation, at low levels, was observed in all LPMO-containing samples, but these levels were insufficient for detection using MALDI-ToF when lignin was present. As expected, higher product levels were obtained in the reaction with added H_2O_2. Importantly, panel (**d**) shows that product levels are identical for the reactions with ascorbic acid (where H_2O_2 generation through oxidation of H_2O will not occur) and the reactions with the two illuminated lignin types (where H_2O_2 generation through oxidation of H_2O might occur). This shows that in all cases the reactions are limited by the same factor, which must be the presence trace amounts of $^{16}O_2$ (i.e., the reactions were not 100 % anerobic).

We did these experiments in $H_2{}^{18}O$ and used $H_2{}^{18}O_2$ in the control reaction with hydrogen peroxide, because such an approach in principle could provide additional evidence for (the absence of) water oxidation. *Sc*AA10C-catalyzed cellulose oxidation involves hydroxylation at the C1-position of the scissile glycosidic bond to form a lactone which is in equilibrium with its hydrated form, the aldonic acid. If lignin oxidizes $H_2{}^{18}O$ to $H_2{}^{18}O_2$ and $^{18}O_2$, the aldonic acid products formed by *Sc*AA10C should display an *m/z* shift of +4 when analyzed by MALDI-TOF MS compared to products generated in a reaction with no ^{18}O present, since both oxygens in the aldonic acid would be ^{18}O. The same would be the case if oxidized products formed in reactions without added $H_2{}^{18}O_2$ would be the result of water oxidation, which would lead to in situ generation of $H_2{}^{18}O_2$. Reactions with AscA (1 mM), acting as reductant, with or without added $H_2{}^{18}O_2$ (0 or approx. 40 µM), in $H_2{}^{18}O$ and in the absence of lignin were performed as controls.

The reaction containing only AscA should not lead to any product formation in true anaerobic conditions whilst a control reaction containing AscA and $H_2{}^{18}O_2$ should provide a positive control for generation oxidized products with an *m/z* of +4. MALDI-ToF MS analyses confirmed the formation of *m/z* of +4 products in the reaction with added $H_2{}^{18}O_2$. Unfortunately, MS analysis of other reaction samples was not conclusive due to the combination of very low product levels and the presence of lignin in the samples. Aldonic acids with *m/z* +4 were not detected in these reactions. Since hardly any products with *m/z* +2 (the result of a reaction involving $^{16}O_2$) were detected neither, the formation of *m/z* +4 products cannot be excluded and the MS data, thus, do not provide additional support for the conclusions drawn from chromatographic product analysis.

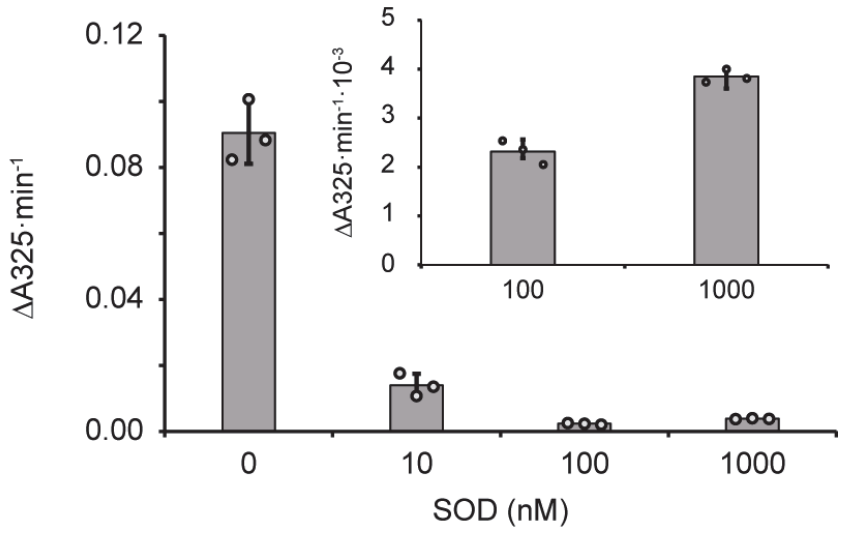

Supplementary Figure 14. Verification of Superoxide Dismutase (SOD) activity. The figure shows the change in absorbance at 325 nm during a 3-min incubation of pyrogallol leading to its autooxidation to purpurogallin, and how increasing amounts of SOD inhibit this reaction. At alkaline pH and aerobic conditions, autooxidation of pyrogallol leads to formation of superoxide radicals that drive formation of purpurogallin, and the latter can be spectrophotometrically measured at 325 nm. Adding SOD removes superoxide and inhibits formation of purpurogallin. The rate was derived using all data points from the 3-min reaction using linear regression. R^2 was > 0.98 for reactions with 0 and 10 nM SOD, while for reactions with 100 and 1000 nM SOD R^2 was > 0.7. The data is presented as mean values and error bars show ± s.d. (n = 3, independent experiments).

Supplementary references

1. Westereng, B. *et al.* Simultaneous analysis of C1 and C4 oxidized oligosaccharides, the products of lytic polysaccharide monooxygenases (LPMOs) acting on cellulose. *J. Chromatogr. A* 46–54 (2016). doi:10.1016/j.chroma.2016.03.064

2. Westereng, B. *et al.* Efficient separation of oxidized cello-oligosaccharides generated by cellulose degrading lytic polysaccharide monooxygenases. *J. Chromatogr. A* **1271**, 144–152 (2013).

3. Lancefield, C. S., Wienk, H. L. J., Boelens, R., Weckhuysen, B. M. & Bruijnincx, P. C. A. Identification of a diagnostic structural motif reveals a new reaction intermediate and condensation pathway in kraft lignin formation. *Chem. Sci.* **9**, 6348–6360 (2018).

4. Ralph, S. A., Ralph, J. & Landucci, L. L. NMR Database of Lignin and Cell Wall Model Compounds. (2009).

Paper IV

Light exposure of lignin affects the saccharification efficiency of LPMO-containing cellulolytic enzyme cocktails

Angeltveit CF, Kommedal EG, Stepnov AA, Eijsink VGH & Horn SJ

Light exposure of lignin affects the saccharification efficiency of LPMO-containing cellulolytic enzyme cocktails

Camilla F. Angeltveit, Eirik G. Kommedal, Anton A. Stepnov, Vincent G. H. Eijsink*, Svein J. Horn*

Faculty of Chemistry, Biotechnology, and Food Science, Norwegian University of Life Sciences (NMBU), Ås, Norway

*Corresponding authors: svein.horn@nmbu.no, vincent.eijsink@nmbu.no

Abstract

Efficient enzymatic saccharification of lignocellulosic substrates requires a blend of different hydrolytic and oxidative enzymes: cellulases, β-glucosidases, and lytic polysaccharide monooxygenases (LPMOs). In aerobic systems, reactions between lignin and oxygen will generate the LPMO co-substrate H_2O_2. This *in situ* generation of H_2O_2 is essential to keep LPMOs active during saccharification processes but is challenging to control, particularly in the presence of transition metals. In this study, H_2O_2 generation and LPMO activity during saccharification reactions with LPMO-containing cellulolytic enzyme cocktails were manipulated by using light of different wavelengths and lignin at different concentrations. The results show that light and its wavelength greatly impact H_2O_2 production resulting from abiotic oxidation of lignin, with major effects on LPMO activity, the stability of both the LPMO and the cellulases, and saccharification efficiency. Light may have a negative effect on the overall efficiency of cellulolytic enzyme cocktails acting on lignin-containing cellulosic material because light may induce excessive production of H_2O_2. Importantly, our data suggest that the LPMO not only contributes by cleaving cellulose, but also by removing excess H_2O_2 that otherwise could harm the cellulases.

Keywords

Photobiocatalysis, enzymatic saccharification, lytic polysaccharide monooxygenase, LPMO, cellulase, lignin, H_2O_2

Introduction

Photobiocatalysis is a renewable and environmentally friendly technology inspired by the conversion of light energy to chemical energy in plant photosynthesis. The aim of photobiocatalysis is to photochemically produce energy to generate redox equivalents to promote the activity of redox-active enzymes [1]. Redox enzymes play numerous important roles in Nature and hold considerable biotechnological potential [2], including the enzymatic saccharification of lignocellulosic biomass, which in part is driven by redox enzymes called lytic polysaccharide monooxygenases (LPMOs) [3,4].

Lignocellulosic biomass is an abundant resource with a high content of polysaccharides that can be enzymatically depolymerized to yield fermentable sugars for further valorization [5]. However, depolymerization is hampered by the presence of lignin because of lignin's direct impeding effect on cellulases [6] and its contribution to the recalcitrance of the material [7]. Complete elimination of lignin from lignocellulosic biomass is typically a challenging and costly process. On the other hand, recent investigations have shown promising results of employing lignin to power LPMOs and other redox enzymes in light-exposed reactions [8,9]. Therefore, understanding how to manage the presence of lignin effectively is crucial for the successful valorization of lignocellulose.

LPMOs are mono-copper enzymes that catalyze oxidative depolymerization of recalcitrant polysaccharide substrates [10]. LPMOs require a priming reduction and H_2O_2 as a co-substrate to oxidize the β-1,4-glycosidic bond in cellulose at the C1 or C4 position, yielding an aldonic acid or a ketoaldose, respectively [11]. While hydrolytic enzymes are only able to bind and cleave individual sugar chains, LPMOs exhibit flat substrate binding interfaces, allowing them to degrade the crystalline surface of the cellulose directly [12].

By reducing crystallinity, LPMOs make cellulose prone to the attack of canonical cellulases [12-14]. The ascomycete fungus *Trichoderma reesei* secretes a variety of lignocellulolytic enzymes, primarily cellulases such as endo- and exo-glucanases and β-glucosidases (BGs), and is the predominant chassis for today's industrial production of cellulase cocktails [15]. The efficiency of cellulolytic enzyme

mixtures has been significantly improved following the discovery and incorporation of LPMOs [4], although the synergy between LPMOs and cellulases remains not fully comprehended. Recently, it has been suggested that LPMO cleavage is followed by a gradual and time-dependent amorphization of the cellulose substrate [16,17].

In a groundbreaking 2016 study, Cannella et al. demonstrated unprecedentedly high LPMO activity, which was obtained by exposing an LPMO reaction mixture containing a combination of plant pigments (thylakoids or chlorophyllin) and ascorbic acid to visible light [18]. After the discovery of the dependence of LPMO activity on H_2O_2 [11], the study by Cannella et al. [18] was revisited, revealing that light-induced formation of H_2O_2 played a pivotal role in regulating LPMO activity in the chlorophyllin/light system [19]. In the following years, the application of other natural materials acting as H_2O_2-generating photocatalysts driving LPMO activity, such as insect exoskeletons [20] and lignin [9] have been investigated. The latter study recently demonstrated that light-exposed lignin could be used to control and significantly increase the degradation efficiency of a bacterial C1-oxidizing LPMO from *Streptomyces coelicolor*, *Sc*AA10C, acting on Avicel [9].

To gain further insight into the impact of light and lignin on enzymatic saccharification of lignocellulosic biomass, we have explored if and how light-exposed lignin can be used to enhance LPMO activity and increase glucan conversion for a microcrystalline model cellulose. A commercial LPMO-poor enzyme cocktail from *T. reesei*, Celluclast 1.5L, together with a BG and two fungal LPMOs originating from *Thermothielavioides terrestris* and *Thermoascus aurantiacus* (*Tt*AA9E and *Ta*AA9A, respectively) were employed, and the effects of light wavelength and lignin concentration were assessed. The results show that light and lignin can facilitate LPMO activity in an LPMO-containing cellulolytic enzyme cocktail but that the impact of the effect on overall saccharification efficiency is not necessarily positive, due the negative effects of excessive light-promoted production of H_2O_2.

Experimental section

Enzymes

*Tt*AA9E from *Thermothielavioides terrestris* (previously called *Thielavia terrestris*), *Ta*AA9A from *Thermoascus aurantiacus*, Celluclast 1.5L, and NZ-BG (equivalent to N188) were kindly provided by Novozymes (Bagsværd, Denmark). The LPMOs were copper saturated as described previously [21] before removing excess copper by using a PD MidiTrap column (G-25; GE Healthcare, Chicago, IL, USA). The enzyme concentrations were determined using the Bradford method with Bovine Serum Albumin (New England BioLabs, Ipswich, MA, USA) as standard. All enzymes were stored at 4°C.

Standard reaction conditions

Standard reactions mixtures contained Avicel (10 g/L; Avicel PH-101, 50 µm particles; Sigma-Aldrich, St. Louis, MO, USA) with or without Kraft lignin (1 g/L; Sigma-Aldrich), in 50 mM sodium phosphate (Sigma-Aldrich) buffer, pH 6.0, and were incubated at 40°C and 1100 rpm. The enzyme concentration was held constant at 4 mg protein per g cellulose in all reactions, where Celluclast 1.5L constituted the majority of the total enzyme amount, namely 3.6 mg/g. NZ-BG was present at 0.4 mg/g to ensure that all disaccharides were converted to monosaccharides. When LPMO was added, 0.4 mg/g of the Celluclast 1.5L cocktail was replaced with either a C1 or predominately C4 active AA9 type LPMO (*Tt*AA9E or *Ta*AA9A, respectively). The reactions were stopped by filtering the reaction mixture using a 96-well filter plate (0.2 µm; Sigma-Aldrich) followed by boiling of the filtrates for 15 min.

All reactions were performed in an EvoluChem PhotoRedOx box (HepatoChem, Beverly, MA, USA) placed on top of a magnetic stirrer and connected to a water bath (Julabo, Seelbach, Germany) for temperature control. A LED light source of cold white light (400-750 nm) with a predominant emission of lower wavelengths (Supplementary Figure S1) was used. In addition, five different LED light sources with lambda max equaling 365 nm, 425 nm, 525 nm, 650 nm, or 740 nm, and a narrow wavelength

distribution were tested. All light sources were purchased from HepatoChem, and all light spectra are shown in Supplementary Figure S1. The reactions were performed with 2 mL reaction volumes in 8 mL capped glass vials with a flat bottom. The inside of the PhotoRedOx box was covered with mirrors to ensure homogenous illumination of the reaction vials. The amount of photons per m^2 per sec (PAR) was measured inside the PhotoRedOx Box with a Skye PAR quantum sensor (Skye instruments, Llandrindod Wells, Wales, United Kingdom) and is shown in Supplementary Table S1.

Analysis of soluble oxidized and native sugars

Oxidized sugars were analyzed by high-performance anion exchange chromatography with a pulsed amperometric detection (HPAEC-PAD) using a Dionex ICS-5000 system (Dionex, Sunnyvale, CA, USA), while glucose levels were analyzed by high-performance liquid chromatography (HPLC) using a Dionex Ultimate 3000 system (Dionex). Analysis of oxidized sugars was done using a CarboPac PA200 3 x 250 mm analytical column, a 5 µL sample loop, and an operational flow of 0.5 mL/min. The gradient from 0-100 % B (A: 100 mM NaOH; B: 100 mM NaOH + 1 M NaOAc) was as follows 0-5.5 % B (linear) over 4.5 min, 5.5-15 % B (Dionex curve 4) over 9 min, 15-100 % B (Dionex curve 8) over 16.5 min, 100-0 % B (linear) over 6 s, 0 % B over 9 min [22]. Glucose was analyzed using a Rezex ROA-organic acid H+ (8 %) 300 mm × 7.8 mm analytical column (Phenomenex, Torrance, CA, USA) at 65°C, a flow rate of 0.6 mL/min and H_2SO_4 (5 mM; Merck, Darmstadt, Germany) as eluent, as described previously [23]. A C1-oxidized monomeric standard, gluconic acid (Glc1A), was purchased from Sigma-Aldrich and diluted as appropriate. C4-oxidized standards, Glc4gemGlc and Glc4gemGlc2, were made as previously described [23,24] using *Nc*AA9C from *Neurospora crassa* (prepared in-house, as described elsewhere [25]). The Chromeleon 7 software package (Dionex) was used to analyze the results.

142 Hydrogen peroxide measurements

143 A solution of Amplex Red (10 mM; Amplex™ Red Reagent, Thermo Fisher Scientific, Waltham, MA,
144 USA) was prepared in Dimethylsulfide (Sigma-Aldrich), protected against light, and stored in aliquots
145 at -18°C. A solution of HRP (Pierce™ Horseradish Peroxidase, Thermo Fisher Scientific) was prepared
146 in milli-Q water, filtered (0.2 µm; VWR, Radnor, PA, USA), and stored at 4°C. The Amplex
147 red/Horseradish Peroxidase (abbreviated AR/HRP) mix consisted of 0.25 mM AR and 0.04 g/L HRP in
148 0.25 M sodium phosphate buffer pH 6.0. 120 µL of sample was mixed with 80 µL AR/HRP mix in a 96-
149 well plate and incubated for 5 min before measuring the fluorescence (Ex: 530 and Em: 590) using a
150 BioTek Synergy H4 hybrid reader (Agilent, Santa Clara, CA, USA). Hydrogen peroxide (VWR) standards
151 were prepared to contain the same amounts of lignin as in the experimental samples (Supplementary
152 Figure S2).

153

154 Stability of C4-oxidized sugars

155 A C4-oxidized standard DP2 was incubated with lignin (1 g/L) or H_2O_2 (1 mM) with or without Cu(II)SO_4
156 (167 µM) in 50 mM sodium phosphate buffer, pH 6.0, at 40°C and 800 rpm in a Thermomixer
157 (Eppendorf, Hamburg, Germany) for 5 h before analysis on the Dionex ICS-5000 as described above.

158

159 Preincubation of the cellulolytic enzyme cocktail with light and lignin

160 A mixture of Celluclast 1.5L and NZ-BG (3.6 mg/g Celluclast 1.5L + 0.4 mg/g NZ-BG) alone or together
161 with Cu(II)SO_4 (100 µM), lignin (1 g/L) or both in 50 mM sodium phosphate buffer, pH 6.0, was pre-
162 incubated at 40°C, 1100 rpm for 6 h while being exposed to cold white, after which Avicel (10 g/L) was
163 added followed by incubation for 24 h at 40°C, 1100 rpm, in the dark. The reactions were stopped by
164 boiling and filtering, after which glucose levels were analyzed using the Dionex Ultimate 3000 HPLC,
165 as described above.

Results and discussion

Using lignin and light to modulate the enzymatic saccharification of cellulose

Lignin is known to have a negative effect on the enzymatic hydrolysis of lignocellulose (also shown in Supplementary Figure S3) [6,26]. Regarding the impact of light on lignin-containing biomass, until recently, the predominant idea was that light-induces lignin degradation, which improves the availability of cell wall polysaccharides for enzymatic conversion by microbial enzymes [27-30]. Recent studies have shown that light-promoted oxidation of lignin leads to the generation of H_2O_2 that can drive biomass-degrading peroxidases and peroxygenases including LPMOs [8,9], providing another explanation for why light affects enzymatic biomass conversion.

A set of experiments was carried out to investigate the effect of lignin concentration and light exposure on LPMO activity and cellulose saccharification. The enzyme blend consisted of a commercial cellulase cocktail without LPMO activity (3.2 mg/g Celluclast 1.5L + 0.4 mg/g NZ-BG) spiked with either a C1- or predominately C4-active fungal LPMO (0.4 mg/g), *Tt*AA9E or *Ta*AA9A, respectively. In this type of experiments, we detected only three major oxidized products, gluconic acid, in reactions with *Tt*AA9E, and C4-oxidized cellobiose and cellotriose, in reactions with *Ta*AA9A. Reaction outcomes were assessed by quantifying these oxidized products as well as glucose.

Reactions run in the dark showed steadily increasing glucose levels over time. Addition of lignin at lower concentrations had a minor and hardly significant positive effect on glucose release (Figures 1B & D). At the highest tested concentration, 3 g/L, lignin had a negative effect on glucose release and, remarkably, this effect was only significant for the reactions with one of the LPMOs, *Tt*AA9E (Figure 1B). In contrast, for the reactions carried out with light exposure, lignin had a clear and to a large extend dose-dependent negative effect on glucose release. For the reactions with *Tt*AA9E, cellulose conversion clearly decreased with increasing lignin concentrations and this decrease was noticeable at each of the three monitored timepoints (Figure 1A). For the reactions with *Ta*AA9A, the effects of lignin were neglectable at the lower lignin concentrations, but at 3 g/L lignin, and after 24 h of reaction,

glucose release was inhibited in the light-exposed reaction (Figure 1C). Of note, control experiments showed that exposure to light does not negatively affect the Celluclast 1.5L cocktail (Supplementary Figure S3).

Compared to the effect on glucose release (Figures 1A-D), light and lignin had a large impact on LPMO activity (Figures 1E-H). For example, the reactions with *Tt*AA9E (Figures 1E & F), reaching similar levels of C1-oxidized sugars required 10 times more lignin (3 g/L) in the dark compared to the light-exposed reaction. Thus, in the dark, more lignin is needed to reduce the LPMO and fuel it with H_2O_2, as has been shown before [9]. Of note, only at 3 g/L does the lignin to cellulose ratio in the reaction (3:10) approach the ratios that one may find in pretreated biomass used in industrial biorefining [31]. In the dark reactions, a consistent and progressive increase in the production of oxidized sugars was observed over time and with increasing lignin concentrations for both LPMOs (Figures 1F & H). Interestingly, Figures 1F & H show clear functional differences between the LPMOs, both in terms of the kinetics of the accumulation of oxidized products (i.e., progress curves with different shapes) and in terms of maximum product levels at early time points of the reactions with the highest lignin concentrations, which are much higher for *Ta*AA9A. Importantly, the data in Figure 1 shows that the combination of light and higher lignin concentrations becomes unfavorable.

The production of oxidized products in the absence of lignin was lower in the reactions with *Ta*AA9A (both in the light and in the dark), but, at the same time, in light exposed reaction with lignin, the reactions with *Ta*AA9A accumulated much more oxidized products compared to the reactions with *Tt*AA9E, at least in the first 6 h of the reaction (Figures 1E & G). After 6 h, the levels of oxidized sugars in the *Ta*AA9A reactions with 1 and 3 g/L lignin decreased (Figure 1G), which is indicative of LPMO inactivation. Of note, C1-oxidized products are stable and, hence, no decrease is observed upon inactivation of the LPMO. On the other hand, several previous studies suggest that C4-oxidized sugars are degraded when H_2O_2 starts accumulating in the reaction, as would be the case if the LPMO is no longer active [32-35]. The latter was confirmed by a control experiment that is described below.

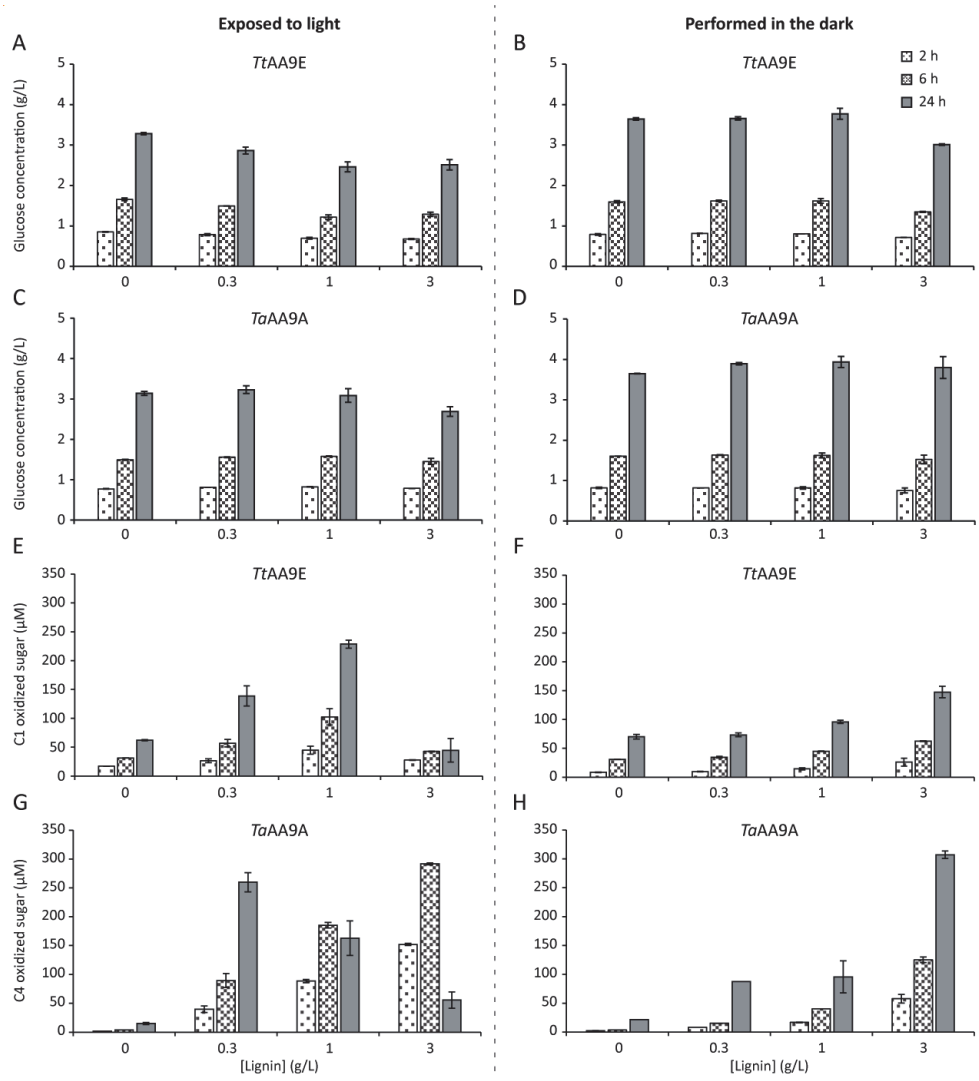

Figure 1. The impact of lignin concentration and light on glucose release and LPMO activity. Saccharification reactions containing 10 g/L Avicel and 0-3 g/L lignin were set up with 3.2 mg/g Celluclast 1.5L + 0.4 mg/g NZ-BG + 0.4 mg/g *Tt*AA9E **(A, B, E & F)** or *Ta*AA9A **(C, D, G & H)**. The reactions were exposed to cold white light **(A, C, E & G)** or performed in the dark **(B, D, F & H)**. The figure shows the glucose release in **Panels A-D**; the generation of C1-oxidized sugars in reactions with *Tt*AA9E is shown in **Panels E & F,** and the generation of C4-oxidized sugars in reactions with *Ta*AA9A is shown in **Panels G & H.** Standard deviations for two biological replicates are shown as error bars.

While it is not easy to fully rationalize the results shown in Figure 1, it is clear that the presence of lignin and the presence of light have considerable effects on LPMO activity and cellulose saccharification. Several important trends stand out. Firstly, reactions with *Ta*AA9A generally yielded higher final glucose levels compared to similar reactions with *Tt*AA9E. Regarding oxidized sugars, the C4-active LPMO showed a higher initial conversion rate, suggesting that, in a reaction with Avicel, the C4-active LPMO is more efficient in productively using *in situ* produced H_2O_2. Secondly, however, while the contribution of LPMO activity to the overall saccharification efficiency of cellulolytic enzyme cocktails is undisputable [13,23,32,36,37], Figure 1 shows a lack of correlation between the levels of oxidized products and saccharification efficiency. Thus, as also seen in a recent study by Østby et al. [38], maximizing LPMO activity is not necessarily beneficial. While this may have to do with optimizing the interplay between synergistically acting enzymes, one needs to keep in mind that high LPMO activity reflects high H_2O_2 levels, which may be damaging not only for the LPMOs but also for the cellulases (see below). Thirdly, and quite remarkably, Figure 1 shows that cellulose saccharification is more efficient in the dark, regardless of the presence of lignin.

As to the difference between *Tt*AA9E and *Ta*AA9A, it should be mentioned that studies indicate that the main component of the Celluclast 1.5L cocktail is the reducing end cellulase Cel7A from *T. reesei,* *Tr*Cel7A [39,40]. As such, C1-active LPMOs have been speculated at having an initial negative effect on the activity of reducing end cellulases, due to their production of reducing end oxidized sugars. For example, a negative synergistic effect has been shown between *Tt*AA9E and *Tr*Cel7A [41-43]. These studies employed short incubation times (1-3 h), whereas multiple studies have shown that positive LPMO-cellulase synergism, reflected in increased glucose conversion, increases with time. This results from a time-dependent amorphization of the crystalline material following the oxidative cuts, thus making it easier for the cellulases to initiate hydrolysis [16,17,44-46]. Thus, it is difficult to say whether the observed difference between the two LPMOs relates to the different interplay with *Tr*Cel7A.

LPMO activity is crucial for maintaining cellulase activity in light-exposed reactions

In recent years, various studies have demonstrated increased production of H_2O_2 when lignin is exposed to light. This phenomenon has been observed under different light conditions, including exposure to violet light (ʎ = 400 nm) [47] and white light (ʎ > 400 nm) [8,9]. A recent study suggested that light-induced oxidation of ring-conjugated olefins within the lignin structure is responsible for the increased production of H_2O_2 [9]. The absorption spectrum of kraft lignin shows strong absorption in the 250 to 400 nm range and comparatively weaker absorption in the 400-700 nm range (Supplementary Figure S4) [9]. To investigate the impact of light in more detail, the impact of wavelength-specific light sources, alongside cold white light, was examined. The goal was to assess wavelength-related variation in H_2O_2-generating lignin oxidation and to study the impact of such variation on LPMO activity and cellulose solubilization.

Saccharification reactions with 1 g/L lignin in the dark, in the absence or presence of *Ta*AA9A, showed a small beneficial effect of the LPMO on the glucose yield that became visible late in the reaction (24 h) (Figures 2A-C). This limited effect is similar to the effects observed in other studies using similarly low substrate concentrations [17,48,49]. The time-delayed effect of LPMO activity can be a result of the slow process of substrate amorphization after the LPMO oxidation [16,44], as discussed above. Interestingly, when applying white light to the reaction, the overall solubilization yield went down, whereas the effect of the LPMO became more pronounced (Figure 2C). Illumination with light of different wavelengths showed a clear correlation: the lower the wavelength, the lower the saccharification yield and the larger the effect of the LPMO. This correlation is clearly visible at 24 h (Figure 2C) but can also be detected at the earlier timepoints (Figures 2A & B) for the lower wavelengths. As an example, in the reaction exposed to 365 nm light, the LPMO increased glucose release by 61 %, as compared to 6 % for the reaction in the dark. Still the glucose yield after 24 in the latter reaction was 100 % higher, compared to the reaction with 365 nm light.

Figure 2D shows that LPMO activity increased with decreasing wavelength. At the lower wavelengths, fast LPMO catalysis is accompanied by LPMO inactivation, as shown by the cessation of product formation and a subsequent decrease in the amount of detected C4-oxidized products. At wavelengths of 525 nm and above, as well as in the dark, the accumulation of oxidized sugars was close to linear for the whole reaction period. The highest level of oxidized sugar after 24 h was observed for the reaction exposed to 525 nm light, about two-fold higher compared to the level of oxidized sugar in the dark reaction. Despite this difference in LPMO activity, the two reactions showed approximately similar glucose yields after 24 h. The lack of correlation between the amount of oxidized products formed and overall glucose solubilization is also clear from Figure 2E, showing the molar ratio of glucose to oxidized sugars. This ratio varied from about 40 to about 190, increased with increasing wavelengths, and showed the highest value for the dark. So, for the reaction with the highest saccharification yield, the relative level of oxidized products was low. Looking at glucose yields, it would seem that for the reaction setups used here, with a low substrate concentration (10 g/L) and lignin-driven LPMO activity, a molar ratio of glucose to oxidized sugar of about 90 and higher seems to reflect a beneficial environment for both LPMO and cellulase activity.

To investigate whether the effects of lignin and light are directly related to *in situ* lignin-induced H_2O_2 production, a series of experiments were carried out to measure H_2O_2 production in the dark and upon irradiation with light at different wavelengths. Exposure of lignin samples (1 g/L) to the wavelength-specific light sources for 1 h showed a clear effect of light and its wavelength on H_2O_2 production (Figure 2F). Furthermore, H_2O_2 production levels under various conditions (Figure 2F) and the initial production levels of oxidized sugars (i.e., after 2 h) depicted in Figure 2D show a clear correlation. These results show that, H_2O_2 is a limiting factor for LPMO activity in this system, and that the *in situ* production of H_2O_2 is highly dependent on light exposure and wavelength. Thus, Figures 2C-F show that when using wavelengths of 525 nm and higher, H_2O_2 production levels and the ability of the LPMO to consume this H_2O_2 over time are such that the reaction stays more or less balanced, leading to overall glucose yields after 24 h that are similar to those obtained in the dark.

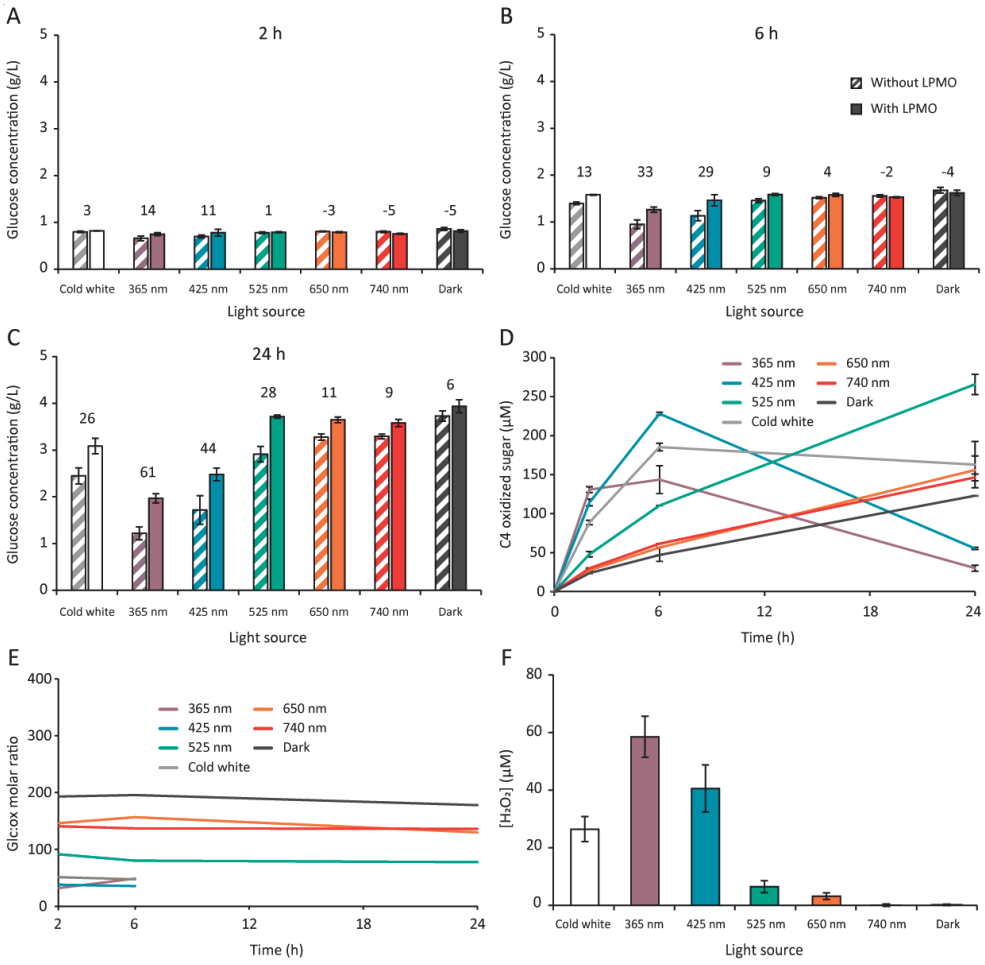

299

300 **Figure 2. The influence of light wavelength on glucose release, *in situ* H_2O_2 production and LPMO**
301 **activity.** In the reactions shown in **Panels A-E**, 10 g/L Avicel and 1 g/L lignin were incubated with 3.2
302 mg/g Celluclast 1.5L + 0.4 mg/g NZ-BG + 0.4 mg/g *Ta*AA9A and exposed to light sources with different
303 wavelengths ranging from 365 to 740 nm, cold white light (400-750 nm) or kept in the dark. The figure
304 shows glucose release after 2 h **(A)**, 6 h **(B),** or 24 h **(C)**, soluble oxidized sugars at all time points **(D)**
305 and the molar ratio of glucose to oxidized sugar (**E).** The numbers above the pairs of bars in **Panels A-**
306 **C** represent the increase in glucose levels (%) resulting from addition of the LPMO. For some reactions,
307 **Panel** E does not show the 24 h point because product degradation took place (see text for more
308 details). **Panel F** shows the apparent H_2O_2 concentration measured with the AR/HRP assay after

exposing 1 g/L lignin to various light sources for 1 hour. Standard deviations for three (or two for **Panel F**) biological replicates are shown as error bars.

Two mechanisms for *in situ* H_2O_2 generation by light-exposed lignin have been proposed [8,47], suggesting either a direct two-electron reduction of O_2 to H_2O_2, or two single-electron reductions, first from O_2 to $O_2^{\bullet-}$ and then further to H_2O_2. In a recent study, the use of superoxide dismutase, an enzyme speeding up the conversion of $O_2^{\bullet-}$ to H_2O_2, was shown to significantly increase the production of oxidized sugars by LPMOs driven by the combination of lignin and light, suggesting that $O_2^{\bullet-}$ indeed is formed an that a two-step reduction of O_2 to H_2O_2 takes place [9]. Thus, multiple reactive oxygen species (ROS) will be present in the light-exposed lignin reactions.

Taken together, these results show that lignin and light have a huge effect on LPMO activity and saccharification efficiency and that variation in H_2O_2 levels likely plays a role. However, the relationship between LPMO activity and saccharification efficiency is not straightforward. Since with decreasing wavelengths, glucose release decreased, while both the (initial) LPMO activity and the impact of the LPMO on saccharification efficiency increased, the outcome of the various reactions described above cannot be explained on the basis of a classical positive synergistic relationship between the LPMO and the cellulases. Instead, what seems to be happening is that LPMO action removes H_2O_2 from the reaction, which not only leads to LPMO activity that is higher than needed for obtaining maximal conversion, but also, importantly, protects the cellulases from H_2O_2-mediated damage. Hydrogen peroxide is a multi-edged sword: it drives LPMO activity, at higher levels it may lead to autocatalytic damage of the LPMO [11], and it may drive unspecific Fenton-type reaction in solutions containing free transition metals and reducing power. Inactivated LPMOs will release their active-site copper into solution [50,51] and in lignin containing reactions there is plenty of reducing power. Fenton-like reactions will generate hydroxyl radicals that damage the cellulases [49]. So, the high positive impact of the LPMO on saccharification efficiency in reactions irradiated with low wavelength light is due to increased protection of the cellulases and not to the increased oxidative cleavage of cellulose.

A control experiment – stability of C4-oxidized products

In the above, apparent degradation of C4-oxidized sugars was observed under conditions that promote high H_2O_2 production and LPMO inactivation, such as at high lignin concentrations (Figure 1G) or upon irradiation of the lignin with short wavelengths (Figure 2D). Similar observations have been made in previous studies [32-35], but causal relationships have not been firmly established or described. The direct effect of H_2O_2 on the C4-oxidized sugar was tested by incubating Glc4gemGlc (C4-oxidized DP2 standard) with H_2O_2 (1 mM), lignin (1 g/L) and/or $Cu(II)SO_4$, and combinations thereof. $Cu(II)SO_4$ was included since inactivation of LPMOs will release copper into the reaction mixture, which again may affect H_2O_2 production [51,52]. Figure 3 shows that incubation with H_2O_2 leads to degradation of Glc4gemGlc, whereas incubation with lignin, $Cu(II)SO_4$ or a combination thereof had no effect. Thus, as suggested by the results described above, and as observed in previous studies, when available H_2O_2 is no longer consumed, for example as a result of LPMO inactivation, degradation of C4-oxidized sugars will occur. Turning this around, monitoring the level of C4-oxidized sugars provides insight into the operational stability of the reaction system.

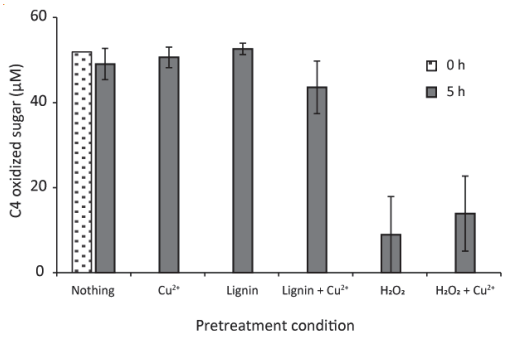

Figure 3. Stability of the C4-oxidized ketoaldose. C4-oxidized DP2 was incubated with lignin (1 g/L) or H_2O_2 (1 mM) in the presence or absence of $Cu(II)SO_4$ (167 µM) at 40°C for 5 h in 50 mM sodium phosphate buffer pH 6.0. Subsequently, the remaining amount of C4-oxidized DP2 was determined using HPAEC-PAD and freshly prepared standards for quantification. Standard deviations for two biological replicates are shown as error bars.

354 The effect of light-exposed lignin on a commercial LPMO-containing enzyme cocktail

355 The impact of light- and lignin-mediated H_2O_2 production was also tested in reactions with a more
356 advanced commercial enzyme cocktail containing LPMO activity, Cellic CTec2, which, according to
357 literature, predominately contains C4-active LPMOs [23,37]. Figure 4 shows that in reactions with
358 Cellic CTec2 glucose release was slightly (approximately 10-30 % after 24 h) higher compared to the
359 LPMO-spiked cellulase system (Celluclast 1.5L + NZ-BG + *Ta*AA9A). As to the impact of light and lignin
360 the trends were similar to those described above for the spiked cellulase cocktails. Reactions in the
361 dark gave the highest glucose levels and lignin had a positive effect on these levels. Irradiation with
362 white light or light at 525 nm had a negative impact on glucose release and this effect became more
363 prominent at higher lignin concentrations. The levels of oxidized products varied with the lignin
364 concentration and irradiation, reflecting a similar trade-off between H_2O_2-mediated activity and H_2O_2-
365 mediated inactivation, where the latter leads to degradation of C4-oxidized products. It is noteworthy
366 that after 24 h of exposure to white light the levels of oxidized sugars produced in the reactions with
367 the *Ta*AA9A-spiked cellulase cocktail and with Cellic CTec2 are similar. Figures 1G & 4B (cold white
368 light reaction) show a large increase in the level of oxidized sugar when going from 0 g/L to 0.3 g/L
369 lignin with maximum values in the range of 250 and 300 µM, while the levels of oxidized sugars
370 decrease at higher lignin concentrations (1 and 3 g/L).

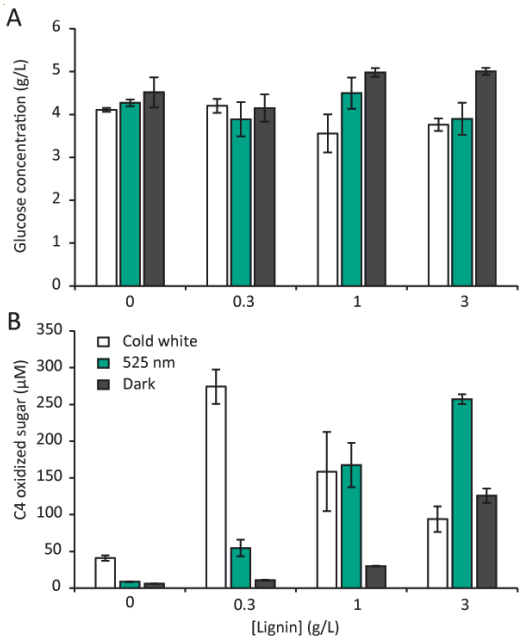

371

372 **Figure 4. The effect of light-exposed lignin on cellulose saccharification with a modern enzyme**
373 **cocktail.** The figure shows the levels of glucose (**A**) and C4-oxidized products (**B**) after 24 h for reactions
374 containing 10 g/L Avicel, 4 mg/g Cellic CTec2 and varying amounts of lignin (0, 0.3, 1 or 3 g/L) exposed
375 to cold white light or 525 nm light, or kept in the dark. Standard deviations for two biological replicates
376 are shown as error bars.

377

378 Reactions at higher dry matter concentration

379 To get closer to industry-relevant conditions and because studies have shown that LPMOs are more
380 beneficial at higher dry matter concentrations [17,48,49], we studied the impact of the LPMO, light
381 and lignin at a five-fold higher substrate concentration (50 g/L), using the Celluclast 1.5L + NZ-BG
382 cocktail spiked with *Tt*AA9E. The ratios of enzyme to glucan (4 mg protein per g of Avicel) and cellulose
383 to lignin (10:1) were identical to the ratios used in the reactions described above.

Figure 5A shows that the reactions without LPMO gave higher saccharification yields early in the reaction, while after 24 h the LPMO-containing reactions were most efficient, both for reactions carried out in the dark and reactions exposed to cold white light. These trends are the same as those seen in reactions with *Ta*AA9A and lower substrate concentrations (Figures 2A-C). Glucose levels after 24 h were four- to five-fold higher for the 50 g/L reaction compared the 10 g/L reaction (compare Figures 1A & B with 5A). Notably, the negative impact of light on glucose yield after 24 h was less for the 50 g/L reaction with *Tt*AA9E (18 % reduction; Figure 5A) compared to the 10 g/L reactions with *Tt*AA9E (53 % reduction; Figures 1A & B). Light effects may become less prominent at higher substrate concentrations due to increased attenuation by substrate particles.

Compared to the reactions with 10 g/L substrate, the levels of soluble oxidized sugars in the 50 g/L reactions only showed a two-fold increase, both in the dark and in the light (compare Figures 1E & F with 5B). It is not immediately obvious why the generation of soluble oxidized products in the dark reaction does not follow the five-fold increase in substrate concentration. It has been shown, however, that the fraction of oxidized products ending up in the soluble fraction rather than in the remaining insoluble material, goes down as the substrate concentration increases [53]. For the light-exposed reaction, which, as expected, leads to generation of higher levels of oxidized products (Figure 5B), the relatively low increase in product levels (compared to 10 g/L reactions) could be due in part to attenuation of the light, which will result in lower H_2O_2 production and, thus, lower LPMO activity. A study employing chlorophyllin for light-induced H_2O_2 production demonstrated recently that more light was needed at higher dry matter concentrations to maintain the same LPMO activity [54]. Taken together, the data in Figure 5 show that the combined effects of lignin and light vary with the substrate concentration and that light effects may become less when working at higher substrate concentration.

Of note, both the data in Figure 2 and the data in Figure 5 show that early in the reaction, replacing the cellulases in Celluclast 1.5L with an LPMO has a negative impact on glucose release, while inclusion of an LPMO leads to improved cellulose conversion at later time points. This observation adds to an

increasing set of observations [17,48] suggesting that LPMOs are particularly important for saccharification efficiency in the later phases of saccharification reactions.

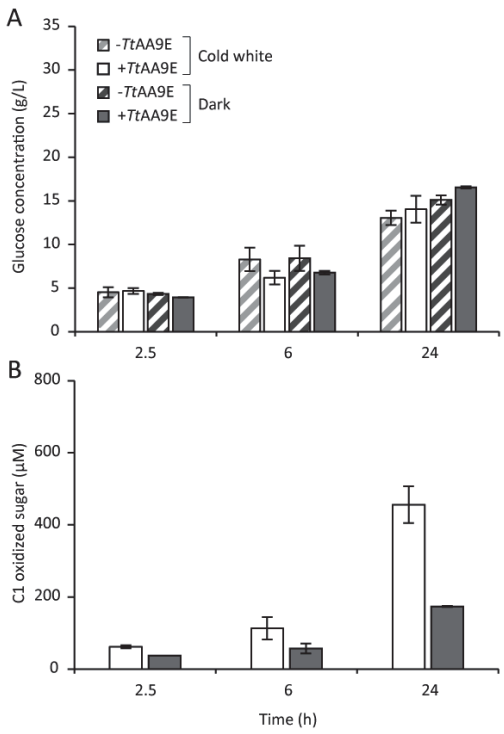

Figure 5. Saccharification reactions with higher, more industry-relevant substrate loading. Reaction mixtures with 50 g/L Avicel and 5 g/L lignin and 3.2 mg/g Celluclast 1.5L + 0.4 mg/g NZ-BG + 0.4 mg/g *Tt*AA9E or 3.6 mg/g Celluclast 1.5L + 0.4 mg/g NZ-BG were exposed to cold white light or kept in the dark. **Panels A** and **B** show glucose release and the level of soluble C1-oxidized sugars, respectively. The errors bars are standard deviations for two biological replicates.

Conclusion

In this study we show that light has a negative effect on the saccharification efficiency of cellulolytic enzyme cocktails and that this effect is increased by the presence of lignin because irradiation of lignin

promotes formation of excessive amounts of H_2O_2. We show that with lignin present, light energy generated H_2O_2 will drive LPMO redox reactions, mimicking processes that may naturally happen in Nature. However, in the context of biomass conversion, increased H_2O_2 levels are not necessarily beneficial. Our data clearly show that high H_2O_2 levels lead to more LPMO activity than needed to reach high saccharification efficiency, and to side reactions that damage both the LPMO and the cellulases. Importantly, the presence of LPMOs in reactions exposed to low wavelength or white light improve the saccharification efficiency in these, notably suboptimal, reactions, not because of increased oxidative cleavage of cellulose, but because the LPMO consumes H_2O_2 that otherwise would harm the cellulolytic enzymes. Thus, in the set-ups used here, the LPMO has a protecting effect on the cellulases by keeping the level of H_2O_2 and other ROS at a non-detrimental levels.

The present results provide further insight into to intricate biochemistry of LPMOs and adds another level of complexity to synergistic interactions between LPMOs and cellulases. Light as a variable in biomass conversion processes has largely been ignored, making it difficult to directly compare literature data. While the effects of light may become less prominent at substrate concentrations higher than those used here, possible light effects need to be kept in mind. We show here that, at low substrate concentrations, the effects of light may be large and that these effects depend on the amount and, likely, the redox state, of the lignin present in the biomass. Thus, it seems necessary to regulate, and report, exposure to light in both laboratory experiments and industrial applications.

Supporting Information

Photon per m^2 per sec (PAR) measurements (Tabel S1) and emission spectra (Figure S1) for the LED lamps used in this study; standard curves prepared with different lignin concentrations used for H_2O_2 quantification with the AR/HRP assay (Figure S2); direct effect of light-exposure and the presence of lignin on the Celluclast 1.5L + NZ-BG cocktail (Figure S3); UV-Vis adsorption spectra of kraft lignin (Figure S4).

Acknowledgements

Celluclast 1.5 L, NZ-BG, Cellic CTec2, *Ta*AA9A, and *Tt*AA9E were all kindly provided by Novozymes.

Author contributions

CFA, SJH, and VGHE conceptualized the study. CFA conducted the experimental procedures. CFA and SJH wrote the initial manuscript. All authors played a role in overseeing the project and interpreting the data, and all contributed to the editing and completion of the final manuscript.

Funding

The Research Council of Norway supported this work through grant no. 257622 (Bio4Fuels).

Notes

The authors declare that there are no competing interests associated with the manuscript.

List of abbreviations

AR: Amplex Red, BG: β-glucosidase, HPAEC-PAD: high-performance anion exchange chromatography with a pulsed amperometric detection, HPLC: high-performance liquid chromatography, HRP: horseradish peroxidase, LPMO: lytic polysaccharide monooxygenase, ROS: reactive oxygen species

References

1. Maciá-Agulló JA, Corma A, Garcia H. Photobiocatalysis: the power of combining photocatalysis and enzymes. Chem - Eur J. 2015; 21(31):10940-59. https://doi.org/10.1002/chem.201406437.
2. Martínez AT, Ruiz-Dueñas FJ, Camarero S, Serrano A, Linde D, Lund H, et al. Oxidoreductases on their way to industrial biotransformations. Biotechnol Adv. 2017; 35(6):815-31. https://doi.org/10.1016/j.biotechadv.2017.06.003.
3. Chylenski P, Bissaro B, Sørlie M, Røhr ÅK, Várnai A, Horn SJ, Eijsink VG. Lytic polysaccharide monooxygenases in enzymatic processing of lignocellulosic biomass. ACS Catal 2019; 9(6):4970-91. https://doi.org/10.1021/acscatal.9b00246.
4. Johansen KS. Discovery and industrial applications of lytic polysaccharide mono-oxygenases. Biochem Soc Trans. 2016; 44(1):143-9. https://doi.org/10.1042/BST20150204.
5. Cherubini F. The biorefinery concept: Using biomass instead of oil for producing energy and chemicals. Energy Conv. 2010; 51(7):1412-21. https://doi.org/10.1016/j.enconman.2010.01.015.

6. Haviland ZK, Nong D, Zexer N, Tien M, Anderson CT, Hancock WO. Lignin impairs Cel7A degradation of in vitro lignified cellulose by impeding enzyme movement and not by acting as a sink. Biotechnol Biofuels. 2024; 17:7. https://doi.org/10.1186/s13068-023-02456-3.
7. Bugg TD, Ahmad M, Hardiman EM, Rahmanpour R. Pathways for degradation of lignin in bacteria and fungi. Nat Prod Rep. 2011; 28(12):1883-96. https://doi.org/10.1039/C1NP00042J.
8. Kim J, Nguyen TVT, Kim YH, Hollmann F, Park CB. Lignin as a multifunctional photocatalyst for solar-powered biocatalytic oxyfunctionalization of C–H bonds. Nat Synth. 2022; 1(3):217-26. https://doi.org/10.1038/s44160-022-00035-2.
9. Kommedal EG, Angeltveit CF, Klau LJ, Ayuso-Fernández I, Arstad B, Antonsen SG, et al. Visible light-exposed lignin facilitates cellulose solubilization by lytic polysaccharide monooxygenases. Nat Commun. 2023; 14(1):1063. https://doi.org/10.1038/s41467-023-36660-4.
10. Vaaje-Kolstad G, Westereng B, Horn SJ, Liu Z, Zhai H, Sorlie M, Eijsink VG. An oxidative enzyme boosting the enzymatic conversion of recalcitrant polysaccharides. Science. 2010; 330(6001):219-22. https://doi.org/10.1126/science.1192231.
11. Bissaro B, Rohr AK, Muller G, Chylenski P, Skaugen M, Forsberg Z, et al. Oxidative cleavage of polysaccharides by monocopper enzymes depends on H_2O_2. Nat Chem Biol. 2017; 13(10):1123-8. https://doi.org/10.1038/nchembio.2470.
12. Horn SJ, Vaaje-Kolstad G, Westereng B, Eijsink VG. Novel enzymes for the degradation of cellulose. Biotechnol Biofuels. 2012; 5(1):45. https://doi.org/10.1186/1754-6834-5-45.
13. Eibinger M, Ganner T, Bubner P, Rosker S, Kracher D, Haltrich D, et al. Cellulose surface degradation by a lytic polysaccharide monooxygenase and its effect on cellulase hydrolytic efficiency. J Biol Chem. 2014; 289(52):35929-38. https://doi.org/10.1074/jbc.M114.602227.
14. Song B, Li BY, Wang XY, Shen W, Park SJ, Collings C, et al. Real-time imaging reveals that lytic polysaccharide monooxygenase promotes cellulase activity by increasing cellulose accessibility. Biotechnol Biofuels. 2018; 11(1):1-11. https://doi.org/10.1186/s13068-018-1023-1.
15. Gupta VK, Kubicek CP, Berrin J-G, Wilson DW, Couturier M, Berlin A, et al. Fungal enzymes for bio-products from sustainable and waste biomass. TIBS. 2016; 41(7):633-45. https://doi.org/10.1016/j.tibs.2016.04.006.
16. Angeltveit CF, Jeoh T, Horn SJ. Lytic polysaccharide monooxygenase activity increases productive binding capacity of cellobiohydrolases on cellulose. Bioresour Technol. 2023; 389:129806. https://doi.org/10.1016/j.biortech.2023.129806.
17. Cannella D, Weiss N, Hsieh C, Magri S, Zarattini M, Kuska J, et al. LPMO-mediated oxidation increases cellulose wettability, surface water retention and hydrolysis yield at high dry matter. Cellulose. 2023; 30:6259–72. https://doi.org/10.1007/s10570-023-05271-z.
18. Cannella D, Möllers K, Frigaard N-U, Jensen P, Bjerrum M, Johansen K, Felby C. Light-driven oxidation of polysaccharides by photosynthetic pigments and a metalloenzyme. Nat Commun. 2016; 7(1):11134. https://doi.org/10.1038/ncomms11134.
19. Bissaro B, Kommedal E, Røhr ÅK, Eijsink VG. Controlled depolymerization of cellulose by light-driven lytic polysaccharide oxygenases. Nat Commun. 2020; 11(1):890. https://doi.org/10.1038/s41467-020-14744-9.
20. Kommedal EG, Sæther F, Hahn T, Eijsink VG. Natural photoredox catalysts promote light-driven lytic polysaccharide monooxygenase reactions and enzymatic turnover of biomass. Proc Natl Acad Sci 2022; 119(34):e2204510119. https://doi.org/10.1073/pnas.2204510119.
21. Loose JSM, Forsberg Z, Fraaije MW, Eijsink VGH, Vaaje-Kolstad G. A rapid quantitative activity assay shows that the *Vibrio cholerae* colonization factor GbpA is an active lytic polysaccharide monooxygenase. FEBS Lett. 2014; 588(18):3435-40. https://doi.org/10.1016/j.febslet.2014.07.036.

22. Hegnar OA, Østby H, Petrović DM, Olsson L, Várnai A, Eijsink VG. Quantifying oxidation of cellulose-associated glucuronoxylan by two lytic polysaccharide monooxygenases from Neurospora crassa. Applied and Environmental Microbiology. 2021; 87(24):e01652-21.
23. Müller G, Varnai A, Johansen KS, Eijsink VG, Horn SJ. Harnessing the potential of LPMO-containing cellulase cocktails poses new demands on processing conditions. Biotechnol Biofuels. 2015; 8(1):187. https://doi.org/10.1186/s13068-015-0376-y.
24. Østby H, Jameson JK, Costa T, Eijsink VGH, Arntzen MO. Chromatographic analysis of oxidized cello-oligomers generated by lytic polysaccharide monooxygenases using dual electrolytic eluent generation. J Chromatogr A. 2022; 1662:462691. https://doi.org/10.1016/j.chroma.2021.462691.
25. Kittl R, Kracher D, Burgstaller D, Haltrich D, Ludwig R. Production of four *Neurospora crassa* lytic polysaccharide monooxygenases in *Pichia pastoris* monitored by a fluorimetric assay. Biotechnol Biofuels. 2012; 5(1):79. https://doi.org/10.1186/1754-6834-5-79.
26. Vermaas JV, Petridis L, Qi X, Schulz R, Lindner B, Smith JC. Mechanism of lignin inhibition of enzymatic biomass deconstruction. Biotechnol Biofuels. 2015; 8:217. https://doi.org/10.1186/s13068-015-0379-8.
27. Austin AT, Ballaré CL. Dual role of lignin in plant litter decomposition in terrestrial ecosystems. Proc Natl Acad Sci 2010; 107(10):4618-22. https://doi.org/10.1073/pnas.0909396107.
28. Austin AT, Méndez MS, Ballaré CL. Photodegradation alleviates the lignin bottleneck for carbon turnover in terrestrial ecosystems. Proc Natl Acad Sci 2016; 113(16):4392-7. https://doi.org/10.1073/pnas.1516157113.
29. Berenstecher P, Vivanco L, Pérez LI, Ballaré CL, Austin AT. Sunlight doubles aboveground carbon loss in a seasonally dry woodland in Patagonia. Curr Biol. 2020; 30(16):3243-51. https://doi.org/10.1016/j.cub.2020.06.005.
30. Austin AT, Vivanco L. Plant litter decomposition in a semi-arid ecosystem controlled by photodegradation. Nature. 2006; 442(7102):555-8. https://doi.org/10.1038/nature05038.
31. Lourenço A, Pereira H. Compositional variability of lignin in biomass. Lignin - Trends and Applications. 2018:65-98. https://doi.org/10.5772/intechopen.71208.
32. Müller G, Chylenski P, Bissaro B, Eijsink VG, Horn SJ. The impact of hydrogen peroxide supply on LPMO activity and overall saccharification efficiency of a commercial cellulase cocktail. Biotechnol Biofuels. 2018; 11(1):209. https://doi.org/10.1186/s13068-018-1199-4.
33. Kadić A, Chylenski P, Hansen MAT, Bengtsson O, Eijsink VG, Lidén G. Oxidation-reduction potential (ORP) as a tool for process monitoring of H_2O_2/LPMO assisted enzymatic hydrolysis of cellulose. Process Biochem. 2019; 86:89-97. https://doi.org/10.1016/j.procbio.2019.08.015.
34. Hansen LD, Østensen M, Arstad B, Tschentscher R, Eijsink VG, Horn SJ, Varnai A. 2-Naphthol impregnation prior to steam explosion promotes LPMO-assisted enzymatic saccharification of spruce and yields high-purity lignin. ACS Sustain Chem Eng. 2022; 10(16):5233-42. https://doi.org/10.1021/acssuschemeng.2c00286.
35. Costa TH, Kadic' A, Chylenski P, Várnai A, Bengtsson O, Lidén G, et al. Demonstration-scale enzymatic saccharification of sulfite-pulped spruce with addition of hydrogen peroxide for LPMO activation. Biofuel Bioprod Biorefin. 2020; 14(4):734-45. https://doi.org/10.1002/bbb.2103.
36. Cannella D, Jørgensen H. Do new cellulolytic enzyme preparations affect the industrial strategies for high solids lignocellulosic ethanol production? Biotechnol Bioeng. 2014; 111(1):59-68. https://doi.org/10.1002/bit.25098.
37. Hu J, Chandra R, Arantes V, Gourlay K, Van Dyk JS, Saddler JN. The addition of accessory enzymes enhances the hydrolytic performance of cellulase enzymes at high solid loadings. Bioresour Technol. 2015; 186:149-53. https://doi.org/10.1016/j.biortech.2015.03.055.
38. Østby H, Várnai A, Gabriel R, Chylenski P, Horn SJ, Singer SW, Eijsink VG. Substrate-Dependent Cellulose Saccharification Efficiency and LPMO Activity of Cellic CTec2 and a Cellulolytic

Secretome from Thermoascus aurantiacus and the Impact of H_2O_2-Producing Glucose Oxidase. ACS Sustain Chem Eng. 2022; 10(44):14433-44. https://doi.org/10.1021/acssuschemeng.2c03341.

39. Martinez D, Berka RM, Henrissat B, Saloheimo M, Arvas M, Baker SE, et al. Genome sequencing and analysis of the biomass-degrading fungus *Trichoderma reesei* (syn. *Hypocrea jecorina*). Nat Biotechnol. 2008; 26(5):553-60. https://doi.org/10.1038/nbt1403.
40. Hu J, Arantes V, Pribowo A, Saddler JN. The synergistic action of accessory enzymes enhances the hydrolytic potential of a "cellulase mixture" but is highly substrate specific. Biotechnol Biofuels. 2013; 6(1):112. https://doi.org/10.1186/1754-6834-6-112.
41. Keller MB, Badino SF, Blossom BMl, McBrayer B, Borch K, Westh P. Promoting and impeding effects of lytic polysaccharide monooxygenases on glycoside hydrolase activity. ACS Sustain Chem Eng. 2020; 8(37):14117-26. https://doi.org/10.1021/acssuschemeng.0c04779.
42. Keller MB, Badino SF, Rojel N, Sorensen TH, Kari J, McBrayer B, et al. A comparative biochemical investigation of the impeding effect of C1-oxidizing LPMOs on cellobiohydrolases. J Biol Chem. 2021; 296:100504. https://doi.org/10.1016/j.jbc.2021.100504.
43. Tokin R, Ipsen ØJ, Westh P, Johansen KS. The synergy between LPMOs and cellulases in enzymatic saccharification of cellulose is both enzyme-and substrate-dependent. Biotechnol Lett. 2020; 42:1975-84. https://doi.org/10.1007/s10529-020-02922-0.
44. Eibinger M, Sattelkow J, Ganner T, Plank H, Nidetzky B. Single-molecule study of oxidative enzymatic deconstruction of cellulose. Nat Commun. 2017; 8(1):894. https://doi.org/10.1038/s41467-017-01028-y.
45. Vermaas JV, Crowley MF, Beckham GT, Payne CM. Effects of lytic polysaccharide monooxygenase oxidation on cellulose structure and binding of oxidized cellulose oligomers to cellulases. J Phys Chem B. 2015; 119(20):6129-43. https://doi.org/10.1021/acs.jpcb.5b00778.
46. Mudedla SK, Vuorte M, Veijola E, Marjamaa K, Koivula A, Linder MB, et al. Effect of oxidation on cellulose and water structure: a molecular dynamics simulation study. Cellulose. 2021; 28(7):3917-33. https://doi.org/10.1007/s10570-021-03751-8.
47. Miglbauer E, Gryszel M, Głowacki ED. Photochemical evolution of hydrogen peroxide on lignins. Green Chem. 2020; 22(3):673-7. https://doi.org/10.1039/C9GC04324A.
48. Tuveng TR, Jensen MS, Fredriksen L, Vaaje-Kolstad G, Eijsink VG, Forsberg Z. A thermostable bacterial lytic polysaccharide monooxygenase with high operational stability in a wide temperature range. Biotechnol Biofuels. 2020; 13:194. https://doi.org/10.1186/s13068-020-01834-5.
49. Angeltveit CF, Várnai A, Eijsink VG, Horn SJ. Enhancing enzymatic saccharification yields of cellulose at high solid loadings by combining different LPMO activities. Biotechnol Biofuels. 2024.
50. Stepnov AA, Christensen IA, Forsberg Z, Aachmann FL, Courtade G, Eijsink VGH. The impact of reductants on the catalytic efficiency of a lytic polysaccharide monooxygenase and the special role of dehydroascorbic acid. FEBS Lett. 2022; 596(1):53-70. https://doi.org/10.1002/1873-3468.14246.
51. Østby H, Tuveng TR, Stepnov AA, Vaaje-Kolstad G, Forsberg Z, Eijsink VG. Impact of copper saturation on lytic polysaccharide monooxygenase performance. ACS Sustain Chem Eng. 2023; 11(43):15566-76. https://doi.org/10.1021/acssuschemeng.3c03714.
52. Stepnov AA, Forsberg Z, Sørlie M, Nguyen G-S, Wentzel A, Røhr ÅK, Eijsink VG. Unraveling the roles of the reductant and free copper ions in LPMO kinetics. Biotechnol Biofuels. 2021; 14:28. https://doi.org/10.1186/s13068-021-01879-0.
53. Courtade G, Forsberg Z, Heggset EB, Eijsink VGH, Aachmann FL. The carbohydrate-binding module and linker of a modular lytic polysaccharide monooxygenase promote localized cellulose oxidation. J Biol Chem. 2018; 293(34):13006-15. https://doi.org/10.1074/jbc.RA118.004269.

54. Blossom BM, Russo DA, Singh RK, Van Oort B, Keller MB, Simonsen TI, et al. Photobiocatalysis by a lytic polysaccharide monooxygenase using intermittent illumination. ACS Sustain Chem Eng. 2020; 8(25):9301-10. https://doi.org/10.1021/acssuschemeng.0c00702.

Graphical abstract

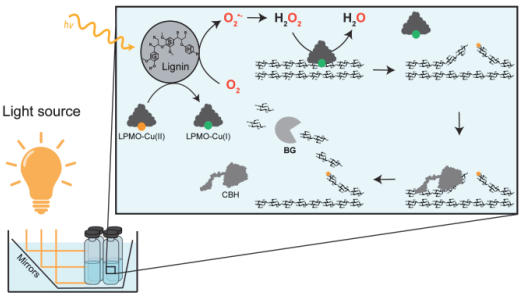

Synopsis

Exposure to light reduce the saccharification efficiency of cellulolytic enzyme cocktails acting on lignin-containing substrates but LPMOs help counteracting this effect.

Supplementary materials

Light exposure of lignin affects the saccharification efficiency of LPMO-containing cellulolytic enzyme cocktails

Camilla F. Angeltveit, Eirik G. Kommedal, Anton A. Stepnov, Vincent G. H. Eijsink*, Svein J. Horn*

Faculty of Chemistry, Biotechnology, and Food Science, Norwegian University of Life Sciences (NMBU), Ås, Norway

*Corresponding authors: svein.horn@nmbu.no, vincent.eijsink@nmbu.no

Table S1. The irradiance intensities of the LED lamps. Photon per m^2 per sec (PAR) measured inside the PhotoRedOx Box.

LED lamp	Cold white	365 nm*	425 nm	525 nm	640 nm	750 nm*
PAR (µmol/m^2/s)	1040	-	275	435	935	-

*Wavelengths outside the sensor's detection range, which was 400 to 700 nm.

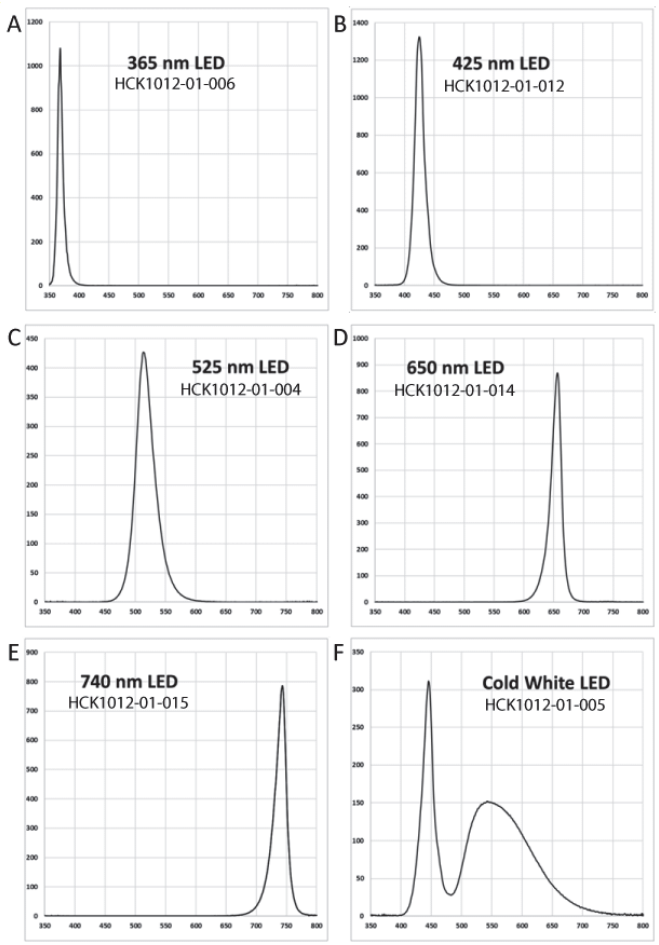

Figure S1. Emission spectra of the different LED lamps used in the PhotoRedOx Box. The spectra were taken from https://www.hepatochem.com/photoreactors-leds-accessories/photoreactor-leds-evoluchem/

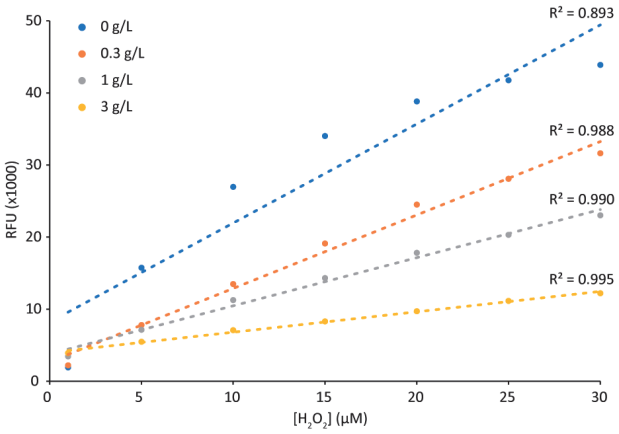

Figure S2. Standard curves used for H_2O_2 quantification in the AR/HRP assay. The H_2O_2 standards were prepared with various lignin concentrations to generate standard curves with the same lignin content and lignin quenching effect as in the experimental samples. The AR/HRP mix consisted of 0.25 mM and 0.04 g/L of Amplex Red and Horseradish Peroxidase, respectively, in 0.25 M sodium phosphate buffer pH 6.0. The fluorescence (Ex: 530 and Em: 590) was measured 5 min after mixing 120 µl of the H_2O_2/lignin sample and 80 µl of the AR/HRP mix.

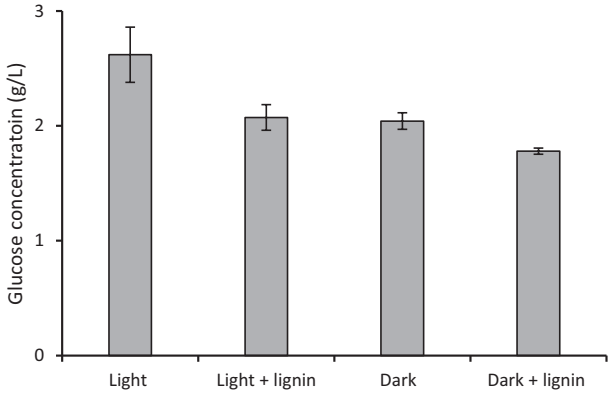

Figure S3. Light-pretreatment of Celluclast 1.5 + NZ-BG. Celluclast 1.5L + NZ-BG was exposed to cold white light for 6 h, either alone or in the presence of lignin (1 g/L), before Avicel was added, and the reaction was run for 24 h in the dark. Control reactions in which Celluclast 1.5L + NZ-BG was pre-incubated in the dark (without light exposure) in the presence or absence of lignin were also performed. Standard deviations for three biological replicates are shown as error bars. The results show that pretreatment with light does not negatively affect the catalytic power of the enzyme cocktail, regardless of the presence of lignin

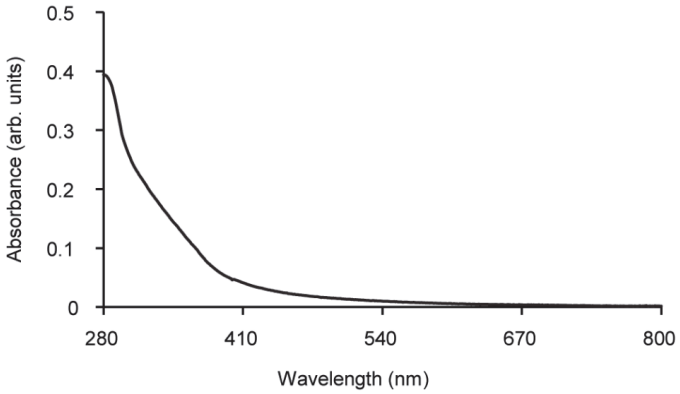

Figure S4. UV-Vis adsorption spectra of kraft lignin. The figure shows the absorption spectra of 0.1 g/L native kraft lignin (Sigma-Aldrich). The data was taken from Kommedal et al. 2023 [1].

Reference

1. Kommedal EG, Angeltveit CF, Klau LJ, Ayuso-Fernández I, Arstad B, Antonsen SG, et al. Visible light-exposed lignin facilitates cellulose solubilization by lytic polysaccharide monooxygenases. Nat Commun. 2023; 14(1):1063. https://doi.org/10.1038/s41467-023-36660-4.

ISBN: 978-82-575-2159-2
ISSN: 1894-6402

Norwegian University
of Life Sciences

Postboks 5003
NO-1432 Ås, Norway
+47 67 23 00 00
www.nmbu.no

120404 / MEDIEHUSET-ANDVORD.NO